Universiteit
Leiden
The Netherlands

Clinical applications of non-invasive imaging techniques in suspected coronary artery disease and in acute myocardial infarction

Nucifora, G.

Citation
Nucifora, G. (2015, April 2). *Clinical applications of non-invasive imaging techniques in suspected coronary artery disease and in acute myocardial infarction*. Retrieved from https://hdl.handle.net/1887/32654

Version:	Corrected Publisher's Version
License:	Licence agreement concerning inclusion of doctoral thesis in the Institutional Repository of the University of Leiden
Downloaded from:	https://hdl.handle.net/1887/32654

Note: To cite this publication please use the final published version (if applicable).

Cover Page

Universiteit Leiden

The handle http://hdl.handle.net/1887/32654 holds various files of this Leiden University dissertation.

Author: Nucifora, Gaetano
Title: Clinical applications of non-invasive imaging techniques in suspected coronary artery disease and in acute myocardial infarction
Issue Date: 2015-04-02

CLINICAL APPLICATIONS OF NON-INVASIVE IMAGING TECHNIQUES IN SUSPECTED CORONARY ARTERY DISEASE AND IN ACUTE MYOCARDIAL INFARCTION

Clinical Applications of Non-invasive Imaging Techniques in Suspected Coronary Artery Disease and in Acute Myocardial Infarction.

The studies described in this thesis were performed at the Department of Cardiology of Leiden University Medical Center, Leiden, The Netherlands

Cover and lay-out: Gaetano Nucifora

Print: Tipografia Tomadini, Udine, Italy

ISBN: 979-12-200-0020-8

Copyright© Gaetano Nucifora, Leiden, The Netherlands. All rights reserved. No part of this book may be reproduced or transmitted, in any form or by any means, without permission of the author.

CLINICAL APPLICATIONS OF NON-INVASIVE IMAGING TECHNIQUES IN SUSPECTED CORONARY ARTERY DISEASE AND IN ACUTE MYOCARDIAL INFARCTION

Proefschrift

Ter verkrijging van de graad van Doctor aan de Universiteit Leiden, op gezag van Rector Magnificus prof. mr. C.J.J.M. Stolker, volgens besluit van het College voor Promoties te verdedigen
op 2 april 2015 klokke 16.15 uur

door

Gaetano Nucifora

Geboren te Udine in 1976

PROMOTIECOMISSIE

Promotor
Prof. Dr. Jeroen J Bax

Co-promotor
Dr. Nina Ajmone Marsan

Overige Leden
Prof. dr. Juhani Knuuti, Turku University Hospital, Turku, Finland
Prof. dr. J.W. Jukema
Prof. dr. Robert J. Klautz
Prof. dr. Johan H.C. Reiber
Dr. Eduard R. Holman
Dr. Victoria Delgado

To Fjoralba and my parents

Table of Contents

Chapter 1. *11*
General Introduction and Outline of the Thesis

PART I. Risk Stratification With MDCT

Chapter 2. *25*
Coronary Artery Calcium Scoring in Cardiovascular Risk Assessment
Cardiovasc Ther 2011;29:e43-53

Chapter 3. *51*
Prevalence of Coronary Artery Disease Across the Framingham Risk Categories: Coronary Artery Calcium Scoring and MSCT Coronary Angiography
J Nucl Cardiol 2009;16:368–75

Chapter 4. *69*
Relation Between Framingham Risk Categories and the Presence of Functionally Relevant Coronary Lesions as Determined on Multislice Computed Tomography and Stress Testing
Am J Cardiol 2009;104:758–763

Chapter 5. *85*
Prevalence of Coronary Artery Disease Assessed by Multislice Computed Tomography Coronary Angiography in Patients With Paroxysmal or Persistent Atrial Fibrillation
Circ Cardiovasc Imaging 2009;2:100-106

Chapter 6. *107*
Relationship Between Obstructive Coronary Artery Disease and Abnormal Stress Testing in Patients With Paroxysmal or Persistent Atrial Fibrillation
Int J Cardiovasc Imaging 2011;27:777–785

Chapter 7. *125*
Usefulness of Echocardiographic Assessment of Cardiac and Ascending Aorta Calcific Deposits to Predict Coronary Artery Calcium and Presence and Severity of Obstructive Coronary Artery Disease
Am J Cardiol 2009;103:1045–1050

Chapter 8. *141*
Incremental Value of Subclinical Left Ventricular Systolic Dysfunction for the Identification of Patients With Obstructive Coronary Artery Disease
Am Heart J 2010;159:148-57

PART II. Assessment of Patients With STEMI: Role of Echocardiographic Techniques

Chapter 9. *167*
Real-time 3-Dimensional Echocardiography Early After Acute Myocardial Infarction: Incremental Value of Echo-Contrast for Assessment of Left Ventricular Function
Am Heart J 2009;157:882.e1-8

Chapter 10. *187*
Left Ventricular Muscle and Fluid Mechanics in Acute Myocardial Infarction
Am J Cardiol 2010;106:1404 –1409

Chapter 11. *205*
Reduced Left Ventricular Torsion Early After Myocardial Infarction Is Related to Left Ventricular Remodeling
Circ Cardiovasc Imaging 2010;3:433-442

Chapter 12. *229*
Impact of Left Ventricular Dyssynchrony Early on Left Ventricular Function After First Acute Myocardial Infarction
Am J Cardiol 2010;105:306–311

Chapter 13. *245*
Temporal Evolution of Left Ventricular Dyssynchrony After Myocardial Infarction: Relation With Changes in Left Ventricular Systolic Function
Eur Heart J Cardiovasc Imaging 2012:13;1041–1046

Summary and Conclusions *261*

Samenvatting en Conclusies *267*

List of Publications *273*

Curriculum Vitae *287*

Acknowledgments *289*

Chapter 1

General Introduction and Outline of the Thesis

GENERAL INTRODUCTION AND OUTLINE OF THE THESIS

Identification of patients at risk of developing coronary artery disease events is one of the most challenging issues in clinical cardiology. The risk of acute coronary events in subjects without known coronary artery disease is related to the presence of cardiovascular risk factors. Several scoring tools that include demographic and clinical characteristics have been developed and are frequently used in clinical practice to predict the 10-year risk of hard coronary events. These tools allow stratification of patients into low-, intermediate, and high-risk categories, in order to determine the need and intensity of risk-modifying interventions.[1-3] However, traditional risk assessment may still fail to identify a considerable proportion of patients with future coronary events, since it provides a statistical probability of having coronary artery disease rather than a direct individual assessment.[4] Indeed, it has been observed that as much as 20% of acute coronary events can occur in the absence of major cardiovascular risk factors.[5]

The potential value of additional risk assessment with stress testing (i.e. electrocardiographic exercise test, stress echocardiography or myocardial perfusion imaging) to improve the identification of patients at risk of coronary events has been extensively evaluated.[6,7] More recently, direct visualization of subclinical atherosclerosis, by coronary artery calcium score (CACS) assessment with electron-beam computed tomography (EBCT) or multi-slice computed tomography (MSCT), and MSCT coronary angiography, has emerged as an extremely rapidly developing non-invasive imaging modality to refine traditional risk assessment. These imaging techniques may be a practical approach since they provide a direct non-invasive estimate of atherosclerotic plaque burden in the coronary arteries (Figure 1).[8] The application of these imaging modalities may be particularly useful among patients with history of atrial fibrillation, since coronary artery disease is considered to be highly prevalent in

patients with atrial fibrillation and may be one of its potential etiologic factors.[9]

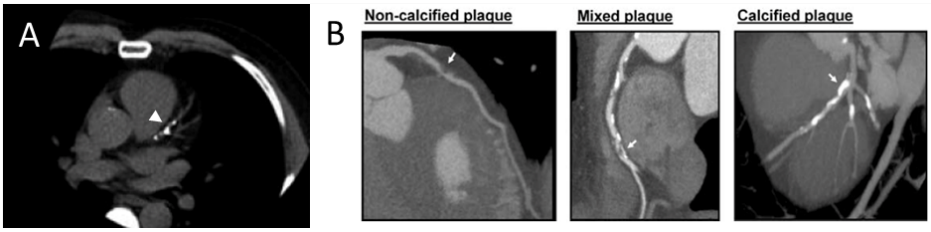

Figure 1. Panel A. Evaluation of CACS by MSCT reveals the presence of coronary calcium in the left anterior descending coronary artery. **Panel B.** Curved multi-planar reconstructions showing three distinct plaque characteristics observed on MSCT with non-calcified plaque (arrow, left panel), mixed plaque (arrow, mid-panel), and calcified plaque (arrow, right panel).

Conventional echocardiography as well as novel echocardiographic techniques, such as speckle-tracking echocardiography, may be of value as well for the identification of patients with obstructive coronary artery disease. Comprehensive echocardiographic assessment of cardiac and ascending aorta calcifications, which have been related to coronary artery disease and cardiovascular events,[10,11] may be a simple, non-invasive, and widely available technique to predict the presence of extensive coronary calcium and obstructive coronary artery disease (Figure 2).

Speckle-tracking echocardiography, a novel non-invasive imaging modality able to quantify myocardial motion and deformation in a region-by-region analysis, may detect the presence of subclinical impairment of myocardial function, which could represent a marker of obstructive coronary artery disease (Figure 3).[12]

Advanced echocardiographic imaging techniques may be of incremental diagnostic and prognostic value among patients with clinically overt cardiac diseases; contrast-enhanced echocardiography, real-time three-dimensional echocardiography (RT3DE) and speckle-tracking imaging have indeed demonstrated their incremental value over conventional echocardiography for the assessment of global and regional left

ventricular function and for a better understand of cardiac mechanics.[13-15] The use of contrast agents allows for the evaluation of cardiac flow dynamics, which are closely related to myocardial motion and deformation, [16,17] and of myocardial blood flow.[18]

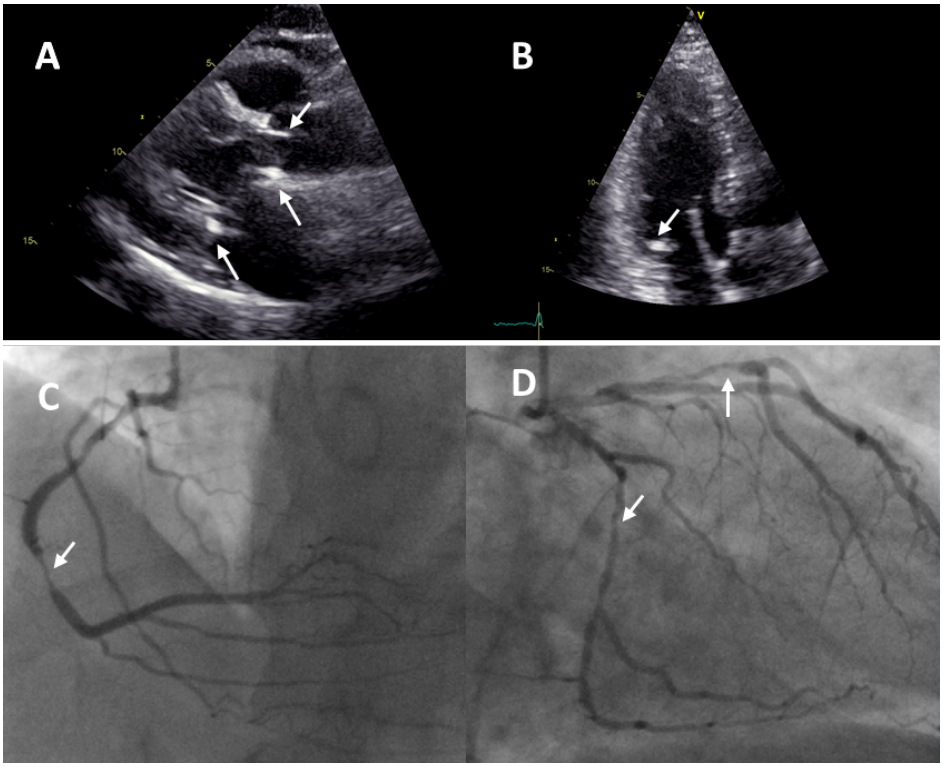

Figure 2. Example of a 50-year-old male with calcified posterior mitral annulus and aortic valve and 3-vessel coronary artery disease. **Panel A** shows the parasternal long-axis view of the left ventricle with calcification of the aortic valve (arrows) and the posterior annulus of the mitral valve (arrow). **Panel B** shows the apical long-axis view of the left ventricle and calcified posterior mitral annulus (arrow). **Panel C** shows the right coronary artery with a significant lesion of the mid segment (arrow) and **panel D** shows the left coronary system with significant lesions in the circumflex coronary artery and first diagonal branch of the left anterior descending coronary artery (arrows).

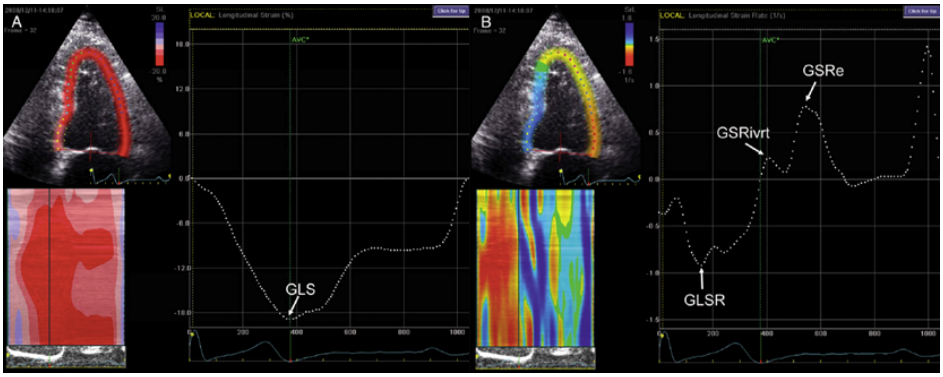

Figure 3. Speckle-tracking echocardiography provides a direct measure of myocardial deformation and can therefore be used to detect subtle abnormalities in LV systolic and diastolic function. Global longitudinal strain and strain rate curves obtained by speckle-tracking analysis from an apical 4-chamber view are shown in **panel A** and **B**, respectively.

Coronary artery calcium scoring and multi-slice computed tomography coronary angiography

EBCT and MSCT have been previously validated as sensitive techniques for the detection of coronary calcium, a marker of coronary atherosclerosis.[19] EBCT was introduced in the early 1980s specifically for cardiac imaging. The use of non-mechanical X-ray source allows for prospective ECG-triggered image acquisition with high temporal resolution (50–100 ms), thereby limiting respiratory and cardiac motion artifacts. Coronary calcifications are defined as hyper-attenuating lesions >130 Hounsfield units with an area of three or more adjacent pixels (at least 1 mm2).[20] To quantify the extent of coronary calcium, a score has been developed by Agatston et al.[21] To express the extent of detected coronary calcium, CACS is commonly classified into four categories: 0, 1–99, 100–399, and ≥400, indicating no calcific deposits, mild, moderate, and severe coronary calcifications, respectively.[22] Several studies have recently demonstrated that CACS obtained using newer generation MSCT scanners (with higher number of detectors and faster X-ray gantry rotation time) are comparable to those obtained with EBCT.[23]

Main disadvantages of calcium scoring are the lack of information on the degree of coronary stenosis and the inability to identify non-calcified plaques. The introduction of MSCT coronary angiography has overcome these limitations, allowing direct non-invasive anatomic assessment of the coronary arteries. For diagnosis, numerous studies support the use of MSCT coronary angiography for rule out of the presence of coronary artery disease with a high accuracy;[24,25] a differentiation can also be made between non-calcified plaques having low attenuation, calcified plaques with high attenuation, and mixed plaques with both non-calcified and calcified elements (Figure 1).[26] Furthermore, plaque remodelling, a marker of vulnerability, can also be appreciated.[26] These advantages have led to an increased use of MSCT as a gatekeeper for further diagnostic testing. In addition, early identification of coronary artery disease with MSCT coronary angiography may be useful for risk stratification.[27]

Echocardiographic assessment of cardiac and ascending aorta calcifications

Previous studies have consistently demonstrated that mitral annular calcium and aortic valve sclerosis are not simple passive degenerative disorders influenced by mechanical stress, but active inflammatory processes with histopathologic features similar to atherosclerosis.[28] Large population cohort studies have also shown that aortic valve sclerosis and mitral annular calcium are associated with increased cardiovascular morbidity and mortality.[10,11] Because it is unlikely that aortic valve sclerosis and mitral annular calcium directly lead to adverse cardiovascular outcomes, their relation with coronary atherosclerosis most likely explains these observations. Accordingly, echocardiographic recognition of cardiac and ascending aorta calcium could be helpful to optimize the identification of patients with obstructive coronary artery disease.

Echocardiographic assessment of myocardial deformation

Speckle-tracking echocardiography has been introduced in the last years for the assessment of myocardial deformation; it allows an angle-independent analysis of myocardial strain (and strain rate) in multiple directions (radial, longitudinal and circumferential), through the detection and tracking of the unique myocardial ultrasound patterns frame by frame. The in-plane frame-to-frame displacement of each pattern over time is used to derive strain.[29] Using this technique, regional and global myocardial contractility can be studied, as well as more complex cardiac mechanics, such as the systolic twisting motion of the left ventricle along its longitudinal axis, which results from the opposite rotation of the left ventricular apex compared with the base. Left ventricular twist has emerged as an important, sensitive parameter of left ventricular systolic function.[30]

Real-time three-dimensional echocardiography

Over the last few decades, advances in ultrasound and computer technologies have enabled on-line real-time display of three-dimensional (3D) images of the heart. Several studies have demonstrated superior accuracy and reproducibility of RT3DE over standard two-dimensional echocardiography for quantification of left ventricular size and function.[31] In addition, the 3D tracking of endocardial motion of volumetric segments refines the analysis of regional left ventricular function and allows the assessment of temporal sequence of regional myocardial contraction, thus providing quantitative data of left ventricular dyssynchrony.[31] In patients with acute myocardial infarction (AMI), the presence of significant left ventricular dyssynchrony has been associated with adverse left ventricular remodelling and functional impairment at follow-up.

Contrast-enhanced echocardiography

Transthoracic echocardiography (and in particular RT3DE) is not able to provide diagnostically useful images in a non-negligible proportion of

patients, mainly because of obesity and lung disease. The use of echo-contrast agents solves these issues, providing cardiac chamber opacification and improving endocardial border definition, thereby allowing a more accurate quantification of left ventricular function (Figure 4).[32]

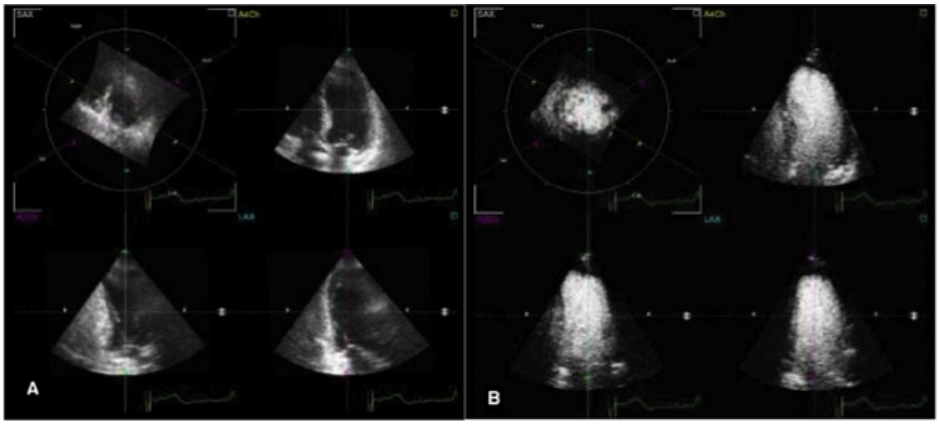

Figure 4. Panel A. Example of fair-quality echocardiogram during nonenhanced RT3DE. **Panel B.** Optimal LV chamber opacification and improved endocardial border definition during contrast-enhanced RT3DE in the same patient. The 3 apical views are shown with the 4-chamber view as a reference view in the top right and the 2- and 3-chamber views in the bottom left and bottom right, respectively. Top left: short-axis view.

Besides improving the assessment of left ventricular function, echo-contrast agents may also be used to assess myocardial perfusion and to investigate left ventricular hydrodynamics. During early left ventricular filling, the blood flow forms an intraventricular rotational body of fluid, which is critical in optimizing the blood flow during systole.[17] Knowledge of abnormalities involving left ventricular hydrodynamics may be useful, since it provides direct information regarding the ultimate goal of left ventricular performance, i.e. optimal blood flow.

OBJECTIVES AND OUTLINE OF THE THESIS

The objectives of the thesis were to investigate the incremental value in clinical practice of different non-invasive imaging techniques in patients with suspected coronary artery disease and in patients with acute myocardial infarction (AMI).

In **Part I**, the use of non-invasive imaging modalities for diagnosis and risk stratification of patients with suspected coronary artery disease will be introduced. An overview of the prognostic value of CACS assessment is provided in **Chapter 2**; in addition, potential other applications of CACS assessment and the limitations of the technique are discussed. The incremental value of CACS and MSCT coronary angiography and the relation between coronary atherosclerosis and presence of abnormal stress testing are subsequently investigated in the general population (**Chapters 3-4**) and among patients with paroxysmal or persistent AF (**Chapters 5-6**). The clinical usefulness of comprehensive echocardiographic assessment of the burden of cardiac and ascending aorta calcium to predict coronary artery calcium and presence and severity of obstructive coronary artery disease is evaluated in **Chapter 7** while in **Chapter 8** the relation between obstructive coronary artery disease and subclinical left ventricular systolic dysfunction, as assessed by speckle-tracking echocardiography, is investigated.

Part II will discuss the diagnostic and prognostic value of novel echocardiographic techniques in patients with AMI. The incremental value of contrast-enhanced RT3DE early after AMI was investigated in **Chapter 9**. The left ventricular hydrodynamics early after AMI and their relation to left ventricular diastolic function and infarct size are evaluated in **Chapter 10**, while the effects of AMI on left ventricular torsional mechanics and on left ventricular dyssynchrony are investigated in **Chapters 11-13**.

REFERENCES

1. Wilson PW, D'Agostino RB, Levy D, et al. Prediction of coronary heart disease using risk factor categories. Circulation 1998;97:1837-1847.
2. Assmann G, Cullen P, Schulte H. Simple scoring scheme for calculating the risk of acute coronary events based on the 10-year follow-up of the prospective cardiovascular Munster (PROCAM) study. Circulation 2002;105:310-315.
3. Conroy RM, Pyorala K, Fitzgerald AP, et al. Estimation of ten-year risk of fatal cardiovascular disease in Europe: the SCORE project. Eur Heart J 2003;24:987-1003.
4. Naghavi M, Libby P, Falk E, et al. From vulnerable plaque to vulnerable patient: a call for new definitions and risk assessment strategies: Part II. Circulation 2003;108:1772-1778.
5. Khot UN, Khot MB, Bajzer CT, et al. Prevalence of conventional risk factors in patients with coronary heart disease. JAMA 2003;290:898-904.
6. Balady GJ, Larson MG, Vasan RS, et al. Usefulness of exercise testing in the prediction of coronary disease risk among asymptomatic persons as a function of the Framingham risk score. Circulation 2004;110:1920-1925.
7. Blumenthal RS, Becker DM, Moy TF, et al. Exercise thallium tomography predicts future clinically manifest coronary heart disease in a high-risk asymptomatic population. Circulation 1996;93:915-923.
8. Nucifora G, Bax JJ, van Werkhoven JM, et al. Coronary artery calcium scoring in cardiovascular risk assessment. Cardiovasc Ther. 2011;29:e43-53.
9. Lip GY, Beevers DG. ABC of atrial fibrillation. History, epidemiology, and importance of atrial fibrillation. BMJ 1995;311:1361-1363.
10. Otto CM, Lind BK, Kitzman DW, et al. Association of aortic-valve sclerosis with cardiovascular mortality and morbidity in the elderly. N Engl J Med. 1999;341:142-147.
11. Fox CS, Vasan RS, Parise H, et al. Mitral annular calcification predicts cardiovascular morbidity and mortality: the Framingham Heart Study. Circulation 2003;107:1492-1496.
12. Edvardsen T, Detrano R, Rosen BD, et al. Coronary artery atherosclerosis is related to reduced regional left ventricular function in individuals without history of clinical cardiovascular disease: the Multiethnic Study of Atherosclerosis. Arterioscler Thromb Vasc Biol. 2006;26:206-211.

13. Mor-Avi V, Lang RM, Badano LP, et al. Current and evolving echocardiographic techniques for the quantitative evaluation of cardiac mechanics: ASE/EAE consensus statement on methodology and indications endorsed by the Japanese Society of Echocardiography. J Am Soc Echocardiogr. 2011;24:277-313.
14. Hoffmann R, von Bardeleben S, Kasprzak JD, et al. Analysis of regional left ventricular function by cineventriculography, cardiac magnetic resonance imaging, and unenhanced and contrast-enhanced echocardiography: a multicenter comparison of methods. J Am Coll Cardiol. 2006;47:121-128.
15. Mor-Avi V, Jenkins C, Kuhl HP, et al. Real-time 3-dimensional echocardiographic quantification of left ventricular volumes: multicenter study for validation with magnetic resonance imaging and investigation of sources of error. JACC Cardiovasc Imaging 2008;1:413-423.
16. Gharib M, Rambod E, Kheradvar A, et al. Optimal vortex formation as an index of cardiac health. Proc Natl Acad Sci U S A. 2006;103:6305-6308.
17. Hong GR, Pedrizzetti G, Tonti G, et al. Characterization and quantification of vortex flow in the human left ventricle by contrast echocardiography using vector particle image velocimetry. JACC Cardiovasc Imaging 2008;1:705-717.
18. Dijkmans PA, Senior R, Becher H, et al. Myocardial contrast echocardiography evolving as a clinically feasible technique for accurate, rapid, and safe assessment of myocardial perfusion: the evidence so far. J Am Coll Cardiol. 2006;48:2168-2177.
19. Rumberger JA, Simons DB, Fitzpatrick LA, et al. Coronary artery calcium area by electron-beam computed tomography and coronary atherosclerotic plaque area. A histopathologic correlative study. Circulation 1995;92:2157-2162.
20. Budoff MJ. Computed tomography. In: Budoff MS, J., ed. Cardiac CT Imaging. London: Springer-Verlag, 2006:1-18.
21. Agatston AS, Janowitz WR, Hildner FJ, et al. Quantification of coronary artery calcium using ultrafast computed tomography. J Am Coll Cardiol. 1990;15:827-832.
22. Rumberger JA, Brundage BH, Rader DJ, et al. Electron beam computed tomographic coronary calcium scanning: a review and guidelines for use in asymptomatic persons. Mayo Clin Proc. 1999;74:243-252.
23. Stanford W, Thompson BH, Burns TL, et al. Coronary artery calcium quantification at multi-detector row helical CT versus electron-beam CT. Radiology 2004;230:397-402.

24. Schuijf JD, Pundziute G, Jukema JW, et al. Diagnostic accuracy of 64-slice multislice computed tomography in the noninvasive evaluation of significant coronary artery disease. Am J Cardiol 2006;98:145-148.
25. Budoff MJ, Dowe D, Jollis JG, et al. Diagnostic performance of 64-multidetector row coronary computed tomographic angiography for evaluation of coronary artery stenosis in individuals without known coronary artery disease: results from the prospective multicenter ACCURACY (Assessment by Coronary Computed Tomographic Angiography of Individuals Undergoing Invasive Coronary Angiography) trial. J Am Coll Cardiol. 2008;52:1724-1732.
26. Schroeder S, Kopp AF, Baumbach A, et al. Noninvasive detection and evaluation of atherosclerotic coronary plaques with multislice computed tomography. J Am Coll Cardiol. 2001;37:1430-1435.
27. Pundziute G, Schuijf JD, Jukema JW, et al. Prognostic value of multislice computed tomography coronary angiography in patients with known or suspected coronary artery disease. J Am Coll Cardiol. 2007;49:62-70.
28. Roberts WC. The senile cardiac calcification syndrome. Am J Cardiol 1986;58:572-574.
29. Brown J, Jenkins C, Marwick TH. Use of myocardial strain to assess global left ventricular function: a comparison with cardiac magnetic resonance and 3-dimensional echocardiography. Am Heart J. 2009;157:102 e101-105.
30. Sengupta PP, Khandheria BK, Narula J. Twist and untwist mechanics of the left ventricle. Heart Fail Clin. 2008;4:315-324.
31. Ng AC, Delgado V, Bertini M, et al. Advanced applications of 3-dimensional echocardiography. Minerva Cardioangiol. 2009;57:415-441.
32. Nucifora G, Faletra FF. Current applications of contrast echocardiography. Minerva Cardioangiol. 2011;59:519-532.

Part I

RISK STRATIFICATION WITH MDCT

Chapter 2

Coronary Artery Calcium Scoring in Cardiovascular Risk Assessment

Gaetano Nucifora, Jeroen J. Bax, Jacob M. van Werkhoven,
Mark J. Boogers, Joanne D. Schuijf

Cardiovasc Ther 2011;29:e43-53

ABSTRACT

Identification of patients at risk of future coronary artery disease (CAD) events traditionally relies on scoring tools that take demographic and clinical characteristics into account (e.g., the Framingham risk score in the United States and the Heart Score in Europe). Although these scoring tools have been shown to have a good predictive value, they may still fail to recognize a proportion of patients with coronary atherosclerosis at risk for future CAD events. In order to improve risk stratification, direct visualization of subclinical atherosclerosis has been advocated. Electron-beam computed tomography and multislice computed tomography provide a direct estimation of coronary calcium, a marker of coronary atherosclerosis. A large amount of data is available supporting the clinical value of the noninvasive assessment of coronary artery calcium score (CACS) with these techniques and its incremental prognostic information over traditional risk stratification. Aim of this review is to provide an overview of the literature regarding the prognostic value of CACS assessment. In addition, potential other applications of CACS assessment as well as the limitations of the technique are discussed.

INTRODUCTION

Identification of patients at risk of developing coronary artery disease (CAD) events is one of the most challenging issues in clinical cardiology. Indeed, in a large proportion of individuals, the initial presentation of CAD is acute myocardial infarction (AMI) or sudden cardiac death.[1] The risk of CAD events in subjects without known CAD is related to the presence of coronary risk factors (i.e., age, gender, diabetes mellitus, systolic blood pressure, total cholesterol and high-density lipoprotein cholesterol level, and smoking history).[1] For this reason, scoring tools that take demographic and clinical characteristics into account (e.g., the Framingham risk score (FRS) in the United States and the Heart Score in Europe) have been developed and are frequently used in clinical practice to predict the 10-year risk of hard CAD events.[2,3] Accordingly, these algorithms allow stratification of individuals into low-, intermediate- and high-risk categories, in order to determine the need and intensity of risk-modifying interventions. However, these scoring tools have several limitations that reduce their ability to provide accurate risk stratification.[4] In particular, cardiovascular risk may not be adequately recognized in certain subset of patients including young individuals and nondiabetic women below the age of 70 years.[4-7] In addition, a variation in CAD severity for each level of risk factor exposure has been observed, likely related to the duration of exposure, genetic susceptibility and other biochemical and environmental risk factors.[8,9]

Several biomarkers and noninvasive imaging techniques have been advocated to refine the traditional risk assessment of CAD events. Among the available noninvasive imaging techniques, coronary artery calcium score (CACS) assessment with electron-beam computed tomography (EBCT) or multislice computed tomography (MSCT) may represent a practical approach since it provides a direct noninvasive estimate of atherosclerotic plaque burden in the coronary arteries. The aim of this review is to provide an overview of the literature regarding the prognostic

value of CACS assessment. In addition, potential other applications of CACS assessment as well as the limitations of the technique are discussed.

EBCT AND MSCT FOR CORONARY ARTERY CALCIUM ASSESSMENT

EBCT and MSCT have been previously validated as sensitive techniques for the detection of coronary calcium, a marker of coronary atherosclerosis.[10] EBCT was introduced in the early 1980s specifically for cardiac imaging. The use of nonmechanical X-ray source allows for prospective ECG-triggered image acquisition with high temporal resolution (50–100 ms), thereby limiting respiratory and cardiac motion artifacts. Usually, 30–40 nonoverlapping slices of 3 mm thickness are obtained during a single 20- to 30-second breath hold to include the whole heart and the entire coronary artery tree.[11] Coronary calcifications are defined as hyper-attenuating lesions >130 Hounsfield units with an area of three or more adjacent pixels (at least 1 mm2).[11] To quantify the extent of coronary calcium, a score has been developed by Agatston et al.[12] Using 3-mm slice thickness images, the CACS is defined as the product of the area of calcification per coronary segment and a factor rated 1 through 4 determined by the maximum calcium CT density within that segment. To express the extent of detected coronary calcium, CACS is commonly classified into four categories: 0, 1–99, 100–399, and ≥400, indicating no calcific deposits, mild, moderate, and severe coronary calcifications, respectively.[13] The presence of coronary calcifications and the extent of CACS has been found to be also gender- and age-related; in particular, a rapid increase in CACS is present in men after age 45 and in women after age 55.[14] These data have been used to derive nomogram tables, in order to compare CACS of asymptomatic subjects with the expected normal values (Table 1).[14] A CACS ≥75th percentile for age- and gender-matched individuals is usually considered as an indicator of elevated coronary calcium burden.[15-17] Several studies have recently demonstrated that

CACS obtained using newer generation MSCT scanners (with higher number of detectors and faster X-ray gantry rotation time) are comparable to those obtained with EBCT.[18-20] However, it should be acknowledged that MSCT has still lower interscan and interreader reproducibility than EBCT.[21] Examples of patients with and without coronary calcium, as detected by MSCT, are shown in Figure 1.

Table 1. Coronary artery calcium scores (CACS) by percentile, gender and age in a large asymptomatic population (N° = 21265) screened with electron-beam computed tomography. Adapted from Wong et al.[14] with permission.

Asymptomatic Women (N° = 6027)					
Age (years)		≤40	41-45	46-50	51-55
N° of subjects		331	407	855	1213
Percentile of CACS					
-25th		0	0	0	0
-50th		0	0	0	0
-75th		0	0	2	7
Age (years)	56-60	61-65	66-70	71-75	>75
N° of subjects	1091	770	626	437	297
Percentile of CACS					
-25th	0	0	0	4	25
-50th	0	2	17	67	157
75th	29	81	163	310	577
Asymptomatic Men (N° = 15238)					
Age (years)	≤35	36-40	41-45	46-50	51-55
N° of subjects	466	1011	1873	2503	2915
Percentile of CACS					
-25th	0	0	0	0	0
-50th	0	0	0	2	14
-75th	0	3	8	41	116
Age (years)	56-60	61-65	66-70	71-75	>75
N° of subjects	2385	1765	1212	679	429
Percentile of CACS					
-25th	1	12	41	81	148
-50th	42	114	211	328	562
75th	227	421	709	918	1409

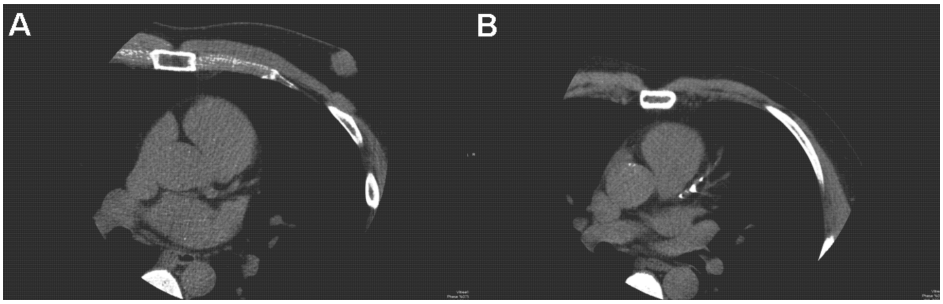

Figure 1. Panel A. 47-year-old asymptomatic female at intermediate risk for future coronary artery disease (CAD) events. Coronary artery calcium score (CACS) assessment by MSCT reveals the absence of coronary calcium. **Panel B.** 55-year-old asymptomatic male patient at intermediate risk for future CAD events. Evaluation of CACS by MSCT reveals the presence of coronary calcium in the left anterior descending coronary artery. Total CACS was >400.

CORONARY ARTERY CALCIFICATIONS AND ATHEROSCLEROSIS

Calcifications of the coronary arteries are strictly related to the process of atherosclerotic plaque formation and evolution.[22] Previous studies have consistently demonstrated that vascular deposition of mineral calcium is not simply a passive precipitation of calcium phosphate crystals in damaged tissues.[23,24] Instead, it is an organized and regulated process similar to bone formation that typically occurs in areas of atherosclerotic lipid accumulation.[23,24] Consequently, the presence of calcific deposits in coronary arteries is considered to be pathognomonic of coronary atherosclerosis. In addition, histopathological and intravascular ultrasound studies found a good correlation between CACS measured using EBCT and the volume of coronary artery atherosclerosis, leading to the concept that CACS may be considered a surrogate of total atherosclerotic plaque burden.[10,25-27] In this regard, however, two main drawbacks of CACS assessment should be acknowledged. Firstly, a large part of the total plaque volume is due to noncalcified tissue, which is not detected. As a result, CACS may underestimate total coronary atherosclerotic plaque burden, particularly in younger individuals.[10] Secondly, the relation of

coronary calcification and the presence of significant stenosis is more variable.[22] Even though a positive relation exists between the amount of CACS and the likelihood of significant luminal narrowing, obstructive plaques can occur at sites with limited calcium, while extensive calcific deposits without stenosis can be observed.[28-32]

RISK STRATIFICATION OF ASYMPTOMATIC SUBJECTS

Numerous studies have previously demonstrated the ability of CACS to predict cardiac events in asymptomatic subjects, with significant incremental value over conventional risk factor assessment. In a retrospective study of 5635 asymptomatic adults at low-intermediate risk (mean age 51±9 years), Kondos et al.[17] observed that CACS >170 measured with EBCT was associated with a relative risk of cardiac events of 7.2 (95% CI 2.0–26.2), after a mean follow-up of 37 months. The prognostic information obtained from CACS assessment was incremental to conventional risk stratification. Similar findings were reported by Shaw and colleagues in a retrospective analysis of 10,377 asymptomatic patients (40% women), with a mean of 5 years follow-up after EBCT evaluation.[33] CACS was an independent predictor of death after adjustment for Framingham risk factors ($p < 0.001$), with an increase of risk that was proportional to the increase of CACS (risk-factor adjusted relative risk of 1.6, 1.7, 2.5, and 4 for CACS 11–100, 101–400, 401–1000, and >1000, respectively). The incremental value of CACS to FRS was illustrated by a significant increase of the area under the ROC curves, from 0.72 for FRS to 0.78 with the addition of CACS ($p < 0.001$). Further follow-up in a large cohort of 25,253 asymptomatic subjects confirmed these data, showing increasing mortality rates after a mean follow-up of 6.8 years with increasing baseline CACS (Figure 2).[34]

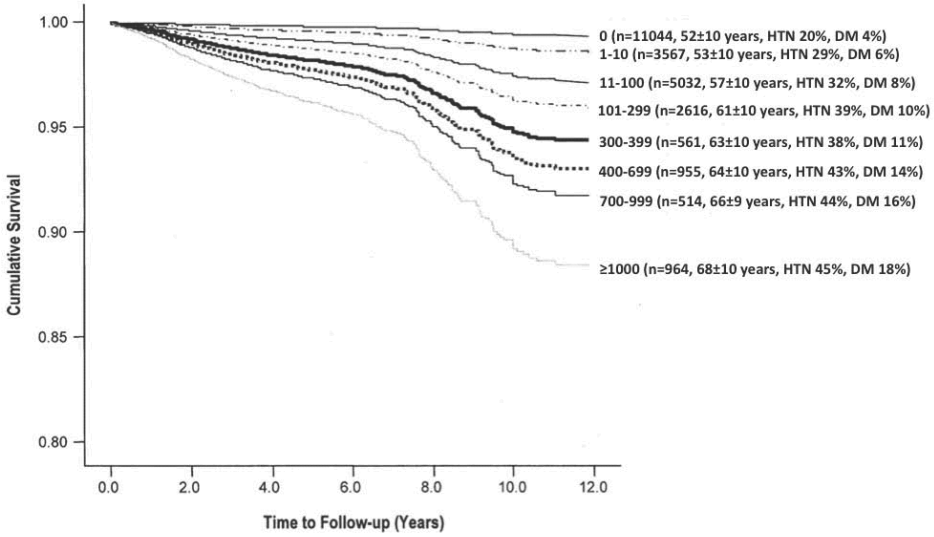

Figure 2. Cumulative survival by coronary artery calcium score (CACS) after adjustment for coronary risk factors (age, hypercholesterolemia, diabetes mellitus, smoking, hypertension, and family history of premature coronary heart disease). Increasing CACS was associated with increased risk of all-cause mortality. DM: diabetes mellitus; HTN: hypertension. Adapted from Budoff et al.[34] with permission.

Prospective studies have confirmed these observations reinforcing the concept that CACS assessment may be of clinical value to refine traditional risk stratification.[35–37] In a prospective observational population-based study, Greenland et al.[35] used EBCT to screen 1029 asymptomatic nondiabetic subjects older than 45 years with at least one coronary risk factor. After a median follow-up of 7 years, a CACS >300 predicted the risk of AMI or cardiac death (hazard ratio 3.9; 95% CI 2.1–7.3; p <0.001) compared with a CACS of zero. Across FRS categories, CACS was predictive of risk among subjects with intermediate and high FRS, but not among subjects with low FRS. Figure 3 shows the predicted 7-year event rates (AMI or cardiac death) across FRS and CACS categories.

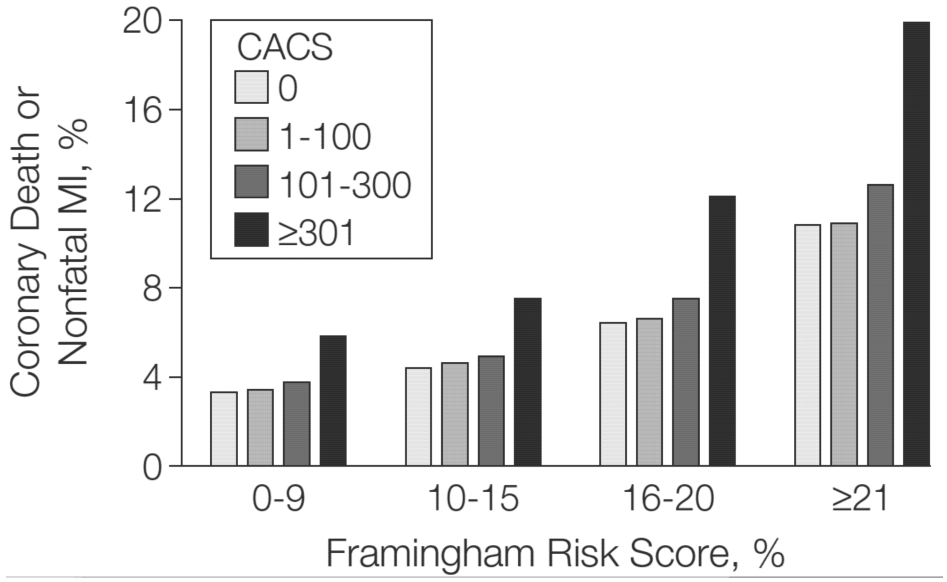

Figure 3. Predicted 7-year event rates for categories of FRS and CACS. Pairwise analyses compared the highest CACS level (>300) with each of the lower levels of CACS within each FRS group. A statistically significant difference between CACS >300 and each of the other three CACS groups was observed for FRS >10% ($p < 0.001$) and between CACS >300 and CACS zero for FRS <10% ($p = 0.01$). From Greenland et al.[35] with permission.

More recently, in the St. Francis Heart Study,[36] screening for CAD by EBCT was performed in 4903 asymptomatic individuals. In the subgroup of 1357 subjects in whom risk factors were measured, CACS was superior in the prediction of CAD events (cardiac death, AMI, surgical, or percutaneous coronary revascularization procedures) after a mean follow-up of 4.3 years as compared to the FRS. Area under the ROC curve for CACS was 0.79 as compared to 0.68 for FRS ($p < 0.001$). In addition, CACS significantly improved the risk stratification based on FRS ($p < 0.001$ for trend).

On the basis of these previous studies, a consensus document from the American College of Cardiology Foundation (ACCF) and the American Heart Association (AHA) has been recently published, providing

recommendations on the use of CACS assessment for risk stratification of asymptomatic subjects.[38] In particular, individuals at intermediate FRS risk are considered to represent potential candidates for evaluation of CACS. In this group, the presence of CACS ≥400 would allow reclassification of individuals to a higher risk category, thereby altering clinical decision-making. Conversely, CACS screening is not recommended in subjects at either low or high FRS. In patients at low risk, the presence of a high CACS would not elevate the individual's risk above the threshold to initiate medical therapy. Conversely, in the latter category, a high risk of CAD events is a priori anticipated on the basis of the high-risk profile, and aggressive medical therapy is already required. Moreover, Blaha et al.[39] recently showed that, after a mean follow-up of 5.6 years, asymptomatic subjects at high risk (in particular diabetic patients and smokers) even in the absence of coronary calcifications, experience more CAD events, as compared to patients at low risk. Accordingly, the ACCF/AHA consensus document does not support the concept that absence of CACS would lower the risk status of individuals with high FRS.

Of note, in opposition to ACCF/AHA consensus document, the US Preventive Services Task Force (USPSTF) did not recommend the use of CACS for risk stratification of asymptomatic subjects.[40] In particular, the USPSTF pointed out that only poor- to fair-quality evidence indicates that higher CACS predicts CAD events independent of Framingham risk factors, on the basis of a systematic review of eight cohort studies. However, it is important to remark that USPSTF did not include in its analysis the results of important large prospective, population-based studies clearly demonstrating the incremental prognostic value of CACS over conventional risk factor assessment.[36,37] Inclusion of these studies may possibly lead the USPSTF to revise its recommendation.

RISK STRATIFICATION OF SYMPTOMATIC PATIENTS

Most of the available data regarding the clinical value of CACS assessment have been obtained in asymptomatic individuals. However, several studies have shown the utility of CACS for risk stratification also in symptomatic subjects. In a prospective, multicenter study of 491 symptomatic patients (mean age 55±12 years) who underwent both invasive coronary angiography and EBCT, Detrano and colleagues observed a strong association between CACS and the occurrence of CAD events.[41] Patients with CACS higher than the median value (75.3) had a six times higher probability of CAD events after a mean follow-up of 30±13 months, as compared to patients with CACS below the median value. Interestingly, at multivariate analysis, log CACS, but not the number of significantly diseased segments at invasive coronary angiography, was selected as an independent predictor of CAD events, suggesting that global plaque burden rather than the degree of stenosis mainly determines the prognosis of CAD.

Keelan et al.[42] further confirmed these preliminary observations. A total of 288 symptomatic subjects who underwent invasive angiography and EBCT were followed-up for 6.9 years. Univariate analysis showed that CACS ≥100 was significantly related to the occurrence of hard CAD events (unadjusted relative risk 3.2, 95% CI 1.17–8.71; p = 0.023). At multivariate analysis, besides increasing age, CACS was the most powerful predictor of future hard CAD events. Conversely, none of the conventional coronary risk factors (except age) nor angiographic stenosis was related to the occurrence of CAD events, supporting the results of Detrano and collegues. In another study, Georgiu et al.[43] screened, by EBCT, 192 patients admitted in the emergency department because of chest pain. A graded relation between increasing CACS values and the incidence of cardiovascular events after a mean follow-up of 50±10 months was observed. In particular, the annualized event rate was 0.6% for the patients without coronary calcium as compared with 13.9% per

year for the patients with CACS >400 (p <0.001). At multivariate analysis, CACS and age- and gender-matched calcium percentiles were the strongest predictors of future events.
The results of these studies demonstrate that CACS assessment also in symptomatic subjects may provide valuable prognostic information.

SELECTION OF PATIENTS REQUIRING TREATMENT

On the basis of the prognostic data previously described, CACS has been proposed to refine medical decision-making. Indeed, the National Cholesterol Education Program's Adult Treatment Panel III guidelines state that the presence of a high CACS (defined as CACS at or above the 75th percentile for age and gender) in subjects at intermediate risk of CAD events identifies advanced coronary atherosclerosis.[44] In these patients, more intensive lipid-lowering therapy is recommended in order to achieve a low-density lipoprotein cholesterol target of less than 100 mg/dl.[44] However, thus far, only few data on the outcome of medical therapy based on CACS are available. In the St. Francis Heart Study,[45] 1005 asymptomatic subjects (mean age 59±6 years) with CACS at or above the 80th percentile for age and gender were randomized to receive atorvastatin 20 mg daily, vitamin C 1 g daily, and vitamin E (alpha-tocopherol) 1000 U daily or placebo. All subjects received aspirin 81 mg daily. Mean duration of treatment was 4.3 years. Treatment significantly reduced total cholesterol by 26.5–30.4% (p <0.0001), low-density lipoprotein cholesterol by 39% (p <0.001), and triglycerides by 11% (p = 0.02). Nevertheless, no significant reduction in atherosclerotic cardiovascular disease event rate was achieved by treatment. Interestingly, however, subanalysis revealed that treatment did reduce event rates in individuals with baseline CACS >400 (8.7% vs. 15.0%, 42% reduction, p <0.046).
More recently, McCullough and Chinnaiyan systematically reviewed five prospective randomized trials evaluating the change in CACS as a

surrogate endpoint for treatment effect in patients at risk for or with CAD and could not demonstrate any consistent treatment effect on CACS progression at 1 year of follow-up.[46] Further randomized studies are therefore needed to clarify whether clinical management based on CACS may positively impact outcome.

SELECTION OF FURTHER DIAGNOSTIC TESTS

CACS provides a relatively simple method for early identification of atherosclerosis. Accordingly, the technique may be used to identify patients that may benefit from further evaluation by means of functional testing. In comparative studies between CACS and myocardial perfusion imaging a relationship has been observed between the presence and extent of calcifications and the presence of ischemia.[47–62] In one of the first comparative studies by He et al.[47] in predominantly asymptomatic individuals, abnormal perfusion was observed in 0% of individuals with a CACS <10, in 2.6% of individuals with a CACS 11–100, in 11.3% of individuals with a CACS 101–400, and in 46% of individuals with a CACS >400. Similar increases in the prevalence of ischemia with increasingly higher CACS have been observed in other studies.[48–52,54–61] Importantly, a CACS above 400 has consistently been shown to imply a high likelihood of ischemia. Accordingly, further evaluation by means of myocardial perfusion imaging in patients with CACS exceeding 400 has been deemed appropriate.[63] Since a CACS >400 is observed in only approximately 10% of asymptomatic individuals,[34] only a small proportion of patients referred for CACS will need further evaluation with ischemia testing. Conversely, in asymptomatic individuals with a CACS <100, further testing using myocardial perfusion imaging may not be needed as the prevalence of ischemia in patients with a CACS <100 is generally very low (< 10%).[47,48,50,58,63,64]

Although this notion may be valid for the general asymptomatic population, some studies have reported a higher prevalence of ischemia in

patients with low CACS. Most likely, the observed discrepancies may reflect differences in study populations.[49,54,56,60] In a large study in asymptomatic patients with diabetes, a higher prevalence of myocardial perfusion defects (18%) was observed in patients with a low CACS between 11 and 100.[53] In a further evaluation by Scholte et al.[60] in asymptomatic diabetics, the prevalence of ischemia in patients with a low CACS <100 was 21%. These observations indicate that CACS should be treated with caution in patients with diabetes, as a low CACS may not invariably rule out the presence of ischemia.

Also in symptomatic patients, a higher prevalence of ischemia (exceeding 10%) has been observed in individuals with a low CACS <100; furthermore, the increased prevalence of ischemia has been linked to the severity of symptoms and the pretest likelihood of CAD.[55,57–59] As compared to patients with minor symptoms or a low pretest likelihood, a higher proportion of patients with more severe symptoms or a higher pretest likelihood appear to have ischemia despite low CACS.[58] In symptomatic patients therefore, CACS may only serve as a reliable gatekeeper for myocardial perfusion imaging in patients with relatively minor symptoms and a low pretest likelihood for CAD.

EVALUATION OF TREATMENT

Serial assessment of CACS has been previously proposed to evaluate the efficacy of treatment with lipid-lowering drugs. Callister and colleagues retrospectively studied 149 asymptomatic patients (age range 32–75 years, 61% men) who underwent two consecutive EBCT examinations for CACS evaluation at least 12 months apart.[65] Patients treated with HMG-CoA reductase inhibitors with a final low-density lipoprotein cholesterol level of less than 120 mg/dl had a significant reduction in CACS (mean change $-7 \pm 23\%$; $p = 0.01$) whereas a significant increase in CACS (mean change $+25 \pm 22\%$, $p < 0.001$) was observed in treated patients with a final low-density lipoprotein cholesterol level of at least 120 mg/dl.

An even larger increase in CACS was observed in untreated patients who had a final low-density lipoprotein cholesterol level of at least 120 mg/dl; in these subjects, a mean change of +52±36% in CACS was observed at follow-up (p <0.001).

Similar results were observed by Budoff et al.[66] and Achenbach et al.[67] Budoff et al.[66] studied 299 asymptomatic subjects (mean age 58±10 years, 76% men) who underwent baseline EBCT for CACS evaluation and follow-up assessment after a minimum of 12 months. The observed mean change in CACS in the study population was 33.2±9.2% per year. The increase in CACS among patients receiving statin therapy was significantly lower, as compared to nontreated patients (15±8% per year vs. 39±12% per year; p <0.001) (Figure 4).

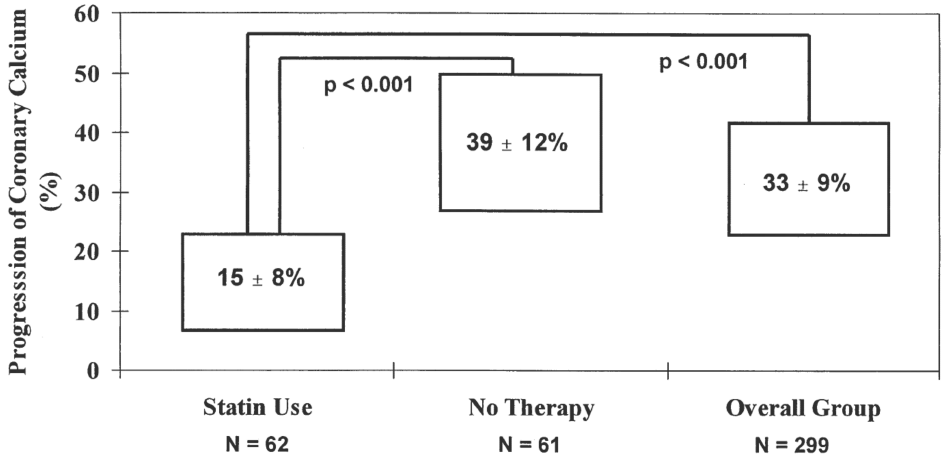

Figure 4. Effect of statin therapy on the progression of coronary calcifications in 299 asymptomatic subjects with high cholesterol levels. The progression of coronary calcifications in the study population was 33.2±9.2% per year (right). The progression of coronary calcifications among patients receiving statins (left) was significantly lower, as compared to nontreated patients (middle). From Budoff et al.[66] with permission.

Achenbach et al.[67] studied 66 asymptomatic subjects with low-density lipoprotein cholesterol level higher than 130 mg/dl, no lipid-lowering treatment and a prior EBCT scan with evidence of coronary calcium (CACS

≥20). A second EBCT scan was performed after a mean interval of 14 months (untreated period) and a third EBCT scan was repeated after 12 months of therapy with cerivastatin (treatment period). During the untreated period, the median annual relative increase in CACS was significantly higher (25%) as compared to the median annual relative increase in CACS during the treatment period (8.8%, p <0.001).

Assessment of CACS progression during statin treatment may be also useful to improve the identification of patients at risk of future CAD events. Raggi and colleagues [68] studied 495 asymptomatic subjects (57±8 years) in whom an initial EBCT study had revealed evidence of coronary calcium (CACS ≥30). After the baseline EBCT study, statin therapy was started and, after a mean interval of 1.9±1 years, the EBCT examination was repeated. During a mean follow-up of 3.2±0.7 years, AMI was observed in 41 patients. Interestingly, CACS progression was significantly higher among patients experiencing AMI as compared to event-free subjects (42±23% per year vs. 17±25% per year; p <0.001). At multivariate analysis, besides CACS at follow-up, CACS progression >15% per year was the most powerful predictor of future AMI (p <0.001).

However, more recent randomized trials failed to confirm these preliminary results. In particular, the St. Francis Heart Study failed to demonstrate that atorvastatin 20 mg daily (together with vitamin C 1 g daily, and vitamin E 1000 U daily) was able to reduce the progression of coronary calcifications in 1005 asymptomatic subjects.[45] Similarly, the BELLES study showed that intensive statin therapy (i.e., atorvastatin 80 mg daily) compared to moderate statin therapy (i.e., pravastatin 40 mg daily) did not reduce the progression of coronary calcifications in 615 hyperlipidemic, postmenopausal women.[69] Consequently, on the basis of these contradictory data, serial CACS scanning to evaluate the efficacy of treatment with lipid-lowering drugs and the progression of coronary calcification cannot be currently advised.

LIMITATIONS OF CALCIUM SCORING

Despite the large amount of data supporting its value as noninvasive marker of coronary atherosclerosis and its clinical utility, some limitations of CACS assessment need to be acknowledged. CACS assessment does not provide information on the degree of coronary stenosis. Previous studies showed that the specificity for obstructive CAD is about 40%.[70] Accordingly, in symptomatic patients, in whom the clinical goal is to determine the cause of symptoms and thus assess the presence of lesions potentially requiring revascularization, the value of CACS assessment may be limited. Moreover, CACS assessment only visualizes calcified plaques, and consequently patients with exclusively noncalcified plaques are not identified. This issue appears to be relevant especially in the setting of diabetes mellitus and (acute) chest pain syndromes.[71–75] Scholte et al.[71] for instance, using MSCT coronary angiography, showed that in asymptomatic patients with type 2 diabetes a nonnegligible proportion of coronary plaques (41%) are noncalcified. Among patients with acute and long-term chest pain syndrome, Rubinshtein and colleagues showed that a low or zero CACS was not able to exclude the presence of obstructive CAD.[72] Use of MSCT coronary angiography revealed single-vessel CAD in all patients with zero CACS, while multivessel CAD was identified in 50% of patients with low CACS (defined as CACS <100).[72] More recently, Gottlieb et al.[75] observed that a nonnegligible proportion (19%) of patients with zero CACS clinically referred for conventional angiography had indeed $\geq$1 obstructive coronary lesion; of note, 12.5% of patients with zero CACS underwent coronary revascularization within 30 days. Similar results were reported by Henneman et al.[73] and Marwan et al.[74] In these studies, a high prevalence of obstructive CAD in the absence of coronary calcifications was observed among patients with acute coronary syndromes.

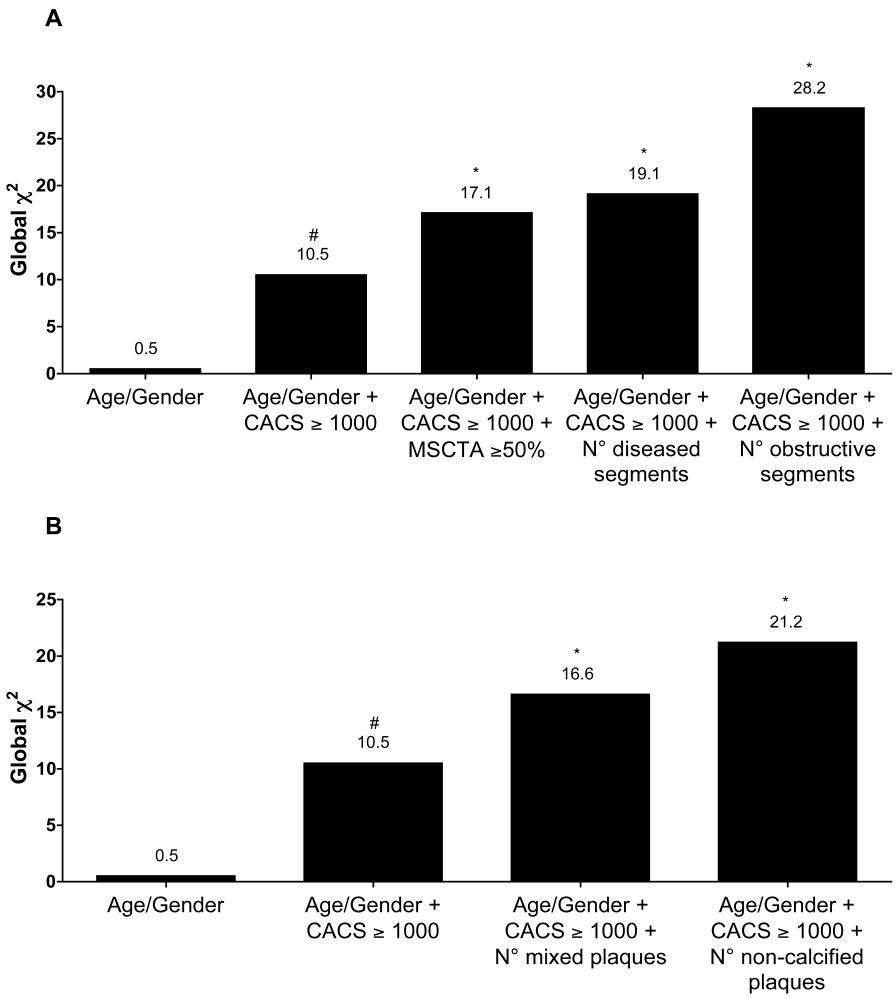

Figure 5. Panel A. Coronary artery calcium score (CACS) has a significant incremental prognostic value (depicted by $\chi 2$ value on the y-axis) over age and gender (#). Obstructive CAD (50% stenosis) on multislice computed tomography coronary angiography (MSCTA) and plaque burden (i.e., number of diseased segments or segments with obstructive CAD on MSCTA) have a further incremental prognostic value over age, gender, and CACS (*). **Panel B.** CACS has a significant incremental prognostic value (depicted by $\chi 2$ value on the y-axis) over age and gender (#). MSCTA plaque composition has a further incremental prognostic value over age, gender, and CACS (*). Adapted from van Werkhoven et al.[76] with permission.

On the basis of these data, noninvasive assessment of coronary atherosclerosis by means of MSCT coronary angiography may further improve identification of high-risk patients. Recently, van Werkhoven et al.[76] demonstrated indeed that evidence of obstructive CAD as well as the number of diseased segments, obstructive segments, and noncalcified plaques at MSCT coronary angiography have significant incremental prognostic value over CACS in symptomatic patients with suspected CAD (Figure 5).

CONCLUSIONS

A large amount of data supports the use of CACS assessment to improve risk stratification as compared to conventional risk assessment. CACS may be particularly valuable in asymptomatic individuals at intermediate risk. In these patients, the information provided by CACS assessment could significantly alter the clinical decision-making.

REFERENCES

1. Kannel WB, Schatzkin A. Sudden death: Lessons from subsets in population studies. J Am Coll Cardiol 1985;5:141B–149B.
2. Wilson PW, D' Agostino RB, Levy D, et al. Prediction of coronary heart disease using risk factor categories. Circulation 1998;97:1837–1847.
3. Conroy RM, Pyorala K, Fitzgerald AP, et al. Estimation of ten-year risk of fatal cardiovascular disease in Europe: The SCORE project. Eur Heart J 2003;24:987–1003.
4. Schlendorf KH, Nasir K, Blumenthal RS. Limitations of the Framingham risk score are now much clearer. Prev Med 2009;48:115–116.
5. Kannel WB, D' Agostino RB, Sullivan L, et al. Concept and usefulness of cardiovascular risk profiles. Am Heart J 2004;148:16–26.
6. Lakoski SG, Greenland P, Wong ND, et al. Coronary artery calcium scores and risk for cardiovascular events in women classified as "low risk" based on Framingham risk score: The multi-ethnic study of atherosclerosis (MESA). Arch Intern Med 2007;167:2437–2442.

7. Nucifora G, Schuijf JD, van Werkhoven JM, et al. Prevalence of coronary artery disease across the Framingham risk categories: Coronary artery calcium scoring and MSCT coronary angiography. J Nucl Cardiol 2009;16:368–375.
8. Desai MY, Nasir K, Braunstein JB, et al. Underlying risk factors incrementally add to the standard risk estimate in detecting subclinical atherosclerosis in low- and intermediate-risk middle-aged asymptomatic individuals. Am Heart J 2004;148:871–877.
9. Kullo IJ, Ballantyne CM. Conditional risk factors for atherosclerosis. Mayo Clin Proc 2005;80:219–230.
10. Rumberger JA, Simons DB, Fitzpatrick LA, et al. Coronary artery calcium area by electron-beam computed tomography and coronary atherosclerotic plaque area. A histopathologic correlative study. Circulation 1995;92:2157–2162.
11. Budoff MJ. Computed tomography. In: Budoff M, Shinbane J, editors. Cardiac CT Imaging. London : Springer-Verlag, 2006;1–18.
12. Agatston AS, Janowitz WR, Hildner FJ, et al. Quantification of coronary artery calcium using ultrafast computed tomography. J Am Coll Cardiol 1990;15:827–832.
13. Rumberger JA, Brundage BH, Rader DJ, et al. Electron beam computed tomographic coronary calcium scanning: A review and guidelines for use in asymptomatic persons. Mayo Clin Proc 1999;74:243–252.
14. Wong ND, Budoff MJ, Pio J, et al. Coronary calcium and cardiovascular event risk: Evaluation by age- and sex-specific quartiles. Am Heart J 2002;143:456–459.
15. Wong ND, Hsu JC, Detrano RC, et al. Coronary artery calcium evaluation by electron beam computed tomography and its relation to new cardiovascular events. Am J Cardiol 2000;86:495–498.
16. Raggi P, Callister TQ, Cooil B, et al. Identification of patients at increased risk of first unheralded acute myocardial infarction by electron-beam computed tomography. Circulation 2000;101:850–855.
17. Kondos GT, Hoff JA, Sevrukov A, et al. Electron-beam tomography coronary artery calcium and cardiac events: A 37-month follow-up of 5635 initially asymptomatic low- to intermediate-risk adults. Circulation 2003;107:2571–2576.
18. Stanford W, Thompson BH, Burns TL, et al. Coronary artery calcium quantification at multi-detector row helical CT versus electron-beam CT. Radiology 2004;230:397–402.

19. Daniell AL, Wong ND, Friedman JD, et al. Concordance of coronary artery calcium estimates between MDCT and electron beam tomography. AJR Am J Roentgenol 2005;185:1542–1545.
20. Mao SS, Pal RS, McKay CR, et al. Comparison of coronary artery calcium scores between electron beam computed tomography and 64-multidetector computed tomographic scanner. J Comput Assist Tomogr 2009;33:175–178.
21. Budoff MJ. Atherosclerosis imaging and calcified plaque: Coronary artery disease risk assessment. Prog Cardiovasc Dis 2003;46:135–148.
22. Rifkin RD, Parisi AF, Folland E. Coronary calcification in the diagnosis of coronary artery disease. Am J Cardiol 1979;44:141–147.
23. Stanford W, Thompson BH. Imaging of coronary artery calcification. Its importance in assessing atherosclerotic disease. Radiol Clin North Am 1999;37:257–272.
24. Demer LL, Tintut Y. Vascular calcification: Pathobiology of a multifaceted disease. Circulation 2008;117:2938–2948.
25. Sangiorgi G, Rumberger JA, Severson A, et al. Arterial calcification and not lumen stenosis is highly correlated with atherosclerotic plaque burden in humans: A histologic study of 723 coronary artery segments using nondecalcifying methodology. J Am Coll Cardiol 1998;31:126–133.
26. Mintz GS, Pichard AD, Popma JJ, et al. Determinants and correlates of target lesion calcium in coronary artery disease: A clinical, angiographic and intravascular ultrasound study. J Am Coll Cardiol 1997;29:268–274.
27. Baumgart D, Schmermund A, Goerge G, et al. Comparison of electron beam computed tomography with intracoronary ultrasound and coronary angiography for detection of coronary atherosclerosis. J Am Coll Cardiol 1997;30:57–64.
28. Fallavollita JA, Brody AS, Bunnell IL, et al. Fast computed tomography detection of coronary calcification in the diagnosis of coronary artery disease. Comparison with angiography in patients <50 years old. Circulation 1994;89:285–290.
29. Rumberger JA, Sheedy PF, III, Breen JF, et al. Coronary calcium, as determined by electron beam computed tomography, and coronary disease on arteriogram. Effect of patient's sex on diagnosis. Circulation 1995;91:1363–1367.
30. Budoff MJ, Georgiou D, Brody A, et al. Ultrafast computed tomography as a diagnostic modality in the detection of coronary artery disease: A multicenter study. Circulation 1996;93:898–904.

31. Rumberger JA, Sheedy PF, Breen JF, et al. Electron beam computed tomographic coronary calcium score cutpoints and severity of associated angiographic lumen stenosis. J Am Coll Cardiol 1997;29:1542–1548.
32. Schmermund A, Baumgart D, Gorge G, et al. Measuring the effect of risk factors on coronary atherosclerosis: Coronary calcium score versus angiographic disease severity. J Am Coll Cardiol 1998;31:1267–1273.
33. Shaw LJ, Raggi P, Schisterman E, et al. Prognostic value of cardiac risk factors and coronary artery calcium screening for all-cause mortality. Radiology 2003;228:826–833.
34. Budoff MJ, Shaw LJ, Liu ST, et al. Long-term prognosis associated with coronary calcification: Observations from a registry of 25,253 patients. J Am Coll Cardiol 2007;49:1860–1870.
35. Greenland P, LaBree L, Azen SP, et al. Coronary artery calcium score combined with Framingham score for risk prediction in asymptomatic individuals. JAMA 2004;291:210–215.
36. Arad Y, Goodman KJ, Roth M, et al. Coronary calcification, coronary disease risk factors, C-reactive protein, and atherosclerotic cardiovascular disease events: The St. Francis Heart Study. J Am Coll Cardiol 2005;46:158–165.
37. Detrano R, Guerci AD, Carr JJ, et al. Coronary calcium as a predictor of coronary events in four racial or ethnic groups. N Engl J Med 2008;358:1336–1345.
38. Greenland P, Bonow RO, Brundage BH, et al. ACCF/AHA 2007 clinical expert consensus document on coronary artery calcium scoring by computed tomography in global cardiovascular risk assessment and in evaluation of patients with chest pain: A report of the American College of Cardiology Foundation Clinical Expert Consensus Task Force (ACCF/AHA Writing Committee to Update the 2000 Expert Consensus Document on Electron Beam Computed Tomography) developed in collaboration with the Society of Atherosclerosis Imaging and Prevention and the Society of Cardiovascular Computed Tomography. J Am Coll Cardiol 2007;49:378–402.
39. Blaha M, Budoff MJ, Shaw LJ, et al. Absence of coronary artery calcification and all-cause mortality. JACC Cardiovasc Imaging 2009;2:692–700.
40. U.S. Preventive Services Task Force. Using nontraditional risk factors in coronary heart disease risk assessment: U.S. Preventive Services Task Force recommendation statement. Ann Intern Med 2009;151:474–482.

41. Detrano R, Hsiai T, Wang S, et al. Prognostic value of coronary calcification and angiographic stenoses in patients undergoing coronary angiography. J Am Coll Cardiol 1996;27:285–290.
42. Keelan PC, Bielak LF, Ashai K, et al. Long-term prognostic value of coronary calcification detected by electron-beam computed tomography in patients undergoing coronary angiography. Circulation 2001;104:412–417.
43. Georgiou D, Budoff MJ, Kaufer E, et al. Screening patients with chest pain in the emergency department using electron beam tomography: A follow-up study. J Am Coll Cardiol 2001;38:105–110.
44. Grundy SM, Cleeman JI, Merz CN, et al. Implications of recent clinical trials for the National Cholesterol Education Program Adult Treatment Panel III guidelines. Circulation 2004;110:227–239.
45. Arad Y, Spadaro LA, Roth M, et al. Treatment of asymptomatic adults with elevated coronary calcium scores with atorvastatin, vitamin C, and vitamin E: The St. Francis Heart Study randomized clinical trial. J Am Coll Cardiol 2005;46:166–172.
46. McCullough PA, Chinnaiyan KM. Annual progression of coronary calcification in trials of preventive therapies: A systematic review. Arch Intern Med 2009;169:2064–2070.
47. He ZX, Hedrick TD, Pratt CM, et al. Severity of coronary artery calcification by electron beam computed tomography predicts silent myocardial ischemia. Circulation 2000;101:244–251.
48. Moser KW, O' Keefe JH, Jr., Bateman TM, et al. Coronary calcium screening in asymptomatic patients as a guide to risk factor modification and stress myocardial perfusion imaging. J Nucl Cardiol 2003;10:590–598.
49. Anand DV, Lim E, Raval U, et al. Prevalence of silent myocardial ischemia in asymptomatic individuals with subclinical atherosclerosis detected by electron beam tomography. J Nucl Cardiol 2004;11:450–457.
50. Berman DS, Wong ND, Gransar H, et al. Relationship between stress-induced myocardial ischemia and atherosclerosis measured by coronary calcium tomography. J Am Coll Cardiol 2004;44:923–930.
51. Wong ND, Rozanski A, Gransar H, et al. Metabolic syndrome and diabetes are associated with an increased likelihood of inducible myocardial ischemia among patients with subclinical atherosclerosis. Diabetes Care 2005;28:1445–1450.
52. Ramakrishna G, Breen JF, Mulvagh SL, et al. Relationship between coronary artery calcification detected by electron-beam computed tomography and

abnormal stress echocardiography: Association and prognostic implications. J Am Coll Cardiol 2006;48:2125–2131.
53. Anand DV, Lim E, Hopkins D, et al. Risk stratification in uncomplicated type 2 diabetes: Prospective evaluation of the combined use of coronary artery calcium imaging and selective myocardial perfusion scintigraphy. Eur Heart J 2006;27:713–721.
54. Blumenthal RS, Becker DM, Yanek LR, et al. Comparison of coronary calcium and stress myocardial perfusion imaging in apparently healthy siblings of individuals with premature coronary artery disease. Am J Cardiol 2006;97:328–333.
55. Schenker MP, Dorbala S, Hong EC, et al. Interrelation of coronary calcification, myocardial ischemia, and outcomes in patients with intermediate likelihood of coronary artery disease: A combined positron emission tomography/computed tomography study. Circulation 2008;117:1693–1700.
56. Rosman J, Shapiro M, Pandey A, et al. Lack of correlation between coronary artery calcium and myocardial perfusion imaging. J Nucl Cardiol 2006;13:333–337.
57. Schuijf JD, Wijns W, Jukema JW, et al. A comparative regional analysis of coronary atherosclerosis and calcium score on multislice CT versus myocardial perfusion on SPECT. J Nucl Med 2006;47:1749–1755.
58. Rozanski A, Gransar H, Wong ND, et al. Use of coronary calcium scanning for predicting inducible myocardial ischemia: Influence of patients' clinical presentation. J Nucl Cardiol 2007;14:669–679.
59. Schepis T, Gaemperli O, Koepfli P, et al. Added value of coronary artery calcium score as an adjunct to gated SPECT for the evaluation of coronary artery disease in an intermediate-risk population. J Nucl Med 2007;48:1424–1430.
60. Scholte AJ, Schuijf JD, Kharagjitsingh AV, et al. Different manifestations of coronary artery disease by stress SPECT myocardial perfusion imaging, coronary calcium scoring, and multislice CT coronary angiography in asymptomatic patients with type 2 diabetes mellitus. J Nucl Cardiol 2008;15:503–509.
61. Nucifora G, Schuijf JD, van Werkhoven JM, et al. Relation between framingham risk categories and the presence of functionally relevant coronary lesions as determined on multislice computed tomography and stress testing. Am J Cardiol 2009;104:758–763.

62. Chang SM, Nabi F, Xu J, et al. The coronary artery calcium score and stress myocardial perfusion imaging provide independent and complementary prediction of cardiac risk. J Am Coll Cardiol 2009; 54:1872–1882.
63. Hendel RC, Berman DS, Di Carli MF, et al. ACCF/ASNC/ACR/AHA/ASE/SCCT/ SCMR/SNM 2009 appropriate use criteria for cardiac radionuclide imaging: A report of the American College of Cardiology Foundation Appropriate Use Criteria Task Force, the American Society of Nuclear Cardiology, the American College of Radiology, the American Heart Association, the American Society of Echocardiography, the Society of Cardiovascular Computed Tomography, the Society for Cardiovascular Magnetic Resonance, and the Society of Nuclear Medicine: Endorsed by the American College of Emergency Physicians. Circulation 2009;119:e561–e587.
64. Ramakrishna G, Miller TD, Breen JF, et al. Relationship and prognostic value of coronary artery calcification by electron beam computed tomography to stress-induced ischemia by single photon emission computed tomography. Am Heart J 2007;153:807–814.
65. Callister TQ, Raggi P, Cooil B, et al. Effect of HMG-CoA reductase inhibitors on coronary artery disease as assessed by electron-beam computed tomography. N Engl J Med 1998;339:1972–1978.
66. Budoff MJ, Lane KL, Bakhsheshi H, et al. Rates of progression of coronary calcium by electron beam tomography. Am J Cardiol 2000;86:8–11.
67. Achenbach S, Ropers D, Pohle K, et al. Influence of lipid-lowering therapy on the progression of coronary artery calcification: A prospective evaluation. Circulation 2002;106:1077–1082.
68. Raggi P, Callister TQ, Shaw LJ. Progression of coronary artery calcium and risk of first myocardial infarction in patients receiving cholesterol-lowering therapy. Arterioscler Thromb Vasc Biol 2004;24:1272–1277.
69. Raggi P, Davidson M, Callister TQ, et al. Aggressive versus moderate lipid-lowering therapy in hypercholesterolemic postmenopausal women: Beyond Endorsed Lipid Lowering with EBT Scanning (BELLES). Circulation 2005;112:563–571.
70. Haberl R, Becker A, Leber A, et al. Correlation of coronary calcification and angiographically documented stenoses in patients with suspected coronary artery disease: Results of 1,764 patients. J Am Coll Cardiol 2001;37:451–457.
71. Scholte AJ, Schuijf JD, Kharagjitsingh AV, et al. Prevalence of coronary artery disease and plaque morphology assessed by multi-slice computed tomography

coronary angiography and calcium scoring in asymptomatic patients with type 2 diabetes. Heart 2008;94:290–295.
72. Rubinshtein R, Gaspar T, Halon DA, et al. Prevalence and extent of obstructive coronary artery disease in patients with zero or low calcium score undergoing 64-slice cardiac multidetector computed tomography for evaluation of a chest pain syndrome. Am J Cardiol 2007;99:472–475.
73. Henneman MM, Schuijf JD, Pundziute G, et al. Noninvasive evaluation with multislice computed tomography in suspected acute coronary syndrome: Plaque morphology on multislice computed tomography versus coronary calcium score. J Am Coll Cardiol 2008;52:216–222.
74. Marwan M, Ropers D, Pflederer T, et al. Clinical characteristics of patients with obstructive coronary lesions in the absence of coronary calcification: An evaluation by coronary CT angiography. Heart 2009;95:1056–1060.
75. Gottlieb I, Miller JM, Arbab-Zadeh A, et al. The absence of coronary calcification does not exclude obstructive coronary artery disease or the need for revascularization in patients referred for conventional coronary angiography. J Am Coll Cardiol 2010;55:627–634.
76. van Werkhoven JM, Schuijf JD, Gaemperli O, et al. Incremental prognostic value of multi-slice computed tomography coronary angiography over coronary artery calcium scoring in patients with suspected coronary artery disease. Eur Heart J 2009;30:2622–2629.

Chapter 3

Prevalence of Coronary Artery Disease Across the Framingham Risk Categories: Coronary Artery Calcium Scoring and MSCT Coronary Angiography

Gaetano Nucifora, Joanne D. Schuijf, Jacob M. van Werkhoven, J. Wouter Jukema, Roxana Djaberi, Arthur J. H. A. Scholte, Albert de Roos, Martin J. Schalij, Ernst E. van der Wall, Jeroen J. Bax

J Nucl Cardiol 2009;16:368–75

ABSTRACT

Background. Non-invasive assessment of subclinical atherosclerosis by means of coronary artery calcium scoring (CACS) and multi-slice computed tomography (MSCT) coronary angiography could improve patients' risk stratification. However, data relating observations on CACS and MSCT coronary angiography to traditional risk assessment are scarce.

Methods and Results. In 314 consecutive outpatients (54±13 years, 56% males) without known CAD, CACS and 64-slice MSCT coronary angiography were performed. According to the Framingham risk score (FRS), 51% of patients were at low, 24% at intermediate and 25% at high risk, respectively. MSCT angiograms showing atherosclerosis were classified as showing obstructive (≥50% luminal narrowing) CAD or not. Both CACS and MSCT coronary angiography showed a high prevalence of normal coronary arteries in low FRS patients (70% and 61%, respectively). An increase in the prevalence of CACS >400 (4% low vs 19% intermediate vs 36% high), CAD (39% low vs 79% intermediate vs 91% high), and obstructive CAD (15% low vs 43% intermediate vs 58% high) was observed across the FRS categories ($p < 0.0001$ for all comparisons).

Conclusions. A strong positive relationship exists between FRS and the prevalence and extent of atherosclerosis. Especially in intermediate FRS patients, CACS and MSCT coronary angiography provide useful information on the presence of subclinical atherosclerosis.

INTRODUCTION

Identification of patients at risk of developing coronary artery disease (CAD) events is one of the most challenging issues in clinical cardiology. For this purpose, several scoring tools that take demographic and clinical characteristics into account have been developed. These tools allow stratification of patients into low-, intermediate-, and high-risk categories, in order to determine the intensity of risk-modifying interventions.[1-3] Among them, the Framingham risk score (FRS) is one of the most frequently used;[1,4] it considers traditional risk factors (age, gender, diabetes mellitus, systolic blood pressure, total cholesterol and HDL cholesterol level, and smoking history) to predict the 10-year risk of hard CAD events. However, traditional risk assessment may still fail to identify a considerable proportion of patients with future CAD events, since it provides a statistical probability of having CAD rather than a direct individual assessment.[5] Indeed, it has been observed that as much as 20% of CAD events can occur in the absence of major cardiovascular risk factors.[6]

To improve risk stratification, direct visualization of subclinical atherosclerosis has been advocated. Indeed, previous studies have shown that non-invasive assessment of the coronary artery calcium score (CACS), by means of electron-beam computed tomography (EBCT) or multi-slice computed tomography (MSCT) provides prognostic information that is incremental to traditional risk stratification.[7] Recently, more detailed visualization of the coronary arteries has become possible with the introduction of MSCT coronary angiography.[8-10] Possibly, MSCT coronary angiography could also improve patients' risk stratification similar to CACS. However, data relating observations on CACS and MSCT coronary angiography to traditional risk assessment are scarce. Aim of the present study therefore was to evaluate the prevalence of CAD across the FRS categories using CACS and MSCT coronary angiography. In

addition, differences in CACS and MSCT coronary angiography findings between asymptomatic and symptomatic patients were explored.

METHODS

Study Population

The study population consisted of 314 consecutive outpatients clinically referred to MSCT for coronary evaluation, due to an increased risk profile and/or stable chest pain complaints. Patients with typical angina, known history of CAD and/or contraindications to MSCT were not included in the study, as well as patients who were not in sinus rhythm during the MSCT examination. History of CAD was defined as the presence of previous acute coronary syndrome, percutaneous or surgical coronary revascularization, and/or one or more angiographically documented coronary artery stenosis ≥50% luminal diameter.[11] Contraindications for MSCT were: *(1)* known allergy to iodinated contrast agent, *(2)* renal failure (defined as glomerular filtration rate <30 ml/min), and *(3)* pregnancy.

For each patient, the presence of coronary risk factors (diabetes mellitus, systemic hypertension, hypercholesterolemia, positive family history, cigarette smoking, and obesity) and the presence of chest pain complaints (atypical angina and non-cardiac chest pain), both defined in accordance to previously published guidelines,[4,12-15] were recorded. The Framingham 10-year risk of hard CAD events was also calculated as previously described in the National Cholesterol Education Program's Adult Treatment Panel III report.[4] In accordance with the FRS, the study population was then categorized as at low (<10%), intermediate (10-20%), and high risk (>20%).[4] In addition, patients were further divided as being asymptomatic or symptomatic.

MSCT Data Acquisition

MSCT coronary angiography was performed with a 64-slice MSCT scanner (Aquilion 64, Toshiba Medical Systems, Japan). The heart rate and blood pressure were monitored before the examination in each patient. In the absence of contraindications, patients with a heart rate ≥65 beats/minute were administered oral ß-blockers (metoprolol, 50 or 100 mg, single dose, 1 hour before the examination).

First, a prospective coronary calcium scan without contrast was performed, followed by 64-slice MSCT coronary angiography, performed according to protocols previously described.[16] Data were subsequently transferred to dedicated workstations for post-processing and evaluation (Advantage, GE Healthcare, USA and Vitrea 2, Vital Images, USA).

MSCT Data Analysis

The MSCT data analysis was performed by two experienced observers who had no knowledge of the patient' s medical history and symptom status; disagreement was solved by consensus or evaluation by a third observer.

Coronary artery calcium score

Coronary artery calcium was identified as a dense area in the coronary artery >130 Hounsfield units. A total CACS was recorded for each patient. In accordance with the value of total CACS, patients were subsequently categorized as having no calcium (total score = 0) or low (total score = 1-100), moderate (total score = 101-400), and severe (total score > 400) CACS.[17]

MSCT coronary angiography

MSCT coronary angiograms were evaluated for the presence of obstructive CAD (≥50% luminal narrowing) on a patient and vessel level. For this purpose, both the original axial dataset as well as curved multi-planar reconstructions were used. Each vessel was evaluated for the

presence of any atherosclerotic plaque, defined as structures >1 mm^2 within and/or adjacent to the coronary artery lumen, which could be clearly distinguished from the vessel lumen and the surrounding pericardial tissue, as described previously.[9] Subsequently, the vessels were further classified as *1.* completely normal, *2.* having non-obstructive CAD when atherosclerotic lesions <50% of luminal diameter were present, or *3.* having obstructive CAD when atherosclerotic lesions ≥50% of luminal diameter were present.

The prevalence of CAD (including obstructive and non-obstructive CAD), obstructive CAD, the presence of obstructive CAD in one vessel (single-vessel disease) or two or three vessels (multi-vessel disease), and location in the left main (LM) and/or proximal left anterior descending (LAD) coronary artery were evaluated. Multi-vessel disease and LM and/or proximal LAD disease were considered to represent high-risk features.

Statistical Analysis

Continuous variables are expressed as mean (standard deviation) or as median (25th to 75th percentile range), when not normally distributed. Categorical variables are expressed as absolute numbers (percentages). The differences in continuous variables were assessed using the Student t test when normally distributed and the Mann-Whitney test when not normally distributed. Chi-square test for greater than two-by-two and Fisher exact for two-by-two contingency tables were computed to test for differences in categorical variables. A P value <0.05 was considered statistically significant. Statistical analyses were performed using SPSS software (version 14.0, SPSS Inc, Chicago, IL, USA).

RESULTS

Patient Characteristics

Baseline characteristics of the study population are shown in Table 1. The mean age was 54±13 years, and 177 (56%) patients were male. A total

of 152 (48%) patients were asymptomatic, while 82 (26%) patients had history of atypical angina and 80 (26%) patients had a history of non-cardiac chest pain. The FRS was low, intermediate, and high, respectively, in 159 (51%), 77 (24%), and 78 (25%) patients.

MSCT Calcium Scoring and Coronary Angiography

Table 2 and Figures 1 and 2 depict the results of calcium scoring and MSCT coronary angiography in the overall population and among asymptomatic and symptomatic patients.

Table 1. Baseline characteristics of the study population

Variable	n = 314
Age (years)	54±13
Gender (male/female)	177/137
Diabetes mellitus	69 (22%)
Hypertension	148 (47%)
- Systolic blood pressure (mmHg)	134±19
- Diastolic blood pressure (mmHg)	81±11
Hypercholesterolemia	105 (33%)
- Total cholesterol (mmol/l)	5.2±1.2
- HDL-cholesterol (mmol/l)	1.5±0.4
Family history of coronary artery disease	123 (39%)
Smoking history	88 (28%)
Overweight	125 (40%)
Obesity	58 (18%)
Body mass index (kg/m²)	27±5
≥ 3 risk factors	84 (27%)
Chest pain complaints	
- Asymptomatic	152 (48%)
- Atypical angina	82 (26%)
- Non-cardiac chest pain	80 (26%)
Framingham risk score	
- Low	159 (51%)
- Intermediate	77 (24%)
- High	78 (25%)

Data are expressed as means±SD and n (%).

Table 2. Results of coronary artery calcium scoring and MSCT coronary angiography in the study population

	Overall population (n = 314)	Asymptomatic patients (n = 152)	Symptomatic patients (n = 162)
Coronary artery calcium			
Coronary artery calcium score	1 (0-159)	0 (0-156)	2 (0-214)
- Zero	157 (50%)	78 (51%)	79 (49%)
- Low	63 (20%)	31 (21%)	32 (20%)
- Moderate	44 (14%)	20 (13%)	24 (15%)
- Severe	50 (16%)	23 (15%)	27 (16%)
MSCT coronary angiography			
- Normal coronary arteries	120 (38%)	59 (39%)	61 (38%)
- Non-obstructive CAD	92 (29%)	46 (30%)	46 (28%)
- Obstructive CAD	102 (33%)	47 (31%)	55 (34%)

Data are expressed as median (25th to 75th percentile range), and n (%). P = ns for all comparisons between asymptomatic vs. symptomatic subjects. CAD: coronary artery disease.

Coronary artery calcium score

As shown in Table 2, the median CACS was 1 (25th to 75th percentile range 0-159). No calcium was observed in 157 (50%), while CACS was low in 63 (20%) patients, moderate in 44 (14%), and severe in 50 (16%) patients.

The median CACS did not differ between asymptomatic and symptomatic patients and the prevalence of no calcium and minimal, mild, moderate, and severe coronary calcifications was not statistically different between the two groups (Table 2).

Relationship between CACS and FRS. As shown in Figure 1A, calcium was absent in 112 (70%) patients with low FRS, 26 (34%) patients with intermediate FRS, and in 19 (24%) patients with high FRS. Overall, a decrease in the prevalence of CACS zero and an increase in the prevalence of severe CACS were observed in line with increasing FRS (Figure 1A). However, among all three FRS categories still a significant proportion of patients presented with low and moderate CACS.

As shown in Figure 1B and C, this positive relationship between FRS and CACS was similarly present among both asymptomatic and symptomatic patients.

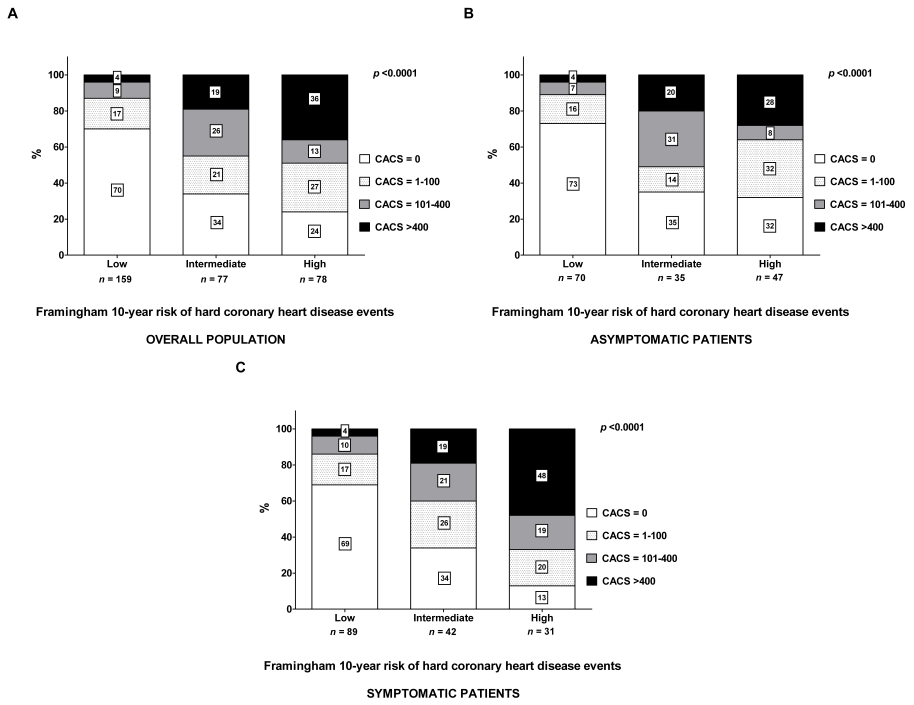

Figure 1. Relationship between CACS and Framingham 10-year risk of hard coronary heart disease events in the overall population (**panel A**), among asymptomatic patients (**panel B**), and among symptomatic patients (**panel C**). The proportion of patients with no calcium, low CACS, intermediate CACS, and severe CACS differed significantly across the three FRS categories. CACS: Coronary artery calcium score; FRS: Framingham risk score.

MSCT coronary angiography

As shown in Table 2, 120 (38%) patients were classified as having no CAD based on MSCT. A total of 92 (29%) patients showed non-obstructive CAD, whereas at least one significant (≥50% luminal narrowing) stenosis was observed in the remaining 102 (33%) patients.

Obstructive single-vessel disease was present in 54 (17%) patients, whereas multi-vessel disease was noted in 48 (15%) patients. Obstructive CAD in the LM and/or proximal LAD was present in 37 (12%) patients, of which 24 also showed multi-vessel disease. Accordingly, 61 (19%) patients were identified as having high-risk features.

No difference in the prevalence of no CAD, and non-obstructive and obstructive CAD was observed between asymptomatic and symptomatic patients (Table 2).

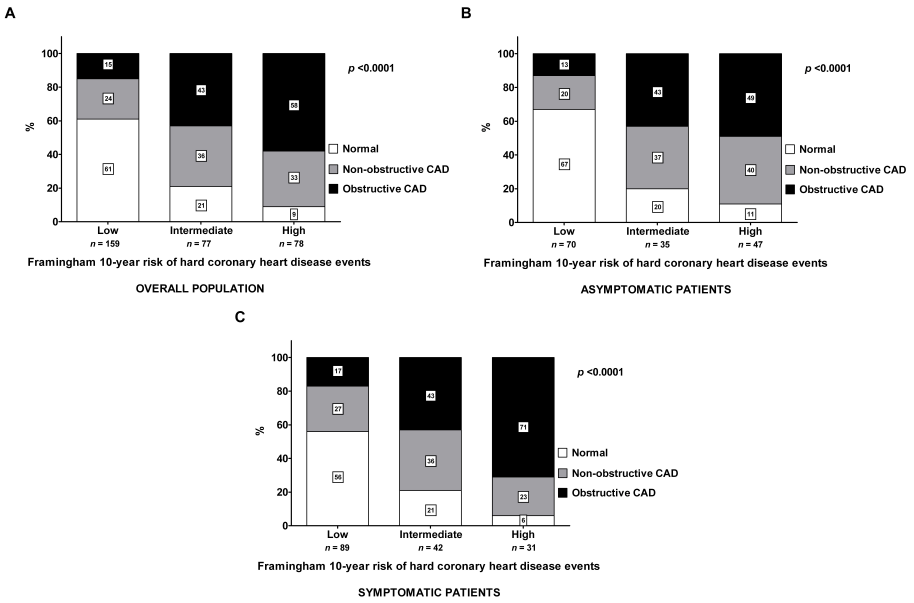

Figure 2. Relationship between MSCT coronary angiography and Framingham 10-year risk of hard coronary heart disease events in the overall population (**panel A**), among asymptomatic patients (**panel B**), and among symptomatic patients (**panel C**). The proportion of patients with normal coronary arteries, non-obstructive CAD, and obstructive CAD differed significantly across the three FRS categories. CAD: Coronary artery disease; FRS: Framingham risk score.

Relationship between MSCT coronary angiography results and FRS. As shown in Figure 2A, normal coronary arteries were observed in 97 (61%) patients with low FRS, 16 (21%) patients with intermediate FRS, and 7

(9%) patient with high FRS. Overall, a decrease in the prevalence of normal coronary arteries and an increase in the prevalence of obstructive CAD were observed in line with increasing FRS (Figure 2A). Moreover, an increase in the prevalence of high-risk features was observed across the FRS categories (13 (8%) patients in the low FRS versus 21 (27%) in the intermediate FRS versus 27 (35%) in the high FRS; p <0.0001). Nevertheless, a significant proportion of patients with non-obstructive CAD was present in each category.
As shown in Figure 2B and C, this positive relationship between FRS and CAD was similarly present among both asymptomatic and symptomatic patients.

DISCUSSION

The present study describes the prevalence and extent of CAD, assessed by means of both CACS and MSCT coronary angiography, across the FRS categories in a large cohort of patients. Both CACS and MSCT coronary angiography showed a high prevalence of normal coronary arteries in low FRS patients (70% and 61%, respectively), which decreased in patients with intermediate and high FRS. Similarly, an increase in the prevalence of high CACS and obstructive or even high-risk CAD were observed with increasing FRS. However, moderate calcium on CACS as well as non-obstructive CAD on MSCT coronary angiography were identified across all FRS categories.
In line with the current observations, an overall increase in the prevalence and extent of atherosclerosis in relation to FRS has been reported in several previous studies.[18-21] At the same time, these studies have also highlighted a discrepancy between the presence of traditional risk factors and the presence of subclinical atherosclerosis: substantial atherosclerosis was frequently observed in patients at low to intermediate risk, while being absent in patients deemed at high risk. Also in the current study, atherosclerosis was identified across all FRS

categories. These observations have led to the notion that (selective) atherosclerosis imaging may provide valuable information in addition to traditional risk assessment. Indeed, several large clinical trials have demonstrated that CACS has incremental value over risk factors.[7,22,23] In a large cohort of 1461 asymptomatic individuals, Greenland et al.[7] demonstrated that knowledge of a high CACS resulted in superior risk stratification as compared to FRS alone. Other investigations have reported similar observations.[22,23] Accordingly, addition of an atherosclerosis marker such as CACS can significantly modify initially predicted risk and can alter clinical decision-making and subsequent therapy/patients management. Knowledge of subclinical atherosclerosis may be of particular value in patients at intermediate risk. In these patients, who represent a substantial part of the population, clinical management is frequently uncertain. In the present study, evaluation by means of MSCT showed that coronary calcium was absent in 34% of patients. In contrast, a CACS exceeding 100 was observed in 45% of patients. Similarly, MSCT coronary angiography showed normal coronary arteries in 21%, whereas obstructive disease was noted in 43% of patients. Moreover, high-risk features were identified in 27%. Accordingly, these observations indicate that underlying atherosclerosis can be identified (but also ruled out) in a substantial proportion of patients at intermediate FRS. Possibly, refinement of risk using atherosclerosis imaging may allow more appropriate targeting of preventive measures in these patients. Indeed, the current American College of Cardiology appropriateness criteria for cardiac computed tomography suggest that assessment of calcium may be a "reasonable approach" among intermediate FRS patients, although substantial uncertainty remains regarding its general applicability.[24]

In low risk patients, the use of imaging remains controversial. In general, the prevalence of abnormal coronary arteries will be low. Indeed, in the present study, the prevalence of normal coronary arteries was high both on CACS and MSCT coronary angiography. Also, prognostic studies

addressing CACS in relation to FRS observed that CACS had no additive value in patients with a FRS <10%.[7] Still, recent data suggest that perhaps in certain subsets of individuals deemed at low risk by FRS, such as women younger than 70 years old, CACS may identify higher risk in a considerable proportion.[25,26] Nevertheless, more data are needed before evaluation of atherosclerosis can be recommended in patients with low FRS.

In patients with high FRS on the other hand, the incremental value of atherosclerosis imaging remains debatable as well. In line with previous investigations, we observed a high prevalence of coronary calcium (76%). Moreover, the prevalence of abnormal coronary arteries on MSCT coronary angiography was even higher, 91%. Finally, a high prevalence of high-risk features was noted on MSCT coronary angiography as well (35%). Indeed, in this group of patients, the presence of high risk has already been established and these patients should receive targeted anti-atherosclerotic measures regardless of imaging results. In this context, assessment with MSCT coronary angiography may be favored over CACS as the former may provide a superior estimate of total plaque burden. Moreover, another advantage of MSCT coronary angiography could be the fact that it allows identification of high-risk features such as left main or multi-vessel disease. Possibly, these patients may benefit from even more aggressive measures, including revascularization, although supporting data in asymptomatic patients are scarce.

It is important to realize that thus far, the majority of data relating coronary atherosclerosis to FRS have been obtained using CACS with EBCT and data relating MSCT coronary angiography to clinical characteristics are scarce. Moreover, MSCT coronary angiography has mainly been applied in high-risk symptomatic patients in order to determine its value in the diagnosis of CAD rather than in risk assessment. As a result, only few data are available concerning its prognostic value.[27,28] Preliminary studies however suggest that MSCT coronary angiography may provide prognostic information incremental to baseline

risk stratification,[29] although no systematic comparisons to FRS are currently available. In addition, no studies are available that evaluate the relative merits of CACS and MSCT coronary angiography with regard to risk stratification. Importantly, efficacy in improving patient outcome remains to be confirmed for both techniques.

The present study has some limitations that should be acknowledged. First, it is a single center experience with a relatively low sample size as compared to previous studies relating CACS to FRS. However, it is also one of the first relating both CACS and MSCT coronary angiography to FRS in patients without symptoms typical for CAD. Unfortunately, no follow-up data were available. Future studies should address whether MSCT coronary angiography may allow re-stratification of risk similar or even superior to CACS. Second, the FRS was developed in, and should be applied to, asymptomatic individuals only; however, due to the radiation exposure associated with MSCT coronary angiography, and the lack of evidence in this setting, use in truly asymptomatic patients cannot be recommended at present. This limitation could be overcome by more extensive implementation of dose-saving algorithms, which are likely to result in substantial dose reduction to <3 mSv, without degradation of image quality.[30,31]

CONCLUSION

A strong positive relationship exists between FRS and the prevalence and extent atherosclerosis on CACS and MSCT coronary angiography. Both techniques showed a high prevalence of normal coronary arteries in low FRS patients versus a low prevalence in high FRS patients. In intermediate FRS patients, however, CACS and MSCT coronary angiography may provide useful information on the presence of subclinical atherosclerosis.

REFERENCES

1. Wilson PW, D' Agostino RB, Levy D, et al. Prediction of coronary heart disease using risk factor categories. Circulation 1998;97:1837-47.
2. Assmann G, Cullen P, Schulte H. Simple scoring scheme for calculating the risk of acute coronary events based on the 10-year follow-up of the prospective cardiovascular Munster (PROCAM) study. Circulation 2002;105:310-5.
3. Conroy RM, Pyorala K, Fitzgerald AP, et al. Estimation of ten-year risk of fatal cardiovascular disease in Europe: The SCORE project. Eur Heart J 2003;24:987-1003.
4.Expert Panel on Detection, Evaluation, and Treatment of High Blood Cholesterol in Adults. Executive summary of the third report of the national cholesterol education program (NCEP) expert panel on detection, evaluation, and treatment of high blood cholesterol in adults (Adult Treatment Panel III). JAMA 2001;285:2486-97.
5. Naghavi M, Libby P, Falk E, et al. From vulnerable plaque to vulnerable patient: A call for new definitions and risk assessment strategies: Part II. Circulation 2003;108:1772-8.
6. Khot UN, Khot MB, Bajzer CT, et al. Prevalence of conventional risk factors in patients with coronary heart disease. JAMA 2003;290:898-904.
7. Greenland P, LaBree L, Azen SP, et al. Coronary artery calcium score combined with Framingham score for risk prediction in asymptomatic individuals. JAMA 2004;291:210-5.
8. Leber AW, Knez A, von Ziegler F, et al. Quantification of obstructive and nonobstructive coronary lesions by 64-slice computed tomography: A comparative study with quantitative coronary angiography and intravascular ultrasound. J Am Coll Cardiol 2005;46:147-54.
9. Leber AW, Knez A, Becker A, et al. Accuracy of multidetector spiral computed tomography in identifying and differentiating the composition of coronary atherosclerotic plaques: A comparative study with intracoronary ultrasound. J Am Coll Cardiol 2004;43:1241-7.
10. Lau GT, Ridley LJ, Schieb MC, et al. Coronary artery stenoses: Detection with calcium scoring, CT angiography, and both methods combined. Radiology 2005;235:415-22.

11. Schuijf JD, Wijns W, Jukema JW, et al. Relationship between noninvasive coronary angiography with multi-slice computed tomography and myocardial perfusion imaging. J Am Coll Cardiol 2006;48:2508-14.
12. American Diabetes Association. Diagnosis and classification of diabetes mellitus. Diabetes Care 2007;30:S42-7.
13. Chobanian AV, Bakris GL, Black HR, et al. Seventh report of the joint national committee on prevention, detection, evaluation, and treatment of high blood pressure. Hypertension 2003;42:1206-52.
14. World Health Organization. Physical status: The use and interpretation of anthropometry. Report of a WHO Expert Committee. World Health Organ Tech Rep Ser 1995;854:1-452.
15. Gibbons RJ, Abrams J, Chatterjee K, et al. ACC/AHA 2002 guideline update for the management of patients with chronic stable angina—summary article: A report of the American College of Cardiology/American Heart Association Task Force on Practice Guidelines (Committee on the Management of Patients With Chronic Stable Angina). Circulation 2003;107:149-58.
16. Schuijf JD, Pundziute G, Jukema JW, et al. Diagnostic accuracy of 64-slice multislice computed tomography in the noninvasive evaluation of significant coronary artery disease. Am J Cardiol 2006;98:145-8.
17. Agatston AS, Janowitz WR, Hildner FJ, et al. Quantification of coronary artery calcium using ultrafast computed tomography. J Am Coll Cardiol 1990;15:827-32.
18. Simon A, Giral P, Levenson J. Extracoronary atherosclerotic plaque at multiple sites and total coronary calcification deposit in asymptomatic men. Association with coronary risk profile. Circulation 1995;92:1414-21.
19. Mahoney LT, Burns TL, Stanford W, et al. Usefulness of the Framingham risk score and body mass index to predict early coronary artery calcium in young adults (Muscatine Study). Am J Cardiol 2001;88:509-15.
20. Taylor AJ, Feuerstein I, Wong H, et al. Do conventional risk factors predict subclinical coronary artery disease? Results from the prospective army coronary calcium project. Am Heart J 2001;141:463-8.
21. Nair D, Carrigan TP, Curtin RJ, et al. Association of coronary atherosclerosis detected by multislice computed tomography and traditional risk-factor assessment. Am J Cardiol 2008;102:316-20.

22. Arad Y, Goodman KJ, Roth M, et al. Coronary calcification, coronary disease risk factors, C-reactive protein, and atherosclerotic cardiovascular disease events: The St. Francis Heart Study. J Am Coll Cardiol 2005;46:158-65.
23. Taylor AJ, Bindeman J, Feuerstein I, et al. Coronary calcium independently predicts incident premature coronary heart disease over measured cardiovascular risk factors: Mean three-year outcomes in the prospective army coronary calcium (PACC) project. J Am Coll Cardiol 2005;46:807-14.
24. Hendel RC, Patel MR, Kramer CM, et al. ACCF/ACR/SCCT/SCMR/ASNC/NASCI/SCAI/SIR 2006 appropriateness criteria for cardiac computed tomography and cardiac magnetic resonance imaging: A report of the American College of Cardiology Foundation Quality Strategic Directions Committee Appropriateness Criteria Working Group, American College of Radiology, Society of Cardiovascular Computed Tomography, Society for Cardiovascular Magnetic Resonance, American Society of Nuclear Cardiology, North American Society for Cardiac Imaging, Society for Cardiovascular Angiography and Interventions, and Society of Interventional Radiology. J Am Coll Cardiol 2006;48:1475-97.
25. Michos ED, Nasir K, Braunstein JB, et al. Framingham risk equation underestimates subclinical atherosclerosis risk in asymptomatic women. Atherosclerosis 2006;184:201-6.
26. Lakoski SG, Greenland P, Wong ND, et al. Coronary artery calcium scores and risk for cardiovascular events in women classified as "low risk" based on Framingham risk score: The multi-ethnic study of atherosclerosis (MESA). Arch Intern Med 2007;167:2437-42.
27. Pundziute G, Schuijf JD, Jukema JW, et al. Prognostic value of multislice computed tomography coronary angiography in patients with known or suspected coronary artery disease. J Am Coll Cardiol 2007;49:62-70.
28. Min JK, Shaw LJ, Devereux RB, et al. Prognostic value of multidetector coronary computed tomographic angiography for prediction of all-cause mortality. J Am Coll Cardiol 2007;50:1161-70.
29. Choi EK, Choi SI, Rivera JJ, et al. Coronary computed tomography angiography as a screening tool for the detection of occult coronary artery disease in asymptomatic individuals. J Am Coll Cardiol 2008;52:357-65.
30. Hausleiter J, Meyer T, Hadamitzky M, et al. Radiation dose estimates from cardiac multislice computed tomography in daily practice: Impact of different scanning protocols on effective dose estimates. Circulation 2006;113:1305-10.

31. Stolzmann P, Leschka S, Scheffel H, et al. Dual-source CT in step-and-shoot mode: Noninvasive coronary angiography with low radiation dose. Radiology 2008;249:71-80.

Chapter 4

Relation Between Framingham Risk Categories and the Presence of Functionally Relevant Coronary Lesions as Determined on Multislice Computed Tomography and Stress Testing

Gaetano Nucifora, Joanne D. Schuijf, Jacob M. van Werkhoven, Roxana Djaberi, Ernst E. van der Wall, Albert de Roos, Arthur J.H.A. Scholte, Martin J. Schalij, J. Wouter Jukema, Jeroen J. Bax

Am J Cardiol 2009;104:758–763

ABSTRACT

Noninvasive assessment of subclinical atherosclerosis by multislice computed tomographic (MSCT) coronary angiography and demonstration of significant, flow-limiting coronary artery disease (CAD) by stress testing may improve patients' risk stratification. However, data relating the complementary information provided by these noninvasive techniques to traditional risk assessment are scarce. In 255 subjects (45% women, mean age 54±12 years) without known CAD, 64-slice MSCT coronary angiography and stress testing (exercise electrocardiographic test or myocardial perfusion imaging) were performed. Framingham risk score (FRS) was calculated from baseline characteristics (50% low, 22% intermediate, 28% high). Angiograms showing atherosclerosis were classified as obstructive (≥50% luminal narrowing) CAD or not. Stress tests were classified as normal or abnormal. Multislice computed tomogram identified 155 patients (61%) with CAD, of whom 78 (31%) showed obstructive CAD. A positive stress test result was observed in 36 patients (46%) with obstructive CAD. In line with increasing FRS categories, a significant increase in the prevalence of functionally relevant obstructive CAD was observed (6% low vs 45% intermediate vs 63% high, $p < 0.001$). In conclusion, a strong positive relation exists between FRS and prevalence of functionally relevant obstructive CAD. Selective use of MSCT coronary angiography and stress testing may refine the traditional risk assessment of CAD events, especially in patients deemed at intermediate and high risk.

INTRODUCTION

Recently, coronary artery calcium score (CACS) and multislice computed tomographic (MSCT) coronary angiography have emerged as useful techniques for the noninvasive direct visualization of coronary atherosclerosis.[1] Their use in selected patients has been suggested to be of potential utility to improve the traditional risk assessment of coronary artery disease (CAD) events.[2-5] However, these imaging techniques, despite providing meaningful information about the presence and extent of coronary atherosclerosis, do not provide information about the functional relevance of the observed coronary lesions.[6-8] This issue appears significant, considering that a large proportion of patients with abnormal CACS or MSCT coronary angiogram has a normal stress test result and thus do not require further invasive imaging.[6,7] Indeed, a better understanding of the complementary information provided by these noninvasive methods (imaging of coronary atherosclerosis vs evidence of inducible ischemia), especially in relation to traditional risk assessment, is needed to define an optimal strategy for patients' risk assessment. The aim of the present study therefore was to evaluate the relation between evidence of coronary atherosclerosis (by CACS and MSCT coronary angiography) and presence of abnormal stress testing result across Framingham risk score (FRS) categories.

METHODS

Two hundred fifty-five consecutive outpatients clinically referred to multislice computed tomography for coronary evaluation were included in the study. In addition, patients underwent stress testing (electrocardiographic exercise test [EET] or myocardial perfusion imaging) within 1 month of MSCT coronary angiography. The patient population is part of an ongoing study protocol addressing the value of

multislice computed tomography and other imaging techniques compared to traditional risk assessment. From this prospective registry, results addressing the relation between CACS and MSCT coronary angiographic data across FRS categories have been recently published.[5]

Patients with typical angina, known history of CAD, and/or contraindications to multislice computed tomography were not included in the study, as were patients who were not in sinus rhythm before MSCT examination. History of CAD was defined as the presence of previous acute coronary syndrome, percutaneous or surgical coronary revascularization, and/or ≥1 angiographically documented coronary artery stenosis ≥50% luminal diameter.[7] Contraindications for multislice computed tomography were *(1)* known allergy to iodinated contrast agent, *(2)* renal failure (defined as glomerular filtration rate <30 ml/min), and *(3)* pregnancy.

For each patient, the presence of coronary risk factors (diabetes mellitus, systemic hypertension, hypercholesterolemia, positive family history, cigarette smoking, and obesity) and the presence of chest pain complaints (atypical angina and noncardiac chest pain), defined in accordance to previously published guidelines,[9-13] were recorded. The Framingham 10-year risk of hard CAD events was also calculated as previously described in the National Cholesterol Education Program's Adult Treatment Panel III report.[11] In accordance to the FRS, the study population was then categorized as at low (<10%), intermediate (10% to 20%), and high (>20%) risk.[11]

MSCT coronary angiography was performed with a 64-slice MSCT scanner (Aquilion 64, Toshiba Medical Systems, Tokyo, Japan). Heart rate and blood pressure were monitored before the examination in each patient. In the absence of contraindications, patients with a heart rate ≥65 beats/min were administered oral β blockers (metoprolol 50 or 100 mg, single dose, 1 hour before the examination).

First, a prospective coronary calcium scan without contrast was performed, followed by 64-slice MSCT coronary angiography, performed

according to protocols previously described.[14] Data were subsequently transferred to dedicated workstations for postprocessing and evaluation (Advantage, GE Healthcare, Milwaukee, Wisconsin; Vitrea 2, Vital Images, Minnetonka, Minnesota).

MSCT data analysis was performed by 2 experienced observers who had no knowledge of a patient's medical history and symptom status; disagreement was solved by consensus or evaluation by a third observer.

CAC was identified as a dense area in the coronary artery >130 HU. A total CACS was recorded for each patient. In accordance to the value of total CACSs, patients were subsequently categorized as having no calcium (total score 0) or a low (total score 1 to 100), moderate (total score 101 to 400), or severe (total score >400) CACS.[15]

MSCT coronary angiograms were evaluated for the presence of obstructive CAD (≥50% luminal narrowing) on a patient and vessel level. For this purpose, the original axial dataset and curved multiplanar reconstructions were used. Each vessel was evaluated for the presence of any atherosclerotic plaque, defined as structures >1 mm2 within and/or adjacent to the coronary artery lumen, which could be clearly distinguished from the vessel lumen and the surrounding pericardial tissue, as described previously.[16] Subsequently, the vessels were further classified as *(1)* completely normal, *(2)* having nonobstructive CAD when atherosclerotic lesions <50% of luminal diameter were present, or *(3)* having obstructive CAD when atherosclerotic lesions ≥50% of luminal diameter were present. Prevalences of CAD (including obstructive and nonobstructive CAD) and obstructive CAD were evaluated.

Symptom-limited EET was performed on a bicycle ergometer according to standard protocols.[17] Patients not able to reach ≥85% of age-predicted maximum heart rate in the absence of ischemic changes were not included in the study. Tests were classified as positive or negative for ischemia. The test was considered positive based on the presence of ≥0.1-mV horizontal or downsloping ST-segment depression at 80 ms

after the J point in 2 contiguous leads during exercise or recovery. All tests were analyzed by an experienced reader without knowledge of the MSCT results.

Myocardial perfusion imaging during stress and at rest was performed with symptom-limited bicycle exercise or pharmacologic (adenosine or dobutamine) stress using technetium-99m tetrofosmin or technetium-99m sestamibi. Images were acquired on a triple-head (GCA 9300/HG, Toshiba Corp., Tokyo, Japan) single-photon emission computed tomographic camera and reconstructed into long- and short-axis projections perpendicular to the heart axis. Perfusion defects were identified on stress images (segmental tracer activity <75% of maximum) and divided into ischemia (reversible defects, with ≥10% increase in tracer uptake on images at rest) or scar tissue (irreversible defects). Accordingly, examinations were classified as negative or positive. Positive examinations were further divided into those demonstrating reversible defects and those demonstrating fixed defects. Gated images were used to assess regional wall motion to improve differentiation between perfusion abnormalities and attenuation artifacts.[18]

Continuous variables are expressed as mean±SD or median (25th to 75th percentile range), when not normally distributed. Categorical variables are expressed as absolute numbers (percentages). Differences in categorical variables were assessed using chi-square test. A p value <0.05 was considered statistically significant. Statistical analyses were performed using SPSS 15.0 (SPSS, Inc., Chicago, Illinois).

RESULTS

Baseline characteristics of the study population are listed in Table 1. Table 2 presents the results of calcium scoring and MSCT coronary angiography, and Table 3 presents the stress testing results.

Table 1. Baseline characteristics of the study population

Variable	n = 255
Age (years)	54±12
Male/female	140/115
Diabetes mellitus	65 (25%)
Hypertension	131 (51%)
- Systolic blood pressure (mmHg)	135±19
- Diastolic blood pressure (mmHg)	81±12
Hypercholesterolemia	92 (36%)
- Total cholesterol (mg/dl)	205±46
- HDL-cholesterol (mg/dl)	58±19
Family history of coronary artery disease	103 (40%)
Smoke	80 (31%)
Obesity	53 (21%)
- Body mass index (kg/m^2)	27±5
≥ 3 risk factors	78 (31%)
Chest pain complaints	
- Asymptomatic	111 (44%)
- Atypical angina pectoris	75 (29%)
- Non-cardiac chest pain	69 (27%)
Framingham risk score	
- Low	127 (50%)
- Intermediate	56 (22%)
- High	72 (28%)

Data are expressed as means±SD and n (%).

Based on calcium scoring, coronary calcifications were found in 37 patients (29%) with a low FRS, 34 patients (61%) with an intermediate FRS, and 53 patients (74%) with a high FRS. Based on MSCT coronary angiogram, normal coronary arteries were found in 79 patients (62%) with a low FRS, 14 patients (25%) with an intermediate FRS, and 7 patients (10%) with a high FRS. Obstructive CAD was found in 17 patients (13%) with a low FRS, 20 patients (36%) with an intermediate FRS, and 41 patients (57%) with a high FRS. Table 3 lists stress testing results. Positive stress test results were observed in 5 patients (4%) with

a low FRS, 16 patients (29%) with an intermediate FRS, and 36 patients (50%) with a high FRS.

Table 2. Results of coronary artery calcium scoring and multi-slice computed tomography coronary angiography in the study population (n = 255)

Coronary artery calcium score	
- Score	0 (0-128)
- Zero	131 (51%)
- Low (total score = 1-100)	50 (20%)
- Moderate (total score = 101-400)	35 (14%)
- Severe (total score >400)	39 (15%)
MSCT coronary angiography	
- Normal coronary arteries	100 (39%)
- Non-obstructive CAD (<50% luminal diameter narrowing)	77 (30%)
- Obstructive CAD (≥50% luminal diameter narrowing)	78 (31%)

Data are expressed as median (25th to 75th percentile range), and n (%).

Table 3. Results of stress testing in the study population (n = 255)

Type of stress test	
- Electrocardiographic exercise test	47 (18%)
- Myocardial perfusion imaging	208 (82%)
Electrocardiographic exercise test	
Mean peak double product	27702±8231
Mean peak workload (Watt)	196±57
Ischemic ST-segment depression	3 (6%)
Myocardial perfusion imaging	
- Symptom-limited bicycle exercise *	80 (38%)
- Pharmacologic stress (adenosine or dobutamine)	128 (62%)
- Stress and rest normal perfusion	154 (74%)
- Reversible perfusion defect	34 (16%)
- Fixed perfusion defect	12 (6%)
- Reversible and fixed perfusion defects	8 (4%)
Overall	
Negative test	198 (78%)
Positive test	57 (22%)

*: In all these patients, ≥85% of maximum age-predicted heart rate was achieved if no stress-induced symptoms or changes in electrocardiogram or blood pressure occurred. Data are expressed as means±SD, and n (%).

Prevalence of positive stress test results in patients with a CACS 0 was low (n = 14, 11%). Conversely, 43 patients (35%) with a CACS >0 had a positive stress test result; as shown in Figure 1, a significant increase in the prevalence of positive stress test results was observed in this group of patients in line with an increasing FRS. Prevalence of positive stress test results in patients with normal coronary arteries or nonobstructive CAD was low (n = 21, 12%). In patients with obstructive CAD, in contrast, a positive stress test result was observed in 36 (46%). As illustrated in Figure 2, a positive relation between prevalence of positive stress test results and FRS was observed in this group of patients and prevalence of positive stress test results increased from 6% in patients with a low FRS and obstructive CAD to 63% in patients with a high FRS and obstructive CAD.

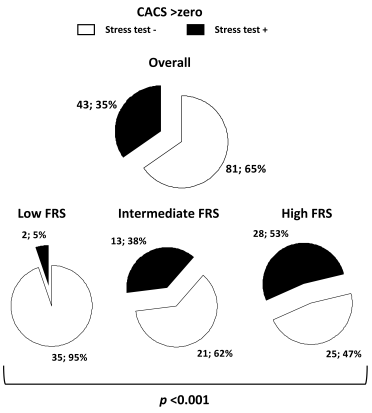

Figure 1. Relation between presence of CAC identified by MSCT calcium scan and stress test results in overall population and across FRS categories.

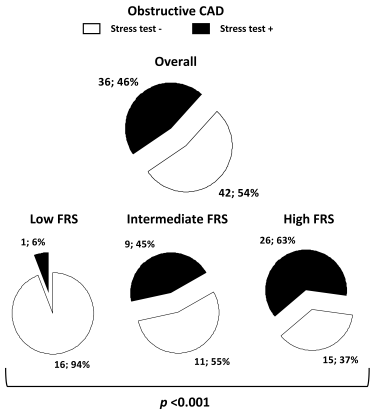

Figure 2. Relation between obstructive CAD identified by MSCT coronary angiography and stress test results in overall population and across FRS categories.

DISCUSSION

The present study describes the prevalence of positive stress testing compared to evidence of coronary atherosclerosis (by CACS and MSCT coronary angiography) across FRS categories. A significant increase in the prevalence of functionally relevant coronary lesions was observed in line with an increasing FRS. In particular, abnormal stress test results were observed in 53% of high-risk patients with abnormal CACSs and 63% of high-risk patients with obstructive CAD on MSCT coronary angiogram.

Previous studies have underlined the potential value of additional risk assessment with stress testing (EET or myocardial perfusion imaging) to improve the identification of patients at risk of CAD events. Gibbons et al,[19] for instance, observed a significant relation between the prognostic information provided by an abnormal EET result in a large cohort of asymptomatic men and the number of coronary risk factors. More recently, Balady et al.[20] showed that different EET variables (including ischemic ST-segment depression) provided incremental prognostic information over the FRS in asymptomatic men. The additional prognostic

value of EET has been confirmed by Cournot et al.[21] in men and women with intermediate and high FRSs.

Fewer data are available regarding the prognostic role of myocardial perfusion imaging in asymptomatic subjects.[22] However, it has been suggested that myocardial perfusion imaging may be of incremental value especially in high-risk patients (i.e., diabetic patients or patients with multiple risk factors), taking into account the high prevalence of myocardial perfusion abnormalities despite the absence of symptoms in this group.[23-25]

Direct visualization of subclinical atherosclerosis, by CACS or MSCT coronary angiography, also may possibly refine traditional risk assessment. Greenland et al,[26] in a large cohort of asymptomatic subjects, demonstrated that a high CACS improved the risk stratification provided by FRS alone. More recently, Budoff et al.[27] demonstrated, in a cohort of 25,253 asymptomatic patients, that CACS is an independent predictor of mortality, with significant incremental value over traditional coronary risk factors. A preliminary analysis by Choi et al.[4] suggested also that MSCT coronary angiography may provide prognostic information incremental to baseline risk stratification. The ability of noninvasive coronary imaging techniques to obtain a direct estimate of total atherosclerotic plaque burden in coronary arteries likely explains these findings. Previous studies indeed have demonstrated that a non-negligible proportion of patients with high plaque burden with CACSs or on MSCT coronary angiogram are not identified as at high risk based on FRS categories.[5,28,29]

Stress testing and noninvasive imaging of coronary arteries provide complementary information about CAD (i.e., evidence of myocardial ischemia and evidence of coronary atherosclerosis, respectively).[6-8] The 2 tests may be useful in refining the risk assessment strategy, but data showing how they relate each other in relation to FRS are still missing. Improved knowledge of the different information provided by stress

testing and noninvasive coronary imaging is needed to appropriately refine the risk assessment strategy.

In the present study, in patients with a low FRS, the prevalence of an abnormal CACS (29%) and of coronary atherosclerosis on MSCT coronary angiogram (38%) was not negligible. In contrast, prevalence of an abnormal stress testing result (4%) was relatively lower. In addition, an abnormal CACS and obstructive CAD on MSCT coronary angiogram rarely resulted in abnormal findings on stress testing (5% and 6%, respectively). Considering the low prevalence of ischemia, use of stress testing seems to carry limited additional value for risk stratification. Conversely, use of atherosclerosis imaging may possibly provide some benefit, considering the non-negligible prevalence of coronary plaques in this group of patients. However, larger studies with long-term follow-up are needed to demonstrate that identification of atherosclerosis may result in improved treatment and outcome before noninvasive coronary atherosclerosis imaging can be recommended in patients with a low FRS. Currently, use of atherosclerosis imaging may be not justified in this group of patients due to the associated radiation exposure (in particular for MSCT coronary angiography).

In patients with a high FRS, a high burden of coronary atherosclerosis and inducible myocardial ischemia were observed. However, in this group of patients, a high prevalence of coronary atherosclerosis is a priori anticipated and based on the high-risk profile; many patients will already have received medical therapy. Noninvasive coronary atherosclerosis imaging therefore is unlikely to further refine patients' risk assessment. Moreover, taking into account that a large proportion of patients with an abnormal CACS or obstructive CAD on MSCT coronary angiogram also showed an abnormal functional test result (53% and 63%, respectively), it seems reasonable to perform stress testing first, to establish or rule out the presence of flow-limiting stenoses. High-risk patients with evidence of inducible myocardial ischemia should then be referred to invasive coronary angiography and possibly may benefit from revascularization

procedures, although supporting data in asymptomatic subjects are scarce.[2]

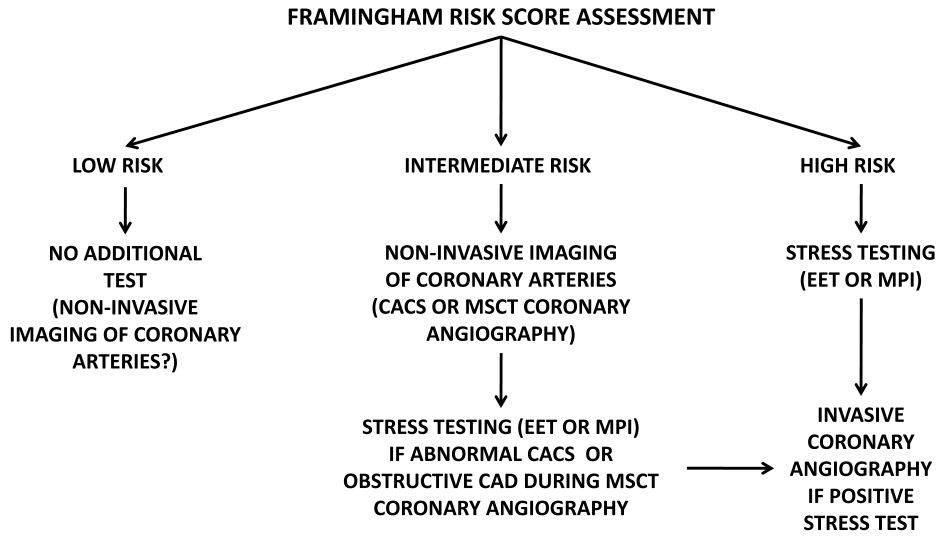

Figure 3. Proposed integration of noninvasive imaging of coronary arteries and stress testing into traditional risk assessment of CAD events. MPI = myocardial perfusion imaging.

In patients with an intermediate-risk profile, however, coronary atherosclerosis imaging may provide valuable information to refine risk stratification and determine further management. A non-negligible prevalence of coronary atherosclerosis (abnormal CACSs in 61% and abnormal MSCT coronary angiographic finding in 75%, including obstructive CAD in 36%) was observed in this population, whereas the prevalence of an abnormal stress test result (29%) was lower. In addition, comparison of coronary imaging data to stress testing data revealed that 38% of patients with an abnormal CACS and 45% of patients with obstructive CAD on MSCT coronary angiogram had an abnormal stress test result. Accordingly, noninvasive imaging of coronary arteries seems to be a reasonable first-line approach to improve risk stratification of

intermediate-risk patients. Patients with an abnormal CACS or obstructive CAD on MSCT coronary angiogram should then be referred to stress testing, to establish or rule out the presence of inducible myocardial ischemia.

A flow chart describing the proposed integration of noninvasive imaging of coronary arteries and stress testing into the traditional risk assessment of CAD events is presented in Figure 3.

REFERENCES

1. Cademartiri F, La Grutta L, Palumbo A, et al. Non-invasive visualization of coronary atherosclerosis: state-of-art. J Cardiovasc Med. 2007; 8: 129–137

2. Naghavi M, Falk E, Hecht HS, et al. The first SHAPE (Screening for Heart Attack Prevention and Education) guideline. Crit Pathw Cardiol. 2006; 5: 187–190

3. Hendel RC, Patel MR, Kramer CM, et al. ACCF/ACR/SCCT/SCMR/ASNC/NASCI/SCAI/SIR 2006 appropriateness criteria for cardiac computed tomography and cardiac magnetic resonance imaging: a report of the American College of Cardiology Foundation Quality Strategic Directions Committee Appropriateness Criteria Working Group, American College of Radiology, Society of Cardiovascular Computed Tomography, Society for Cardiovascular Magnetic Resonance, American Society of Nuclear Cardiology, North American Society for Cardiac Imaging, Society for Cardiovascular Angiography and Interventions, and Society of Interventional Radiology. J Am Coll Cardiol. 2006; 48: 1475–1497

4. Choi EK, Choi SI, Rivera JJ, et al. Coronary computed tomography angiography as a screening tool for the detection of occult coronary artery disease in asymptomatic individuals. J Am Coll Cardiol. 2008; 52: 357–365

5. Nucifora G, Schuijf JD, van Werkhoven JM, et al. Prevalence of coronary artery disease across the Framingham risk categories: coronary artery calcium scoring and MSCT coronary angiography. J Nucl Cardiol. 2009; 16: 368–375

6. Berman DS, Wong ND, Gransar H, et al. Relationship between stress-induced myocardial ischemia and atherosclerosis measured by coronary calcium tomography. J Am Coll Cardiol. 2004; 44: 923–930

7. Schuijf JD, Wijns W, Jukema, JW, et al. Relationship between noninvasive coronary angiography with multi-slice computed tomography and myocardial perfusion imaging. J Am Coll Cardiol. 2006; 48: 2508–2514

8. Petretta M, Costanzo P, Acampa W, et al. Noninvasive assessment of coronary anatomy and myocardial perfusion: going toward an integrated imaging approach. J Cardiovasc Med. 2008; 9: 977–986
9. American Diabetes Association. Diagnosis and classification of diabetes mellitus. Diabetes Care. 2007; 30: S42–S47
10. Chobanian AV, Bakris GL, Black HR, et al. Seventh report of the Joint National Committee on prevention, detection, evaluation, and treatment of high blood pressure. Hypertension. 2003; 42: 1206–1252
11. Executive summary of the Third Report of the National Cholesterol Education Program (NCEP) expert panel on detection, evaluation, and treatment of high blood cholesterol in adults (Adult Treatment Panel III). JAMA. 2001; 285: 2486–2497
12. Physical status: the use and interpretation of anthropometry (Report of a WHO expert committee). World Health Organ Tech Rep Ser. 1995; 854: 1–452
13. Gibbons RJ, Abrams J, Chatterjee K, et al. ACC/AHA 2002 guideline update for the management of patients with chronic stable angina—summary article: a report of the American College of Cardiology/American Heart Association task force on practice guidelines (committee on the management of patients with chronic stable angina). Circulation. 2002; 2003: 149–158
14. Schuijf JD, Pundziute G, Jukema JW, et al. Diagnostic accuracy of 64-slice multislice computed tomography in the noninvasive evaluation of significant coronary artery disease. Am J Cardiol. 2006; 98: 145–148
15. Agatston AS, Janowitz WR, Hildner FJ, et al. Quantification of coronary artery calcium using ultrafast computed tomography. J Am Coll Cardiol. 1990; 15: 827–832
16. Leber AW, Knez A, Becker A, et al. Accuracy of multidetector spiral computed tomography in identifying and differentiating the composition of coronary atherosclerotic plaques: a comparative study with intracoronary ultrasound. J Am Coll Cardiol. 2004; 43: 1241–1247
17. Fletcher GF, Balady G, Froelicher VF, et al. Exercise standards (A statement for healthcare professionals from the American Heart Association. Writing Group). Circulation. 1995; 91: 580–615
18. Smanio PE, Watson DD, Segalla DL, et al. Value of gating of technetium-99m sestamibi single-photon emission computed tomographic imaging. J Am Coll Cardiol. 1997; 30: 1687–1692

19. Gibbons LW, Mitchell TL, Wei M, et al. Maximal exercise test as a predictor of risk for mortality from coronary heart disease in asymptomatic men. Am J Cardiol. 2000; 86: 53–58
20. Balady GJ, Larson MG, Vasan RS, et al. Usefulness of exercise testing in the prediction of coronary disease risk among asymptomatic persons as a function of the Framingham risk score. Circulation. 2004; 110: 1920–1925
21. Cournot M, Taraszkiewicz D, Galinier M, et al. Is exercise testing useful to improve the prediction of coronary events in asymptomatic subjects?. Eur J Cardiovasc Prev Rehabil. 2006; 13: 37–44
22. Blumenthal RS, Becker DM, Moy TF, et al. Exercise thallium tomography predicts future clinically manifest coronary heart disease in a high-risk asymptomatic population. Circulation. 1996; 93: 915–923
23. Klocke FJ, Baird MG, Lorell BH, et al. ACC/AHA/ASNC guidelines for the clinical use of cardiac radionuclide imaging—executive summary: a report of the American College of Cardiology/American Heart Association task force on practice guidelines (ACC/AHA/ASNC committee to revise the 1995 guidelines for the clinical use of cardiac radionuclide imaging). Circulation. 2003; 108: 1404–1418
24. Lee SJ, Lee KH, Park SM, et al. Myocardial perfusion defects and coronary risk factors in symptomatic and asymptomatic elderly women. Int J Cardiovasc Imaging. 2008; 24: 277–281
25. Scholte AJ, Schuijf JD, Kharagjitsingh AV, et al. Prevalence and predictors of an abnormal stress myocardial perfusion study in asymptomatic patients with type 2 diabetes mellitus. Eur J Nucl Med Mol Imaging. 2009; 36: 567–575
26. Greenland P, LaBree L, Azen SP, et al. Coronary artery calcium score combined with Framingham score for risk prediction in asymptomatic individuals. JAMA. 2004; 291: 210–215
27. Budoff MJ, Shaw L.J, Liu ST, et al. Long-term prognosis associated with coronary calcification: observations from a registry of 25,253 patients. J Am Coll Cardiol. 2007; 49: 1860–1870
28. Nasir K, Michos ED, Blumenthal RS, et al. Detection of high-risk young adults and women by coronary calcium and National Cholesterol Education Program Panel III guidelines. J Am Coll Cardiol. 2005; 46: 1931–1936
29. Johnson KM, Dowe DA, Brink JA. Traditional clinical risk assessment tools do not accurately predict coronary atherosclerotic plaque burden: a CT angiography study. Am J Roentgenol. 2009; 192: 235–243

Chapter 5

Prevalence of Coronary Artery Disease Assessed by Multislice Computed Tomography Coronary Angiography in Patients With Paroxysmal or Persistent Atrial Fibrillation

Gaetano Nucifora, Joanne D. Schuijf, Laurens F. Tops, Jacob M. van Werkhoven, Sami Kajander, J. Wouter Jukema, Joop H.M. Schreur, Mark W. Heijenbrok, Serge A. Trines, Oliver Gaemperli, Olli Turta, Philipp A. Kaufmann, Juhani Knuuti, Martin J. Schalij, Jeroen J. Bax

Circ Cardiovasc Imaging 2009;2:100-106

ABSTRACT

Background. Although atrial fibrillation (AF) has been linked to underlying coronary artery disease (CAD), data supporting this association have been based on ECG and clinical history for the definition of CAD rather than direct visualization of atherosclerosis.

Methods and Results. The prevalence of CAD among patients with paroxysmal or persistent AF and without history of CAD was evaluated using multislice computed tomography. Multislice computed tomography was performed in 150 patients with AF (61±11 years, 67% males, 58% asymptomatic) with predominantly low (59%) or intermediate (25%) pretest likelihood of CAD. CAD was classified as obstructive (≥50% luminal narrowing) or not. A population of 148 patients without history of AF, similar to the AF group as to age, gender, symptomatic status, and pretest likelihood, served as a control group. Logistic regression analysis was applied to evaluate the relationship between demographic and clinical data and the presence of obstructive CAD. On the basis of multislice computed tomography, 18% of patients with AF were classified as having no CAD, whereas 41% showed nonobstructive CAD and the remaining 41% had obstructive CAD. Among patients without AF, 32% were classified as having no CAD, whereas 41% showed nonobstructive CAD and 27% had obstructive CAD ($p = 0.010$ compared with patients with AF). At logistic regression analysis, age, male gender, and the presence of AF were significantly related to obstructive CAD.

Conclusion. A higher prevalence of obstructive CAD was observed among patients with AF, confirming the hypothesis that AF could be a marker of advanced coronary atherosclerosis.

INTRODUCTION

Atrial fibrillation (AF) is the most common sustained cardiac arrhythmia, with an estimated prevalence of 0.4% to 1% in the general population.[1] In addition, the mortality rate of patients with AF is almost double than that of patients in normal sinus rhythm. This observation has been attributed to an increased cardiac death rate due to underlying heart disease [2–5] rather than to thromboembolism.[6]

Coronary artery disease (CAD) is considered to be highly prevalent among patients with AF and may be one of its underlying causes.[7] Furthermore, it has been suggested that AF may be the sole manifestation of CAD.[8] However, most data supporting this association have been derived from studies using the presence of ECG abnormalities and a history of ischemic heart disease to define CAD [4,9,10] rather than direct visualization of atherosclerosis. Thus far, only 2 cardiac imaging studies are available. In these investigations, stress myocardial perfusion single-photon emission computed tomography (SPECT) was applied to evaluate the prevalence of CAD in patients with AF.[11,12] Abidov et al.[11] showed a significantly higher prevalence of abnormal myocardial perfusion SPECT studies in patients with AF as compared with patients without AF. However, in this study patients with symptoms and known CAD were included while investigation of a strictly asymptomatic population, as performed by Askew et al,[12] failed to confirm this observation.

Recently, multislice computed tomography (MSCT) has been introduced as an alternative cardiac imaging modality.[13,14] This technique allows noninvasive direct visualization of the coronary arteries, including detection of coronary atherosclerosis by assessing the coronary artery calcium burden (calcium scoring) and by performing noninvasive angiography. Accordingly, this technique allows evaluation of CAD at an early stage.

The aim of the present study was to evaluate the prevalence of CAD, by means of MSCT, among patients with paroxysmal or persistent AF and compare findings to patients without a history of AF.

METHODS

Study Population

The study population consisted of 150 patients from the outpatient clinic with a history of paroxysmal (n = 99, 66%) or persistent (n = 51, 34%) AF referred to MSCT for coronary evaluation, due to an elevated risk profile and/or chest pain. Patients with history of CAD and contraindications to MSCT were excluded, as well as patients who were not in sinus rhythm during MSCT examination. Paroxysmal and persistent AF were diagnosed according to the American Heart Association/American College of Cardiology/European Society of Cardiology criteria.[1] Briefly, paroxysmal AF was defined as self-terminating episodes of AF lasting ≤7 days whereas persistent AF was defined as episodes lasting >7 days, requiring pharmacological or electric cardioversion, respectively. Accordingly, no patient with permanent (defined as long-lasting) AF was included in the study; all the patients were in sinus rhythm during the MSCT examination.[1] A history of CAD was defined as the presence of previous acute coronary syndrome, percutaneous or surgical coronary revascularization, and/or one or more angiographically documented coronary stenosis ≥50% luminal diameter.[15] Contraindications for MSCT were *(1)* known allergy to iodinated contrast agent, *(2)* renal failure, and *(3)* pregnancy.

For each patient, the presence of coronary risk factors (diabetes mellitus, systemic hypertension, hypercholesterolemia, positive family history, and cigarette smoking) and symptoms was recorded. In addition, the prevalence of ≥3 coronary risk factors and the pretest likelihood of obstructive CAD was evaluated using the Diamond and Forrester' s criteria.[16,17]

Using the same exclusion criteria, a population of 148 patients from the outpatient clinic without a history of AF, similar to the AF group as to age, gender, chest pain complaints, and pretest likelihood of obstructive CAD, who underwent MSCT for coronary evaluation due to an elevated risk profile and/or chest pain, was identified from the clinical database to serve as a control group for comparison purposes.

Patients were included at 4 centers in 3 different countries (Leiden University Medical Center, Leiden, the Netherlands; Medisch Centrum Haaglanden, Leidschendam, The Netherlands; Turku PET Center, Turku, Finland; University Hospital Zurich, Zurich, Switzerland).

MSCT Data Acquisition

MSCT coronary angiography was performed with 2 different 16-slice MSCT scanners (Aquilion 16, Toshiba Medical Systems, n = 39; and Discovery STE, GE Healthcare, n = 8) and 3 different 64-slice MSCT scanners (Aquilion 64, Toshiba Medical Systems, n = 202; LightSpeed VCT, GE Healthcare, n = 19; and Discovery VCT, GE Healthcare, n = 30). The heart rate and blood pressure were monitored before the examination in each patient. In the absence of contraindications, patients with a heart rate $\geq$65 bpm were administered β-blocking medication (50 to 100 mg metoprolol, oral or 5 to 10 mg metoprolol, intravenous). First, a prospective coronary calcium scan without contrast was performed, followed by 16- or 64-slice MSCT coronary angiography performed according to protocols described previously.[13,18,19] Data were subsequently transferred to dedicated workstations for postprocessing and evaluation (Advantage, GE Healthcare; Vitrea 2, Vital Images; and Aquarius, TeraRecon).

MSCT Data Analysis

The MSCT data analysis was performed in each center by 2 experienced observers who had no knowledge of the patient's medical history and

symptom status; disagreement was solved by consensus or evaluation by a third observer. Standardized MSCT data evaluation methodology and scoring system described later were used in each center.

Coronary Artery Calcium Score

Coronary artery calcium was identified as a dense area in the coronary artery >130 Hounsfield units. A total coronary artery calcium score was recorded for each patient. In accordance to the value of total calcium score, the study population was then categorized as having no calcium (total score = 0) or minimal (total score = 1 to 10), mild (total score = 11 to 100), moderate (total score = 101 to 400), and severe (total score >400) coronary calcifications.[20]

Coronary Angiography

MSCT coronary angiograms obtained with 16- and 64-slice scanners were evaluated for the presence of obstructive CAD (≥50% luminal narrowing) on a patient, vessel, and segment level. For this purpose, both the original axial dataset and curved multiplanar reconstructions were used. Coronary segments were evaluated in accordance to the 17 segments American Heart Association classification.[21] First, each segment was classified as interpretable or not. Then, the interpretable segments were evaluated for the presence of any atherosclerotic plaque, defined as structures >1 mm2 within and/or adjacent to the coronary artery lumen, which could be clearly distinguished from the vessel lumen and the surrounding pericardial tissue, as described previously.[22] One coronary plaque was assigned per coronary segment. Subsequently, segments were further classified as *(1)* completely normal, *(2)* having nonobstructive CAD when atherosclerotic lesions <50% of luminal diameter were present, or *(3)* having obstructive CAD when atherosclerotic lesions ≥50% of luminal diameter were present.

The prevalence of CAD (including obstructive and nonobstructive CAD), obstructive CAD, the presence of obstructive CAD in 1 vessel (single-

vessel disease) or 2 or 3 vessels (multivessel disease) and location in the left main (LM) and/or proximal left anterior descending (LAD) coronary artery were evaluated. In addition, the number of diseased coronary segments (segments containing plaques) and the number of coronary segments with obstructive as well as nonobstructive plaques were determined for each patient.

Statistical Analysis

Continuous variables are expressed as mean and standard deviation. Categorical variables are expressed as absolute numbers and percentages.

The differences in continuous variables were assessed using the Student t test when normally distributed and the Mann–Whitney test when not normally distributed. All continuous variables were normally distributed, except coronary artery calcium score, the number of diseased coronary segments, of segments with obstructive CAD and nonobstructive CAD per patient. Chi-square test was computed to test for differences in categorical variables.

Multivariable logistic regression analyses (backward stepwise with retention level set at 0.1) were performed to evaluate the relationship between demographic and clinical data (age, gender, coronary risk factors, symptoms, pretest likelihood of CAD, and history of AF) and the presence of CAD and obstructive CAD at MSCT coronary angiography. Only significant univariate predictors were entered as covariates in the multivariable models. Odds ratios and 95% CI were calculated.

The diagnostic accuracy of MSCT coronary angiography for the detection of obstructive (≥50% luminal narrowing) coronary artery stenoses was assessed in the subgroup of patients who underwent invasive coronary angiography. The sensitivity and specificity, including 95% CI, were calculated using invasive coronary angiography as the reference standard.

A probability value <0.05 was considered statistically significant. Statistical analyses were performed using SPSS software (version 14.0, SPSS Inc).

Statement of Responsibility

The authors had full access to and take full responsibility for the integrity of the data. All authors have read and agree to the manuscript as written.

RESULTS

Patient Characteristics

Baseline characteristics of each group are shown in Table 1. In accordance to the study design, AF and non-AF groups did not differ as to mean age (61±11 versus 59±10 years), male gender (67% versus 65%), symptomatic status, and pretest likelihood of CAD. In particular, a history of typical or atypical angina pectoris was present in 42% of patients with AF and in 43% of patients without AF and the pretest likelihood of CAD according to Diamond and Forrester was low, intermediate, and high, respectively, in 59%, 25%, and 16% of patients with AF and in 58%, 28%, and 14% of patients without AF.

Patients with AF, as compared with patients without AF, were less frequently diabetic (13% versus 28%, p <0.001) and smoker (21% versus 31%, p = 0.027). Overall, the prevalence of ≥3 coronary risk factors was not statistically different between the 2 groups.

MSCT Calcium Scoring and Noninvasive Angiography

A total of 24 (16%) patients with AF and 23 (16%) patients without AF underwent examination with 16-slice MSCT, whereas the remaining study population underwent 64-slice MSCT. Table 2 and Figures 1-3 depict the results of calcium scoring and MSCT coronary angiography in the study population.

Coronary Artery Calcium Score

Coronary artery calcium score was effectively performed in 133 (89%) patients with AF and in all patients without AF. The median Agatston calcium score did not differ between patients with AF and patients without AF (27, interquartile range 0 to 308, versus 75, interquartile range 0 to 350; p = 0.19). The prevalence of no calcium and minimal, mild, moderate, and severe coronary calcifications was not statistically different between the 2 groups, although absence of any calcium was less frequently observed among patients with AF (Figure 1).

Table 1. Baseline characteristics of the study population

	AF patients (n = 150)	Non-AF patients (n = 148)	p value
Age (years)	61±11	59±10	0.16
Male gender	100 (67%)	96 (65%)	0.81
Diabetes mellitus	19 (13%)	41 (28%) *	0.001
Hypertension	92 (61%)	94 (63%)	0.72
Hypercholesterolemia	64 (43%)	57 (39%)	0.48
Family history of CAD	46 (31%)	59 (40%)	0.062
Current or previous smoking	31 (21%)	46 (31%) †	0.027
≥ 3 coronary risk factors	37 (25%)	48 (32%)	0.16
Body mass index (kg/m²)	26.2±5.7	26.8±4.4	0.31
Symptoms			0.98
- Asymptomatic	87 (58%)	85 (57%)	
- Atypical angina	38 (25%)	37 (25%)	
- Typical angina	25 (17%)	26 (18%)	
Pre-test likelihood of CAD			0.80
- Low	89 (59%)	86 (58%)	
- Intermediate	37 (25%)	41 (28%)	
- High	24 (16%)	21 (14%)	

Data are expressed as mean±SD and n (%).

Noninvasive Coronary Angiography

Noninvasive coronary angiography was successfully performed in all the patients of the study population. Mean heart rate during the scan was 64±6 bpm among patients with AF and 65±9 bpm among patients without AF (p = 0.24).

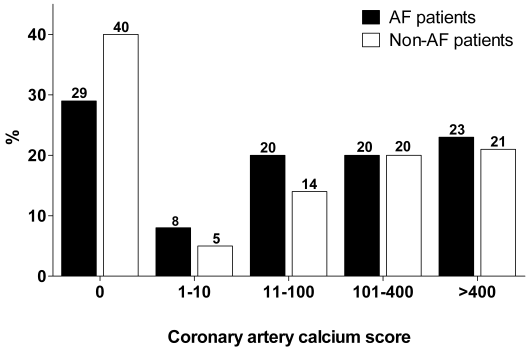

Figure 1. Bar graph showing the coronary artery calcium score categories in patients with and without history of paroxysmal or persistent AF. Solid bars indicate patients with AF; open bars, patients without AF. P = 0.31 for comparison between the 2 groups.

As shown in Figure 2, 28 (18%) patients with AF were classified as having no CAD based on MSCT, whereas 61 (41%) showed nonobstructive CAD and at least 1 significant (≥50%) luminal narrowing was observed in the remaining 61 (41%) patients. The prevalence of CAD among patients without AF was significantly lower: 47 (32%) were classified as having no CAD, whereas 61 (41%) showed nonobstructive CAD and 40 (27%) had obstructive CAD, based on MSCT (p = 0.010 compared with patients with AF).

Obstructive single-vessel disease was present in 35 (23%) patients with AF, whereas obstructive LM and/or proximal LAD disease was present in 37 (25%) patients with AF. Multivessel disease was observed in 26 (17%) (Figure 3).

As also indicated by Figure 3, patients without AF showed a significantly lower prevalence of obstructive single-vessel disease and obstructive LM and/or proximal LAD disease, as compared with patients with AF, but not a significantly lower prevalence of multivessel disease. Obstructive single-vessel disease was indeed observed in 19 (13%) patients without AF, obstructive CAD in the LM and/or proximal LAD in 15 (10%) and multivessel disease in 21 (14%) (p = 0.024, p = 0.001, and p = 0.53, respectively, compared with patients with AF).

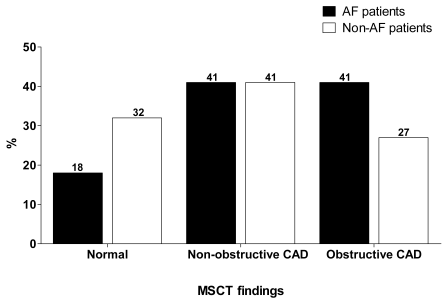

Figure 2. Prevalence of CAD in patients without and with history of paroxysmal or persistent AF. Solid bars indicate patients with AF; open bars, patients without AF. P = 0.010 for comparison between the 2 groups.

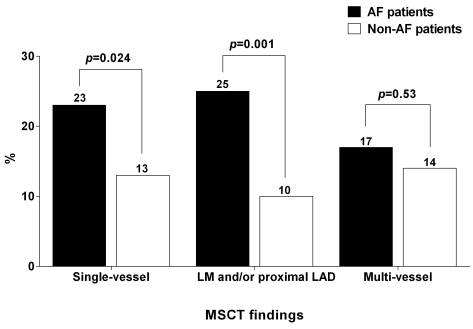

Figure 3. Prevalence of obstructive single-vessel, LM, or proximal LAD CAD and of multivessel disease in patients with and without history of paroxysmal or persistent AF. Solid bars indicate patients with AF; open bars, patients without AF.

Because of motion artifacts, 39 (1.5%) segments in the AF group and 38 (1.5%) segments in the non-AF group were excluded from the segment-based analysis, respectively. A significantly higher number of diseased coronary segments, of segments with obstructive CAD and nonobstructive CAD per patient was present in the AF group, as compared with non-AF group (5.5±3.9 versus 4.0±4.0, p = 0.001; 1.1±1.9 versus 0.8±1.7, p = 0.010 and 4.4±3.2 versus 3.2±3.3, p = 0.001, respectively).

Age (p <0.001), male gender (p = 0.002), diabetes mellitus (p = 0.004), hypertension (p <0.001), hypercholesterolemia (p <0.001), and history of AF (p = 0.010) were selected as significant univariate predictors of (any) CAD. Age (p <0.001), male gender (p = 0.014), hypertension (p = 0.006), hypercholesterolemia (p = 0.026), pretest likelihood of CAD (p = 0.021), and history of AF (p = 0.013) were selected as significant univariate predictors of obstructive CAD. At multivariable logistic regression analysis, age, history of AF, male gender, and hypercholesterolemia were identified as significantly associated to the presence of (any) CAD whereas the variables age, history of AF, and male gender were identified as significantly associated to obstructive CAD (Table 2).

Table 2. Multivariable logistic regression analysis: demographic and clinical variables related to coronary artery disease

CORONARY ARTERY DISEASE			
	p value	**OR**	**CI**
Age	<0.0001	1.13	1.09-1.18
Atrial fibrillation	0.006	2.52	1.30-4.90
Male gender	<0.0001	3.80	1.93-7.61
Hypercholesterolemia	0.033	2.2	1.06-4.44
OBSTRUCTIVE CORONARY ARTERY DISEASE			
	p value	**OR**	**CI**
Age	<0.0001	1.10	1.04-1.19
Atrial fibrillation	0.049	1.70	1.00-2.89
Male gender	0.001	2.67	1.48-4.84

CI: confidence intervals; OR: odds ratio.

Figure 4 shows an example of an asymptomatic patient with paroxysmal AF and evidence of extensive coronary atherosclerosis on MSCT.

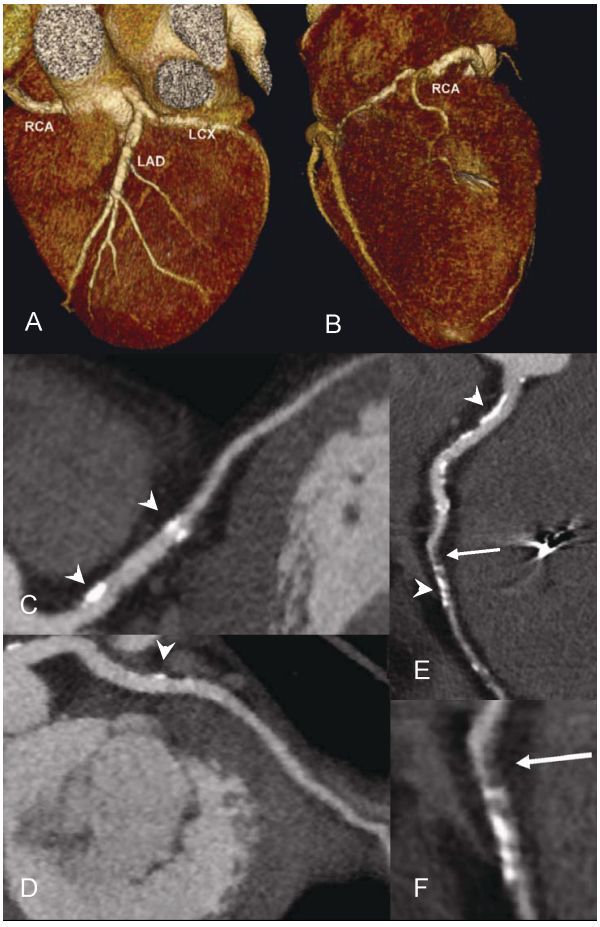

Figure 4. Example of a patient with extensive coronary atherosclerosis on MSCT. **Panel A** and **B**. 3D volume-rendered reconstructions are provided, showing the LAD, left circumflex (LCX), and right coronary arteries (RCA). **Panel C–E.** Curved multiplanar reconstructions of the LAD, LCX, and RCA, respectively. Calcifications (arrowheads) can be observed in the entire coronary tree (particularly in the LAD and RCA). An obstructive noncalcified plaque is present in the RCA (arrow in **panel E** and enlargement in **panel F**).

Diagnostic Accuracy of MSCT Coronary Angiography

A total of 79 patients underwent invasive coronary angiography. The overall number of obstructive (≥50% luminal narrowing) coronary artery stenoses was 151. The sensitivity/specificity of MSCT coronary angiography was 92.1% (95% CI, 86.5% to 95.8%) and 96.4% (95% CI, 95% to 97.4%), respectively.

DISCUSSION

This is one of first studies using anatomic assessment to examine the prevalence of CAD among patients with paroxysmal or persistent AF and without a history of CAD.[23] A higher prevalence of obstructive CAD was detected among patients with AF, as compared with a cohort of patients without AF, with similar age and pretest likelihood of CAD, but with a higher prevalence of diabetes mellitus. Moreover, LM and/or proximal LAD disease was more frequently identified (25% of patients with AF versus 10% of patients without AF). At logistic regression analysis, AF, together with age and male gender, was identified as an independent predictor of the presence of obstructive CAD.

Although a casual relationship between CAD and AF has not yet been established, CAD is considered to be highly prevalent among patients with AF and may be one of its potential etiologic factors.[7] Indeed, AF and CAD may simply be different, concurrent consequences of long-lasting exposure to coronary risk factors, but, on the other hand, AF could be a consequence of CAD, directly or indirectly, through an increase of left atrial pressure secondary to episodes of left ventricular ischemia.[24,25] Previous population studies such as the Framingham [9] and Manitoba [4] studies reported CAD to be one of the etiologic factors most commonly associated with the development of AF. Moreover, once diagnosed with AF, the presence of CAD has been shown to be related with recurrent AF episodes,[26] presence of symptoms (including arrhythmic, heart failure, and angina symptoms) [27] and increased risk of death.[28,29] Interestingly,

epidemiological data disclosed that ischemic heart disease is one of the most common underlying cause of death among patients with AF [30] and a more recent community-based longitudinal cohort study showed that patients diagnosed with first AF but yet without established CAD constitute a high-risk group with increased risk for subsequent new coronary ischemic events and mortality.[31]

Accordingly, these observations have lead to an increased interest in the evaluation of underlying CAD in patients with AF. Two recent studies assessed the value of cardiac imaging to detect CAD in patients with AF, using stress myocardial perfusion SPECT.[11,12] Abidov et al.[11] reported that patients with AF have larger perfusion abnormalities on SPECT and a higher risk of cardiac death as compared with patients without AF. However, >50% of enrolled patients had symptoms and/or known CAD, and the reported difference in SPECT studies results was mostly due to a higher amount of hypoperfused myocardium at rest in the AF group. More recently, Askew et al.[12] showed a prevalence of abnormal myocardial perfusion SPECT studies of 51.6% among asymptomatic patients with AF. After an average follow-up of 5.7 years, a significantly higher mortality rate was observed in patients with AF as compared with patients without AF. Interestingly, no significant difference in the rate of abnormal SPECT studies between patients with and without AF was observed, suggesting that the increased mortality was not related to a higher prevalence of obstructive CAD.

However, SPECT reflects only indirectly the presence of CAD, because it is based on the detection of coronary lesions that result in compromised blood flow during stress,[15] whereas the actual prevalence of atherosclerosis in patients with AF may be higher.

In this study, imaging of atherosclerosis with MSCT was used to determine the prevalence of CAD. By means of calcium scoring, the presence and extensions of coronary calcifications was not statistically different between patients with AF and patients without AF. However, using

noninvasive coronary angiography, patients with AF were found to have more frequently coronary atherosclerosis (82%) and obstructive CAD (41%), as compared with patients without AF (68% and 27%, respectively). Furthermore, LM/proximal LAD disease was identified in 25% of patients with AF versus 10% of patients without AF. These findings are particular striking, when considering that the patients of the study population were mostly asymptomatic and with low pretest likelihood for CAD. In addition, a higher prevalence of diabetes, a condition that is generally associated with a significantly higher extent of CAD, was observed in patients without AF. Indeed, at multivariable logistic regression analysis, only AF, age and male gender were identified as significantly related to the presence of obstructive CAD.

Clinical Implications

Because of the lack of follow-up data, the clinical significance and implications of these findings are still unknown at this time. However, taking into account the suspected association between AF, underlying CAD and increased risk for coronary events,[11,12] our observations suggest that patients with AF (despite the absence of symptoms) potentially may benefit from noninvasive diagnostic procedures to evaluate the presence of CAD. In this study, the feasibility of MSCT coronary angiography was evaluated, showing a higher prevalence of atherosclerosis and even obstructive CAD in patients with AF, as compared with patients without AF, confirming the hypothesis that AF could be a marker of advanced coronary atherosclerosis. However, in this regard, it remains important to realize that MSCT coronary angiography does not provide information about the hemodynamic consequences of observed coronary lesions.[15] In patients with obstructive CAD on MSCT functional testing remains needed to determine the presence of ischemia and to guide further therapeutic decisions (aggressive medical therapy and risk factor modification or referral for invasive angiography with potentially revascularization).

Study Limitations

This study has several limitations that should be acknowledged. First, it is a case-control study, the limitations of which are well known. Moreover, no prognostic data were available. A larger study, with follow-up data, may provide more conclusive information. Second, only patients with paroxysmal or persistent AF were studied. We preferred to exclude patients with permanent AF. Despite the introduction of 64-slice MSCT, the technique still suffers from limited diagnostic accuracy in case of irregular heart rate. With the more recent generations of dual source and 320-slice MSCT scanners, imaging in patients with permanent AF could potentially be possible, although no consistent data are available. Third, MSCT coronary angiography is not able to discriminate between flow-limiting and non–flow-limiting stenoses; accordingly, no data regarding the hemodynamic consequences of observed coronary lesions can be provided. Fourth, because the presence of history of paroxysmal or persistent AF was used to identify the study population, it is possible that some patients with unacknowledged episodes of paroxysmal AF have been included in the control group. In addition, although standardized MSCT evaluation protocols were used in the participating centers, acquisition protocols were not completely uniform as scanners from different generations and manufacturers were used. This, however, reflects the daily clinical routine and confers generalized applicability to our observations. In addition, no off-site reading of MSCT coronary angiography was performed, possibly influencing interobserver variability. Finally, MSCT coronary angiography still has a high radiation exposure, which limits its use in asymptomatic patients. However, the use of more recent generation scanners and the implementation of dose-saving algorithms is likely to result in substantial dose reduction, without degradation of image quality.[32]

CONCLUSIONS

A higher prevalence of obstructive CAD was detected among patients with AF, as compared with patients without AF, confirming the hypothesis that AF could be a marker of advanced coronary atherosclerosis. In addition, the presence of AF was identified as a significant and independent predictor of the presence of obstructive CAD.

REFERENCES

1. Fuster V, Ryden LE, Cannom DS, et al. ACC/AHA/ESC 2006 Guidelines for the Management of Patients with Atrial Fibrillation: a report of the American College of Cardiology/American Heart Association Task Force on Practice Guidelines and the European Society of Cardiology Committee for Practice Guidelines (Writing Committee to Revise the 2001 Guidelines for the Management of Patients With Atrial Fibrillation): developed in collaboration with the European Heart Rhythm Association and the Heart Rhythm Society. Circulation. 2006; 114: e257–e354.
2. Flegel KM, Shipley MJ, Rose G. Risk of stroke in non-rheumatic atrial fibrillation. Lancet. 1987; 1: 526–529.
3. Kannel WB, Abbott RD, Savage DD, et al. Coronary heart disease and atrial fibrillation: the Framingham Study. Am Heart J. 1983; 106: 389–396.
4. Krahn AD, Manfreda J, Tate RB, et al. The natural history of atrial fibrillation: incidence, risk factors, and prognosis in the Manitoba Follow-Up Study. Am J Med. 1995; 98: 476–484.
5. Psaty BM, Manolio TA, Kuller LH, et al. Incidence of and risk factors for atrial fibrillation in older adults. Circulation. 1997; 96: 2455–2461.
6. Dries DL, Exner DV, Gersh BJ, et al. Atrial fibrillation is associated with an increased risk for mortality and heart failure progression in patients with asymptomatic and symptomatic left ventricular systolic dysfunction: a retrospective analysis of the SOLVD trials. Studies of left ventricular dysfunction. J Am Coll Cardiol. 1998; 32: 695–703.
7. Lip GY, Beevers DG. ABC of atrial fibrillation. History, epidemiology, and importance of atrial fibrillation. BMJ. 1995; 311: 1361–1363.

8. Schoonderwoerd BA, Van Gelder I, Crijns HJ. Left ventricular ischemia due to coronary stenosis as an unexpected treatable cause of paroxysmal atrial fibrillation. J Cardiovasc Electrophysiol. 1999; 10: 224–228.
9. Kannel WB, Abbott RD, Savage DD, et al. Epidemiologic features of chronic atrial fibrillation: the Framingham study. N Engl J Med. 1982; 306: 1018–1022.
10. Baseline characteristics of patients with atrial fibrillation: the AFFIRM Study. Am Heart J. 2002; 143: 991–1001.
11. Abidov A, Hachamovitch R, Rozanski A, et al. Prognostic implications of atrial fibrillation in patients undergoing myocardial perfusion single-photon emission computed tomography. J Am Coll Cardiol. 2004; 44: 1062–1070.
12. Askew JW, Miller TD, Hodge DO, et al. The value of myocardial perfusion single-photon emission computed tomography in screening asymptomatic patients with atrial fibrillation for coronary artery disease. J Am Coll Cardiol. 2007; 50: 1080–1085.
13. Schuijf JD, Pundziute G, Jukema JW, et al. Diagnostic accuracy of 64-slice multislice computed tomography in the noninvasive evaluation of significant coronary artery disease. Am J Cardiol. 2006; 98: 145–148.
14. Mollet NR, Cademartiri F, van Mieghem CA, et al. High-resolution spiral computed tomography coronary angiography in patients referred for diagnostic conventional coronary angiography. Circulation. 2005; 112: 2318–2323.
15. Schuijf JD, Wijns W, Jukema JW, et al. Relationship between noninvasive coronary angiography with multi-slice computed tomography and myocardial perfusion imaging. J Am Coll Cardiol. 2006; 48: 2508–2514.
16. Diamond GA, Forrester JS. Analysis of probability as an aid in the clinical diagnosis of coronary-artery disease. N Engl J Med. 1979; 300: 1350–1358.
17. Gibbons RJ, Balady GJ, Bricker JT, et al. ACC/AHA 2002 guideline update for exercise testing: summary article: a report of the American College of Cardiology/American Heart Association Task Force on Practice Guidelines (Committee to Update the 1997 Exercise Testing Guidelines). Circulation. 2002; 106: 1883–1892.
18. Schuijf JD, Bax JJ, Salm LP, et al. Noninvasive coronary imaging and assessment of left ventricular function using 16-slice computed tomography. Am J Cardiol. 2005; 95: 571–574.

19. Gaemperli O, Schepis T, Koepfli P, et al. Accuracy of 64-slice CT angiography for the detection of functionally relevant coronary stenoses as assessed with myocardial perfusion SPECT. Eur J Nucl Med Mol Imaging. 2007; 34: 1162–1171.
20. Agatston AS, Janowitz WR, Hildner FJ, et al. Quantification of coronary artery calcium using ultrafast computed tomography. J Am Coll Cardiol. 1990; 15: 827–832.
21. Austen WG, Edwards JE, Frye RL, et al. A reporting system on patients evaluated for coronary artery disease. Report of the Ad Hoc Committee for Grading of Coronary Artery Disease, Council on Cardiovascular Surgery, American Heart Association. Circulation. 1975; 51: 5–40.
22. Leber AW, Knez A, Becker A, et al. Accuracy of multidetector spiral computed tomography in identifying and differentiating the composition of coronary atherosclerotic plaques: a comparative study with intracoronary ultrasound. J Am Coll Cardiol. 2004; 43: 1241–1247.
23. Androulakis A, Aznaouridis KA, Aggeli CJ, et al. Transient ST-segment depression during paroxysms of atrial fibrillation in otherwise normal individuals: relation with underlying coronary artery disease. J Am Coll Cardiol. 2007; 50: 1909–1911.
24. Nattel S. Therapeutic implications of atrial fibrillation mechanisms: can mechanistic insights be used to improve AF management? Cardiovasc Res. 2002; 54: 347–360.
25. Casaclang-Verzosa G, Gersh BJ, Tsang TS. Structural and functional remodeling of the left atrium: clinical and therapeutic implications for atrial fibrillation. J Am Coll Cardiol. 2008; 51: 1–11.
26. Suttorp MJ, Kingma JH, Koomen EM, et al. Recurrence of paroxysmal atrial fibrillation or flutter after successful cardioversion in patients with normal left ventricular function. Am J Cardiol. 1993; 71: 710–713.
27. Flaker GC, Belew K, Beckman K, et al. Asymptomatic atrial fibrillation: demographic features and prognostic information from the Atrial Fibrillation Follow-up Investigation of Rhythm Management (AFFIRM) study. Am Heart J. 2005; 149: 657–663.
28. Corley SD, Epstein AE, DiMarco JP, et al. Relationships between sinus rhythm, treatment, and survival in the Atrial Fibrillation Follow-Up Investigation of Rhythm Management (AFFIRM) Study. Circulation. 2004; 109: 1509–1513.
29. Curtis AB, Gersh BJ, Corley SD, et al. Clinical factors that influence response to treatment strategies in atrial fibrillation: the Atrial Fibrillation Follow-up

Investigation of Rhythm Management (AFFIRM) study. Am Heart J. 2005; 149: 645–649.

30. Wattigney WA, Mensah GA, Croft JB. Increased atrial fibrillation mortality: United States, 1980–1998. Am J Epidemiol. 2002; 155: 819–826.

31. Miyasaka Y, Barnes ME, Gersh BJ, et al. Coronary ischemic events after first atrial fibrillation: risk and survival. Am J Med. 2007; 120: 357–363.

32. McCollough CH, Primak AN, Saba O, et al. Dose performance of a 64-channel dual-source CT scanner. Radiology. 2007; 243: 775–784.

Chapter 6

Relationship Between Obstructive Coronary Artery Disease and Abnormal Stress Testing in Patients With Paroxysmal or Persistent Atrial Fibrillation

Gaetano Nucifora, Joanne D. Schuijf, Jacob M. van Werkhoven, Serge A. Trines, Sami Kajander, Laurens F. Tops, Olli Turta, J. Wouter Jukema, Joop H. M. Schreur, Mark W. Heijenbrok, Oliver Gaemperli, Philipp A. Kaufmann, Juhani Knuuti, Ernst E. van der Wall, Martin J. Schalij, Jeroen J. Bax

Int J Cardiovasc Imaging 2011; 27:777–785

ABSTRACT

Atrial fibrillation (AF) has been linked to the presence of underlying coronary artery disease (CAD). However, whether the higher burden of CAD observed in AF patients translates into higher burden of myocardial ischemia is unknown. In 87 patients (71% male, mean age 61±10 years) with paroxysmal or persistent AF and without history of CAD, MSCT coronary angiography and stress testing (exercise ECG test or myocardial perfusion imaging) were performed. CAD was classified as obstructive (≥50% luminal narrowing) or not. Stress tests were classified as normal or abnormal. A population of 122 patients without history of AF, similar to the AF group as to age, gender, symptomatic status and pre-test likelihood, served as a control group. Based on MSCT, 17% of AF patients were classified as having no CAD, whereas 43% showed non-obstructive CAD and the remaining 40% had obstructive CAD. A positive stress test was observed in 49% of AF patients with obstructive CAD. Among non-AF patients, 34% were classified as having no CAD, while 41% showed non-obstructive CAD and 25% had obstructive CAD ($p = 0.013$ compared to AF patients). A positive stress test was observed in 48% of non-AF patients with obstructive CAD. In conclusion, the higher burden of CAD observed in AF patients is not associated to higher burden of myocardial ischemia.

INTRODUCTION

Atrial fibrillation (AF) has been shown to be an independent risk factor for future coronary artery disease (CAD) events.[1–6] Accordingly, evaluation of AF patients for CAD may potentially be useful, in order to improve their outcome.

Multi-slice computed tomography (MSCT) coronary angiography has emerged as an accurate technique for the non-invasive imaging of coronary atherosclerosis.[7] In a recent study using MSCT coronary angiography, a higher prevalence of CAD and obstructive CAD was found among patients with paroxysmal or persistent AF, as compared to patients without a history of AF; in addition, a significant independent relation between AF and CAD was observed.[8] However, MSCT coronary angiography does not provide information about the hemodynamic consequences of observed coronary lesions;[9,10] therefore, whether the higher burden of CAD observed in AF patients is associated also to a higher burden of myocardial ischemia remains to be determined.

Accordingly, the aim of the present study was to evaluate the relation between the evidence of coronary atherosclerosis (by means of MSCT coronary angiography) and the presence of abnormal stress testing among patients with paroxysmal or persistent AF and compare findings to patients without a history of AF.

METHODS

Patient population

A total of 87 patients from the outpatient clinic with a history of paroxysmal (n = 54, 62%) or persistent (n = 33, 38%) AF, referred to MSCT for coronary evaluation, due to an elevated risk profile and/or chest pain, were included. In addition, patients underwent stress testing (exercise ECG testing [EET] or myocardial perfusion imaging [MPI]) within 1 month of MSCT coronary angiography.

The patient population is part of an ongoing study protocol addressing the value of MSCT and other imaging techniques in patients with paroxysmal or persistent AF. From this prospective registry, results addressing the prevalence of CAD by MSCT coronary angiography in AF patients have been recently published.[8]

Patients with history of CAD and contraindications to MSCT were excluded. Only patients in sinus rhythm were included, and patients with AF at the time of SPECT or MPI were excluded. Paroxysmal and persistent AF were diagnosed according to the American Heart Association/American College of Cardiology/European Society of Cardiology criteria.[11] A history of CAD was defined as the presence of previous acute coronary syndrome, percutaneous or surgical coronary revascularization, and/or one or more angiographically documented coronary stenosis ≥50% luminal diameter.[9] Contraindications for MSCT were *(1)* known allergy to iodinated contrast agent, *(2)* renal failure, *(3)* pregnancy.

For each patient, the presence of coronary risk factors (diabetes, systemic hypertension, hypercholesterolemia, positive family history of CAD and cigarette smoking) and symptoms was recorded. In addition, the pre-test likelihood of obstructive CAD was evaluated using the Diamond and Forrester criteria.[12,13]

A control group was selected from the clinical database for comparison purposes. Accordingly, 122 patients were included without history of AF and with similar baseline clinical characteristics; these patients were clinically referred to MSCT for coronary evaluation and stress testing within 1 month.

Patients were included at 4 centers in 3 different countries (Leiden University Medical Center, Leiden, the Netherlands; Medisch Centrum Haaglanden, Leidschendam, The Netherlands; Turku PET Center, Turku, Finland; University Hospital Zurich, Zurich, Switzerland).

MSCT data acquisition

The heart rate and blood pressure were monitored before the examination in each patient. In the absence of contraindications, patients with a heart rate ≥65 beats/min were administered beta-blocking medication (50–100 mg metoprolol, oral or 5–10 mg metoprolol, intravenous).

MSCT coronary angiography was performed with either 16-slice MSCT scanner (n = 39; Aquilion 16, Toshiba Medical Systems, Japan and Discovery STE, General Electrics, USA) or 64-slice MSCT scanner (n = 170; Aquilion 64, Toshiba Medical Systems, Japan, LightSpeed VCT, GE Healthcare, USA and Discovery VCT, General Electrics, USA). The estimated radiation dose was between 10 and 18 mSv.

Data were subsequently transferred to dedicated workstations for post-processing and evaluation (Advantage, GE Healthcare, USA; Vitrea 2, Vital Images, USA; and Aquarius, TeraRecon, USA).

MSCT data analysis

The MSCT data analysis was performed in each center by two experienced observers who had no knowledge of the patient's medical history, symptom status and stress testing results; disagreement was solved by consensus or evaluation by a third observer. Standardized MSCT data evaluation methodology and scoring system described below were used in each center.

MSCT coronary angiograms obtained with 16 and 64-slice scanners were evaluated for the presence of obstructive CAD (≥50% luminal narrowing) on a patient and vessel level. For this purpose, both the original axial dataset as well as curved multiplanar reconstructions were used. Each vessel was evaluated for the presence of any atherosclerotic plaque, defined as structures >1 mm^2 within and/or adjacent to the coronary artery lumen, which could be clearly distinguished from the vessel lumen and the surrounding pericardial tissue, as described previously.[14] Subsequently, the vessels were further classified as *(1)* completely normal, *(2)* having non-obstructive CAD when atherosclerotic lesions

<50% of luminal diameter were present or *(3)* having obstructive CAD when atherosclerotic lesions ≥50% of luminal diameter were present.
The presence of CAD (including obstructive and non-obstructive CAD), and obstructive CAD were evaluated. In addition, the presence of *(1)* single-vessel disease (obstructive CAD in one vessel); *(2)* multi-vessel disease (obstructive CAD in more than one vessel) and *(3)* obstructive CAD in the left main (LM) and/or proximal left anterior descending (LAD) coronary artery was evaluated. Multi-vessel disease and LM and/or proximal LAD disease were considered to represent high-risk features.

Stress testing

Stress testing was performed in all patients within 1 month of MSCT coronary angiography after an adequate pharmacological wash-out; beta-blockers, long-acting nitrates and calcium channel blockers were discontinued at least 48 h before the test.

Exercise ECG test

Symptom-limited EET was performed on a bicycle ergometer according to standard protocols.[15] Patients not able to reach ≥85% age-predicted maximum heart rate in the absence of ischemic changes were not included in the study.
The test was analyzed by an experienced reader who had no knowledge of the MSCT results and was classified as positive or negative for ischemia. The test was considered positive based on the presence of ≥0.1 mV horizontal or downsloping ST-segment depression at 80 ms after the J point in two contiguous leads during exercise or recovery.

Myocardial perfusion imaging

Stress-rest MPI was performed with symptom-limited bicycle exercise or pharmacologic (adenosine or dobutamine) stress using either technetium-99 m tetrofosmin or technetium-99 m sestamibi. Images were acquired with either a dual-head (Millenium VG & Hawkeye; GE Healthcare,

Waukesha, Wisconsin) or a triple-head (GCA 9300/HG, Toshiba Corp., Japan) single-photon emission computed tomographic (SPECT) camera, and reconstructed into long- and short-axis projections perpendicular to the heart axis. The estimated radiation dose for stress-rest MPI was approximately 7 mSv.

The test was analyzed by an experienced reader who had no knowledge of the MSCT results. Perfusion defects were identified on the stress images (segmental tracer activity <75% of maximum) and divided into ischemia (reversible defects, with ≥10% increase in tracer uptake on the resting images) or scar tissue (irreversible defects). Accordingly, examinations were classified as being either negative or positive. Positive examinations were further divided into those demonstrating reversible defects and those demonstrating fixed defects. The gated images were used to assess regional wall motion to improve differentiation between perfusion abnormalities and attenuation artifacts.[16]

Statistical analysis

Continuous variables are expressed as mean and standard deviation. Categorical variables are expressed as absolute numbers and percentages.

The differences in continuous variables were assessed using the Student t test. Chi-square or Fisher exact test, when appropriate, were computed to test for differences in categorical variables.

A p value < 0.05 was considered statistically significant. Statistical analyses were performed using SPSS software (version 15.0, SPSS Inc, Chicago, Il, USA).

RESULTS

Patient characteristics

Baseline characteristics of each group are shown in Table 1. By definition, AF and non-AF groups did not differ as to mean age (61±10 vs. 59±11

years), male gender (71% vs. 66%), symptomatic status and pre-test likelihood of CAD. In addition, no difference in coronary risk factor profile was observed between the two groups.

Table 1. Baseline characteristics of the study population

	AF patients (n = 87)	Non-AF patients (n = 122)	p value
Age (years)	61±10	59±11	0.25
Male gender	62 (71%)	80 (66%)	0.39
Diabetes	13 (15%)	30 (25%)	0.089
Hypertension	56 (64%)	79 (65%)	0.95
Hypercholesterolemia	44 (51%)	53 (43%)	0.31
Family history of coronary artery disease	30 (35%)	50 (41%)	0.34
Current or previous smoking	23 (26%)	39 (32%)	0.39
≥ 3 coronary risk factors	26 (30%)	40 (33%)	0.66
Body mass index (kg/m^2)	26.4±3.6	26.4±3.7	0.97
Symptoms			0.84
- Asymptomatic	45 (52%)	68 (56%)	
- Atypical angina	24 (28%)	30 (25%)	
- Typical angina	18 (21%)	24 (20%)	
Pre-test likelihood of coronary artery disease			0.63
- Low	46 (53%)	69 (57%)	
- Intermediate	23 (26%)	34 (28%)	
- High	18 (21%)	19 (16%)	
Medical therapy			
Digoxin	8 (9%)	0 (0%)	0.001
Beta-blockers	28 (32%)	32 (26%)	0.35
Nitrates	13 (15%)	13 (11%)	0.36
Non-dihydropyridinic calcium antagonists	9 (10%)	5 (4%)	0.075

Data are expressed as mean±SD and n (%).

MSCT coronary angiography

Table 2 shows the results of MSCT coronary angiography among AF and non-AF patients. Overall, a significantly higher prevalence of obstructive

CAD was observed among AF patients, as compared to non-AF patients (p = 0.013; Table 2). Single-vessel disease and LM and/or proximal LAD disease were more frequently observed in AF patients (p = 0.027 and p = 0.003, respectively; Table 2).

Table 2. MSCT coronary angiography results in the study population

	AF patients (n = 87)	Non-AF patients (n = 122)	p value
Type of MSCT scanner			0.53
- 16-slice	18 (21%)	21 (17%)	
- 64-slice	69 (79%)	101 (83%)	
Mean heart rate during the scan (beats/min)	64±7	66±10	0.13
Prevalence of CAD			0.013
- Normal coronary arteries	15 (17%)	41 (34%)	
- Non-obstructive CAD	37 (43%)	50 (41%)	
- Obstructive CAD	35 (40%)	31 (25%)	
Obstructive single-vessel disease	19 (22%)	13 (11%)	0.027
Multi-vessel disease	16 (18%)	18 (15%)	0.48
LM and/or proximal LAD	22 (25%)	12 (10%)	0.003
High-risk features	24 (28%)	21 (17%)	0.072

Data are expressed as mean±SD and n (%).

Stress testing

Table 3 shows the stress testing results among AF and non-AF patients. Symptom-limited EET was performed in 38 (44%) AF patients and in 48 (39%) non-AF patients. Ischemic ST-segment depression was observed in 15 (39%) AF patients and in 14 (29%) non-AF patients (p = 0.32; Table 3). When considering only the symptomatic patients, symptom-limited EET was performed in 13 AF patients and in 23 non-AF patients. In this sub-group of asymptomatic subjects, ischemic ST-segment depression was observed in 8 (62%) AF patients and in 5 (22%) non-AF patients (p = 0.030).

Table 3. Stress testing results in the study population

	AF patients (n = 87)	Non-AF patients (n = 122)	p value
Type of stress test			0.53
- Exercise ECG test	38 (44%)	48 (39%)	
- Myocardial perfusion imaging	49 (56%)	74 (61%)	
Exercise ECG test			
Mean peak double product	28996±7346	28854±6678	0.93
Mean peak workload (Watt)	191±52	186±41	0.60
Ischemic ST-segment depression	15 (39%)	14 (29%)	0.32
Myocardial perfusion imaging			
Myocardial perfusion findings			0.47
- Normal perfusion	30 (61%)	50 (68%)	
- Reversible perfusion defect	17 (35%)	17 (23%)	
- Fixed perfusion defect	2 (4%)	5 (7%)	
- Reversible and fixed perfusion defects	-	2 (2%)	
Overall			0.23
Negative test	53 (61%)	84 (69%)	
Positive test	34 (39%)	38 (31%)	

Data are expressed as mean±SD and n (%).

Stress-rest MPI was performed in 49 (56%) AF patients and in 74 (61%) non-AF patients. Symptom-limited bicycle exercise was performed in 21 AF patients and in 11 non-AF patients; in all these patients, ≥85% of maximum age-predicted heart rate was achieved if no stress-induced symptoms or changes in electrocardiogram or blood pressure occurred. Pharmacologic stress using adenosine or dobutamine was applied in 28 AF patients and in 63 non-AF patients.

Thirty (61%) AF patients had normal perfusion at both stress and rest. In the remaining 19 (39%) AF patients, reversible and fixed defects were observed in 17 and 2 patients, respectively. None of the AF patients showed both reversible and fixed defects (Table 3). The prevalence of abnormal MPI scans among non-AF patients was similar. Normal myocardial perfusion was observed in 50 (68%) non-AF patients. In the remaining 24 (32%) non-AF patients, reversible, fixed and both reversible

and fixed defects were observed in 17, 5 and 2 patients, respectively (see Table 3). When considering only the symptomatic patients, stress-rest MPI was performed in 29 symptomatic AF patients and in 31 symptomatic non-AF patients. The prevalence of abnormal MPI scans between these two groups of patients was similar (8, 28% vs. 11, 36%; p = 0.58).

Overall, considering the combined EET and stress-rest MPI results, no statistically significant difference in the prevalence of abnormal stress tests was observed between AF and non-AF patients (39% vs. 31%, p = 0.23; Table 3). Similarly, no statistically significant difference in the prevalence of abnormal stress tests was observed between symptomatic AF and non-AF patients (38% vs. 30%, p = 0.38).

Relationship between obstructive coronary artery disease and abnormal stress testing

Figure 1 illustrates the relationship between observations on MSCT coronary angiography and stress test results among AF and non-AF patients. The majority of AF and non-AF patients with normal coronary arteries had a normal stress test (87% vs. 88%; p = 0.90). In patients with (any) CAD, 32 (44%) AF patients and 33 (41%) non-AF patients had an abnormal stress test (p = 0.64).

Figure 2 illustrates the relationship between non-obstructive and obstructive CAD identified by MSCT coronary angiography and stress test results among AF and non-AF patients. The majority of AF and non-AF patients with non-obstructive CAD had a normal stress test (59% vs. 64%; p = 0.66). In patients with obstructive CAD, 17 (49%) AF patients and 15 (48%) non-AF patients had an abnormal stress test (p = 0.98).

DISCUSSION

The results of the present study show that AF patients have a higher prevalence of CAD, and in particular of obstructive CAD, as compared to

non-AF patients. However, no difference in the prevalence of abnormal stress testing and of functionally relevant coronary lesions was observed between the two groups.

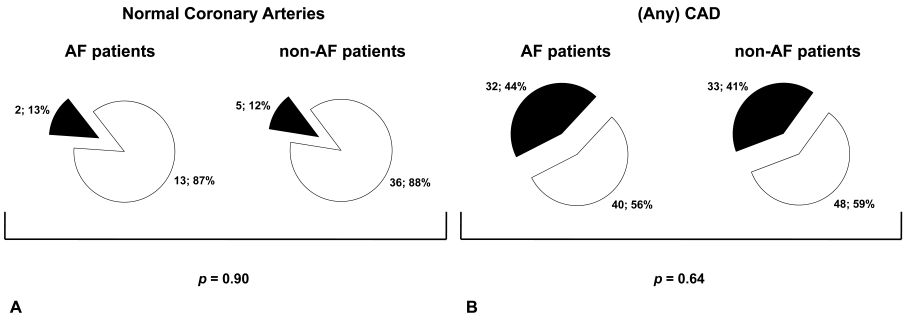

Figure 1. Pie charts illustrating the relationship between normal coronary arteries (**panel A**) and any coronary artery disease (CAD) (**panel B**) identified by MSCT coronary angiography and stress test results among atrial fibrillation (AF) and non-AF patients. White: negative stress test. Black: positive stress test.

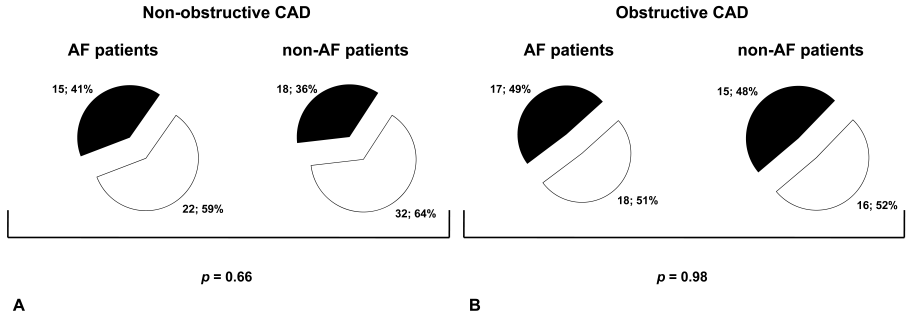

Figure 2. Pie charts illustrating the relationship between non-obstructive coronary artery disease (CAD) (**panel A**) and obstructive CAD (**panel B**) identified by MSCT coronary angiography and stress test results among atrial fibrillation (AF) and non-AF patients. White: negative stress test. Black: positive stress test.

Clinical relevance of CAD in AF patients

Previous studies have shown that AF patients have a low risk of CAD events at the time of first AF,[17,18] but a higher long-term risk, as

compared to patients without AF.[3,6] Aronow et al.[3], for instance, in a prospective study of 1359 patients, demonstrated that AF patients have a 2.2 times increased probability of developing CAD events during a follow-up of 42±26 months, as compared to non-AF patients. A more recent community-based longitudinal cohort study of 2768 patients showed that AF patients without known CAD represent a high-risk group with increased risk for subsequent new coronary ischemic events and mortality during a follow-up of 6.0±5.2 years.[6]

These observations raise the question whether routine evaluation of underlying CAD in AF patients should be recommended.[19] Thus far, only few studies addressed this issue. Abidov et al.[20], for instance, assessed the prevalence of CAD in 384 AF patients using stress-rest MPI; a higher prevalence of abnormal MPI studies was observed in AF patients as compared to patients without AF. However, in that study, a non-negligible proportion of enrolled patients had symptoms and/or known CAD, and the observed difference in MPI studies results was mainly related to a higher amount of fixed defects in the AF group. Conversely, Askew et al.[19] showed a similar prevalence of abnormal stress-rest MPI studies in 374 asymptomatic AF patients with no history of CAD, as compared to 374 age- and gender-matched controls without AF. More recently, the prevalence of CAD in 150 AF patients was assessed using MSCT coronary angiography; a significantly higher prevalence of CAD and obstructive CAD was observed among AF patients, as compared to 148 patients with similar age, gender, and pre-test likelihood of obstructive CAD. In addition, AF was independently related to the presence of CAD and obstructive CAD, strengthening the hypothesis that AF could be a marker of advanced coronary atherosclerosis.[8]

Atherosclerosis versus abnormal stress testing in AF patients

Stress testing and MSCT coronary angiography provide different, complementary information about CAD (i.e. evidence of myocardial ischemia and evidence of coronary atherosclerosis, respectively).[9,10]

However, how these data relate each other in AF patients is still unknown. In the present study, the relation between evidence of coronary atherosclerosis, assessed by means of MSCT coronary angiography, and the presence of abnormal stress testing was assessed among 87 patients with paroxysmal or persistent AF. Findings were compared to 122 patients without a history of AF. In line with the study of Askew et al.[19], a similar prevalence of abnormal stress tests was observed between AF and non-AF patients (39% vs. 31%). In addition, and importantly, no difference in the prevalence of functionally-relevant obstructive coronary lesions was observed between the two groups of patients (49% vs. 48%). These data suggest that the higher atherosclerotic burden associated to the presence of AF is not associated with a higher burden of myocardial ischemia.

Clinical implications

The results of the present and of previous studies suggest that a history of AF, per se, should not represent an indication to stress testing as indiscriminate first-line approach to rule out the presence of CAD.[19] AF patients have indeed a similar prevalence of functionally-relevant coronary lesions as compared to non-AF patients. Nevertheless, a higher burden of subclinical coronary atherosclerosis is observed in patients with AF and this higher prevalence may potentially explain the previously observed higher long-term risk of CAD event in this group.[3,6] Accordingly, more aggressive medical therapy and risk factor modification may be justified in AF patients. Further follow-up studies, with follow-up data, are however needed in order to confirm this hypothesis.

Study limitations

This study has several limitations that should be acknowledged. First, it is a case–control study, the limitations of which are well known. Moreover, the patient population is relatively small, including both symptomatic and asymptomatic subjects, and no prognostic data are available; a larger

study, with follow-up data, may provide more conclusive information. Second, only patients with paroxysmal or persistent AF were enrolled, while patients with permanent AF were not included. Sixty-four-slice MSCT suffers indeed from limited diagnostic accuracy in case of irregular heart rate. More recent generations of dual source MSCT or 320-row scanners could potentially allow imaging of the coronary arteries also in patients with permanent AF.[21] Third, MSCT scanners from different generations as well as manufacturers were used and the stress testing protocol was not standardized, including either symptom-limited EET or stress-rest MPI; this, however, reflects the daily clinical practice, and allows wider applicability to the present observations. In addition, no off-site reading of MSCT coronary angiography and stress testing was performed, possibly influencing inter-observer variability.

CONCLUSIONS

AF patients have a higher prevalence of CAD, and in particular of obstructive CAD, as compared to non-AF patients. However, the higher burden of CAD observed in AF patients is not associated with a higher burden of myocardial ischemia, as compared to non-AF patients.

REFERENCES

1. Kannel WB, Abbott RD, Savage DD, et al. Coronary heart disease and atrial fibrillation: the Framingham Study. Am Heart J 1983;106:389–396
2. Krahn AD, Manfreda J, Tate RB, et al. The natural history of atrial fibrillation: incidence, risk factors, and prognosis in the Manitoba Follow-Up Study. Am J Med 1995;98:476–484
3. Aronow WS, Ahn C, Mercando AD, et al. Correlation of atrial fibrillation, paroxysmal supraventricular tachycardia, and sinus rhythm with incidences of new coronary events in 1, 359 patients, mean age 81 years, with heart disease. Am J Cardiol 1995;75:182–184

4. Psaty BM, Manolio TA, Kuller LH, et al. Incidence of and risk factors for atrial fibrillation in older adults. Circulation 1997;96:2455–2461
5. Kopecky SL, Gersh BJ, McGoon MD, et al. Lone atrial fibrillation in elderly persons: a marker for cardiovascular risk. Arch Intern Med 1999;159:1118–1122
6. Miyasaka Y, Barnes ME, Gersh BJ, et al. Coronary ischemic events after first atrial fibrillation: risk and survival. Am J Med 2007;120:357–363
7. Cademartiri F, La Grutta L, Palumbo A, et al. Non-invasive visualization of coronary atherosclerosis: state-of-art. J Cardiovasc Med (Hagerstown) 2007;8:129–137
8. Nucifora G, Schuijf JD, Tops LF, et al. Prevalence of coronary artery disease assessed by multislice computed tomography coronary angiography in patients with paroxysmal or persistent atrial fibrillation. Circ Cardiovasc Imaging 2009;2:100–106
9. Schuijf JD, Wijns W, Jukema JW, et al. Relationship between noninvasive coronary angiography with multi-slice computed tomography and myocardial perfusion imaging. J Am Coll Cardiol 2006;48:2508–2514
10. Petretta M, Costanzo P, Acampa W, et al. Noninvasive assessment of coronary anatomy and myocardial perfusion: going toward an integrated imaging approach. J Cardiovasc Med (Hagerstown) 2008;9:977–986
11. Fuster V, Ryden LE, Cannom DS, et al. ACC/AHA/ESC 2006 guidelines for the management of patients with atrial fibrillation: a report of the American College of Cardiology/American Heart Association Task Force on Practice Guidelines and the European Society of Cardiology Committee for Practice Guidelines (Writing Committee to Revise the 2001 Guidelines for the Management of Patients With Atrial Fibrillation): developed in collaboration with the European Heart Rhythm Association and the Heart Rhythm Society. Circulation 2006;114:e257–e354
12. Diamond GA, Forrester JS. Analysis of probability as an aid in the clinical diagnosis of coronary-artery disease. N Engl J Med 1979;300:1350–1358
13. Gibbons RJ, Balady GJ, Bricker JT, et al. ACC/AHA 2002 guideline update for exercise testing: summary article: a report of the American College of Cardiology/American Heart Association Task Force on Practice Guidelines (Committee to Update the 1997 Exercise Testing Guidelines). Circulation 2002;106:1883–1892
14. Leber AW, Knez A, Becker A, et al. Accuracy of multidetector spiral computed tomography in identifying and differentiating the composition of coronary

atherosclerotic plaques: a comparative study with intracoronary ultrasound. J Am Coll Cardiol 2004;43:1241–1247

15. Fletcher GF, Balady G, Froelicher VF, et al. Exercise standards. a statement for healthcare professionals from the american heart association. writing group. Circulation 1995;91:580–615

16. Smanio PE, Watson DD, Segalla DL, et al. Value of gating of technetium-99 m sestamibi single-photon emission computed tomographic imaging. J Am Coll Cardiol 1997;30:1687–1692

17. Friedman HZ, Weber-Bornstein N, Deboe SF, et al. Cardiac care unit admission criteria for suspected acute myocardial infarction in new-onset atrial fibrillation. Am J Cardiol 1987;59:866–869

18. Zimetbaum PJ, Josephson ME, McDonald MJ, et al. Incidence and predictors of myocardial infarction among patients with atrial fibrillation. J Am Coll Cardiol 2000;36:1223–1227

19. Askew JW, Miller TD, Hodge DO, et al. The value of myocardial perfusion single-photon emission computed tomography in screening asymptomatic patients with atrial fibrillation for coronary artery disease. J Am Coll Cardiol 2007;50:1080–1085

20. Abidov A, Hachamovitch R, Rozanski A, et al. Prognostic implications of atrial fibrillation in patients undergoing myocardial perfusion single-photon emission computed tomography. J Am Coll Cardiol 2004;44:1062–1070

21. Marwan M, Pflederer T, Schepis T, et al. Accuracy of dual-source computed tomography to identify significant coronary artery disease in patients with atrial fibrillation: comparison with coronary angiography. Eur Heart J. 2010;31, 2230–2237

Chapter 7

Usefulness of Echocardiographic Assessment of Cardiac and Ascending Aorta Calcific Deposits to Predict Coronary Artery Calcium and Presence and Severity of Obstructive Coronary Artery Disease

Gaetano Nucifora, Joanne D. Schuijf, Jacob M. van Werkhoven, J. Wouter Jukema, Nina Ajmone Marsan, Eduard R. Holman, Ernst E. van der Wall, Jeroen J. Bax

Am J Cardiol 2009;103:1045–1050

ABSTRACT

The presence of cardiac and aortic calcific deposits has been related to coronary artery disease (CAD) and cardiovascular events. The present study aimed to evaluate whether comprehensive echocardiographic assessment of cardiac and ascending aorta calcific deposits could predict coronary calcium and obstructive CAD. A total of 140 outpatients (age 61±11 years; 90 men) without a history of CAD were studied. Aortic valve sclerosis and mitral annular, papillary muscle, and ascending aorta calcific deposits were assessed using echocardiography and semiquantified using an echocardiography-derived calcium score (ECS) ranging from 0 (no calcium visible) to 8 (severe calcific deposits). Coronary calcium scoring and noninvasive coronary angiography were performed using multislice computed tomography. Angiograms showing atherosclerosis were classified as having obstructive (≥50% luminal narrowing) CAD or not. The relation between ECS and multislice computed tomographic findings was explored using multivariate and receiver-operator characteristic curve analyses. Only ECS was associated with coronary calcium score >400 (odds ratio [OR] 3.6, 95% confidence interval [CI] 2.4 to 5.5, p <0.001). Similarly, only ECS (OR 1.8, 95% CI 1.4 to 2.4, p <0.001) and pretest likelihood of CAD (OR 1.7, 95% CI 1.0 to 2.8, p = 0.04) were associated with obstructive CAD. ECS ≥3 had high sensitivity and specificity in identifying patients with coronary calcium score >400 (87% for both) and obstructive CAD (74% and 82%, respectively). In conclusion, echocardiographic assessment of cardiac and ascending aorta calcium may allow detection of patients with extensive calcified coronary arterial atherosclerotic plaques.

INTRODUCTION

The presence of cardiac and aortic calcium has been related to coronary artery disease (CAD) and cardiovascular events.[1-4] Moreover, it was suggested that mitral annular calcium and aortic valve sclerosis were not merely passive age-related degenerative processes. Rather, these phenomena may be a form of atherosclerosis, sharing many risk factors and a similar cause with both systemic and coronary atherosclerosis.[5-7] Possibly, recognition of cardiac and ascending aorta calcific deposits using transthoracic echocardiography, a simple, noninvasive, and widely available technique, could be helpful for the identification of patients with obstructive CAD. Therefore, the aim of the present study was to determine whether an echocardiography-derived calcium score (ECS), obtained using comprehensive assessment of the burden of cardiac and ascending aorta calcium, was able to predict coronary artery calcium score (CACS) and the presence of obstructive CAD, assessed using multislice computed tomographic (MSCT) coronary angiography.

METHODS

A total of 140 consecutive outpatients referred for MSCT for coronary evaluation because of increased risk profile and/or stable chest pain symptoms were included. Transthoracic echocardiography was performed in all patients within 1 month of MSCT coronary angiography. Patients with aortic valve stenosis, rheumatic valvular disease, prosthetic valves, or bicuspid aortic valves were excluded. Also, patients with a history of CAD, cardiomyopathy, rhythm other than sinus, suboptimal echocardiographic studies (i.e., inadequate visualization of the left ventricular endocardium, valves, and ascending aorta), or contraindications to multislice computed tomography were excluded. History of CAD was defined as the presence of previous acute coronary

syndromes, percutaneous or surgical coronary revascularization, and/or ≥1 angiographically documented coronary stenosis ≥50% luminal diameter.[8] Contraindications for multislice computed tomography were *(1)* known allergy to iodinated contrast agent, *(2)* renal insufficiency, and *(3)* pregnancy.

MSCT coronary angiography was performed using a 64-slice MSCT scanner (Aquilion 64; Toshiba Medical Systems, Tokyo, Japan). Heart rate and blood pressure were monitored before the examination in each patient. In the absence of contraindications, patients with a heart rate ≥65 beats/min were administered oral β blockers (metoprolol 50 or 100 mg, single dose, 1 hour before the examination). First, a prospective coronary calcium scan without contrast enhancement was performed, followed by MSCT coronary angiography performed according to the protocol described elsewhere.[9] Data were subsequently transferred to dedicated workstations for postprocessing and evaluation (Advantage; GE Healthcare, Milwaukee, Wisconsin, and Vitrea 2; Vital Images, Minnetonka, Minnesota). MSCT data analysis was performed by 2 experienced observers who had no knowledge of the patient's medical history and symptom status. Disagreement was solved by consensus or evaluation by a third observer. Coronary artery calcium was identified as a dense area in the coronary artery >130 Hounsfield units. A total CACS was recorded for each patient. According to the total CACS, patients were subsequently categorized as having no calcium (total score = 0) or low (total score = 1 to 100), moderate (total score = 101 to 400), and severe (total score >400) coronary artery calcium.[10] MSCT coronary angiograms were evaluated for the presence of CAD on patient, vessel, and segment levels. For this purpose, both the original axial data set and curved multiplanar reconstructions were used. Coronary arteries were divided into 17 segments according to the modified American Heart Association classification.[11] Each segment was evaluated for the presence of atherosclerotic plaque, and 1 coronary plaque was assigned per coronary segment. Subsequently, type of plaque was determined as *(1)*

noncalcified plaques, plaques with a lower density compared with the contrast-enhanced vessel lumen; *(2)* calcified plaques, plaques with high density; and *(3)* mixed plaques, plaques with noncalcified and calcified elements within a single plaque. Finally, plaques were classified as obstructive (≥50% luminal narrowing) or nonobstructive.

Table 1. Grading system of the cardiac and ascending aorta calcifications

Grade	Aortic valve sclerosis	Mitral annular calcification	Papillary muscles calcification	Ascending aorta calcification
0	Absent	Absent	Absent	Absent
1	Mild	<5 mm	Present	Present
2	Moderate	5-10 mm		
3	Severe	>10 mm		

Aortic valve sclerosis (AVS) was defined by focal areas of increased echogenicity and thickening of the aortic valve leaflets with a velocity ≤2.5 m/s across the aortic valve. Each aortic valve leaflet was graded according to leaflet thickening and calcification. The highest score for a given cusp was assigned as the overall degree of AVS. Mitral annular calcification (MAC) was defined as an intense and bright echo-producing structure located at the junction of the atrio-ventricular groove and posterior mitral valve leaflet and was measured from the leading anterior to the trailing posterior edge. Papillary muscle calcification was defined as a bright echo involving the head of one or both papillary muscles. Ascending aorta calcification was defined as a focal or diffuse area of increased echoreflectance and thickening in the aortic root on the parasternal long-axis view.

Complete transthoracic echocardiographic studies were performed using a commercially available system (Vivid 7 Dimension; GE Healthcare, Horten, Norway) equipped with a M3S phased-array transducer (3.5 MHz). A careful search for cardiac calcific deposits was systematically performed. All studies were digitally stored for off-line analysis. Off-line analysis was performed using dedicated software (EchoPAC 7.0.0; GE Healthcare, Horten, Norway) by an observer who had no knowledge of clinical data and MSCT coronary angiography results. Criteria for judging aortic valve sclerosis, mitral annular calcium, and ascending aorta and

papillary muscle calcium were similar to grading systems used in previous studies [3,12-14] and are listed in Table 1. Accordingly, a final score was derived as the sum of all identified cardiac calcific deposits and was in the range of 0 (no calcium visible) to 8 (extensive cardiac and ascending aorta calcific deposits).

A total of 40 patients were randomly selected and analyzed again 1 month later by a second observer to assess interobserver agreement for the ECS. According to weighted κ test, interobserver agreement was good (weighted $\kappa = 0.84$).

Continuous variables were expressed as mean ± SD or median and 25th to 75th percentile range when non-normally distributed. Categorical variables were expressed as absolute number and percentage. Multivariable logistic regression analysis (backward stepwise with retention level set at 0.1) was applied to evaluate the association between clinical and echocardiographic data and the presence of severe coronary artery calcium and obstructive CAD at MSCT coronary angiography. Variables entered in multivariable models were age, gender, diabetes mellitus, hypertension, hypercholesterolemia, positive family history, smoking, pretest likelihood of CAD, mitral annular calcium, aortic valve sclerosis, papillary muscle calcium, ascending aorta calcium, and ECS. Odds ratios (ORs) and 95% confidence intervals (CIs) were calculated. Relations between ECS and the presence of severe coronary artery calcium, presence of obstructive CAD, number of significantly diseased vessels, number of significantly diseased segments, and numbers of segments with noncalcified, calcified, and mixed plaques were also evaluated. The general population was divided into 3 groups accordingly to ECS (group 1, ECS <3; group 2, ECS 3 to 5; and group 3, ECS >5). Comparison between continuous variables was performed using 1-way analysis of variance test with polynomial contrast to assess the presence of a linear trend across ordered levels of ECS. Chi-square test for >2 × 2 and Fisher's exact test for 2 × 2 contingency tables were computed to assess differences in categorical variables. Receiver-

operator characteristic (ROC) curves were used to evaluate the ability of the ECS to predict the presence of severe coronary artery calcium and the presence of obstructive CAD at MSCT coronary angiography. In addition, ROC curve analysis was performed to evaluate the ability of the CACS to predict the presence of obstructive CAD at MSCT coronary angiography. A p value <0.05 was considered statistically significant. Statistical analyses were performed using SPSS software (version 15.0; SPSS Inc., Chicago, Illinois).

RESULTS

Table 2 lists baseline characteristics of the study population, and Table 3 lists results of MSCT coronary angiography and transthoracic echocardiography.

Table 2. Baseline characteristics of the study population

Variable	n = 140
Age (years)	61±11
Men/women	90/50
Diabetes mellitus	54 (39%)
Hypertension	89 (64%)
Hypercholesterolemia (total cholesterol ≥240 mg/dl)	73 (52%)
Family history of CAD	44 (31%)
Current or previous smoker	53 (38%)
Body mass index (kg/m^2)	27±4
Previous chest pain	65 (46%)
- Typical	31 (22%)
- Atypical	34 (24%)
Pre-test likelihood of CAD	
- Low	71 (51%)
- Intermediate	40 (28%)
- High	29 (21%)

Table 3. Results of multislice computed tomographic (MSCT) coronary angiography and transthoracic echocardiography (n = 140)

MSCT coronary angiography	
CACS	385 (29-967)
- No calcium	22 (16%)
- Low	27 (19%)
- Moderate	21 (15%)
- Severe	70 (50%)
CAD	123 (88%)
Obstructive CAD	80 (57%)
- Single vessel disease	33 (24%)
- Multivessel disease	47 (34%)
- Left main/proximal left anterior descending coronary artery disease	37 (26%)
Segments	
- n° of diseased segments	7.3±4.0
- n° of segments with obstructive plaques	2.0±2.6
- n° of segments with nonobstructive plaques	5.3±3.4
- n° of segments with non calcified plaques	1.9±2.3
- n° of segments with calcified plaques	3.7±3.5
- n° of segments with mixed plaques	1.6±1.9
Transthoracic echocardiography	
Aortic valve sclerosis	77 (55%)
Mitral annular calcium	55 (39%)
Papillary muscle calcium	21 (15%)
Ascending aorta calcium	61 (44%)
ECS	2.5±2.0
- <3	70 (50%)
- 3–5	48 (34%)
- >5	22 (16%)

Multivariable logistic regression analysis identified ECS as the only variable among the clinical and echocardiographic variables with a significant association with severe coronary artery calcium (OR 3.6, 95% CI 2.4 to 5.5, p <0.001). ECS (OR 1.8, 95% CI 1.4 to 2.4, p <0.001) and pretest likelihood of CAD (OR 1.7, 95% CI 1.0 to 2.8, p = 0.04) were identified as significantly associated with obstructive CAD.

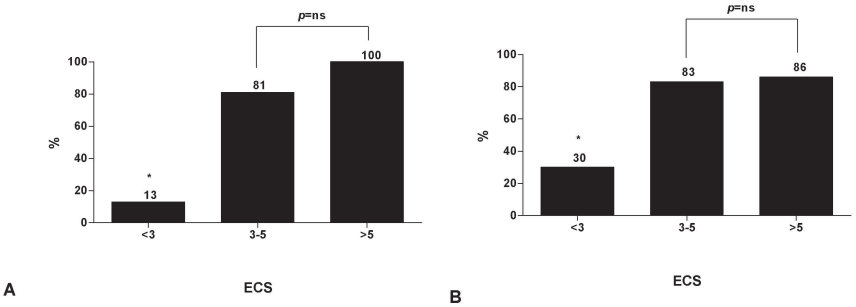

Figure 1. Relation between ECS and (**panel A**) severe coronary artery calcium and (**panel B**) obstructive CAD. *p <0.001 in comparison to the other 2 groups.

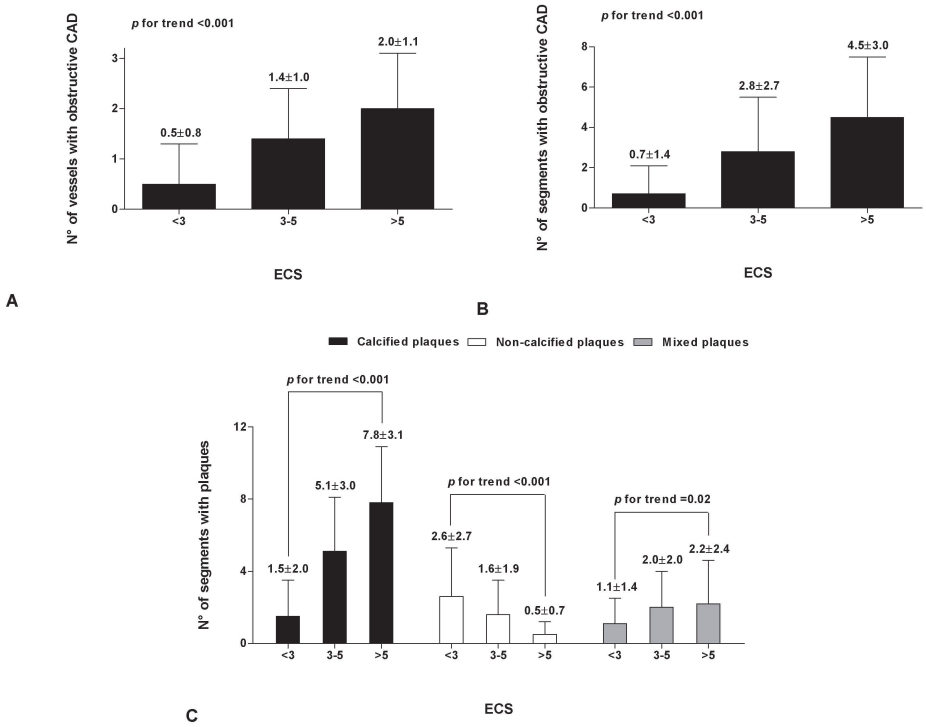

Figure 2. Relation between ECS and (**panel A**) number of vessels with obstructive CAD, (**panel B**) number of segments with obstructive CAD, and (**panel C**) number of segments with calcified, noncalcified, and mixed plaque.

As shown in Figure 1, patients with ECS of 3 to 5 and >5 more frequently had severe coronary artery calcium and obstructive CAD compared with the group with ECS <3 (p <0.001). Furthermore, a significant increasing linear trend in number of vessels with obstructive plaques, number of segments with obstructive plaques, and number of segments with calcified plaques was observed across the ordered levels of ECS (p <0.001, respectively; Figure 2).

At ROC curve analysis (Figure 3), ECS ≥3 had the highest sensitivity and specificity for identification of patients with severe coronary artery calcium (87% for both) and obstructive CAD (74% and 82%, respectively). Moreover, the ability of ECS to predict obstructive CAD was similar to that shown by the CACS (Figure 3).

DISCUSSION

Results of the present study showed that an ECS obtained through comprehensive assessment of cardiac and ascending aorta calcium was able to predict the presence of extensive coronary calcium and obstructive CAD, assessed using MSCT coronary angiography. Furthermore, significant linear trends were observed between ECS and extent and severity of coronary atherosclerosis and number of calcified coronary artery lesions.

Vascular deposition of mineral calcium is an organized and regulated process that typically occurs in areas of atherosclerotic lipid accumulation, sharing many features with cortical bone formation.[7] In the last 2 decades, the clinical relevance of vascular calcific deposits has emerged. The amount of calcium in both coronary arteries and the aorta correlates with atherosclerotic plaque burden in each vascular bed [15,16] and is associated with increased risk of cardiovascular events.[4,17] Severe coronary calcific deposits are associated with the presence of myocardial ischemia,[18] and extent of calcium in the aorta is related to coronary, carotid, and peripheral artery disease.[14]

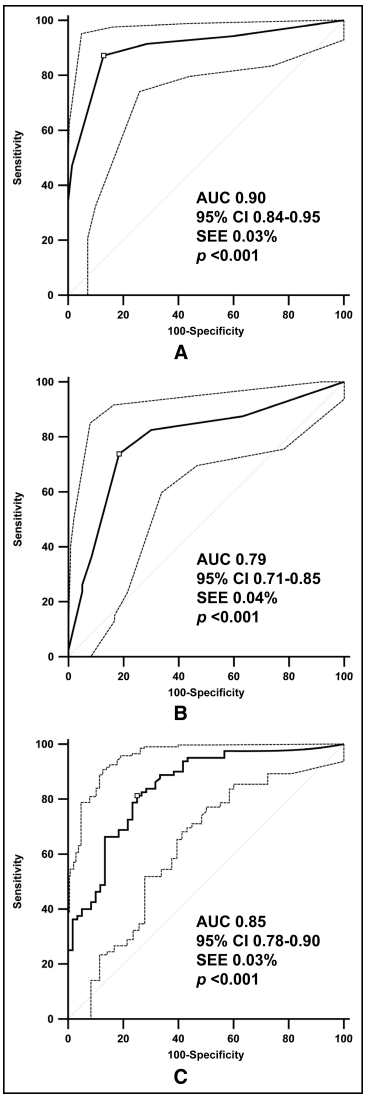

Figure 3. ROC curve analyses. **Panel A.** Area under the ROC curve (AUC) of the ECS for the prediction of severe coronary artery calcium. The highest sensitivity and specificity in identification of patients with severe coronary artery calcium (87% for both) was provided by ECS ≥3. **Panel B.** AUC of the ECS for the prediction of obstructive CAD. The highest sensitivity and specificity in the identification of patients with obstructive CAD (74% and 82%, respectively) was provided by ECS ≥3. **Panel C.** AUC of CACS for the prediction of obstructive CAD. The highest sensitivity and specificity in the identification of patients with obstructive CAD (81% and 75%, respectively) was provided by CACS ≥208.

Mitral annular calcium and aortic valve sclerosis appears to be the result of similar pathologic processes. Both are not simple passive degenerative disorders influenced by mechanical stress, but active inflammatory processes with histopathologic features similar to atherosclerosis.[5-7]

Previous clinical studies have shown significant associations between mitral annular calcium and aortic valve sclerosis with cardiovascular risk factors,[12,19] impaired coronary microvascular function,[20,21] subclinical systemic calcified atherosclerosis,[22] inducible myocardial ischemia,[13] and obstructive CAD at conventional coronary angiography.[23,24] Large population cohort studies showed that aortic valve sclerosis and mitral annular calcium are associated with increased cardiovascular morbidity and mortality.[1-3] Because it is unlikely that aortic valve sclerosis and mitral annular calcium directly lead to adverse cardiovascular outcomes, their relation with coronary atherosclerosis most likely explains these observations.

Calcific deposits of the papillary muscles are less commonly observed in the general population and usually limited to their apical portion. Similarly to mitral annular calcium and aortic valve sclerosis, papillary muscle calcium is associated with the presence of CAD despite potentially different underlining mechanisms,[5] more likely a consequence of necrosis or fibrosis caused by narrowing of the coronary arterial lumen by atherosclerosis.[25]

Noninvasive modalities for the diagnosis of CAD are important for both screening of asymptomatic subjects and risk stratification of symptomatic patients to identify those who could benefit from invasive coronary angiography. Recently, MSCT coronary angiography has emerged as a feasible and accurate technique allowing detection of coronary atherosclerosis by assessing the coronary artery calcium burden and performing noninvasive angiography.[9] However, it is expensive and not widely available. Moreover, it still carries high radiation exposure, which limits its widespread use in asymptomatic patients, and a potential associated risk of allergic reactions and nephrotoxicity related to the use of iodinated contrast agents.

According to the previously described association between cardiovascular calcific deposits and coronary atherosclerosis, recognition of cardiac and ascending aorta calcium using transthoracic echocardiography could be

helpful to optimize the identification of patients with obstructive CAD. Transthoracic echocardiography has the advantage of being a simple, low-cost, radiation-free technique that is widely available and used in clinical practice. Based on previous echocardiographic studies, sensitivity and specificity of aortic valve sclerosis and mitral annular calcium for the detection of obstructive CAD has been reported to be in the range of 38% to 64% and 60% to 86% and 57% to 60% and 33% to 56%, respectively.[23,26-28] However, most studies had drawbacks, such as *(1)* inclusion of patients with a history of CAD; *(2)* use of invasive coronary angiography for the diagnosis of CAD, possibly introducing a selection bias; *(3)* lack of information about coronary plaque composition; and *(4)* simple assessment of the presence/absence of single cardiac calcific deposits, rather than a graded approach.

In the present study, in a consecutive group of patients without a history of CAD, comprehensive echocardiographic assessment of cardiac and ascending aorta calcific deposits was performed. Moreover, not only the presence/absence of calcific deposits was assessed, but their burden was also quantified, deriving a global score. MSCT coronary angiography was used to diagnose CAD. Use of this technique allowed us to show coronary atherosclerosis even in patients asymptomatic or with low pretest likelihood and assess coronary plaque composition, thereby reducing (although not completely obviating) the selection bias that hampered previous studies relying on invasive coronary angiography.[23,26-28] The derived global ECS was able to predict the presence of severe coronary artery calcium with sensitivity and specificity of 87% for both and the presence of obstructive CAD with sensitivity of 74% and specificity of 82%. Furthermore, a linear trend between ECS and number of vessels and segments with obstructive CAD and number of segments with calcified plaques was observed, strengthening the evidence of a relation between cardiac and aortic calcific deposits and advanced calcified coronary atherosclerosis.

This study had some limitations that should be acknowledged. First, it is a single-center experience. Second, conventional coronary angiography, the gold standard for diagnosing CAD, was not used. However, 64-slice MSCT coronary angiography has been validated against invasive angiography and intravascular ultrasound, allowing detection of significant stenoses and assessment of plaque composition with high accuracy.[9,29] Moreover, the higher spatial resolution and lower voxel size of 64-slice MSCT compared with 16-slice MSCT decreased the blooming artifacts related to coronary calcifications.30 Third, no follow-up data were available. Therefore, it is unknown whether comprehensive assessment of cardiac and ascending aorta calcific deposits could provide incremental prognostic information.

REFERENCES

1. Otto CM, Lind BK, Kitzman DW, et al. Association of aortic-valve sclerosis with cardiovascular mortality and morbidity in the elderly. N Engl J Med. 1999; 341: 142–147

2. Fox CS, Vasan RS, Parise H, et al. Mitral annular calcification predicts cardiovascular morbidity and mortality: the Framingham Heart Study. Circulation. 2003; 107: 1492–1496

3. Barasch E, Gottdiener JS, Marino Larsen EK, et al. Cardiovascular morbidity and mortality in community-dwelling elderly individuals with calcification of the fibrous skeleton of the base of the heart and aortosclerosis (the Cardiovascular Health Study). Am J Cardiol. 2006; 97: 1281–1286

4. Witteman JC, Kannel WB, Wolf PA, et al. Aortic calcified plaques and cardiovascular disease (the Framingham Study). Am J Cardiol. 1990; 66: 1060–1064

5. Roberts WC. The senile cardiac calcification syndrome. Am J Cardiol. 1986; 58: 572–574

6. Farzaneh-Far A, Proudfoot D, Shanahan C, et al. Vascular and valvar calcification: recent advances. Heart. 2001; 85: 13–17

7. Demer LL, Tintut Y. Vascular calcification: pathobiology of a multifaceted disease. Circulation. 2008; 117: 2938–2948

8. Schuijf JD, Wijns W, Jukema JW, et al. Relationship between noninvasive coronary angiography with multi-slice computed tomography and myocardial perfusion imaging. J Am Coll Cardiol. 2006; 48: 2508–2514
9. Schuijf JD, Pundziute G, Jukema JW, et al. Diagnostic accuracy of 64-slice multislice computed tomography in the noninvasive evaluation of significant coronary artery disease. Am J Cardiol. 2006; 98: 145–148
10. Agatston AS, Janowitz WR, Hildner FJ, et al. Quantification of coronary artery calcium using ultrafast computed tomography. J Am Coll Cardiol. 1990; 15: 827–832
11. Austen WG, Edwards JE, Frye RL, et al. A reporting system on patients evaluated for coronary artery disease (Report of the Ad Hoc Committee for Grading of Coronary Artery Disease, Council on Cardiovascular Surgery, American Heart Association). Circulation. 1975; 51: 5–40
12. Stewart BF, Siscovick D, Lind BK, et al. Clinical factors associated with calcific aortic valve disease (Cardiovascular Health Study). J Am Coll Cardiol. 1997; 29: 630–634
13. Jeon DS, Atar S, Brasch AV, et al. Association of mitral annulus calcification, aortic valve sclerosis and aortic root calcification with abnormal myocardial perfusion single photon emission tomography in subjects age < or = 65 years old. J Am Coll Cardiol. 2001; 38: 1988–1993
14. Tolstrup K, Roldan CA, Qualls CR, et al. Aortic valve sclerosis, mitral annular calcium, and aortic root sclerosis as markers of atherosclerosis in men. Am J Cardiol. 2002; 89: 1030–1034
15. Rumberger JA, Simons DB, Fitzpatrick LA, et al. Coronary artery calcium area by electron-beam computed tomography and coronary atherosclerotic plaque area (A histopathologic correlative study). Circulation. 1995; 92: 2157–2162
16. Takasu J, Katz R, Nasir K, et al. Relationships of thoracic aortic wall calcification to cardiovascular risk factors: the Multi-Ethnic Study of Atherosclerosis (MESA). Am Heart J. 2008; 155: 765–771
17. Greenland P, LaBree L, Azen SP, et al. Coronary artery calcium score combined with Framingham score for risk prediction in asymptomatic individuals. JAMA. 2004; 291: 210–215
18. Ho J, FitzGerald S, Stolfus L, et al. Severe coronary artery calcifications are associated with ischemia in patients undergoing medical therapy. J Nucl Cardiol. 2007; 14: 341–346

19. Boon A, Cheriex E, Lodder J, et al. Cardiac valve calcification: characteristics of patients with calcification of the mitral annulus or aortic valve. Heart. 1997; 78: 472–474
20. Bozbas H, Pirat B, Yildirir A, et al. Mitral annular calcification associated with impaired coronary microvascular function. Atherosclerosis. 2008; 198: 115–121
21. Bozbas H, Pirat B, Yildirir A, et al. Coronary flow reserve is impaired in patients with aortic valve calcification. Atherosclerosis. 2008; 197: 846–852
22. Allison MA, Cheung P, Criqui MH, et al. Mitral and aortic annular calcification are highly associated with systemic calcified atherosclerosis. Circulation. 2006; 113: 861–866
23. Adler Y, Herz I, Vaturi M, F et al. Mitral annular calcium detected by transthoracic echocardiography is a marker for high prevalence and severity of coronary artery disease in patients undergoing coronary angiography. Am J Cardiol. 1998; 82: 1183–1186
24. Kannam H, Aronow WS, Chilappa K, et al. Comparison of prevalence of >70% diameter narrowing of one or more major coronary arteries in patients with versus without mitral annular calcium and clinically suspected coronary artery disease. Am J Cardiol. 2008; 101: 467–470
25. Roberts WC, Cohen LS. Left ventricular papillary muscles (Description of the normal and a survey of conditions causing them to be abnormal). Circulation. 1972; 46: 138–154
26. Acarturk E, Bozkurt A, Cayli M, et al. Mitral annular calcification and aortic valve calcification may help in predicting significant coronary artery disease. Angiology. 2003; 54: 561–567
27. Conte L, Rossi A, Cicoira M, et al. Aortic valve sclerosis: a marker of significant obstructive coronary artery disease in patients with chest pain?. J Am Soc Echocardiogr. 2007; 20: 703–708
28. Sui SJ, Ren MY, Xu FY, et al. A high association of aortic valve sclerosis detected by transthoracic echocardiography with coronary arteriosclerosis. Cardiology. 2007; 108: 322–330
29. Schroeder S, Kopp AF, Baumbach A, et al. Noninvasive detection and evaluation of atherosclerotic coronary plaques with multislice computed tomography. J Am Coll Cardiol. 2001; 37: 1430–1435
30. Pundziute G, Schuijf JD, Jukema JW, et al. Impact of coronary calcium score on diagnostic accuracy of multislice computed tomography coronary angiography for detection of coronary artery disease. J Nucl Cardiol. 2007; 14: 36–43

Chapter 8

Incremental Value of Subclinical Left Ventricular Systolic Dysfunction for the Identification of Patients With Obstructive Coronary Artery Disease

Gaetano Nucifora, Joanne D. Schuijf, Victoria Delgado, Matteo Bertini, Arthur J.H.A. Scholte, Arnold C.T. Ng, Jacob M. van Werkhoven, J. Wouter Jukema, Eduard R. Holman, Ernst E. van der Wall, Jeroen J. Bax

Am Heart J 2010;159:148-57

ABSTRACT

Background. Left ventricular (LV) diastolic dysfunction and subclinical systolic dysfunction may be markers of coronary artery disease (CAD). However, whether these markers are useful for prediction of obstructive CAD is unknown.

Methods. A total of 182 consecutive outpatients (54±10 years, 59% males) without known CAD and overt LV systolic dysfunction underwent 64-slice multislice computed tomography (MSCT) coronary angiography and echocardiography. The MSCT angiograms showing atherosclerosis were classified as showing obstructive (≥50% luminal narrowing) CAD or not. Conventional echocardiographic parameters of LV systolic and diastolic function were obtained; in addition, *(1)* global longitudinal strain (GLS) and strain rate (indices of systolic function) and *(2)* global strain rate during the isovolumic relaxation period and during early diastolic filling (indices of diastolic function) were assessed using speckle-tracking echocardiography. In addition, the pretest likelihood of obstructive CAD was assessed using the Duke Clinical Score.

Results. Based on MSCT, 32% of patients were classified as having no CAD, whereas 33% showed nonobstructive CAD and the remaining 35% had obstructive CAD. Multivariate analysis of clinical and echocardiographic characteristics showed that only high pretest likelihood of CAD (odds ratio [OR] 3.21, 95% 1.02-10.09, p = 0.046), diastolic dysfunction (OR 3.72, 95% CI 1.44-9.57, p = 0.006), and GLS (OR 1.97, 95% CI 1.43-2.71, p <0.001) were associated with obstructive CAD. A value of GLS ≥−17.4 yielded high sensitivity and specificity in identifying patients with obstructive CAD (83% and 77%, respectively), providing a significant incremental value over pretest likelihood of CAD and diastolic dysfunction.

Conclusions. The GLS impairment aids detection of patients without overt LV systolic dysfunction having obstructive CAD.

INTRODUCTION

Among patients with suspected coronary artery disease (CAD), scoring tools that take demographic and clinical characteristics into account are traditionally used to estimate the likelihood of obstructive CAD and to identify those who could benefit from further diagnostic tests.[1-3] In the diagnostic workup of these patients, the assessment of left ventricular (LV) function can provide additional information, refining the initial clinical evaluation.[4] In particular, the presence of reduced LV ejection fraction (EF) or wall motion abnormalities significantly increase the likelihood of obstructive CAD.[4,5] In addition, the presence of LV diastolic dysfunction may also be a marker of coronary atherosclerosis, even when global LV systolic function is normal.[6-8]

In patients without overt LV systolic dysfunction, the presence of subclinical reduction of myocardial function may be a marker of CAD as well.[9] For instance, the Multiethnic Study of Atherosclerosis (MESA) observed that a progressive impairment of myocardial contraction (despite normal LVEF) was associated with an increasing severity of coronary atherosclerosis (detected by multislice computed tomography [MSCT] or electron-beam computed tomography).[9]

Although LV diastolic dysfunction and subclinical LV systolic dysfunction have been shown as possible markers of CAD, it is unknown whether their detection could improve patients' stratification. Accordingly, the aim of the present evaluation was 2-fold. *First*, to explore the relation between obstructive CAD, LV diastolic dysfunction, and subclinical LV systolic dysfunction. *Second*, to assess the potential incremental value of LV diastolic dysfunction and subclinical LV systolic dysfunction over the initial estimate of pretest likelihood of obstructive CAD. The MSCT coronary angiography was performed to detect coronary atherosclerosis and obstructive CAD;[10] 2-dimensional echocardiography with speckle-tracking analysis was used to evaluate LV systolic and diastolic function.[11-13]

METHODS

Patient population

A total of 182 consecutive outpatients referred to MSCT for coronary evaluation, because of increased risk profile and/or stable chest pain, were included. Two-dimensional echocardiography with speckle-tracking analysis was performed in all patients within 1 month of MSCT coronary angiography. Both MSCT coronary angiography and extensive echocardiographic examination are part of clinical diagnostic workup of patients with known or suspected CAD.

Patients with overt LV systolic dysfunction (LVEF <50%) or with LV wall motion abnormalities were excluded. Also, patients with a history of CAD, cardiomyopathy, significant (moderate or severe) valvular heart disease, congenital heart disease, rhythm other than sinus, conduction abnormalities, technically inadequate echocardiographic studies, or contraindications to MSCT were excluded. Known CAD was defined as history of acute coronary syndrome, percutaneous or surgical coronary revascularization, and/or angiographically documented coronary stenoses ≥50% luminal diameter.[14] Contraindications for MSCT were known allergy to iodinated contrast agent, renal failure (defined as glomerular filtration rate <30 ml/min), and pregnancy.

For each patient, the presence of coronary risk factors (diabetes, systemic hypertension, hypercholesterolemia, positive family history, cigarette smoking) and the presence of chest pain were recorded. In addition, the pretest likelihood of obstructive CAD was assessed using the Duke Clinical Score,[2] which takes age, gender, coronary risk factors, and type of chest pain into account. In accordance to the Duke Clinical Score, the patient population was then categorized as having a low (≤30%), intermediate (31-70%), or high (>70%) pretest likelihood of obstructive CAD.[15]

Two-dimensional echocardiography

Echocardiography was performed using a commercially available system (Vivid 7 Dimension, GE Health care, Horten, Norway) equipped with a 3.5-MHz transducer. Standard M-mode, 2-dimensional images, and Doppler and color Doppler data were acquired from the parasternal and apical views (4, 2, and 3 chambers) and digitally stored in cine-loop format; analyses were subsequently performed off-line using EchoPAC version 7.0.0 (GE Health care, Horten, Norway).

Left ventricular end-diastolic volume (EDV) and end-systolic volume (ESV) were measured according to the Simpson's biplane method, and LVEF was calculated as [(EDV-ESV)/EDV] ×100. The LV mass was calculated using the formula proposed by Lang et al.[16] and Devereux and Reicheck [17] and normalized for body surface area (LV mass index, gram per square meter).

Transmitral and pulmonary vein flows were obtained by pulsed-wave Doppler tracings, obtained in accordance to the recommendations of the American Society of Echocardiography.[18] Early (E) and late (A) diastolic waves, deceleration time (DT) of E wave, and pulmonary vein systolic (PVs) and diastolic (PVd) velocities were measured. Diastolic function was then classified as follows:[19] *(1)* normal, when the E/A ratio = 0.9-1.5, DT = 160-240 milliseconds, and PVs ≥ PVd; *(2)* diastolic dysfunction grade 1 (mild), when the E/A ratio was <0.9, DT >240 milliseconds, and PVs > > PVd; *(3)* diastolic dysfunction grade 2 (moderate), when the E/A ratio = 0.9-1.5, DT = 160-240 milliseconds, and PVs < PVd; *(4)* diastolic dysfunction grade 3 (severe), when the E/A ratio >2.0, DT <160 milliseconds, and PVs > > PVd; and *(5)* diastolic dysfunction grade 4 (severe), when the E/A ratio >2.5, DT <130 milliseconds, and PVs > > PVd.

In addition, the septal mitral annulus early (E') velocity was measured by tissue Doppler imaging and the E/E' ratio was calculated, as estimate of LV filling pressures.[19,20]

Speckle-tracking analysis

Longitudinal strain analysis of the LV was performed by speckle-tracking imaging (EchoPAC version 7.0.0). Grayscale 2-dimensional apical images of the LV (4-, 2-, and 3-chamber views) were used with frame rate ranging from 80 to 100 frames/s. From an end-systolic frame, the endocardial border was manually traced, and the software traces automatically 2 more concentric regions of interest to include the entire myocardial wall. Speckle-tracking analysis detects and tracks the unique myocardial ultrasound patterns frame by frame. The in-plane frame-to-frame displacement of each pattern over time is used to derive strain. The software validates automatically the segmental tracking along the cardiac cycle and allows the operator further adjustment of the region of interest to improve the tracking quality.

As described previously,[11] mean global longitudinal strain (GLS) and strain rate (GLSR) were calculated, as indices of global LV systolic function, by averaging the global longitudinal strains and strain rates obtained automatically from each apical view (Figure 1). Similarly, the following indices of diastolic function were obtained (Figure 1):[21] *(1)* global strain rate during the isovolumic relaxation period (GSRivrt) and *(2)* global strain rate during early diastolic filling (GSRe).

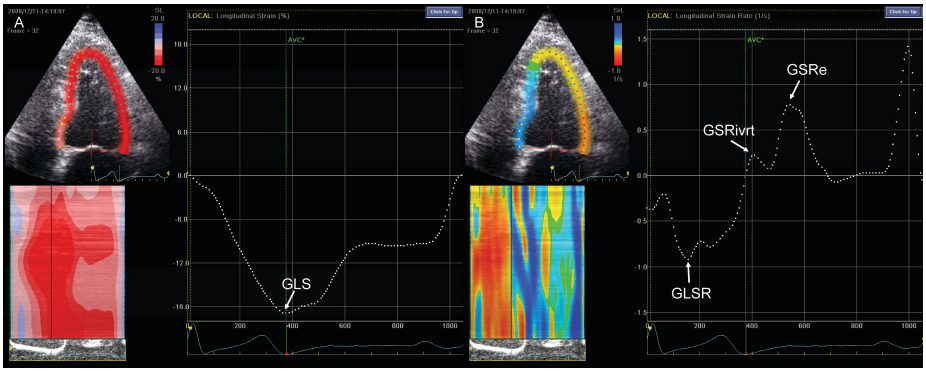

Figure 1. Global longitudinal strain and strain rate curves. Global longitudinal strain (**panel A**) and strain rate (**panel B**) curves obtained by speckle-tracking analysis from an apical 4-chamber view.

Multislice computed tomography

Data acquisition

The MSCT coronary angiography was performed with a 64-slice MSCT scanner (Aquilion 64, Toshiba Medical Systems, Tokyo, Japan). The heart rate and blood pressure were monitored before the examination in each patient. In the absence of contraindications, patients with a heart rate ≥ 65 beat/min were administered oral β-blockers (metoprolol 50 or 100 mg, single dose, 1 hour before the examination). Noninvasive MSCT coronary angiography was therefore performed according to protocols previously described.[10] Data were subsequently transferred to dedicated workstations for postprocessing and evaluation (Vitrea 2, Vital Images, Minnetonka, Minnesota, USA).

Data analysis

The MSCT data analysis was performed by 2 experienced observers who had no knowledge of the patient's medical history, symptom status, and echocardiographic data; disagreement was solved by consensus or evaluation by a third observer. The MSCT coronary angiograms were evaluated for the presence of obstructive CAD (≥50% luminal narrowing) on a patient level. For this purpose, both the original axial dataset as well as curved multiplanar reconstructions were used. Each coronary artery was evaluated for the presence of any atherosclerotic plaque, defined as structures >1 mm2 within and/or adjacent to the coronary artery lumen, which could be clearly distinguished from the vessel lumen and the surrounding pericardial tissue, as described previously.[22] Subsequently, the coronary arteries were further classified as *(1)* completely normal, *(2)* having nonobstructive CAD when atherosclerotic lesions <50% of luminal diameter were present, or *(3)* having obstructive CAD when atherosclerotic lesions ≥50% of luminal diameter were present. The prevalence of normal coronary arteries, (any) CAD (including obstructive

and nonobstructive CAD), and obstructive CAD in the patient population was evaluated.

Statistical analysis

Continues variables are expressed as mean and SD. Categorical data are presented as absolute numbers and percentages. Differences in continuous and categorical variables between patients with normal coronary arteries, nonobstructive CAD, and obstructive CAD at MSCT coronary angiography were assessed using the 1-way analysis of variance test and the chi-square test, respectively; if the result of the analysis was significant, post hoc test with Bonferroni's correction was applied.

Univariate and multivariate logistic regression analysis (enter model) were performed to evaluate the association between the presence of obstructive CAD at MSCT coronary angiography, the traditional assessment of pretest likelihood of obstructive CAD (Duke Clinical Score), and the following echocardiographic variables: LVEF, LV mass index, presence of diastolic dysfunction, E/E' ratio, GLS, GLSR, GSRivrt, and GSRe. Only significant ($p < 0.05$) univariate predictors were entered as covariates in the multivariate model. Odds ratios and 95% CI were calculated. Model discrimination was assessed using C-statistic, and model calibration was assessed using Hosmer-Lemeshow statistic.

Receiver operator characteristic (ROC) curve analysis was performed to determine the accuracy of GLS to detect obstructive CAD, with an area under the curve value of 0.50 indicating no accuracy and a value of 1.00 indicating maximal accuracy. In addition, to determine the potential incremental value of diastolic dysfunction and GLS over the traditional assessment of pretest likelihood of obstructive CAD (Duke Clinical Score), ROC curves were constructed for 3 models: *model 1*, Duke Clinical Score alone; *model 2*, combination of Duke Clinical Score and presence of diastolic dysfunction; and *model 3*, combination of Duke Clinical Score, diastolic dysfunction, and GLS. For this purpose, the statistical significance of the difference between the areas under the ROC curves

was tested using the method proposed by Hanley and McNeil.[23] The Bayes' theorem was then applied to estimate the posttest likelihood of obstructive CAD yielded by the variables that provided incremental value over the pretest likelihood of obstructive CAD (Duke Clinical Score).

In addition, variability and reproducibility of speckle-tracking measurements were assessed. The coefficient of variation (ie, the ratio between the mean value and the SD) was computed for each parameter. Reproducibility of speckle-tracking measurements was analyzed with repeated measurements by 1 experienced observer at 2 different time points and by a second experienced observer in 20 randomly selected individuals. Intraobserver and interobserver agreements for each parameter were evaluated by Bland-Altman analysis. Furthermore, intraclass correlation coefficients were used as indicators of reproducibility.

All statistical tests were 2 sided, and a P value <0.05 was considered statistically significant. Statistical analysis was performed using the SPSS software package (SPSS 15.0; SPSS Inc, Chicago, IL).

The authors are solely responsible for the design and conduct of this study, all study analyses, and the drafting and editing of the paper and its final contents. No extramural funding was used to support this work.

RESULTS

Clinical and echocardiographic characteristics of the patient population

Clinical and echocardiographic characteristics of the patient population are summarized in Table 1. The mean age was 54±10 years, and 108 patients (59%) were male. A total of 76 patients (42%) were asymptomatic, whereas 76 patients (42%) had history of noncardiac chest pain or atypical angina, and 30 patients (16%) had a history of typical angina. The Duke Clinical Score was low, intermediate, and high, respectively, in 88 (48%), 60 (33%), and 34 (19%) patients.

Table 1. Baseline characteristics of the patient population

Variable	n = 182
Age (years)	54±10
Male gender	108 (59%)
Family history of CAD	81 (45%)
Diabetes	42 (23%)
Hypertension	95 (52%)
Smoker	59 (32%)
Hypercholesterolemia	74 (41%)
BMI	26.9±4.5
Symptoms	
- asymptomatic	76 (42%)
- non-anginal or atypical chest pain	76 (42%)
- typical chest pain	30 (16%)
Duke Clinical Score	
- low	88 (48%)
- intermediate	60 (33%)
- high	34 (19%)
LVEDV (ml)	108±30
LVESV (ml)	41±15
LVEF (%)	62±7
LV mass index (g/m^2)	100±26
Diastolic function	
- normal	99 (55%)
- diastolic dysfunction grade 1	79 (43%)
- diastolic dysfunction grade 2	4 (2%)
E/E' ratio	10.0±4.3
GLS (%)	-17.6±2.4
GLSR (s^{-1})	-0.87±0.13
GSRivrt (s^{-1})	0.31±0.13
GSRe (s^{-1})	0.97±0.28

BMI: body mass index; CAD: coronary artery disease; EDV: end-diastolic volume; EF: ejection fraction; ESV: end-systolic volume; GLS: global longitudinal strain; GLSR: global longitudinal strain rate; GSRe: global strain rate during early diastolic filling; GSRivrt: global strain rate during the isovolumic relaxation period; LV: left ventricular.

By definition, LVEF was within normal limits in all patients, whereas diastolic dysfunction was observed in 83 patients (45%). Regarding the speckle-tracking–derived parameters, GLS was −17.6±2.4%, GLSR was

-0.87 ± 0.13 s^{-1}, GSRivrt was 0.31 ± 0.13 s^{-1}, and GSRe was 0.97 ± 0.28 s^{-1}.

Coronary artery disease: correlation with clinical and echocardiographic parameters

Based on the results of MSCT coronary angiography, 59 patients (32%) were classified as having no CAD. A total of 60 patients (33%) showed nonobstructive CAD, whereas at least 1 significant (≥50% luminal narrowing) stenosis was observed in the remaining 63 patients (35%).

The clinical and echocardiographic characteristics of these 3 groups are summarized in Table 2 and Figure 2. Patients with normal coronary arteries were younger and more frequently female; in addition, they showed a lower prevalence of coronary risk factors and less often had typical angina. Consequently, the pretest likelihood of obstructive CAD, assessed using the Duke Clinical Score, was significantly lower in this group of patients as compared to those with nonobstructive CAD and obstructive CAD (analysis of variance $p < 0.001$). No significant difference in LVEF was noted among the 3 groups, whereas the patients with obstructive CAD showed a higher prevalence of diastolic dysfunction, as compared to the other 2 groups (Table 2).

A progressive impairment of the speckle-tracking parameters was observed across the 3 groups of patients (Figure 2); specifically, patients with obstructive CAD had significantly impaired GLS and GLSR, as compared to the other 2 groups (Figure 2). In addition, patients with obstructive CAD showed significantly impaired GSRivrt and GSRe, as compared to the patients with normal coronary arteries (Figure 2).

Table 2. Clinical and echocardiographic characteristics of the patient population in relation to the presence of coronary artery disease

	No CAD (n = 59)	Non-obstructive CAD (n = 60)	Obstructive CAD (n = 63)	p value
Age (years)	49±9 * †	54±9	57±10	<0.001
Male gender	26 (44%) ‡	35 (58%)	47 (75%)	0.003
Family history of CAD	29 (49%)	24 (40%)	28 (44%)	0.60
Diabetes	8 (14%)	15 (25%)	19 (30%)	0.086
Hypertension	25 (42%)	30 (50%)	40 (64%)	0.060
Smoker	13 (22%) §	19 (32%)	27 (43%)	0.048
Hypercholesterolemia	11 (19%) * †	26 (43%)	37 (59%)	<0.001
BMI	26.2±4.6	27.8±4.7	26.5±4.0	0.11
Symptoms	§			0.046
- asymptomatic	27 (46%)	27 (45%)	22 (35%)	
- non-anginal or atypical chest pain	29 (49%)	21 (35%)	26 (41%)	
- typical chest pain	3 (5%)	12 (20%)	15 (24%)	
Duke Clinical Score	† ‖			<0.001
- low	49 (83%)	25 (42%)	14 (22%)	
- intermediate	7 (12%)	25 (42%)	28 (45%)	
- high	3 (5%)	10 (16%)	21 (33%)	
LVEDV (ml)	107±32	105±30	111±29	0.51
LVESV (ml)	41±15	40±15	43±15	0.56
LVEF (%)	63±8	62±7	62±8	0.86
LV mass index (g/m^2)	92±22 ‡	99±23	109±30	0.001
Diastolic function	§	§		0.007
- normal	38 (64%)	38 (63%)	23 (37%)	
- diastolic dysfunction grade 1	21 (36%)	21 (35%)	37 (59%)	
- diastolic dysfunction grade 2	-	1 (2%)	3 (5%)	
E/E' ratio	8.7±2.7 §	10.2±3.5	10.9±5.8	0.014

* = p <0.05 vs. CAD <50%. † = p <0.001 vs. CAD ≥50%. ‡ = p <0.01 vs. CAD ≥50%. § = p <0.05 vs. CAD ≥50%. ‖ = p <0.001 vs. CAD <50%. Abbreviations as in Table 1.

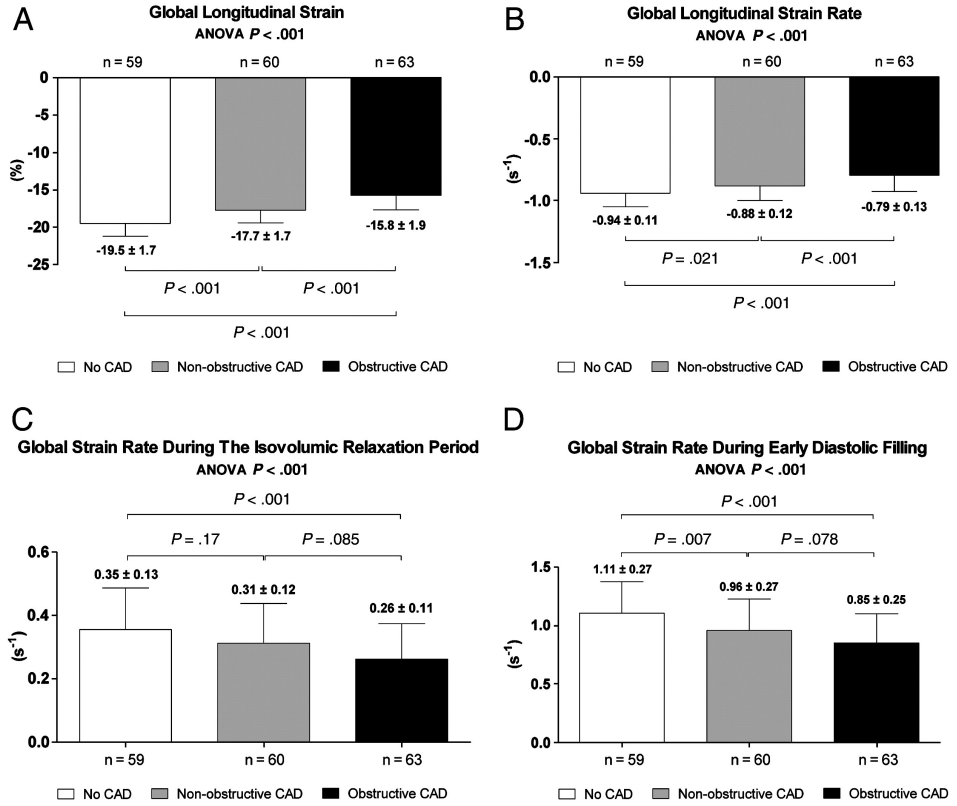

Figure 2. Progressive impairment of the speckle-tracking parameters with increasing severity of CAD. Differences in GLS (**panel A**), GLSR (**panel B**), GSRivrt (**panel C**), and GSRe (**panel D**) among patients with no CAD (white bars), nonobsructive CAD (gray bars), and obstructive CAD (black bars).

Univariate and multivariate analysis

Table 3 shows the results of the univariate and multivariate logistic regression analysis performed to determine the independent correlates of obstructive CAD. At univariate analysis, several variables were significantly related to obstructive CAD as follows: Duke Clinical Score, LV mass index, presence of diastolic dysfunction, GLS, GLSR, GSRivrt, and GSRe. However, at multivariate analysis, only high Duke Clinical Score (odds ratio [OR] 3.21, 95% CI 1.02-10.09, p = 0.046), presence of diastolic dysfunction (OR 3.72, 95% CI 1.44-9.57, p = 0.006), and GLS

(OR 1.97, 95% CI 1.43-2.71, p <0.001) were independent factors associated with obstructive CAD.

At ROC curve analysis (Figure 3), GLS ≥−17.4% had the highest sensitivity and specificity for identification of patients with obstructive CAD (83% and 77%, respectively).

Table 3. Univariate and multivariate logistic regression analyses to determine the independent correlates of obstructive coronary artery disease

	Univariate		Multivariate	
	OR (95% CI)	**p value**	**OR (95% CI)**	**p value**
Duke Clinical Score				
- intermediate vs. low	4.63 (2.16-9.93)	<0.001	2.30 (0.87-6.04)	0.092
- high vs. low	8.54 (3.48-20.94)	<0.001	3.21 (1.02-10.09)	0.046
LVEF *	0.99 (0.95-1.03)	0.60	-	-
LV mass index *	1.02 (1.01-1.04)	0.001	1.01 (0.99-1.03)	0.33
Presence of diastolic dysfunction	3.07 (1.63-5.80)	0.001	3.72 (1.44-9.57)	0.006
E/E' ratio *	1.09 (0.99-1.19)	0.055	-	-
GLS *	2.20 (1.73-2.80)	<0.001	1.97 (1.43-2.71)	<0.001
GLSR †	2.36 (1.69-3.28)	<0.001	1.39 (0.91-2.13)	0.13
GSRivrt †	0.62 (0.48-0.82)	0.001	0.88 (0.61-1.27)	0.50
GSRe †	0.77 (0.68-0.88)	<0.001	1.17 (0.96-1.44)	0.12
			C-statistic = 0.89	

*: OR and 95% CI are intended for 1 unit increase. †: OR and 95% CI are intended for 0.1 unit increase. CI: confidence intervals; OR: odds ratio. Other abbreviations as in Table 1.

Incremental value of GLS to predict obstructive CAD

The ROC curves were generated to determine the predictive value of Duke Clinical Score alone (model 1), Duke Clinical Score combined with the presence of diastolic dysfunction (model 2), and Duke Clinical Score combined with the presence of diastolic dysfunction and GLS (model 3), with respect to obstructive CAD. As shown in Figure 4, the presence of diastolic dysfunction did not provide any incremental value over the Duke Clinical Score (p = .25 for model 2 vs model 1). In contrast, by adding GLS (with ≥−17.4% used as cutoff value) (model 3), the ability to detect

obstructive CAD was significantly improved (area under the curve 0.83, 95% CI 0.77-0.88, p <0.001 vs model 1 and model 2).

The diagnostic impact of GLS on the estimated pretest likelihood of obstructive CAD is shown in Figure 5.

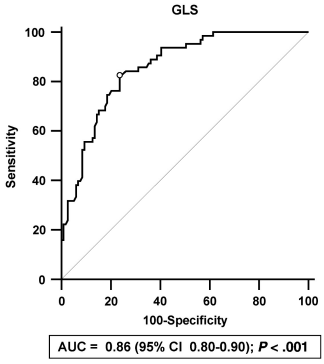

Figure 3. Accuracy of GLS to detect obstructive CAD. Receiver-operator characteristic curve, testing the accuracy of GLS to detect obstructive CAD. GLS ≥−17.4% provided the highest sensitivity (83%) and specificity (77%) for identification of patients with obstructive CAD (positive likelihood ratio 3.51, negative likelihood ratio 0.23). AUC indicates area under the curve.

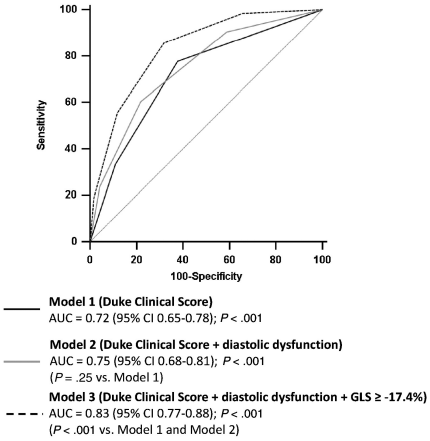

Figure 4. Incremental value of GLS. Receiver-operator characteristic curves testing the potential incremental value of diastolic dysfunction and GLS ≥−17.4% over the Duke Clinical Score to detect obstructive CAD. AUC indicates area under the curve.

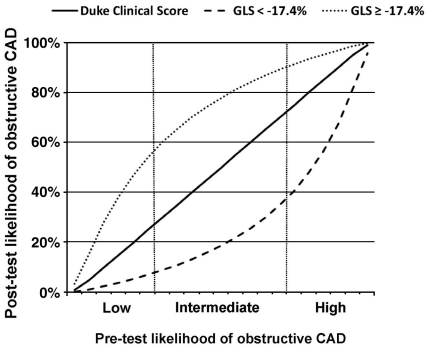

Figure 5. Effect of GLS on probability of obstructive CAD as a function of pretest likelihood. Estimated posttest likelihood of obstructive CAD yielded by the GLS compared to the pretest likelihood of obstructive CAD estimated using the Duke Clinical Score. The positive and negative likelihood ratios provided in the legend of Figure 3 were used to calculate the estimated posttest likelihood of obstructive CAD.

Variability and reproducibility of speckle-tracking parameters

Variability and reproducibility of speckle-tracking measurements are shown in Table 4. The assessment of GLS had lower variability and higher reproducibility, as compared to the assessment of strain rate parameters.

Table 4. Variability and reproducibility of speckle-tracking measurements

	Variability	Intraobserver agreement		Interobserver agreement	
	CV	Mean±2SD	ICC	Mean±2SD	ICC
GLS	0.14	-0.20±0.53%	99%	-0.25±1.37%	97%
GLSR	0.15	-0.02±0.07s^{-1}	97%	-0.03±0.10s^{-1}	93%
GSRivrt	0.42	–0.01±0.10s^{-1}	95%	0.01±0.13s^{-1}	91%
GSRe	0.29	0.03±0.14s^{-1}	97%	-0.02±0.21s^{-1}	95%

CV: coefficient of variation; ICC: intraclass correlation coefficient; SD: standard deviation. Other abbreviations as in Table 1.

DISCUSSION

The results of the present evaluation can be summarized as follows: *(1)* both LV diastolic dysfunction and subclinical LV systolic dysfunction are independently related to obstructive CAD and *(2)* only the presence of subclinical LV systolic dysfunction provides significant incremental value over the Duke Clinical Score for the identification of patients having obstructive CAD.

Relation between CAD and LV diastolic dysfunction

Coronary artery disease is considered one of the potential causes of LV diastolic dysfunction.[24] Previous studies indeed showed a high prevalence of global and regional LV diastolic dysfunction in patients with CAD and normal LV systolic function.[6-8] Moreover, a progressive impairment of LV relaxation has been observed in relation to the severity of coronary atherosclerosis and the number of diseased vessels,[6,25] and a reversal of these abnormalities has been described after percutaneous coronary intervention.[26,27] Several mechanisms have been proposed to explain this association. In particular, it has been postulated that repetitive episodes of subclinical ischemia may impair LV relaxation, which is an active, energy-dependent process.[28] In addition, the presence of severely reduced coronary flow may induce structural remodeling of the myocardium (ie, myocardial fibrosis and hypertrophy and glycogen accumulation), leading to LV diastolic dysfunction.[6]

Confirming these previous observations, an independent relation between LV diastolic dysfunction and obstructive CAD was observed in the present evaluation. However, the clinical use of this relation appeared to be limited because the presence of LV diastolic dysfunction did not provide any incremental value over the traditional assessment of pretest likelihood of obstructive CAD (Duke Clinical Score). Indeed, other factors (ie, diabetes mellitus, hypertension) also can play a role in determining LV

diastolic dysfunction,[29,30] potentially reducing its accuracy in identifying patients with obstructive CAD.

Relation between CAD and subclinical LV systolic dysfunction

Few previous studies addressed the issue of subclinical LV systolic dysfunction in relation to CAD, providing contradictory results. For instance, Bolognesi et al.[31] observed an impairment of LV longitudinal shortening (assessed by tissue-Doppler and long-axis M-mode echocardiography), despite normal LVEF, among patients with obstructive CAD. Conversely, Yuda et al.[6] did not observe any difference in systolic myocardial velocity and strain rate (assessed by tissue-Doppler echocardiography) between LV segments subtended by vessels with and without obstructive CAD. More recently, Edvardsen et al.[9] evaluated the relation between myocardial systolic strain and strain rate (assessed by tagged magnetic resonance imaging) and CAD (expressed as calcium score by MSCT or electron-beam computed tomography) in a large cohort of patients without history of CAD and with normal LVEF. An impairment of regional LV systolic function was observed in relation to the presence of coronary atherosclerosis.

In the present evaluation, speckle-tracking echocardiography and MSCT coronary angiography were used to evaluate the presence of subclinical LV systolic dysfunction and CAD, respectively, in a cohort of patients with increased risk profile and/or stable chest pain and normal LVEF. Speckle-tracking echocardiography (used to assess strain and strain rate) provides a direct measure of myocardial deformation and can therefore be used to detect subtle abnormalities in LV systolic function.[13] The MSCT coronary angiography provides direct noninvasive visualization of the coronary arteries, allowing evaluation of CAD at an early stage.[10]

Interestingly, a progressive impairment of GLS and GLSR was observed with increasing severity of CAD; in addition, an independent relation between GLS and obstructive CAD was found. These data support the hypothesis that subclinical myocardial damage may be a marker of

coronary atherosclerosis even in the absence of myocardial infarction, mainly because of small-vessel microembolization, endothelial dysfunction, or chronic ischemia.[9]

Clinical implications

Besides demonstrating a strong independent relation between subclinical LV systolic dysfunction and obstructive CAD, the present evaluation showed a significant incremental value of GLS over the Duke Clinical Score for identification of patients with obstructive CAD. Especially among the patients with low or intermediate Duke Clinical Score, the presence of subclinical LV systolic dysfunction significantly increased the likelihood of having obstructive CAD. Importantly, the assessment of GLS had lower variability and higher reproducibility, as compared to the assessment of strain rate parameters; these data further confirm the clinical use of GLS and may partially explain why strain rate parameters were not independently related to obstructive CAD.

Accordingly, routine screening for subclinical LV systolic dysfunction among patients with coronary risk factors and/or stable chest pain may possibly refine the traditional clinical assessment and may be useful for selection of further diagnostic tests.

CONCLUSIONS

The LV diastolic dysfunction and subclinical systolic dysfunction are independently related to the presence of obstructive CAD. In particular, subclinical LV systolic dysfunction provides significant incremental value over the Duke Clinical Score for the identification of patients having obstructive CAD.

REFERENCES

1. Diamond GA, Forrester, JS. Analysis of probability as an aid in the clinical diagnosis of coronary-artery disease. N Engl J Med. 1979; 300: 1350–1358
2. Pryor DB, Harrell FE Jr., Lee KL, et al. Estimating the likelihood of significant coronary artery disease. Am J Med. 1983; 75: 771–780
3. Morise AP, Haddad WJ, Beckner, D. Development and validation of a clinical score to estimate the probability of coronary artery disease in men and women presenting with suspected coronary disease. Am J Med. 1997; 102: 350–356
4. Cheitlin MD, Armstrong WF, Aurigemma GP, et al. ACC/AHA/ASE 2003 guideline update for the clinical application of echocardiography—summary article: a report of the American College of Cardiology/American Heart Association Task Force on Practice Guidelines (ACC/AHA/ASE Committee to Update the 1997 Guidelines for the Clinical Application of Echocardiography). J Am Coll Cardiol. 2003; 42: 954–970
5. Chen YZ, Sherrid MV, Dwyer, EM Jr. Value of two-dimensional echocardiography in evaluating coronary artery disease: a randomized blinded analysis. J Am Coll Cardiol. 1985; 5: 911–917
6. Yuda S, Fang ZY, Marwick, TH. Association of severe coronary stenosis with subclinical left ventricular dysfunction in the absence of infarction. J Am Soc Echocardiogr. 2003; 16: 1163–1170
7. Lee KW, Blann AD, Lip, GY. Impaired tissue Doppler diastolic function in patients with coronary artery disease: relationship to endothelial damage/dysfunction and platelet activation. Am Heart J. 2005; 150: 756–766
8. Liang HY, Cauduro S, Pellikka P, et al. Usefulness of two-dimensional speckle strain for evaluation of left ventricular diastolic deformation in patients with coronary artery disease. Am J Cardiol. 2006; 98: 1581–1586
9. Edvardsen T, Detrano R, Rosen BD, et al. Coronary artery atherosclerosis is related to reduced regional left ventricular function in individuals without history of clinical cardiovascular disease: the Multiethnic Study of Atherosclerosis. Arterioscler Thromb Vasc Biol. 2006; 26: 206–211
10. Schuijf JD, Pundziute G, Jukema JW, et al. Diagnostic accuracy of 64-slice multislice computed tomography in the noninvasive evaluation of significant coronary artery disease. Am J Cardiol. 2006; 98: 145–148

11. Reisner SA, Lysyansky P, Agmon Y, et al. Global longitudinal strain: a novel index of left ventricular systolic function. J Am Soc Echocardiogr. 2004; 17: 630–633
12. Amundsen BH, Helle-Valle T, Edvardsen T, et al. Noninvasive myocardial strain measurement by speckle tracking echocardiography: validation against sonomicrometry and tagged magnetic resonance imaging. J Am Coll Cardiol. 2006; 47: 789–793
13. Delgado V, Mollema SA, Ypenburg C, et al. Relation between global left ventricular longitudinal strain assessed with novel automated function imaging and biplane left ventricular ejection fraction in patients with coronary artery disease. J Am Soc Echocardiogr. 2008; 21: 1244–1250
14. Schuijf JD, Wijns W, Jukema JW, et al. Relationship between noninvasive coronary angiography with multi-slice computed tomography and myocardial perfusion imaging. J Am Coll Cardiol. 2006; 48: 2508–2514
15. Meijboom WB, van Mieghem CA, Mollet NR, et al. 64-slice computed tomography coronary angiography in patients with high, intermediate, or low pretest probability of significant coronary artery disease. J Am Coll Cardiol. 2007; 50: 1469–1475
16. Lang RM, Bierig M, Devereux RB, et al. Recommendations for chamber quantification: a report from the American Society of Echocardiography's Guidelines and Standards Committee and the Chamber Quantification Writing Group, developed in conjunction with the European Association of Echocardiography, a branch of the European Society of Cardiology. J Am Soc Echocardiogr. 2005; 18: 1440–1463
17. Devereux RB, Reichek, N. Echocardiographic determination of left ventricular mass in man. Anatomic validation of the method. Circulation. 1977; 55: 613–618
18. Quinones MA, Otto CM, Stoddard M, et al. Recommendations for quantification of Doppler echocardiography: a report from the Doppler Quantification Task Force of the Nomenclature and Standards Committee of the American Society of Echocardiography. J Am Soc Echocardiogr. 2002; 15: 167–184
19. Lester SJ, Tajik AJ, Nishimura RA, et al. Unlocking the mysteries of diastolic function: deciphering the Rosetta Stone 10 years later. J Am Coll Cardiol. 2008; 51: 679–689

20. Nagueh SF, Middleton KJ, Kopelen HA, et al. Doppler tissue imaging: a noninvasive technique for evaluation of left ventricular relaxation and estimation of filling pressures. J Am Coll Cardiol. 1997; 30: 1527–1533
21. Wang J, Khoury DS, Thohan V, et al. Global diastolic strain rate for the assessment of left ventricular relaxation and filling pressures. Circulation. 2007; 115: 1376–1383
22. Leber AW, Knez A, Becker A, et al. Accuracy of multidetector spiral computed tomography in identifying and differentiating the composition of coronary atherosclerotic plaques: a comparative study with intracoronary ultrasound. J Am Coll Cardiol. 2004; 43: 1241–1247
23. Hanley JA, McNeil, BJ. A method of comparing the areas under receiver operating characteristic curves derived from the same cases. Radiology. 1983; 148: 839–843
24. Fischer M, Baessler A, Hense HW, et al. Prevalence of left ventricular diastolic dysfunction in the community. Results from a Doppler echocardiographic-based survey of a population sample. Eur Heart J. 2003; 24: 320–328
25. Rydberg E, Willenheimer R, Erhardt, L. The prevalence of impaired left ventricular diastolic filling is related to the extent of coronary atherosclerosis in patients with stable coronary artery disease. Coron Artery Dis. 2002; 13: 1–7
26. Bonow RO, Kent KM, Rosing DR, et al. Improved left ventricular diastolic filling in patients with coronary artery disease after percutaneous transluminal coronary angioplasty. Circulation. 1982; 66: 1159–1167
27. Tanaka H, Kawai H, Tatsumi K, et al. Improved regional myocardial diastolic function assessed by strain rate imaging in patients with coronary artery disease undergoing percutaneous coronary intervention. J Am Soc Echocardiogr. 2006; 19: 756–762
28. Reduto LA, Wickemeyer WJ, Young JB, et al. Left ventricular diastolic performance at rest and during exercise in patients with coronary artery disease. Assessment with first-pass radionuclide angiography. Circulation. 1981; 63: 1228–1237
29. Galderisi M. Diastolic dysfunction and diabetic cardiomyopathy: evaluation by Doppler echocardiography. J Am Coll Cardiol. 2006; 48: 1548–1551
30. Slama M, Susic D, Varagic J, et al. Diastolic dysfunction in hypertension. Curr Opin Cardiol. 2002; 17: 368–373
31. Bolognesi R, Tsialtas D, Barilli AL, et al. Detection of early abnormalities of left ventricular function by hemodynamic, echo-tissue Doppler imaging, and mitral

Doppler flow techniques in patients with coronary artery disease and normal ejection fraction. J Am Soc Echocardiogr. 2001; 14: 764–772

Part II

ASSESSMENT OF PATIENTS WITH STEMI: ROLE OF ECHOCARDIOGRAPHIC TECHNIQUES

Chapter 9

Real-time 3-Dimensional Echocardiography Early After Acute Myocardial Infarction: Incremental Value of Echo-Contrast for Assessment of Left Ventricular Function

Gaetano Nucifora, Nina Ajmone Marsan, Eduard R. Holman, Hans-Marc J. Siebelink, Jacob M. van Werkhoven, Arthur J. Scholte, Ernst E. van der Wall, Martin J. Schalij, Jeroen J. Bax

Am Heart J 2009;157:882.e1-8

ABSTRACT

Background. Accurate and reproducible assessment of left ventricular (LV) systolic function is important in patients with acute myocardial infarction (AMI). Real-time 3-dimensional echocardiography (RT3DE) is an accurate technique, but it relies heavily on good image quality. The aim of the present study was to evaluate the incremental value of contrast-enhanced RT3DE.

Methods. A total of 140 consecutive patients (58±11 years, 78% men) with ST-elevation AMI clinically underwent nonenhanced and contrast-enhanced RT3DE within 24 hours from AMI to evaluate global and regional LV systolic function. Endocardial border definition was graded for each of the 16 LV segments as follows: *0* = border invisible, *1* = border visualized only partially, and *2* = complete visualization of the border. Three image-quality groups (good, fair, and uninterpretable) were identified. Left ventricular volumes and ejection fraction were measured off-line. Wall motion was graded for each visible segment as follows: *1* = normal, *2* = hypokinetic, *3* = akinetic, and *4* = dyskinetic.

Results. During contrast-enhanced RT3DE, as compared with nonenhanced RT3DE, the number of segments with complete visualization of the endocardial border increased from 66% to 84% ($p < 0.001$); and the number of patients with a good-quality echocardiogram increased from 59% to 94% ($p < 0.001$). Intra- and interobserver agreement for assessment of global and regional LV systolic function improved during contrast-enhanced RT3DE, as compared with nonenhanced RT3DE.

Conclusions. Assessment of LV systolic function in AMI patients with RT3DE is frequently hampered by suboptimal echocardiographic quality. Contrast-enhanced RT3DE is of incremental value, improving the endocardial border visualization and the reproducibility of LV function assessment.

INTRODUCTION

The assessment of global and regional left ventricular (LV) systolic function is extremely important among patients with acute myocardial infarction (AMI) because it carries significant therapeutic and prognostic implications.[1-6] Recently, real-time 3-dimensional echocardiography (RT3DE) has been introduced for assessment of LV function and volumes. Real-time 3D echocardiography has been validated against magnetic resonance imaging and found to be more accurate and reproducible as compared with 2-dimensional echocardiography (2DE).[7-13] However, even more than 2DE, RT3DE relies heavily on the presence of good image quality.[14,15] The use of intravenous contrast agents during 2DE has been shown to be of incremental value, improving LV endocardial border visualization among patients with suboptimal image quality and increasing the accuracy and reproducibility of LV systolic function measurements.[16-22] In contrast, data regarding the use of echo-contrast during RT3DE are scarce.[14,23-25] In particular, no specific data exist about the efficacy of contrast-enhanced RT3DE performed early after AMI; the safety of contrast-enhanced echocardiography early after AMI was recently reported.[26] The aim of the present study was therefore to investigate, in a large cohort of consecutive patients with AMI, the potential incremental value of contrast-enhanced RT3DE over nonenhanced RT3DE for assessment of LV function and volumes.

METHODS

Study population

The study population consisted of 140 patients admitted to the coronary care unit because of ST-elevation AMI. The diagnosis of ST-elevation AMI was made on the basis of typical electrocardiographic changes and/or ischemic chest pain associated with elevation of cardiac biomarkers.[27]

All patients underwent immediate coronary angiography and primary percutaneous coronary intervention. As part of the clinical workup, RT3DE (with echo-contrast) was performed in the coronary care unit within 24 hours from patients' admission to accurately evaluate global and regional LV systolic function. Of note, the safety profile of echo-contrast infusion in 115 of these patients has been recently reported using conventional 2DE.[26]

Echocardiography

Patients were imaged in left lateral decubitus position with a commercially available system (Vivid 7; GE Healthcare, Horten, Norway) equipped with a 3-V phased array transducer (2.5 MHz). First, apical full-volume 3D data sets were acquired in harmonic mode, integrating, during a brief breath hold, 8 R wave–triggered subvolumes into a larger pyramidal volume (90° by 90°) with a complete capture of the LV. Thereafter, the same acquisition was repeated during echo-contrast administration (Luminity; Bristol-Myers Squibb Pharma, Bruxelles, Belgium) to optimize LV border delineation. Each patient received an intravenous infusion of 1.3 ml of echo-contrast diluted in 50 ml of 0.9% NaCl solution; the rate of infusion was initially set at 4.0 ml/min and then titrated to achieve optimal LV chamber opacification and endocardial border delineation.[28] Contrast-enhanced RT3DE was performed in harmonic mode at low mechanical index (0.26), and care was taken to record the images at a phase when echo-contrast flow was relatively stable with absent or minimal swirling in the apex. The 3D data sets were digitally stored for the off-line analysis.

Echocardiographic analysis

The 3D data sets were analyzed online for the analysis of LV chamber opacification and off-line for the analysis of LV endocardial border definition and LV volumes and function. The off-line analysis was performed using a dedicated software (4D LV-Analysis; TomTec, Munich, Germany) by an observer who had no knowledge of the patient's identity,

medical history, and symptom status. As described elsewhere,[29] the software automatically displays in a quad screen the 4-chamber view, as a reference view; the 2- and 3- chamber views with default interplane angles at 60° ; and a short-axis view (Figure 1). The interplane angles can be manually modified to obtain adequate orientation of the 3 apical views, and their meeting point can be adjusted in the middle of the LV cavity to avoid LV foreshortening. This procedure can also be used to evaluate regions between the 3 adjacent conventional apical views.

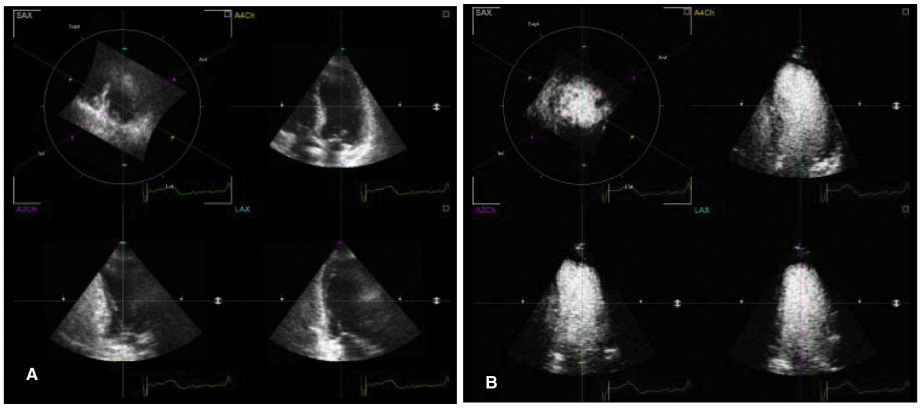

Figure 1. Panel A. Example of fair-quality echocardiogram during nonenhanced RT3DE. **Panel B.** Optimal LV chamber opacification and improved endocardial border definition during contrast-enhanced RT3DE in the same patient. The 3 apical views are shown with the 4-chamber view as a reference view in the top right and the 2- and 3-chamber views in the bottom left and bottom right, respectively. Top left: short-axis view.

LV chamber opacification

The degree of LV chamber opacification during echo-contrast administration was graded according to 5-point rating scale:[17,28] *0* = no contrast enhancement, *1* = weak or little contrast enhancement, *2* = adequate contrast enhancement that facilitates image interpretation, *3* = full contrast enhancement that definitely aids image interpretation, and *4* = excessive contrast enhancement that hampers interpretation. The

percentage of patients with adequate-to-full contrast enhancement was calculated. The mean time needed to achieve adequate-to-full contrast enhancement was measured.

LV endocardial border definition

Qualitative assessment of the endocardial border was performed in both nonenhanced and contrast-enhanced images. A standard 16-segment model was used.[30] Adequacy of LV endocardial border definition was graded for each of the 16 cardiac segments as follows:[22] *0* = border invisible, *1* = border visualized only partially throughout the cardiac cycle and/or incomplete segment length, and *2* = complete visualization of the border. A global endocardial visualization score was calculated as the sum of each LV segment's score.

On basis of the global score, 3 image-quality groups were defined: good (score 25-32), fair (score 17-24), and uninterpretable (score $\leq$16).[15,22] Uninterpretable echocardiograms were deemed nondiagnostic, and further analyses of LV volumes and global and regional LV functions were considered not feasible.

LV volumes and global systolic function

The algorithm used by the software to calculate LV end-diastolic volume (EDV), LV end-systolic volume (ESV), and LV ejection fraction (EF) is described in detail elsewhere.[29] Briefly, the endocardial border is manually traced in the 3 apical views (including LV trabeculations and papillary muscles within the cavity) in both the end-diastolic and end-systolic frames. Subsequently, the software automatically identifies the endocardial border in the entire 3D data set; further manual adjustments are possible in approximately 30 coronal and sagittal planes. Finally, a reconstruction of the LV model is generated; and LV volumes and LVEF are obtained.

LV regional function

Qualitative assessment of the regional wall motion was performed in both nonenhanced and contrast-enhanced images, according to the same 16-segment model used for the evaluation of LV endocardial border definition.[30] Segments with invisible endocardial border were excluded from this analysis. Wall motion was graded for each of the visualized segments as follows: *1* = normal, *2* = hypokinetic, *3* = akinetic, and *4* = dyskinetic. A global wall motion score index (WMSI) was calculated as the sum of each LV segment's score divided by the number of visualized segments.

Reproducibility of RT3DE measurements

The data sets of 20 patients with a good-quality echocardiogram and 20 patients with a fair-quality echocardiogram during nonenhanced RT3DE were randomly selected and analyzed again 1 month later by the original observer and by a second observer who was blinded to the results of the previous analysis. Intra- and interobserver agreement was assessed for the measurements of LV volumes and LVEF and the grading of regional wall motion.

Statistical analysis

Continues variables are expressed as mean and SD. Categorical data are presented as absolute numbers and percentages. The global endocardial visualization score and the measurements of LV volumes, LVEF, and WMSI were compared between the 2 imaging techniques with the paired t test. To determine whether there was a statistically significant difference in the comparison between categorical variables, the McNemar test was performed for binary data and the marginal homogeneity test for multinomial response data.

Intra- and interobserver agreement in the measurements of LV volumes and LVEF were assessed using Bland-Altman analysis and expressed as

the mean difference between the 2 measurements ±2 SDs. To evaluate intra- and interobserver agreement in the grading of regional wall motion, weighted κ test was used and the level of agreement was interpreted as follows: 0 to 0.2 = poor to slight, 0.21 to 0.4 = fair, 0.41 to 0.6 = moderate, 0.61 to 0.8 = substantial, and 0.81 to 1.0 = nearly perfect. A p value < 0.05 was considered statistically significant. Statistical analysis was performed using the SPSS software package (SPSS 15.0, Chicago, IL).

The authors are solely responsible for the design and conduct of this study, all study analyses, the drafting and editing of the paper, and its final contents. No extramural funding was used to support this work.

Table 1. Clinical and echocardiographic patient characteristics

Variable	n = 140
Age (years)	58±11
Gender (male/female)	109/31
Diabetes	16 (11%)
Family history of coronary artery disease	54 (39%)
Hypercholesterolemia	26 (19%)
Hypertension	50 (36%)
Current or previous smoking	85 (61%)
Previous myocardial infarction	15 (11%)
Previous myocardial revascularization	12 (9%)
Body mass index (kg/m^2)	27±4
Current anterior myocardial infarction	60 (43%)
Current infarct-related artery	
- left anterior descending coronary artery	60 (43%)
- left circumflex coronary artery	19 (13%)
- right coronary artery	61 (44%)
Multi-vessel coronary artery disease	51 (36%)

RESULTS

Study population

The baseline characteristics of the study population are summarized in Table 1. Mean age of the patients was 58±11 years; 109 (78%) were

male. The infarct-related artery was the left anterior descending coronary artery in 60 (43%) patients, the left circumflex coronary artery in 19 (13%), and the right coronary artery in 61 (44%). Obstructive multivessel disease (ie, >1 vessel with a luminal narrowing ≥70%) was present in 51 (36%) patients.

Echocardiography

The mean infusion rate of echo-contrast was 3.0±0.6 ml/min, and the total infusion dose was on average 16 μL/kg.

LV chamber opacification

Adequate-to-full enhancement during echo-contrast infusion was noted in 130 (93%) patients. Weak or little contrast enhancement was observed in 9 (6%) patients and excessive contrast enhancement in 1 (1%) patient. The mean time needed to achieve adequate-to-full LV contrast enhancement was 65±20 seconds.

LV endocardial border definition

During nonenhanced RT3DE, from the total number of 2,240 LV segments, the endocardial border was invisible in 243 (11%) and visualized only partially in 509 (23%). A complete visualization of the border was possible in 1,488 (66%) segments (Table 2). The mean global endocardial visualization score was 25±6. A total of 82 (59%) patients had a good-quality echocardiogram, whereas 44 (31%) and 14 (10%) had a fair-quality and uninterpretable echocardiogram, respectively (Figure 2).

Table 2. Left ventricular endocardial border definition with non-enhanced and contrast-enhanced RT3DE

	Non-enhanced RT3DE	Contrast-enhanced RT3DE	p value
Overall segments (n = 2240)			<0.001
- border invisible	243 (11%)	16 (1%)	
- border visualized only partially	509 (23%)	334 (15%)	
- complete visualization of the border	1488 (66%)	1890 (84%)	
Anterior wall segments (n = 420)			<0.001
- border invisible	118 (28%)	4 (1%)	
- border visualized only partially	145 (35%)	139 (33%)	
- complete visualization of the border	157 (37%)	277 (66%)	
Antero-lateral wall segments (n = 420)			<0.001
- border invisible	40 (10%)	1 (0%)	
- border visualized only partially	151 (36%)	46 (11%)	
- complete visualization of the border	229 (54%)	373 (89%)	
Anterior septum segments (n = 280)			<0.001
- border invisible	55 (20%)	5 (2%)	
- border visualized only partially	64 (23%)	57 (20%)	
- complete visualization of the border	161 (57%)	218 (78%)	
Inferior wall segments (n = 420)			0.04
- border invisible	13 (3%)	2 (1%)	
- border visualized only partially	52 (12%)	52 (12%)	
- complete visualization of the border	355 (85%)	366 (87%)	
Infero-lateral wall segments (n = 280)			<0.001
- border invisible	7 (2%)	2 (1%)	
- border visualized only partially	67 (24%)	29 (10%)	
- complete visualization of the border	206 (74%)	249 (89%)	
Inferior septum segments (n = 420)			<0.001
- border invisible	10 (2%)	2 (1%)	
- border visualized only partially	30 (7%)	11 (2%)	
- complete visualization of the border	380 (91%)	407 (97%)	

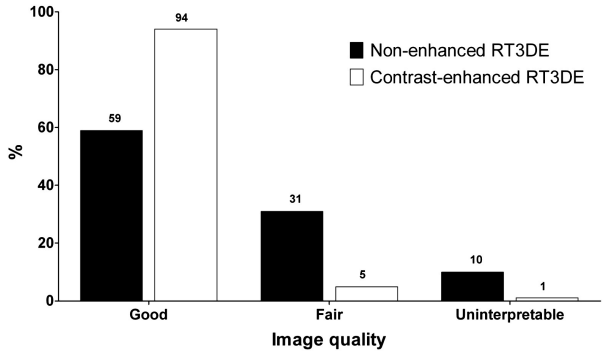

Figure 2. Image quality during nonenhanced and contrast-enhanced RT3DE. P <0.001 for comparison between the 2 imaging techniques.

During contrast-enhanced RT3DE, a complete visualization of the border was possible in 1,890 (84%) segments (p <0.001 vs nonenhanced RT3DE) (Table 2). The LV endocardial border definition significantly improved in the segments of each LV wall (Table 2). As compared with nonenhanced RT3DE, the mean global endocardial visualization score improved to 29±3 (p <0.001). A total of 131 (94%) patients had a good-quality echocardiogram, whereas 7 (5%) and 2 (1%) had a fair-quality and uninterpretable echocardiogram, respectively (p <0.001 vs nonenhanced RT3DE) (Figure 2).

An example of LV chamber opacification and improved endocardial border definition during contrast-enhanced RT3DE, as compared with nonenhanced RT3DE, is displayed in Figure 1.

LV volumes and global systolic function

Nonenhanced RT3DE provided significantly lower values of LVEDV as compared with contrast-enhanced RT3DE (107±28 vs 113±27 ml, p <0.001). The values of LVESV were not statistically different between the 2 techniques (59±21 vs 61±20 ml, p = not significant). Accordingly, nonenhanced RT3DE provided slightly but significantly lower values of

LVEF (45±9% [median 46%, interquartile range 39-51%] vs 47±9% [median 47%, interquartile range 39-53%], p = 0.003).

LV regional systolic function

Wall motion score index assessed on nonenhanced and contrast-enhanced images was 1.8±0.4 and 1.7±0.4, respectively (p = 0.04).

Reproducibility of RT3DE measurements

Intra- and interobserver agreement for the measurements of LV volumes and LVEF and the grading of regional wall motion obtained with the 2 techniques is shown in Table 3 and Table 4. The weakest agreements were observed among patients with a fair-quality echocardiogram. Contrast-enhanced RT3DE improved intra- and interobserver agreement in both good and fair echocardiograms.

Table 3. Intra- and inter-observer agreements for the measurements of left ventricular volumes and left ventricular global function, in relation to image quality during non-enhanced RT3DE

	Good quality echocardiogram during non-enhanced RT3DE		Fair quality echocardiogram during non-enhanced RT3DE	
Intra-observer agreement				
	Non-enhanced	**Contrast-enhanced**	**Non-enhanced**	**Contrast-enhanced**
LVEDV	-1.5±28.0	-0.7±6.8	-4.5±42	4.0±12.8
LVESV	-1.0±17.0	0.2±5.4	-2.7±24.8	3.1±5.6
LVEF	-0.1±10.0	-0.4±4.6	1.7±14.8	-0.8±5.0
Inter-observer agreement				
	Non-enhanced	**Contrast-enhanced**	**Non-enhanced**	**Contrast-enhanced**
LVEDV	-6.1±36.2	-0.6±13.8	-6.6±44.2	4.8±17.4
LVESV	-4.2±20.2	0.5±9.2	-6.4±36.2	3.8±12.6
LVEF	1.0±12.8	-0.7±7.4	2.2±22.4	-1.4±8.8

Intra- and interobserver agreements for the measurements of LV volumes and LVEF were assessed using the method proposed by Bland and Altman and expressed as the mean difference between the 2 measurements ±2 SDs.

Table 4. Intra- and inter-observer agreements for the grading of left ventricular regional wall motion, in relation to image quality during non-enhanced RT3DE

	Good quality echocardiogram during non-enhanced RT3DE		Fair quality echocardiogram during non-enhanced RT3DE	
Intra-observer agreement				
	Non-enhanced	**Contrast-enhanced**	**Non-enhanced**	**Contrast-enhanced**
LV RWM	0.77	0.95	0.69	0.92
Inter-observer agreement				
	Non-enhanced	**Contrast-enhanced**	**Non-enhanced**	**Contrast-enhanced**
LV RWM	0.65	0.87	0.54	0.85

Intra- and interobserver agreements for the grading of LV RWM were assessed using the weighted κ test and expressed as weighted κ value. RWM: regional wall motion.

DISCUSSION

The current results show that, among unselected patients in the early stage of AMI, contrast-enhanced RT3DE has a high feasibility (93%) and is of incremental value for the assessment of LV systolic function. Specifically, as compared with nonenhanced RT3DE, *(1)* it significantly increased the number of LV segments with a complete visualization of the endocardial border (from 66% to 84%); *(2)* it increased the number of good-quality echocardiograms (from 59% to 94%); and *(3)* it reduced the number of fair-quality and uninterpretable echocardiograms (from 41% to 6%). Moreover, intra- and interobserver agreement for the measurements of global and regional LV systolic function improved during contrast-enhanced RT3DE, particularly among patients with fair-quality echocardiogram during nonenhanced RT3DE.

Advantages and limitations of RT3DE

The most commonly used imaging modality for the evaluation of global and regional LV systolic function is 2DE. However, 2DE relies on

significant geometric assumptions, resulting in modest agreement with reference methods and fair reproducibility.[17,31]

More recently, RT3DE has been proposed to overcome the above-mentioned limitations of 2DE; RT3DE correlated well with magnetic resonance imaging for assessment of LV volumes and LVEF.[8-11] In addition, it has been suggested that RT3DE has potential advantages for the evaluation of regional LV function in regions/planes that could not be adequately visualized with 2DE.[7,13]

Because of its higher accuracy and reproducibility, RT3DE could be extremely useful for serial assessment of systolic function.[32] Real-time 3D echocardiography would be particularly useful in AMI patients, in whom accurate assessment of LV function and volumes is important for prediction of future adverse events.[2,3]

However, RT3DE still has several limitations; particularly, RT3DE image quality is highly dependent on the acoustic window because of a lower spatial and temporal resolution as compared with 2DE.[11,24] Accordingly, adequate endocardial border delineation may be difficult on RT3DE still frames, even in the presence of relatively good-quality 2DE.[33] Because of this limitation, most of the previous RT3DE studies included only patients with an optimal acoustic window.[8-10] Few studies explored the feasibility of RT3DE, in relation to the image quality, for the assessment of LV systolic function in unselected population and reported a prevalence of uninterpretable or poor-quality RT3DE images in the range of 35%.[15,24] This issue may be even more prominent in patients with AMI, in whom adequate assessment of LV function and volumes is important for prognosis, but in whom RT3DE data acquisition may be hampered by reduced patient mobility.[12,34] In the present study, 41% of 140 consecutive patients referred to RT3DE within 24 hours from AMI had a fair-quality or uninterpretable echocardiogram. This percentage is in line with previous studies [15,24] and may also be related to technical limitations associated to the performance of RT3DE in the coronary care unit, as well as the high body mass index of our study population.

Incremental value of contrast-enhanced RT3DE

In the subset of patients with inadequate RT3DE images, contrast agents could improve LV endocardial border visualization, increasing the feasibility, accuracy, and reproducibility of LV function assessment as previously reported with 2DE.[16-22]

Thus far, few small studies [14,23-25] (16, 20, 39, and 50 patients, respectively) previously assessed the accuracy of contrast-enhanced RT3DE, reporting a good agreement between contrast-enhanced RT3DE and magnetic resonance imaging for assessment of LV function and volumes.

However, data regarding the feasibility of contrast-enhanced RT3DE and its incremental value over nonenhanced RT3DE (in terms of improved image quality) have not been shown. In the present study, we reported our experience on the feasibility and efficacy of contrast-enhanced RT3DE in a large, unselected cohort of patients in the early stage of AMI. Echo-contrast infusion ensured optimal LV opacification in 93% of the patients. Moreover, the definition of the endocardial border significantly increased with the use of echo-contrast, allowing more reliable and reproducible assessment of regional wall motion abnormalities. Of note, visualization of the anterior and anterolateral walls particularly improved with the use of echo-contrast.

Overall, the prevalence of good-quality echocardiograms increased from 59% to 94% with the intravenous contrast. The prevalence of fair image quality and uninterpretable echocardiograms decreased from 31% to 5% and from 10% to 1%, respectively.

Taking into account these data, the use of echo-contrast should therefore be advocated whenever a confident and reproducible assessment of LV systolic function is not possible because of suboptimal RT3DE images to increase the number of patients who could benefit from an RT3DE assessment of LV systolic function.

Study limitations

The present study has some limitations that should be acknowledged. First, the semiautomated algorithm used for LV volume analysis requires manual tracing of the endocardial border in the 3 apical planes, which is a subjective procedure that could alter the reproducibility of the technique. Second, an independent criterion standard (eg, magnetic resonance imaging) was not performed; and therefore, data about accuracy of contrast-enhanced RT3DE could not be provided.

REFERENCES

1. Nishimura RA, Reeder GS, Miller FA Jr, et al. Prognostic value of predischarge 2-dimensional echocardiogram after acute myocardial infarction. Am J Cardiol. 1984; 53: 429–432

2. Serruys PW, Simoons ML, Suryapranata H, et al. Preservation of global and regional left ventricular function after early thrombolysis in acute myocardial infarction. J Am Coll Cardiol. 1986; 7: 729–742

3. White HD, Norris RM, Brown MA, et al. Left ventricular end-systolic volume as the major determinant of survival after recovery from myocardial infarction. Circulation. 1987; 76: 44–51

4. Berning J, Steensgaard-Hansen F. Early estimation of risk by echocardiographic determination of wall motion index in an unselected population with acute myocardial infarction. Am J Cardiol. 1990; 65: 567–576

5. Volpi A, De Vita C, Franzosi MG, et al. Determinants of 6-month mortality in survivors of myocardial infarction after thrombolysis. Results of the GISSI-2 data base. The Ad hoc Working Group of the Gruppo Italiano per lo Studio della Sopravvivenza nell'Infarto Miocardico (GISSI)-2 Data Base. Circulation. 1993; 88: 416–429

6. Oh JK, Gibbons RJ, Christian TF, et al. Correlation of regional wall motion abnormalities detected by two-dimensional echocardiography with perfusion defect determined by technetium 99m sestamibi imaging in patients treated with reperfusion therapy during acute myocardial infarction. Am Heart J. 1996; 131: 32–37

7. Collins M, Hsieh A, Ohazama CJ, et al. Assessment of regional wall motion abnormalities with real-time 3-dimensional echocardiography. J Am Soc Echocardiogr. 1999; 12: 7–14
8. Jenkins C, Bricknell K, Hanekom L, et al. Reproducibility and accuracy of echocardiographic measurements of left ventricular parameters using real-time three-dimensional echocardiography. J Am Coll Cardiol. 2004; 44: 878–886
9. Sugeng L, Mor-Avi V, Weinert L, et al. Quantitative assessment of left ventricular size and function: side-by-side comparison of real-time three-dimensional echocardiography and computed tomography with magnetic resonance reference. Circulation. 2006; 114: 654–661
10. Jenkins C, Bricknell K, Chan J, et al. Comparison of two- and three-dimensional echocardiography with sequential magnetic resonance imaging for evaluating left ventricular volume and ejection fraction over time in patients with healed myocardial infarction. Am J Cardiol. 2007; 99: 300–306
11. Badano LP, Dall'Armellina E, Monaghan MJ, et al. Real-time three-dimensional echocardiography: technological gadget or clinical tool?. J Cardiovasc Med (Hagerstown). 2007; 8: 144–162
12. Arruda-Olson AM, Bursi F, Gerber Y, et al. Three-dimensional echocardiography for evaluating left ventricular function in patients with ST elevation myocardial infarction: a pilot study. Mayo Clin Proc. 2008; 83: 372–373
13. Jaochim Nesser H, Sugeng L, Corsi C, et al. Volumetric analysis of regional left ventricular function with real-time three-dimensional echocardiography: validation by magnetic resonance and clinical utility testing. Heart. 2007; 93: 572–578
14. Corsi C, Coon P, Goonewardena S, et al. Quantification of regional left ventricular wall motion from real-time 3-dimensional echocardiography in patients with poor acoustic windows: effects of contrast enhancement tested against cardiac magnetic resonance. J Am Soc Echocardiogr. 2006; 19: 886–893
15. Tighe DA, Rosetti M, Vinch CS, et al. Influence of image quality on the accuracy of real time three-dimensional echocardiography to measure left ventricular volumes in unselected patients: a comparison with gated-SPECT imaging. Echocardiography. 2007; 24: 1073–1080
16. Hundley WG, Kizilbash AM, Afridi I, et al. Administration of an intravenous perfluorocarbon contrast agent improves echocardiographic determination of left ventricular volumes and ejection fraction: comparison with cine magnetic resonance imaging. J Am Coll Cardiol. 1998; 32: 1426–1432

17. Kitzman DW, Goldman ME, Gillam LD, et al. Efficacy and safety of the novel ultrasound contrast agent perflutren (definity) in patients with suboptimal baseline left ventricular echocardiographic images. Am J Cardiol. 2000; 86: 669–674
18. Thomson HL, Basmadjian AJ, Rainbird AJ, et al. Contrast echocardiography improves the accuracy and reproducibility of left ventricular remodeling measurements: a prospective, randomly assigned, blinded study. J Am Coll Cardiol. 2001; 38: 867–875
19. Malm S, Frigstad S, Sagberg E, et al. Accurate and reproducible measurement of left ventricular volume and ejection fraction by contrast echocardiography: a comparison with magnetic resonance imaging. J Am Coll Cardiol. 2004; 44: 1030–1035
20. Hoffmann R, von Bardeleben S, ten Cate F, et al. Assessment of systolic left ventricular function: a multi-centre comparison of cineventriculography, cardiac magnetic resonance imaging, unenhanced and contrast-enhanced echocardiography. Eur Heart J. 2005; 26: 607–616
21. Hoffmann R, von Bardeleben S, Kasprzak JD, et al. Analysis of regional left ventricular function by cineventriculography, cardiac magnetic resonance imaging, and unenhanced and contrast-enhanced echocardiography: a multicenter comparison of methods. J Am Coll Cardiol. 2006; 47: 121–128
22. Galema TW, Geleijnse ML, Yap SC, et al. Assessment of left ventricular ejection fraction after myocardial infarction using contrast echocardiography. Eur J Echocardiogr. 2008; 9: 250–254
23. Caiani EG, Coon P, Corsi C, et al. Dual triggering improves the accuracy of left ventricular volume measurements by contrast-enhanced real-time 3-dimensional echocardiography. J Am Soc Echocardiogr. 2005; 18: 1292–1298
24. Krenning BJ, Kirschbaum SW, Soliman OI. et al. Comparison of contrast agent-enhanced versus non-contrast agent-enhanced real-time three-dimensional echocardiography for analysis of left ventricular systolic function. Am J Cardiol. 2007; 100: 1485–1489
25. Jenkins C, Moir S, Chan J, et al. Left ventricular volume measurement with echocardiography: a comparison of left ventricular opacification, three-dimensional echocardiography, or both with magnetic resonance imaging. Eur Heart J. 2009; 30: 98–106

26. Nucifora G, Ajmone Marsan N, Siebelink HM, et al. Safety of contrast-enhanced echocardiography within 24 h after acute myocardial infarction. Eur J Echocardiogr. 2008; 9: 816–818
27. Thygesen K, Alpert JS, White HD, et al. Universal definition of myocardial infarction. Circulation. 2007; 116: 2634–2653
28. Weissman NJ, Cohen MC, Hack TC, et al. Infusion versus bolus contrast echocardiography: a multicenter, open-label, crossover trial. Am Heart J. 2000; 139: 399–404
29. Soliman OI, Krenning BJ, Geleijnse ML, et al. A comparison between QLAB and TomTec full volume reconstruction for real time three-dimensional echocardiographic quantification of left ventricular volumes. Echocardiography. 2007; 24: 967–974
30. Lang RM, Bierig M, Devereux RB, et al. Recommendations for chamber quantification: a report from the American Society of Echocardiography's Guidelines and Standards Committee and the Chamber Quantification Writing Group, developed in conjunction with the European Association of Echocardiography, a branch of the European Society of Cardiology. J Am Soc Echocardiogr. 2005; 18: 1440–1463
31. McGowan JH, Cleland, JG. Reliability of reporting left ventricular systolic function by echocardiography: a systematic review of 3 methods. Am Heart J. 2003; 146: 388–397
32. Chan J, Jenkins C, Khafagi F, et al. What is the optimal clinical technique for measurement of left ventricular volume after myocardial infarction? A comparative study of 3-dimensional echocardiography, single photon emission computed tomography, and cardiac magnetic resonance imaging. J Am Soc Echocardiogr. 2006; 19: 192–201
33. Nemes A, Geleijnse ML, Krenning BJ, et al. Usefulness of ultrasound contrast agent to improve image quality during real-time three-dimensional stress echocardiography. Am J Cardiol. 2007; 99: 275–278
34. Olszewski R, Timperley J, Szmigielski C, et al. The clinical applications of contrast echocardiography. Eur J Echocardiogr. 2007; 8: S13–S23

Chapter 10

Left Ventricular Muscle and Fluid Mechanics in Acute Myocardial Infarction

Gaetano Nucifora, Victoria Delgado, Matteo Bertini, Nina Ajmone Marsan, Nico R. Van de Veire, Arnold C.T. Ng, Hans-Marc J. Siebelink, Martin J. Schalij, Eduard R. Holman, Partho P. Sengupta, Jeroen J. Bax

Am J Cardiol 2010;106:1404–1409

ABSTRACT

Left ventricular (LV) diastolic filling is characterized by the formation of intraventricular rotational bodies of fluid (termed "vortex rings") that optimize the efficiency of LV ejection. The aim of the present study was to evaluate the morphology and dynamics of LV diastolic vortex ring formation early after acute myocardial infarction (AMI), in relation to LV diastolic function and infarct size. A total of 94 patients with a first ST-segment elevation AMI (59±11 years; 78% men) were included. All patients underwent primary percutaneous coronary intervention. After 48 hours, the following examinations were performed: 2-dimensional echocardiography with speckle-tracking analysis to assess the LV systolic and diastolic function, the vortex formation time (VFT, a dimensionless index for characterizing vortex formation), and the LV untwisting rate; contrast echocardiography to assess LV vortex morphology; and myocardial contrast echocardiography to identify the infarct size. Patients with a large infarct size (≥3 LV segments) had a significantly lower VFT ($p < 0.001$) and vortex sphericity index ($p < 0.001$). On univariate analysis, several variables were significantly related to the VFT, including anterior AMI, LV end-systolic volume, LV ejection fraction, grade of diastolic dysfunction, LV untwisting rate, and infarct size. On multivariate analysis, the LV untwisting rate ($\beta = -0.43$, $p < 0.001$) and infarct size ($\beta = -0.33$, $p = 0.005$) were independently associated with VFT. In conclusion, early in AMI, both the LV infarct size and the mechanical sequence of diastolic restoration play key roles in modulating the morphology and dynamics of early diastolic vortex ring formation.

INTRODUCTION

The assessment of left ventricular (LV) diastolic function usually relies on noninvasive measures of LV relaxation and stiffness.[1] More recently, the evaluation of LV muscle and fluid mechanics, using novel echocardiographic indexes and techniques, has been proposed to refine the assessment of LV diastolic function.[2-5] In particular, 2-dimensional speckle tracking imaging enables the assessment of the complex torsional mechanics of the left ventricle. During systole, the contraction of the helically arranged subendocardial and subepicardial layers leads to the opposite rotation of the LV apex and LV base, the so-called LV twist.[3,6] During isovolumic relaxation, the reverse rotation of the LV apex and LV base (LV untwisting) releases the energy stored during LV systole. The restoring forces generate intraventricular pressure gradients contributing to early LV filling.[3,6,7] These complex LV mechanics are associated with characteristic intraventricular fluid dynamics.[4,8] During early LV filling, the blood flow forms intraventricular rotational bodies of fluid (so-called vortex rings) that are critical in optimizing the blood flow during LV ejection.[4,8] These diastolic fluid dynamics can be noninvasively evaluated using color Doppler echocardiography or contrast echocardiography.[9] In addition, a novel echocardiographic dimensionless index (vortex formation time [VFT]) has recently been introduced to quantitatively characterize the optimal conditions leading to vortex formation.[5]

It is well known that myocardial injuries, such as those induced by acute myocardial infarction (AMI), negatively affect the LV diastolic function;[10] conversely, not much data regarding the effect of AMI on the VFT or vortex morphology are available. The knowledge of abnormalities involving the LV vortex formation in clinical setting would be useful, because it would provide direct information regarding the ultimate goal of LV performance (i.e., optimal blood flow). Accordingly, the aim of the present study was to quantify vortex ring formation using the dimensionless index of the VFT and to estimate the morphology of the

vortex during routine contrast echocardiography early after AMI. In addition, we sought to correlate the dynamics of vortex ring formation with LV diastolic function, torsional mechanics, and the extent of myocardial damage (i.e., infarct size).

METHODS

The population consisted of 110 consecutive patients admitted to the coronary care unit for a first ST-segment elevation AMI. The diagnosis of AMI was determined from typical electrocardiographic changes and/or ischemic chest pain associated with the elevation of cardiac biomarkers.[11] All patients underwent immediate coronary angiography and primary percutaneous coronary intervention. The infarct-related artery was identified by the site of coronary occlusion during coronary angiography and electrocardiographic criteria.

The clinical evaluation included 2-dimensional echocardiography with speckle-tracking analysis to assess the LV systolic and diastolic function, dimensionless index of VFT (see paragraph with equation below), and LV untwisting rate; contrast echocardiography to assess LV vortex morphology; and myocardial contrast echocardiography (MCE) to assess the extent of perfusion abnormalities and infarct size. These echocardiographic examinations were performed 48 hours after primary percutaneous coronary intervention. Subsequently, the relations between VFT and vortex morphology with LV diastolic function, LV untwisting rate, and infarct size (as assessed from MCE) were evaluated.

Patients with significant (moderate or severe) valvular heart disease or rhythm other than sinus were not included.

The local ethical committee approved the study protocol, and all patients provided informed consent.

All patients with AMI underwent imaging in the left lateral decubitus position using a commercially available system (Vivid 7 Dimension, GE Healthcare, Horten, Norway) equipped with a 3.5-MHz transducer.

Standard 2-dimensional images and Doppler and color Doppler data were acquired from the parasternal and apical views (2-, 3- and 4-chamber) and digitally stored in cine-loop format. The analyses were subsequently performed off-line using EchoPAC, version 7.0.0 (GE Healthcare, Horten, Norway). The LV end-diastolic and end-systolic volumes were measured according to the Simpson's biplane method, and the LV ejection fraction was calculated as [(end-diastolic volume − end-systolic volume)/end-diastolic volume] × 100.[12]

As previously reported,[1] transmitral and pulmonary vein pulsed-wave Doppler tracings were used to classify the diastolic function as normal, diastolic dysfunction grade 1 (mild), diastolic dysfunction grade 2 (moderate), diastolic dysfunction grade 3 (severe), or diastolic dysfunction grade 4 (severe).

The VFT, a dimensionless index that characterizes the optimal conditions for vortex formation during diastole was calculated as follows:[5,13]

$$VFT = \frac{4(1-\beta)}{\pi D^3} \times SV$$

where SV is the stroke volume, β the fraction of stroke volume contributed from the atrial component of LV filling and calculated from Doppler spectra of the E and A waves, and D the mitral valve diameter in centimeters. The mitral valve diameter was obtained by averaging the largest mitral orifice diameters measured during early diastolic filling in the 2-, 3-, and 4-chamber apical views.

Speckle tracking analysis was applied to evaluate the LV untwisting rate. Parasternal short-axis images of the left ventricle were acquired at 2 different levels: the basal level, identified by the mitral valve and the apical level, identified as the smallest cavity achievable distally to the papillary muscles (moving the probe down and slightly laterally, if needed). The frame rate was 60 to 100 frames/s, and 3 cardiac cycles for each short-axis level were stored in cine-loop format for off-line analysis (EchoPAC, version 7.0.0, GE Healthcare). The endocardial border

was traced at an end-systolic frame, and the region of interest was chosen to fit the whole myocardium. The software allows the operator to check and validate the tracking quality and to adjust the endocardial border or modify the width of the region of interest, if needed. Each short-axis image was automatically divided into 6 standard segments: septal, anteroseptal, anterior, lateral, posterior, and inferior. The software calculated the LV rotation from the apical and basal short-axis images as the average angular displacement of the 6 standard segments, referring to the ventricular centroid, frame by frame. Counterclockwise rotation was marked as a positive value and clockwise rotation as a negative value when viewed from the LV apex. LV twist was defined as the net difference (in degrees) of the apical and basal rotation at the isochronal points. The opposite rotation after LV twist was defined as the LV untwist and the time derivative of the LV untwist was defined as the LV untwisting rate (° /s).

Immediately after 2-dimensional echocardiography, contrast echocardiography was performed using the same ultrasound system. Luminity (Bristol-Myers Squibb Pharma, Brussels, Belgium) was used as the contrast agent. A slow intravenous bolus of echocardiographic contrast (0.1 to 0.2 ml) was administered, followed by 1 to 3 ml of normal saline flush.[4] Apical 3- and 4-chamber views were acquired using a low-power technique (0.1 to 0.4 mechanical index), and the focus was set in the middle of the left ventricle. The machine settings were optimized to obtain the best possible visualization of LV vortex formation. The frame rate was 60 to 100 frames/s, and ≥3 cardiac cycles were stored in cine-loop format for off-line analysis (EchoPAC, version 7.0.0, GE Healthcare). For the evaluation of vortex morphology, the vortex length and width relative to the LV volume were measured during early diastolic filling in the apical 3-chamber view. A vortex sphericity index was calculated as the vortex length/vortex width ratio.

Immediately after contrast echocardiography, MCE was performed to evaluate myocardial perfusion to assess the infarct size after AMI. The

same ultrasound system was used, and the 3 standard apical views were acquired using a low-power technique (0.1 to 0.26 mechanical index). The background gains were set such that minimal tissue signal was seen, and the focus was set at the level of the mitral valve. Luminity (Bristol-Myers Squibb Pharma) was used as the contrast agent. Each patient received an infusion of 1.3 ml of echocardiographic contrast diluted in 50 ml of 0.9% NaCl solution through a 20-gauge intravenous catheter in a proximal forearm vein. The infusion rate was initially set at 4.0 ml/min and then titrated to achieve optimal myocardial enhancement without attenuation artifacts.[14] The machine settings were optimized to obtain the best possible myocardial opacification with minimal attenuation. At least 15 cardiac cycles after high mechanical index (1.7) microbubble destruction were stored in cine-loop format for off-line analysis (EchoPAC, version 7.0.0, GE Healthcare).[15] The left ventricle was divided according to a standard 16-segment model, and a semiquantitative scoring system was used to assess contrast intensity after microbubble destruction:[12] *1*, normal/homogenous opacification; *2*, reduced/patchy opacification; and *3*, minimal or absent contrast opacification.[15,16] A myocardial perfusion index (MPI) was derived by adding the contrast scores of all segments and dividing by the total number of segments.[15,16] In accordance with the number of segments showing minimal or absent contrast opacification, patients were categorized as having a small infarct size (<3 segments with minimal or absent contrast opacification) or a large infarct size (≥3 segments with minimal or absent contrast opacification).[17]

Continues variables are expressed as the mean±SD, when normally distributed, and as the median and interquartile range, when non-normally distributed. Categorical data are presented as absolute numbers and percentages. Differences in continuous variables were assessed using the Student t test or the Mann-Whitney U test, as appropriate. The chi-square test or Fisher's exact test, if appropriate, were computed to assess differences in categorical variables.

Linear regression analyses were performed to evaluate the relation between the VFT and the vortex sphericity index; the vortex parameters and the grade of diastolic dysfunction; the vortex parameters and the LV untwisting rate; and the vortex parameters and infarct size (as assessed from MCE). Univariate and multivariate linear regression analyses (enter model) were performed to evaluate the relation between VFT and the following clinical and echocardiographic variables: age, gender, infarct location (anterior vs nonanterior), multivessel disease, LV end-diastolic volume, LV end-systolic volume, LV ejection fraction, diastolic dysfunction grade, LV untwisting rate, and MPI. Only significant variables on univariate analysis were entered as covariates in the multivariate model. A p value of <0.05 was considered statistically significant. Statistical analysis was performed using the Statistical Package for Social Sciences software package, version 15.0 (SPSS, Chicago, Illinois).

RESULTS

A total of 16 patients were excluded because of suboptimal echocardiographic images that prevented adequate analysis of the speckle-tracking data, vortex morphology, or myocardial perfusion. The clinical characteristics of the 94 patients included in the study are listed in Table 1, and the echocardiographic characteristics are listed in Table 2. The mean LV ejection fraction was $47 \pm 10\%$. Most (54%) had grade 1 diastolic dysfunction. From the speckle tracking analysis findings, the diastolic function was characterized by a mean peak untwisting rate of $-94 \pm 32°$ /s. From the LV hydrodynamics evaluation, the VFT was 1.4 ± 0.6, and the vortex sphericity index was 1.1 ± 0.2.

As shown in Figure 1, a good relation between the VFT and vortex sphericity index was observed ($r = 0.61$; $p < 0.001$). Both LV vortex parameters were weakly related to the LV diastolic function (Figure 2). In contrast, good relations between the VFT and the LV untwisting rate ($r =$

0.65; p <0.001) and between the vortex sphericity index and the LV untwisting rate (r = 0.61; p <0.001) were observed (Figure 3).

Table 1. Clinical patient characteristics

Variable	n = 94
Age (years)	59±11
Men	73 (78%)
Diabetes mellitus	12 (13%)
Hypercholesterolemia *	15 (16%)
Hypertension †	37 (39%)
Current or previous smoking	52 (55%)
Anterior wall myocardial infarction	47 (50%)
Infarct-related coronary artery	
- left anterior descending	47 (50%)
- left circumflex	16 (17%)
- right	31 (33%)
Multi-vessel coronary disease	36 (38%)
Peak troponin T (μg/l)	2.9 (1.6-7.5)

Data are expressed as mean±SD or median (interquartile range), and n (%). *: Defined as total cholesterol ≥240 mg/dl. †: Defined as systolic blood pressure ≥140 mmHg and/or diastolic blood pressure ≥90 mmHg.

According to the results from MCE, 69 patients (73%) with AMI had a small infarct size (<3 segments with minimal or absent contrast opacification) and 25 (27%) had a large infarct size (≥3 segments with minimal or absent contrast opacification). The echocardiographic characteristics of these 2 groups are summarized in Table 2. Patients with a small infarct size had a significant greater LV ejection fraction compared to patients with a large infarct size (51±8% vs 39±8%; p <0.001).

No significant difference in the grade of diastolic dysfunction was observed between patients with a small and large infarct size; most of the patients in both groups (52% and 60%, respectively) had grade 1 diastolic dysfunction. However, the LV untwisting rate was significantly impaired in the patients with a large infarct size (−69±27° /s vs −103±29° /s; p <0.001). Regarding the vortex parameters, patients with a large infarct size had a significantly lower VFT (1.0±0.5 vs

1.6±0.5; p <0.001) and vortex sphericity index (0.9±0.2 vs 1.2±0.2; p <0.001). As shown in Figure 4, a good relation between the VFT and MPI (expressing infarct size) (r = 0.63; p <0.001) and between the vortex sphericity index and MPI (r = 0.71; p <0.001) was observed.

Table 2. Echocardiographic characteristics

	All AMI patients (n = 94)	Small infarct (n = 69)	Large infarct (n = 25)	p value
Left ventricular end-diastolic volume (ml)	105±28	104±25	107±36	0.69
Left ventricular end-systolic volume (ml)	56±22	52±18	66±29	0.024
Left ventricular ejection fraction (%)	47±10	51±8	39±8	<0.001
E wave velocity (cm/sec)	62±0.18	62±0.18	62±0.18	0.97
E wave deceleration time (msec)	201±59	207±55	184±67	0.11
A wave velocity (cm/sec)	68±0.17	68±0.13	70±0.25	0.76
Diastolic function				0.18
- grade 0	35 (37%)	29 (42%)	6 (24%)	
- grade 1	51 (54%)	36 (52%)	15 (60%)	
- grade 2	5 (6%)	3 (4%)	2 (8%)	
- grade 3-4	3 (3%)	1 (1%)	2 (8%)	
Untwisting rate (° /sec)	-94±32	-103±29	-69±27	<0.001
Vortex formation time	1.4±0.6	1.6±0.5	1.0±0.5	<0.001
Vortex length/left ventricular volume (cm/ml)	0.02±0.01	0.02±0.01	0.01±0.01	0.19
Vortex width/left ventricular volume (cm/ml)	0.01±0.01	0.01±0.01	0.02±0.01	0.026
Vortex sphericity index	1.1±0.2	1.2±0.2	0.9±0.2	<0.001
Myocardial perfusion index	1.4±0.3	1.2±0.2	1.7±0.3	<0.001

Data are expressed as mean±SD and n (%).

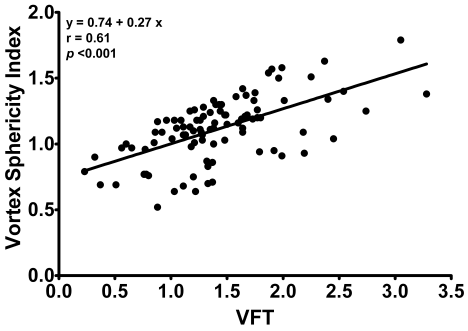

Figure 1. Relation between VFT and vortex sphericity index.

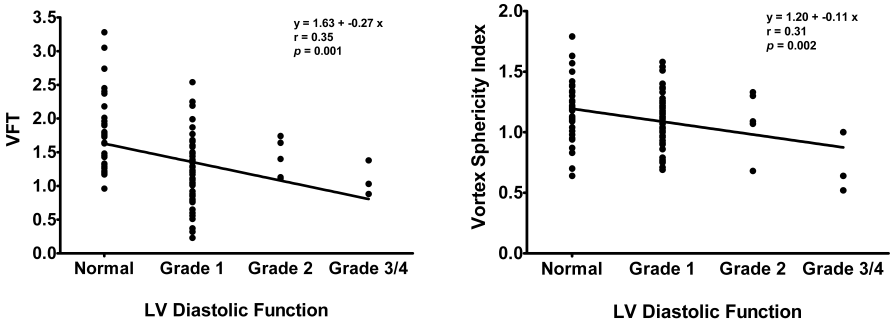

Figure 2. Relation between grades of LV diastolic dysfunction and (**left panel**) VFT and (**right panel**) vortex sphericity index.

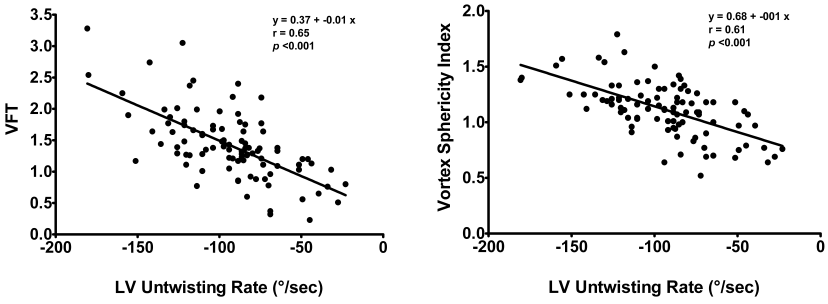

Figure 3. Relation between LV untwisting rate and (**left panel**) VFT and (**right panel**) vortex sphericity index.

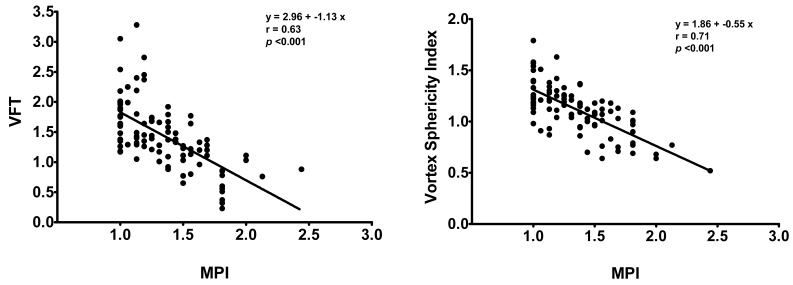

Figure 4. Relation between infarct size (expressed as MPI) and (**left panel**) VFT and (**right panel**) vortex sphericity index.

Table 3 lists the results of the univariate and multivariate linear regression analyses performed to determine the factors related to VFT among patients with AMI. On univariate analysis, several variables were significantly related to VFT, including anterior AMI, LV end-systolic volume, LV ejection fraction, diastolic dysfunction grade, LV untwisting rate, and MPI. On multivariate analysis, only the LV untwisting rate ($\beta = -0.43$, $p < 0.001$) and MPI ($\beta = -0.33$, $p = 0.005$) were independently associated with the VFT.

Table 3. Univariate and multivariate linear regression analyses to determine independent correlates of vortex formation time (VFT)

	Univariate		Multivariate	
	β	**p value**	**β**	**p value**
Age	-0.16	0.12	-	-
Men	-0.024	0.82	-	-
Anterior myocardial infarction	-0.37	<0.001	-0.059	0.49
Multi-vessel disease	-0.15	0.16	-	-
Left ventricular end-diastolic volume	0.065	0.53	0.18	0.62
Left ventricular end-systolic volume	-0.21	0.039	0.053	0.91
Left ventricular ejection fraction	0.53	<0.001	0.092	0.70
Grade of diastolic dysfunction	-0.35	0.001	-0.081	0.31
Untwisting rate	-0.65	<0.001	-0.43	<0.001
Myocardial perfusion index	-0.63	<0.001	-0.33	0.005

Abbreviations as in Table 2.

DISCUSSION

The results of the present study can be summarized as follows: both the VFT and the vortex sphericity index were weakly related to global LV diastolic function, and a good relation was observed between the LV vortex parameters and LV untwisting rate. Second, both the VFT and the vortex sphericity index had a good relation with infarct size (as assessed by MCE), indicating progressive impairment of LV diastolic fluid dynamics with an increasing extent of myocardial damage. Finally, on multivariate analysis, a significant independent relation was observed between VFT and both the LV untwisting rate and the MPI.

Several investigators have previously demonstrated the process of vortex formation during LV filling using numeric or physical models and flow visualization techniques (i.e., cardiac magnetic resonance imaging, color Doppler echocardiography, and MCE) in clinical studies.[4,8,9,18-21] The process of vortex formation starts immediately after the onset of the early diastolic phase, lasting the whole diastolic period.[4] It is related to the difference in velocity between the high-speed inflow jet after mitral valve opening and the surrounding still fluid in the left ventricle. The shear layer between the moving and the still part of the blood promotes a natural swirling of flow inside the left ventricle, leading to the vortex formation.[4,22]

The LV vortex has been shown to optimize the diastolic fluid dynamics and the efficiency of systolic ejection of blood. The LV vortex redirects the blood flow from the LV base to the LV apex during isovolumic relaxation and toward the LV outflow tract and aorta during isovolumic contraction.[4,22,23] In addition, the LV vortex constitutes a kinetic energy reservoir (storing the kinetic energy of the high-speed inflow jet) and, consequently, enhances the ejection of blood during systole.[24] The premature loss or absence of diastolic LV vortex would conversely lead to the dissipation of the stored kinetic energy, resulting in an increased myofiber cardiac work and oxygen demand.[24]

In the present study, the effect of AMI on LV vortex flow was assessed. In particular, the morphology of the intraventricular vortex was evaluated using contrast echocardiography. In addition, the dimensionless index of VFT was also evaluated. The VFT is a recently proposed parameter for characterizing the process of vortex ring formation.[5] It is a measure of the length/diameter ratio of the fluid column and is directly proportional to the time-averaged velocity of flow through the mitral valve and inversely proportional to the mitral valve size.[5] A previous in vitro study showed that a range of VFT from 3.3 to 4.5 characterizes the optimal hemodynamic conditions for vortex ring formation.[5]

A good linear relation was observed between the vortex sphericity index and the VFT, indicating that suboptimal hemodynamic conditions for vortex ring formation (i.e., low values of VFT) are associated with short and wide LV vortex rings. In addition, both the VFT and the vortex sphericity index were weakly related to the global LV diastolic function, and a good relation was observed between the LV vortex parameters and LV untwisting rate. This finding suggests that LV hydrodynamics are mainly related to LV diastolic suction rather than to global LV diastolic function. Suction gradients are necessary for the redirection of flow from the LV base to the LV apex and, consequently, for vortex ring formation. In addition, suction gradients are mainly determined by the LV untwisting mechanics.[7] Reduced LV untwisting after AMI might attenuate these suction gradients, leading finally to abnormal LV vortex ring formation.

In the present study, the relation between LV vortex flow and infarct size was also evaluated. Both the VFT and the vortex sphericity index had a significant linear relation with infarct size (as assessed by MCE), indicating that larger infarctions are associated with a more severe alteration in LV intracavitary blood flow dynamics. This finding is in line with the study by Hong et al,[4] showing abnormal LV vortex morphology among patients with reduced LV systolic function compared to normal controls. As a consequence of impaired VFT and abnormal vortex morphology, the relative stasis and delay or modification of the normal blood flow during

the cardiac cycle might occur, predisposing to LV thrombus formation.[9] Moreover, taking into account the essential role of LV vortex rings in optimizing the ejection of blood during systole, a significant impairment of LV vortex ring formation might contribute to a progressive decrease in LV systolic function.[24] However, follow-up studies that also include other parameters of diastolic function (e.g., tissue-Doppler parameters, isovolumic relaxation time, and time of untwisting) are needed to demonstrate the prognostic role of LV hydrodynamics parameters for the prediction of post-AMI complications and outcome.

REFERENCES

1. Lester SJ, Tajik AJ, Nishimura RA, et al. Unlocking the mysteries of diastolic function: deciphering the Rosetta Stone 10 years later. J Am Coll Cardiol. 2008; 51: 679–689
2. Thomas JD, Popovic, ZB. Assessment of left ventricular function by cardiac ultrasound. J Am Coll Cardiol. 2006; 48: 2012–2025
3. Sengupta PP, Khandheria BK, Narula, J. Twist and untwist mechanics of the left ventricle. Heart Fail Clin. 2008; 4: 315–324
4. Hong GR, Pedrizzetti G, Tonti G, et al. Characterization and quantification of vortex flow in the human left ventricle by contrast echocardiography using vector particle image velocimetry. JACC Cardiovasc Imaging. 2008; 1: 705–717
5. Gharib M, Rambod E, Kheradvar A, et al. Optimal vortex formation as an index of cardiac health. Proc Natl Acad Sci USA. 2006; 103: 6305–6308
6. Bertini M, Nucifora G, Ajmone Marsan N, et al. Left ventricular rotational mechanics in acute myocardial infarction and in chronic (ischemic and non-ischemic) heart failure patients. Am J Cardiol. 2009; 103: 1506–1512
7. Burns AT, La Gerche A, Prior DL, et al. Left ventricular untwisting is an important determinant of early diastolic function. JACC Cardiovasc Imaging. 2009; 2: 709–716
8. Kim WY, Walker PG, Pedersen EM, et al. Left ventricular blood flow patterns in normal subjects: a quantitative analysis by three-dimensional magnetic resonance velocity mapping. J Am Coll Cardiol. 1995; 26: 224–238
9. Sengupta PP, Burke R, Khandheria BK, et al. Following the flow in chambers. Heart Fail Clin. 2008; 4: 325–332

10. Popovic AD. Old and new paradigms on diastolic function in acute myocardial infarction. Am Heart J. 1999; 138: S84–S88
11. Thygesen K, Alpert JS, White HD, et al. Universal definition of myocardial infarction. Circulation. 2007; 116: 2634–2653
12. Lang RM, Bierig M, Devereux RB, et al. Recommendations for chamber quantification: a report from the American Society of Echocardiography's Guidelines and Standards Committee and the Chamber Quantification Writing Group, developed in conjunction with the European Association of Echocardiography, a branch of the European Society of Cardiology. J Am Soc Echocardiogr. 2005; 18: 1440–1463
13. Jiamsripong P, Calleja AM, Alharthi MS, et al. Impact of acute moderate elevation in left ventricular afterload on diastolic transmitral flow efficiency: analysis by vortex formation time. J Am Soc Echocardiogr. 2009; 22: 427–431
14. Weissman NJ, Cohen MC, Hack TC, et al. Infusion versus bolus contrast echocardiography: a multicenter, open-label, crossover trial. Am Heart J. 2000; 139: 399–404
15. Dwivedi G, Janardhanan R, Hayat SA, et al. Prognostic value of myocardial viability detected by myocardial contrast echocardiography early after acute myocardial infarction. J Am Coll Cardiol. 2007; 50: 327–334
16. Main ML, Magalski A, Kusnetzky LL, et al. Usefulness of myocardial contrast echocardiography in predicting global left ventricular functional recovery after anterior wall acute myocardial infarction. Am J Cardiol. 2004; 94: 340–342
17. Caldas MA, Tsutsui JM, Kowatsch I, et al. Value of myocardial contrast echocardiography for predicting left ventricular remodeling and segmental functional recovery after anterior wall acute myocardial infarction. J Am Soc Echocardiogr. 2004; 17: 923–932
18. Bellhouse BJ. Fluid mechanics of a model mitral valve and left ventricle. Cardiovasc Res. 1972; 6: 199–210
19. Baccani B, Domenichini F, Pedrizzetti G, et al. Fluid dynamics of the left ventricular filling in dilated cardiomyopathy. J Biomech. 2002; 35: 665–671
20. Steen T, Steen S. Filling of a model left ventricle studied by colour M mode Doppler. Cardiovasc Res. 1994; 28: 1821–1827
21. Vierendeels JA, Riemslagh K, Dick E, et al. Computer simulation of intraventricular flow and pressure gradients during diastole. J Biomech Eng. 2000; 122: 667–674

22. Domenichini F, Pedrizzetti G, Baccani B. Three-dimensional filling flow into a model left ventricle. J Fluid Mech. 2005; 539: 179–198
23. Sengupta PP, Khandheria BK, Korinek J, et al. Left ventricular isovolumic flow sequence during sinus and paced rhythms: new insights from use of high-resolution Doppler and ultrasonic digital particle imaging velocimetry. J Am Coll Cardiol. 2007; 49: 899–908
24. Pedrizzetti G, Domenichini F. Nature optimizes the swirling flow in the human left ventricle. Phys Rev Lett. 2005; 95: 108101

Chapter 11

Reduced Left Ventricular Torsion Early After Myocardial Infarction Is Related to Left Ventricular Remodeling

Gaetano Nucifora, Nina Ajmone Marsan, Matteo Bertini, Victoria Delgado, Hans-Marc J. Siebelink, Jacob M. van Werkhoven, Arthur J. Scholte, Martin J. Schalij, Ernst E. van der Wall, Eduard R. Holman, Jeroen J. Bax

Circ Cardiovasc Imaging 2010;3:433-442

ABSTRACT

Background. Left ventricular (LV) torsion is emerging as a sensitive parameter of LV systolic myocardial performance. The aim of the present study was to explore the effects of acute myocardial infarction (AMI) on LV torsion and to determine the value of LV torsion early after AMI in predicting LV remodeling at 6-month follow-up.

Methods and Results. A total of 120 patients with a first ST-segment elevation AMI (mean±SD age, 59±10 years; 73% male) were included. All patients underwent primary percutaneous coronary intervention. After 48 hours, speckle-tracking echocardiography was performed to assess LV torsion; infarct size was assessed by myocardial contrast echocardiography. At 6-month follow-up, LV volumes and LV ejection fraction were reassessed to identity patients with LV remodeling (defined as a ≥15% increase in LV end-systolic volume). Compared with control subjects, peak LV torsion in AMI patients was significantly impaired (1.54±0.64° /cm vs 2.07±0.27° /cm, p <0.001). By multivariate analysis, only LV ejection fraction (β = 0.36, p <0.001) and infarct size (β = −0.47, p <0.001) were independently associated with peak LV torsion. At 6-month follow-up, 19 patients showed LV remodeling. By multivariate analysis, only peak LV torsion (odds ratio = 0.77; 95% CI, 0.65–0.92; p = 0.003) and infarct size (odds ratio = 1.04; 95% CI, 1.01–1.07; p = 0.021) were independently related to LV remodeling. Peak LV torsion provided modest but significant incremental value over clinical, echocardiographic, and myocardial contrast echocardiography variables in predicting LV remodeling. By receiver-operating characteristics curve analysis, peak LV torsion ≤1.44° /cm provided the highest sensitivity (95%) and specificity (77%) to predict LV remodeling.

Conclusions. LV torsion is significantly impaired early after AMI. The amount of impairment of LV torsion predicts LV remodeling at 6-month follow-up.

INTRODUCTION

Remodeling of the left ventricle (LV) after acute myocardial infarction (AMI) is associated with the development of heart failure and a poor survival rate.[1,2] Accordingly, identification of patients prone to develop postinfarction LV remodeling represents an important issue in clinical cardiology. These considerations have stimulated research for new parameters able to provide quantitative and objective estimation of post-AMI myocardial damage and to identify patients at risk of LV remodeling.[3] The systolic twisting motion of the LV along its longitudinal axis, resulting from opposite rotation of the LV apex compared with the base, is emerging as an important, sensitive parameter of LV systolic function.[4] Recently, echocardiographic assessment of LV torsional mechanics based on speckle-tracking analysis has been introduced and validated against sonomicrometry and magnetic resonance imaging.[5,6] In the clinical setting, however, not much data on changes in LV torsion after AMI are available,[7,8] and no specific data exist concerning the role of LV torsion in predicting postinfarction LV remodeling. Accordingly, the aim of the present evaluation was 2-fold. *First*, we sought to determine the correlates of LV torsion after AMI, and *second*, we aimed to explore the relation between LV torsion and the development of LV remodeling at 6-month follow-up.

METHODS

Patient Population and Protocol

The population consisted of 146 consecutive patients admitted to the coronary care unit because of a first ST-segment elevation AMI. Diagnosis of AMI was made on the basis of typical ECG changes and/or ischemic chest pain associated with elevation of cardiac biomarkers.[9] All patients underwent immediate coronary angiography and primary percutaneous coronary intervention (PCI). The infarct-related artery was identified

during coronary angiography and by ECG criteria. During PCI, final TIMI (Thrombolysis In Myocardial Infarction) flow was assessed.

Clinical evaluation included 2-dimensional (2D) echocardiography with speckle-tracking analysis to assess LV global longitudinal strain (GLS) and torsion, and myocardial contrast echocardiography (MCE) was performed 48 hours after PCI to assess the extent of perfusion abnormalities and infarct size. At 6-month follow-up, 2D echocardiography was performed to reassess LV volumes and ejection fraction (LVEF). These echocardiographic examinations are part of the routine, comprehensive assessment of AMI patients in our clinics.

In addition, 20 subjects without evidence of structural heart disease and without known risk factors for coronary artery disease, matched for age, sex, and body surface area and who underwent 2D echocardiography, were included as a normal control group. These individuals were derived from the echocardiographic database and were clinically referred for echocardiographic evaluation because of atypical chest pain, palpitations, or syncope without murmur.

To determine the reduction in LV torsion after AMI, patient data were compared with data from the normal controls. In addition, the independent correlates of LV torsion after AMI were investigated, and the role of LV torsion in predicting LV remodeling (defined as a $\geq$15% increase in LV end-systolic volume [ESV]) at 6-month follow-up was assessed.[1,10]

2D Echocardiography

All AMI patients and control subjects were imaged in the left lateral decubitus position with a commercially available system (Vivid 7 Dimension, GE Healthcare, Horten, Norway) equipped with a 3.5-MHz transducer. Standard 2D images and Doppler and color-Doppler data were acquired from parasternal and apical views (4-, 2-, and 3-chamber views) and digitally stored in cine-loop format; analyses were subsequently performed offline with EchoPAC version 7.0.0 software (GE Healthcare). LV end-diastolic volume (LVEDV) and LVESV were measured according to

Simpson's biplane method, and LVEF was calculated as [(LVEDV−LVESV)/LVEDV]×100.[11]

Qualitative assessment of regional wall motion was performed according to the 16-segment model of the American Society of Echocardiography, and the global wall-motion score index (WMSI) was calculated for each patient.[11] As previously described,[12] transmitral and pulmonary vein pulsed-wave Doppler tracings were used to classify diastolic function as *(1)* normal, *(2)* diastolic dysfunction grade 1 (mild), *(3)* diastolic dysfunction grade 2 (moderate), or *(4)* diastolic dysfunction grade 3 (severe).

Speckle-Tracking Analysis

Longitudinal Strain Analysis

Longitudinal strain analysis of the LV was performed by speckle-tracking imaging (EchoPAC version 7.0.0). Gray-scale 2D apical images of the LV (4-, 2-, and 3-chamber views) were used with a frame rate ranging from 60 to 100 frames per second. From an end-systolic frame, the endocardial border was manually traced, and the software automatically traces 2 more concentric regions of interest (ROIs) to include the entire myocardial wall. Speckle-tracking analysis detects and tracks the unique myocardial ultrasound patterns frame by frame. The in-plane frame-to-frame displacement of each pattern over time is used to derive strain. The software automatically validates the segmental tracking throughout the cardiac cycle and allows the operator further adjustment of the ROI to improve tracking quality. As previously described,[13] mean GLS was calculated, as an index of global LV systolic function, by averaging the GLSs obtained automatically from each apical view.

Torsional Mechanics Analysis

Speckle-tracking analysis was applied to evaluate LV basal and apical rotations, LV twist, and LV torsion. Parasternal short-axis images of the LV were acquired at 2 different levels: *(1)* basal level, identified by the

mitral valve, and *(2)* apical level, as the smallest cavity achievable distally to the papillary muscles (by moving the probe downward and slightly laterally, if needed). Frame rate was 60 to 100 frames per second, and 3 cardiac cycles for each short-axis level were stored in cine-loop format for offline analysis (EchoPAC version 7.0.0). The endocardial border was traced at an end-systolic frame, and the ROI was chosen to fit the whole myocardium. The software allows the operator to check and validate the tracking quality and to adjust the endocardial border or modify the width of the ROI, if needed. Each short-axis image was automatically divided into 6 standard segments: septal, anteroseptal, anterior, lateral, posterior, and inferior. The software calculated LV rotation from the apical and basal short-axis images as the average angular displacement of the 6 standard segments by referring to the ventricular centroid, frame by frame. Counterclockwise rotations were marked as positive values and clockwise rotations, as negative values when viewed from the LV apex. LV twist was defined as the net difference (in degrees) of apical and basal rotations at isochronal time points. LV torsion was then calculated as the ratio between LV twist (in degrees) and the LV diastolic longitudinal length (in cm) between the LV apex and the mitral plane.[14]

Twenty patients were randomly selected to assess the reproducibility of peak LV twist. Bland-Altman analysis was performed to evaluate intraobserver and interobserver agreement by repeating the analysis 1 month later by the same observer and by a second independent observer. Intraobserver agreement was excellent. According to Bland-Altman analysis, the mean difference ±2 SD for peak LV twist was 0.05±0.35°. Interobserver agreement was also good. According to Bland-Altman analysis, the mean difference ±2 SD for peak LV twist was 0.16±1.50°.

Myocardial Contrast Echocardiography

Immediately after 2D echocardiography, MCE was performed to evaluate myocardial perfusion to assess infarct size after AMI. The same ultrasound system was used, and the 3 standard apical views were

acquired with a low-power technique (mechanical index of 0.1 to 0.26). Background gains were set so that minimal tissue signal was seen, and the focus was set at the level of the mitral valve. Luminity (Perflutren, Bristol-Myers Squibb Pharma, Brussels, Belgium) was used as the contrast agent. Each patient received an infusion of 1.3 ml of echo contrast diluted in 50 ml of 0.9% NaCl solution through a 20-gauge intravenous catheter in a proximal forearm vein. Infusion rate was initially set at 4.0 ml/min and then titrated to achieve optimal myocardial enhancement without attenuation artifacts.[15] Machine settings were optimized to obtain the best possible myocardial opacification with minimal attenuation. At least 15 cardiac cycles after high-mechanical-index (1.7) microbubble destruction were stored in cine-loop format for offline analysis (EchoPAC version 7.0.0).[16] The LV was divided according to a standard 16-segment model, and a semiquantitative scoring system was used to assess contrast intensity after microbubble destruction: *(1)* normal/homogenous opacification, *(2)* reduced/patchy opacification, or *(3)* minimal or absent contrast opacification.[11,16] Minimal or absent contrast opacification identifies myocardial segments with a >50% transmural extent of infarction with high accuracy, as previously demonstrated by Janardhanan et al.[17] A myocardial perfusion index (MPI), indicating the extent of infarct size, was derived by adding contrast scores of all segments and dividing by the total number of segments.[16]

Twenty patients were randomly selected to assess the reproducibility of perfusion scoring. A weighted κ test was performed to evaluate intraobserver and interobserver agreement by repeating the analysis 1 month later by the same observer and by a second independent observer. Both intraobserver and interobserver agreements were good (weighted κ = 0.86 and = 0.84, respectively). To avoid measurements bias, all analyses were performed in blinded fashion.

Statistical Analysis

Continuous variables are expressed as mean±SD, when normally distributed, and as median and interquartile range, when not normally distributed. Categorical data are presented as absolute numbers and percentages.

Differences in continuous variables between 2 groups were assessed with the Student t test or Mann-Whitney U test, where appropriate. Chi-square test or Fisher's exact test, where appropriate, was computed to assess differences in categorical variables. Differences in continuous variables between >2 groups were assessed by 1-way ANOVA or Kruskal-Wallis test, where appropriate; when the result of the analysis was significant, a post hoc test with Bonferroni's correction was applied.

Univariate and multivariate linear-regression analyses (with an automatic stepwise selection procedure with backward elimination) were performed to evaluate the relation between peak LV torsion among AMI patients and the following variables: age, sex, infarct location (anterior versus nonanterior), multivessel disease, TIMI flow grade 3 after PCI, peak troponin T value, LVEDV, LVESV, LVEF, WMSI, presence of diastolic dysfunction, peak LV GLS, and MPI. Age and sex were entered into the multivariate model independently of their probability value by univariate analysis and were kept fixed throughout the stepwise selection procedure. Regarding the remaining variables, only those with a probability value <0.20 by univariate analysis were entered as covariates in the multivariate model. Linear-regression analyses were performed to evaluate the relation between peak LV torsion at baseline and LVESV at 6-month follow-up, as well as the change in LVESV after 6-month follow-up compared with the baseline value.

Univariate and multivariate logistic-regression analyses (with automatic stepwise selection procedure with backward elimination) were performed to evaluate the relation between the occurrence of LV remodeling at 6-month follow-up and the following baseline variables: age, sex, infarct location (anterior versus nonanterior), multivessel disease, TIMI flow

grade 3 after PCI, peak troponin T value, LVEDV, LVESV, LVEF, WMSI, presence of diastolic dysfunction, peak LV GLS, peak LV torsion, and MPI. Age, sex, and LVESV were entered into the multivariate model independently of their probability value by univariate analysis and were kept fixed throughout the stepwise selection procedure. Regarding the remaining variables, only those with a probability value <0.20 by univariate analysis were entered as covariates in the multivariate model. The incremental predictive value of peak LV torsion over clinical, echocardiographic, and MCE variables was assessed by calculating the global χ^2 values.

Receiver-operator-characteristics curve analysis was performed to determine the accuracy of baseline peak LV torsion to predict LV remodeling at 6-month follow-up in the overall patient population and among anterior and nonanterior AMI patients. A probability value <0.05 was considered statistically significant. Statistical analysis was performed with the SPSS software package (SPSS 15.0, Chicago, Ill).

RESULTS

Reliable speckle-tracking curves for rotation analysis and diagnostic MCE data were obtained in 120 patients; consequently, 26 patients were excluded from further analysis. Of note, no significant difference was observed between included and excluded patients with regard to age (59±10 versus 57±10 years, p = 0.31), male sex (87 [73%] versus 17 [65%], p = 0.47), anterior location of AMI (55 [46%] versus 13 [50%], p = 0.70), and peak value of troponin T (3.04 μg/L [1.65 to 7.03] versus 3.18 μg/L [1.74 to 12.62], p = 0.58). All control subjects had reliable speckle-tracking curves.

Clinical and Echocardiographic Characteristics

Clinical and echocardiographic characteristics of control subjects and AMI patients are listed in Table 1.

Table 1. Baseline clinical and echocardiographic characteristics of control subjects and AMI patients

	Control subjects (n = 20)	AMI patients (n = 120)	p value
Age (years)	56±10	59±10	0.37
Male gender	15 (75%)	87 (73%)	0.82
Diabetes	-	13 (11%)	
Family history of coronary artery disease	-	45 (37%)	
Hypercholesterolemia	-	16 (13%)	
Hypertension	-	43 (36%)	
Current or previous smoking	-	67 (56%)	
Anterior myocardial infarction	-	55 (46%)	
Infarct-related artery			
- left anterior descending	-	55 (46%)	
coronary artery	-	21 (17%)	
- left circumflex coronary artery	-	44 (37%)	
- right coronary artery			
Multi-vessel disease	-	41 (34%)	
TIMI flow grade 3	-	101 (84%)	
Peak troponin T (μg/l)	-	3.04 (1.65-7.03)	
LVEDV (ml)	103±22	104±27	0.91
LVESV (ml)	40±10	55±21	<0.001
LVEF (%)	61±7	48±9	<0.001
LV diastolic longitudinal length (cm)	8.6±0.6	8.3±0.8	0.18
WMSI	-	1.72±0.34	
Diastolic function			<0.001
- grade 0	20 (100%)	47 (39%)	
- grade 1	-	63 (52%)	
- grade 2	-	8 (7%)	
- grade 3	-	2 (2%)	
Peak LV GLS (%)	-19.4±1.7	-14.0±3.8	<0.001
Peak LV basal rotation (°)	-6.8±2.7	-5.1±2.7	0.013
Peak LV apical rotation (°)	11.6±2.8	8.4±4.6	<0.001
Peak LV twist (°)	17.7±2.1	12.7±5.2	<0.001
Peak LV torsion (°/cm)	2.07±0.27	1.54±0.64	<0.001
MPI	-	1.28 (1.08-1.50)	

Abbreviations are as defined in text.

By definition, control subjects and AMI patients did not differ in age or sex. Among AMI patients, the infarct-related artery was the left anterior descending coronary artery in 55 (46%) patients; obstructive multivessel disease (ie, >1 vessel with a luminal narrowing ≥70%) was present in 41 (34%) patients. Peak value of troponin T was 3.04 μg/L (1.65 to 7.03 μg/L). Mean LVEF was 48±9%.

Compared with control subjects, AMI patients had significantly reduced peak LV basal rotation (−5.1±2.7° versus −6.8±2.7° , p = 0.013), reduced peak LV apical rotation (8.4±4.6° versus 11.6±2.8° , p <0.001), and consequently decreased peak LV twist (12.7±5.2° versus 17.7±2.1° , p <0.001) and peak LV torsion (1.54±0.64° /cm versus 2.07±0.27° /cm, p <0.001). Among AMI patients, those with an anterior AMI had significantly lower peak LV apical rotation, LV twist, and LV torsion compared with the remaining AMI patients (6.5±4.3° versus 10.1±4.2° , p <0.001; 11.1±5.4° versus 14.0±4.7° , p = 0.002; and 1.35±0.65° /cm versus 1.70±0.58° /cm, p = 0.003, respectively), whereas peak LV basal rotation was not different (−5.4±2.6° versus −4.9±2.8° , p = 0.31). Of note, no significant difference was observed in peak LV basal rotation, apical rotation, LV twist, and LV torsion between patients (n = 37) with anterior AMI due to proximal LAD occlusion versus patients (n = 18) with anterior AMI due to mid or distal LAD occlusion (−5.2±2.5° versus −5.8±2.7° , p = 0.38; 6.9±4.3° versus 5.6±4.2° , p = 0.30; 11.4±5.2° versus 10.7±5.8° , p = 0.67; and 1.36±0.63° /cm versus 1.35±0.72° /cm, p = 0.95, respectively). Examples of LV rotational mechanics curves obtained by speckle-tracking analysis in a control subject and in a patient with AMI are shown in Figure 1.

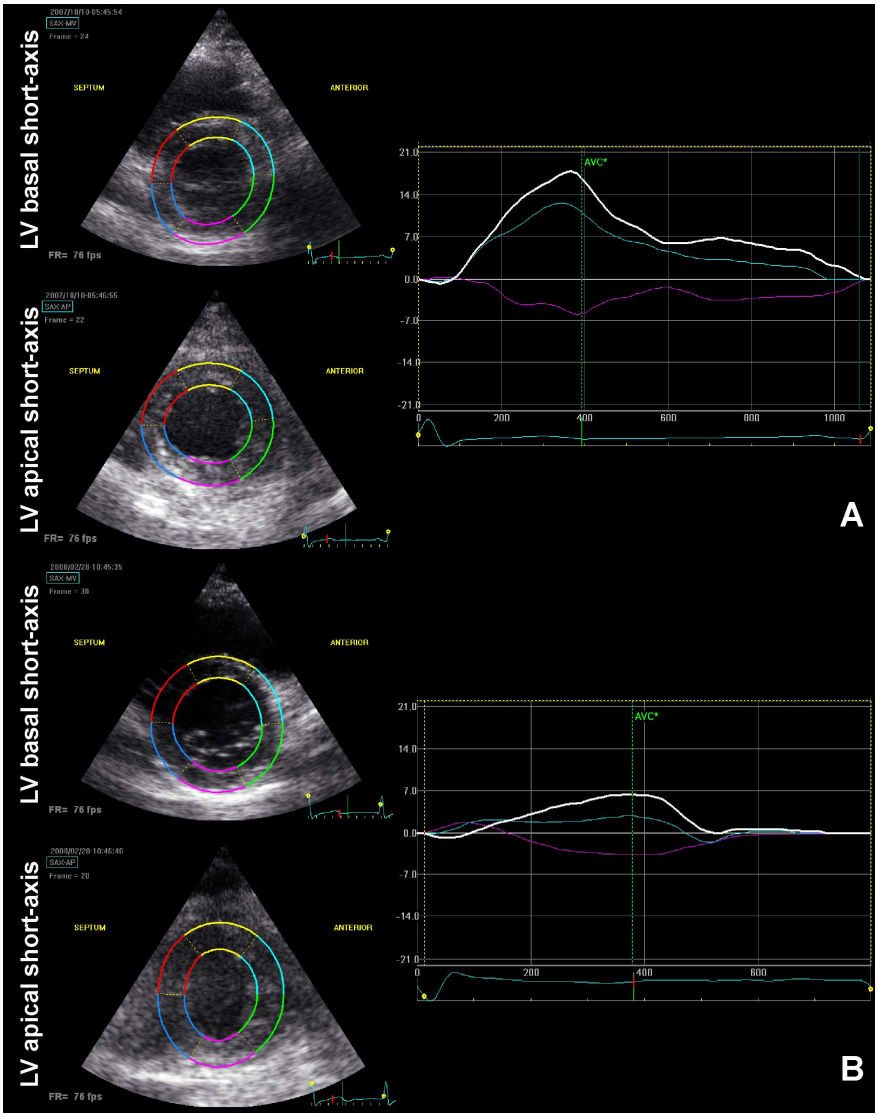

Figure 1. LV rotational mechanics curves of a control subject (**panel A**) and of a patient with anterior AMI (**panel B**). A, Speckle-tracking analysis shows normal peak LV basal (purple line) and apical (green line) rotations and normal peak LV twist (18.4° ; white line). B, Speckle-tracking analysis shows impaired peak LV basal (purple line) and apical (green line) rotations and reduced peak LV twist (6.8° ; white line).

Determinants of LV Torsion Among AMI Patients

Table 2 shows the results of univariate and multivariate linear regression analyses performed to determine the factors related to peak LV torsion among AMI patients. By univariate analysis, several variables were significantly related to peak LV torsion: anterior AMI, TIMI flow grade 3 after PCI, peak troponin T value, LVEDV, LVESV, LVEF, WMSI, presence of diastolic dysfunction, peak LV GLS, and MPI. However, by multivariate analysis, only LVEF (β = 0.36, p <0.001) and MPI (β = -0.47, p <0.001) were independently associated with peak LV torsion. The relation between peak LV torsion and MPI is shown in Figure 2.

Patients without myocardial segments with minimal or absent contrast opacification had higher peak LV torsion compared with patients with ≥1 myocardial segment with minimal or absent contrast opacification (1.84±0.49° /cm versus 1.27±0.63° /cm; p <0.001). In addition, a progressive reduction of peak LV torsion with increasing number of myocardial segments with minimal or absent contrast opacification was observed (Figure 3).

LV Remodeling at 6-Month Follow-Up

Eight of 120 AMI patients included in the initial population did not complete the 6-month follow-up; consequently, data at baseline and at 6-month follow-up were available for 112 patients. At 6-month follow-up, mean LVEDV was 114±37 ml, whereas mean LVESV was 54±29 ml and mean LVEF was 55±10%. A total of 19 patients developed LV remodeling.

Baseline clinical and echocardiographic characteristics of AMI patients with versus without LV remodeling are summarized in Table 3. At baseline, patients who developed LV remodeling had larger LVESVs (p = 0.036), lower LVEFs (p <0.001), and higher MPIs (p <0.001), indicating larger infarct size. Regarding LV rotational mechanics parameters, at baseline patients with LV remodeling had significantly lower peak LV apical rotation (p <0.001), peak LV twist (p <0.001), and peak LV

torsion (p <0.001) compared with patients without LV remodeling; conversely, no difference in peak LV basal rotation was observed between the 2 groups. Patients with more impaired peak LV torsion at baseline had larger LVESVs at 6-month follow-up and a higher change in LVESV in the 6-month follow-up period (Figure 4).

Table 2. Univariate and multivariate linear regression analyses to determine the independent correlates of peak LV torsion in AMI patients

	Univariate		Multivariate	
	β	**p value**	**β**	**p value**
Age	-0.080	0.38	0.057	0.37
Male	-0.048	0.61	-0.046	0.46
Anterior myocardial infarction	-0.27	0.003	-	-
Multi-vessel disease	-0.13	0.17	-	-
TIMI flow grade 3	0.25	0.005	-	-
Peak troponin T	-0.40	<0.001	-	-
LVEDV	-0.25	0.007	-	-
LVESV	-0.51	<0.001	-	-
LVEF	0.65	<0.001	0.36	<0.001
WMSI	-0.66	<0.001	-	-
Presence of diastolic dysfunction	-0.23	0.011	-	-
Peak LV GLS	-0.56	<0.001	-	-
MPI	-0.69	<0.001	-0.47	<0.001

Abbreviations are as defined in text.

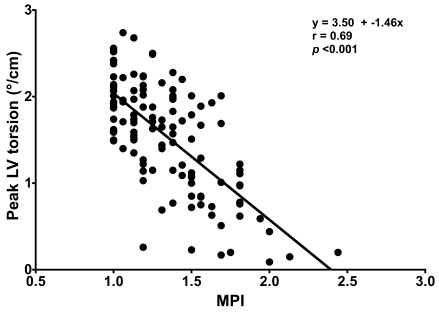

Figure 2. Linear regression analysis illustrating the relation between peak LV torsion and MPI.

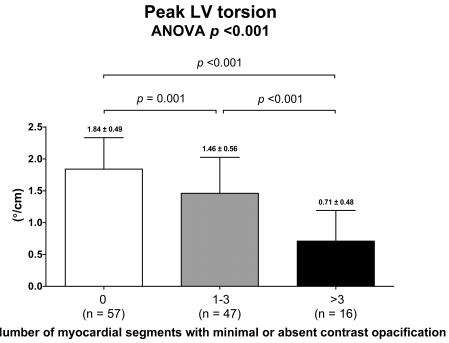

Figure 3. Relation between peak LV torsion and number of myocardial segments with minimal or absent contrast opacification.

Table 4 shows the results of univariate and multivariate logistic regression analyses performed to determine the relation between clinical and echocardiographic characteristics at baseline and LV remodeling at 6-month follow-up. By univariate analysis, several variables were significantly related to LV remodeling: anterior AMI, peak troponin T value, LVESV, LVEF, WMSI, presence of diastolic dysfunction, peak LV GLS, peak LV torsion, and MPI. However, by multivariate analysis, only peak LV torsion (odds ratio = 0.77; 95% CI, 0.65 to 0.92; p = 0.003) and MPI (odds ratio = 1.04; 95% CI, 1.01 to 1.07; p = 0.021) were independently related to the development of LV remodeling. Furthermore, peak LV torsion provided modest but significant incremental value over clinical, echocardiographic, and MCE variables in predicting LV remodeling (Figure 5).

By receiver-operator-characteristics curve analysis (Figure 6), peak LV torsion $\leq$1.44° /cm provided the highest sensitivity (95%) and specificity (77%) to predict LV remodeling; diagnostic accuracy was high in both anterior and nonanterior AMI patients (Figure 6).

Table 3. Baseline clinical and echocardiographic characteristics of AMI patients without vs with LV remodeling

	No LV remodeling (n = 93)	LV remodeling (n = 19)	p value
Age (years)	58±10	61±9	0.20
Male gender	66 (71%)	15 (79%)	0.48
Diabetes	9 (10%)	2 (11%)	0.91
Family history of coronary artery disease	36 (39%)	7 (37%)	0.88
Hypercholesterolemia	13 (14%)	2 (11%)	0.74
Hypertension	34 (37%)	6 (32%)	0.68
Current or previous smoking	54 (58%)	9 (47%)	0.39
Anterior myocardial infarction	35 (38%)	13 (68%)	0.013
Multi-vessel disease	29 (31%)	9 (47%)	0.18
TIMI flow grade 3	81 (87%)	14 (74%)	0.16
Peak troponin T (μg/l)	2.54 (1.29-5.25)	9.63 (4.96-12.51)	<0.001
LVEDV (ml)	101±23	106±34	0.59
LVESV (ml)	51±15	63±24	0.036
LVEF (%)	50±8	40±8	<0.001
LV diastolic longitudinal length (cm)	8.2±0.7	8.3±0.6	0.76
WMSI	1.63±0.30	2.05±0.21	<0.001
Presence of diastolic dysfunction	52 (56%)	16 (84%)	0.021
Peak LV GLS (%)	-15.0±3.3	-11.1±3.3	<0.001
Peak LV basal rotation (°)	-5.4±2.6	-4.6±2.5	0.20
Peak LV apical rotation (°)	9.7±4.1	3.5±3.0	<0.001
Peak LV twist (°)	14.4±4.3	6.6±3.5	<0.001
Peak LV torsion (°/cm)	1.75±0.51	0.80±0.44	<0.001
MPI	1.19 (1.00-1.41)	1.75 (1.38-1.81)	<0.001
Medical therapy at discharge			
- Antiplatelets	93 (100%)	19 (100%)	1.00
- Angiotensin-converting enzyme inhibitors and/or angiotensin receptor blockers	93 (100%)	19 (100%)	1.00
- Beta-blockers	89 (96%)	18 (95%)	1.00
- Statins	93 (100%)	19 (100%)	

Abbreviations are as defined in text.

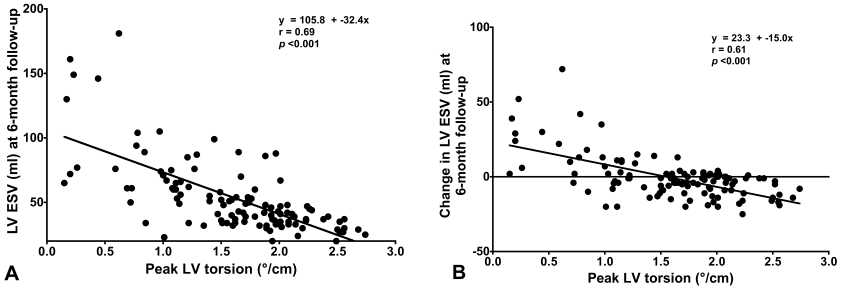

Figure 4. Relation between peak LV torsion at baseline and LVESV at 6-month follow-up (**panel A**) and the change in LVESV after 6-month follow-up compared with baseline value (**panel B**).

Table 4. Univariate and multivariate logistic regression analyses to determine the independent predictors of LV remodeling at 6-month follow-up

	Univariate		Multivariate	
	OR (95%CI)	p value	OR (95%CI)	p value
Age	1.03 (0.98-1.09)	0.20	1.00 (0.93-1.08)	0.94
Male	1.53 (0.47-5.04)	0.48	3.62 (0.66-19.8)	0.14
Anterior myocardial infarction	3.59 (1.25-10.3)	0.017	-	-
Multi-vessel disease	1.99 (0.73-5.40)	0.18	-	-
TIMI flow grade 3	0.42 (0.13-1.36)	0.15	-	-
Peak troponin T	1.23 (1.11-1.36)	<0.001	-	-
LVEDV	1.01 (0.99-1.03)	0.47		
LVESV	1.04 (1.01-1.07)	0.006	0.99 (0.94-1.04)	0.77
LVEF	0.85 (0.78-0.92)	<0.001	-	-
WMSI*	1.73 (1.34-2.24)	<0.001	-	-
Presence of diastolic dysfunction	4.21 (1.15-15.4)	0.030	-	-
Peak LV GLS	1.43 (1.19-1.71)	<0.001	-	-
Peak LV torsion*	0.72 (0.62-0.82)	<0.001	0.77 (0.65-0.92)	0.003
MPI*	1.79 (1.39-2.31)	<0.001	1.04 (1.01-1.07)	0.021

*: OR and 95%CI are intended for 0.1 unit increase. Abbreviations are as defined in text. OR indicates odds ratio. C-statistic = 0.93.

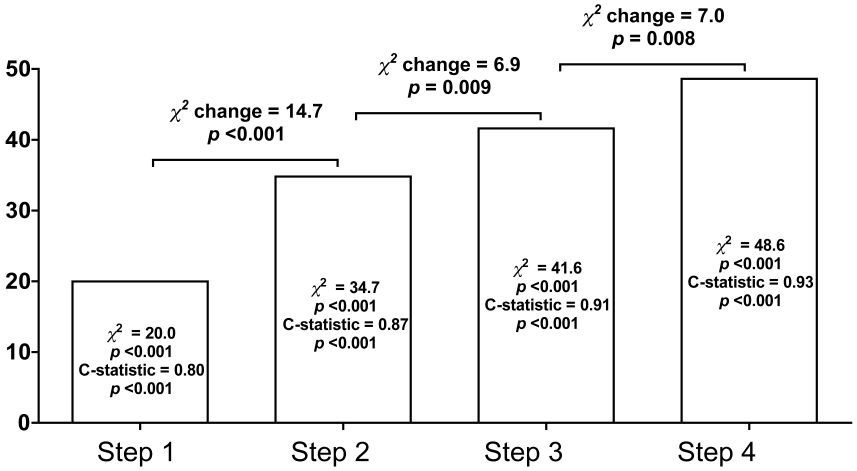

Step 1 included clinical variables (i.e. age, male gender, anterior myocardial infarction, multi-vessel disease, TIMI flow grade 3 and peak troponin T).
Step 2 included clinical and echocardiographic variables (i.e. left ventricular end-systolic volume, left ventricular ejection fraction, wall motion score index, presence of diastolic dysfunction and peak left ventricular global longitudinal strain).
Step 3 included clinical and echocardiographic variables and myocardial contrast echocardiography estimated infarct size (i.e. myocardial perfusion index).
Step 4 included clinical, echocardiographic and myocardial contrast echocardiography variables, and peak LV torsion.

Figure 5. Incremental value of peak LV torsion over clinical, echocardiographic, and MCE variables in predicting LV remodeling at 6-month follow-up.

DISCUSSION

The results of the present evaluation show that LV torsion is significantly impaired early after AMI, owing to a reduction of both basal and apical rotations. Infarct size (assessed by MCE) was independently related to LV torsion. In addition, LV torsion early after AMI was significantly and independently related to the occurrence of LV remodeling at 6-month follow-up.

Impact of AMI on LV Rotational Mechanics

Previous experimental and clinical studies have consistently shown an impairment of LV torsional deformation in the setting of acute and chronic MI.[7,8,18–21] In addition, LV torsion was related to global LV systolic

function and the extent of wall-motion abnormalities.[7,8,21] The present evaluation confirms and extends these previous observations. LV systolic function was indeed significantly related to LV torsion. More important, an independent correlation between infarct size (assessed by MCE and expressed as MPI) and LV torsion was noted on multivariate analysis. The larger damage of the LV subepicardial myofibers and the greater disarrangement of the typical architecture of LV myofibers secondary to larger infarcts may explain the observed relation between infarct size and LV torsion.

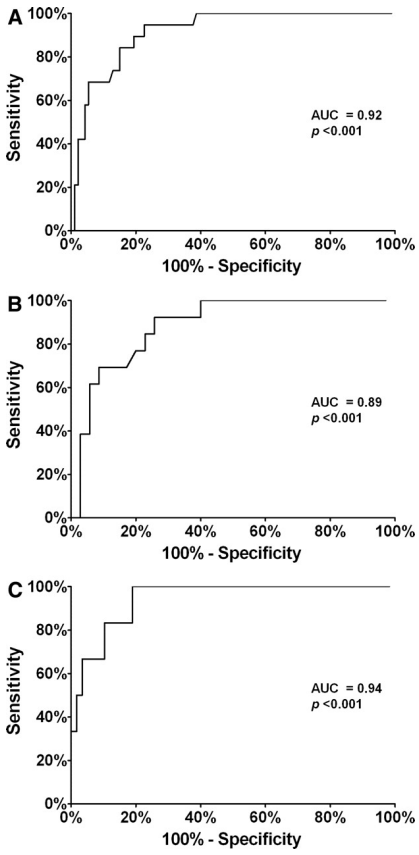

Figure 6. Receiver-operator-characteristics curve, testing the accuracy of peak LV torsion to predict LV remodeling at 6-month follow-up. **Panel A**. In the overall patient population, peak LV torsion ≤1.44° /cm provided the highest sensitivity (95%) and specificity (77%) to predict LV remodeling. **Panel B.** Among patients with anterior AMI, peak LV torsion ≤1.29° /cm provided the highest sensitivity (92%) and specificity (74%) to predict LV remodeling. **Panel C.** Among patients with nonanterior AMI, peak LV torsion ≤1.44° /cm provided the highest sensitivity (100%) and specificity (81%) to predict LV remodeling. AUC indicates area under the curve.

Epicardial myofibers are indeed extremely important to maintain LV torsional deformation.[4] Epicardial myofibers (compared with endocardial fibers) produce larger torque (related to the larger radius) and determine the overall direction of rotation.[4] Damage to epicardial fibers therefore appears mandatory for an impairment of LV torsional mechanics. Indeed, the present evaluation underscores that larger infarcts (as indicated by higher MPI values), leading to more extensive, transmural damage (spreading to epicardial myofibers),[17] result in a larger impairment of LV torsion. Previous experimental studies in an occlusion-reperfusion model provide evidence for this hypothesis by showing that LV torsion was impaired in the presence of transmural ischemia, whereas LV torsion was preserved in the presence of subendocardial ischemia only.[22,23] In addition, LV myofibers have a typical spiral architecture that is also extremely important in determining the LV systolic wringing motion. Large infarcts may be associated with extensive distortion of the typical architecture of LV myofibers, altering their obliquity and eventually impairing LV torsion.[24]

Role of LV Torsion in Predicting LV Remodeling

Besides being strictly related to the myocardial damage after AMI, LV torsion at baseline was found to be a strong predictor of LV remodeling at 6-month follow-up; interestingly, this relation remained even after adjustment for other univariate predictors of LV remodeling, including infarct size (expressed as MPI). Peculiar properties of the LV systolic twisting motion may explain this finding.

LV torsion indeed is not simply an index of global LV systolic function; previous mathematical models revealed the essential role of LV torsion in optimizing LV oxygen demand and the efficiency of LV systolic thickening by uniformly distributing myofiber stress across the myocardial wall.[25] A significant impairment of LV torsion after AMI will therefore result in increased myofiber stress and oxygen demand of the remaining noninfarcted myocardium. This low-efficiency state would further impair

myocardial contractility, possibly representing the initial step of a vicious circle of progressive LV dilatation and decline in LV systolic function.[18,24]

Clinical Implications

The present evaluation underscores the value of LV torsion as a sensitive global parameter of LV systolic myocardial performance. Its impairment early after AMI is strictly related to the extent of myocardial damage and possibly plays an important role in the development of LV remodeling. Indeed, peak LV torsion provided modest but significant incremental value over clinical, echocardiographic, and MCE variables in predicting LV remodeling. Accordingly, this parameter may be used in clinical practice as an early marker for risk stratification. Early assessment of LV torsion after AMI by speckle tracking echocardiography could identify patients (with reduced LV torsion) who may benefit from aggressive medical therapy to prevent LV remodeling, heart failure, and poor outcome.

Limitations

Some limitations should be acknowledged. First, only patients with ST-segment elevation AMI were included; consequently, the results cannot be extrapolated to patients with non–ST-segment elevation AMI. Another important limitation concerns the acquisition of short-axis images. The acquisition of true LV apical short-axis images is indeed dependent on the acoustic window (more than the basal short-axis view) and may be technically difficult to acquire in some patients. In addition, transducer position has a strong impact on the assessment of apical rotation by speckle-tracking echocardiography. It should, however, be emphasized that the most caudal transducer position was used to acquire the parasternal short-axis apical view; moreover, all patients without true LV apical short-axis images were not included in the present evaluation. Furthermore, motion throughout the planes at the basal level may reduce the accuracy of measurement of LV basal rotation. Finally, the impairment of LV torsion observed early after AMI may be partially related to the

presence of myocardial stunning; further studies are needed to assess the evolution of LV torsion after the acute phase of AMI.

CONCLUSIONS

LV torsion is significantly impaired early after AMI. The amount of impairment of LV torsion is related to infarct size. In addition, LV torsion at baseline predicts the occurrence of LV remodeling at 6-month follow-up, with modest but significant incremental value over clinical, echocardiographic, and MCE variables.

REFERENCES

1. White HD, Norris RM, Brown MA, et al. Left ventricular end-systolic volume as the major determinant of survival after recovery from myocardial infarction. Circulation. 1987;76:44–51.
2. John Sutton M, St, Pfeffer MA, Plappert T, et al. Quantitative two-dimensional echocardiographic measurements are major predictors of adverse cardiovascular events after acute myocardial infarction: the protective effects of captopril. Circulation. 1994;89:68–75.
3. Bolognese L, Cerisano G. Early predictors of left ventricular remodeling after acute myocardial infarction. Am Heart J. 1999;138:S79–S83.
4. Sengupta PP, Khandheria BK, Narula J. Twist and untwist mechanics of the left ventricle. Heart Fail Clin. 2008;4:315–324.
5. Notomi Y, Lysyansky P, Setser RM, et al. Measurement of ventricular torsion by two-dimensional ultrasound speckle tracking imaging. J Am Coll Cardiol. 2005;45:2034–2041.
6. Helle-Valle T, Crosby J, Edvardsen T, et al. New noninvasive method for assessment of left ventricular rotation: speckle tracking echocardiography. Circulation. 2005;112:3149–3156.
7. Takeuchi M, Nishikage T, Nakai H, et al. The assessment of left ventricular twist in anterior wall myocardial infarction using two-dimensional speckle tracking imaging. J Am Soc Echocardiogr. 2007;20:36–44.

8. Bansal M, Leano RL, Marwick TH. Clinical assessment of left ventricular systolic torsion: effects of myocardial infarction and ischemia. J Am Soc Echocardiogr. 2008;21:887–894.
9. Thygesen K, Alpert JS, White HD, et al. Universal definition of myocardial infarction. Circulation. 2007;116:2634–2653.
10. Himelman RB, Cassidy MM, Landzberg JS, et al. Reproducibility of quantitative two-dimensional echocardiography. Am Heart J. 1988;115:425–431.
11. Lang RM, Bierig M, Devereux RB, et al. Recommendations for chamber quantification: a report from the American Society of Echocardiography's Guidelines and Standards Committee and the Chamber Quantification Writing Group, developed in conjunction with the European Association of Echocardiography, a branch of the European Society of Cardiology. J Am Soc Echocardiogr. 2005;18:1440–1463.
12. Lester SJ, Tajik AJ, Nishimura RA, et al. Unlocking the mysteries of diastolic function: deciphering the Rosetta Stone 10 years later. J Am Coll Cardiol. 2008;51:679–689.
13. Reisner SA, Lysyansky P, Agmon Y, et al. Global longitudinal strain: a novel index of left ventricular systolic function. J Am Soc Echocardiogr. 2004;17:630–633.
14. Kim HK, Sohn DW, Lee SE, et al. Assessment of left ventricular rotation and torsion with two-dimensional speckle tracking echocardiography. J Am Soc Echocardiogr. 2007;20:45–53.
15. Weissman NJ, Cohen MC, Hack TC, et al. Infusion versus bolus contrast echocardiography: a multicenter, open-label, crossover trial. Am Heart J. 2000;139:399–404.
16. Dwivedi G, Janardhanan R, Hayat SA, et al. Prognostic value of myocardial viability detected by myocardial contrast echocardiography early after acute myocardial infarction. J Am Coll Cardiol. 2007;50:327–334.
17. Janardhanan R, Moon JC, Pennell DJ, et al. Myocardial contrast echocardiography accurately reflects transmurality of myocardial necrosis and predicts contractile reserve after acute myocardial infarction. Am Heart J. 2005;149:355–362.
18. Tibayan FA, Rodriguez F, Langer F, et al. Alterations in left ventricular torsion and diastolic recoil after myocardial infarction with and without chronic ischemic mitral regurgitation. Circulation. 2004;110(suppl II):II-109–II-114.

19. Sun JP, Niu J, Chou D, et al. Alterations of regional myocardial function in a swine model of myocardial infarction assessed by echocardiographic 2-dimensional strain imaging. J Am Soc Echocardiogr. 2007;20:498–504.
20. Nagel E, Stuber M, Lakatos M, et al. Cardiac rotation and relaxation after anterolateral myocardial infarction. Coron Artery Dis. 2000;11:261–267.
21. Garot J, Pascal O, Diebold B, et al. Alterations of systolic left ventricular twist after acute myocardial infarction. Am J Physiol Heart Circ Physiol. 2002;282:H357–H362.
22. Kroeker CA, Tyberg JV, Beyar R. Effects of ischemia on left ventricular apex rotation: an experimental study in anesthetized dogs. Circulation. 1995;92:3539–3548.
23. Knudtson ML, Galbraith PD, Hildebrand KL, et al. Dynamics of left ventricular apex rotation during angioplasty: a sensitive index of ischemic dysfunction. Circulation. 1997;96:801–808.
24. Buchalter MB, Rademakers FE, Weiss JL, et al. Rotational deformation of the canine left ventricle measured by magnetic resonance tagging: effects of catecholamines, ischaemia, and pacing. Cardiovasc Res. 1994;28:629–635.
25. Beyar R, Sideman S. Left ventricular mechanics related to the local distribution of oxygen demand throughout the wall. Circ Res. 1986;58:664–677.

Chapter 12

Impact of Left Ventricular Dyssynchrony Early on Left Ventricular Function After First Acute Myocardial Infarction

Gaetano Nucifora, Matteo Bertini, Nina Ajmone Marsan, Victoria Delgado, Arthur J. Scholte, Arnold C.T. Ng, Jacob M. van Werkhoven, Hans-Marc J. Siebelink, Eduard R. Holman, Martin J. Schalij, Ernst E. van der Wall, Jeroen J. Bax

Am J Cardiol 2010;105:306–311

ABSTRACT

The impact of left ventricular (LV) dyssynchrony after acute myocardial infarction (AMI) on LV ejection fraction (EF) is unknown. One hundred twenty-nine patients with a first ST-elevation AMI (58±11 years, 78% men) and QRS duration <120 ms were included. All patients underwent primary percutaneous coronary intervention. Real-time 3-dimensional echocardiography and myocardial contrast echocardiography were performed to assess LV function, LV dyssynchrony, and infarct size. LV dyssynchrony was defined as the SD of the time to reach the minimum systolic volume for 16 LV segments, expressed in percent cardiac cycle (systolic dyssynchrony index [SDI]). Myocardial perfusion at myocardial contrast echocardiography was scored (*1* = normal/homogenous; *2* = decreased/patchy; *3* = minimal/absent) using a 16-segment model; a myocardial perfusion index, expressing infarct size, was derived by summing segmental contrast scores and dividing by the number of segments. SDI in patients with AMI was 5.24±2.23% compared to 2.02±0.70% of controls (p <0.001). Patients with AMI and LVEF <45% had significantly higher SDI compared to patients with LVEF ≥45% (4.29±1.44 vs 6.95±2.40, p <0.001). At multivariate analysis, SDI was independently related to LVEF; in addition, the impact of SDI on LV systolic function was incremental to infarct size and anterior location of AMI (F change 16.9, p <0.001). In conclusion, LV synchronicity is significantly impaired soon after AMI. LV dyssynchrony is related to LVEF and has an additional detrimental effect on LV function, beyond infarct size and the anterior location of AMI.

INTRODUCTION

Advances in echocardiographic techniques, i.e., tissue Doppler echocardiography, speckle-tracking echocardiography, and real-time 3-dimensional echocardiography (RT3DE) have recently demonstrated an impaired left ventricular (LV) synchronicity in patients with acute myocardial infarction (AMI).[1-3] In the setting of chronic heart failure, LV dyssynchrony is a phenomenon extensively described and related to impaired LV systolic function and poor prognosis.[4-8] In the setting of AMI, however, it is unclear whether LV dyssynchrony is independently associated with LV ejection fraction (EF). Moreover, the detrimental effect of LV dyssynchrony on LV systolic function in addition to other variables remains unknown. Accordingly, the aim of the present study was twofold: *(1)* to assess the decrease in LV synchronicity after AMI (compared to normal values) and *(2)* to explore the relation between this decrease in LV synchronicity and LV systolic function. In particular, the effect of LV dyssynchrony on LVEF in addition to other variables was assessed.

METHODS

The population consisted of 159 consecutive patients admitted to the coronary care unit because of a first ST-segment elevation AMI. Patients with a QRS complex duration >120 ms were excluded from the study.
The diagnosis of AMI was made based on typical electrocardiographic changes and/or ischemic chest pain associated with increased cardiac biomarkers.[9] All patients underwent immediate coronary angiography and primary percutaneous coronary intervention (PCI). The infarct-related artery was identified by the site of coronary occlusion during coronary angiography and electrocardiographic criteria. During PCI, the final Thrombolysis In Myocardial Infarction flow was assessed. In addition, time

from onset of symptoms to first balloon dilatation (symptoms-to-balloon time) was determined.

Using the electrocardiograms acquired on admission and 1 hour after PCI, the ST-segment resolution was assessed, as previously described.[10] The sum of ST-segment elevations was measured 60 ms after the J point in leads I, aVL, and V1 to V6 for anterior AMI and leads II, III, aVF, V5, and V6 for nonanterior AMI. Percent resolution of ST-segment elevation from before to after PCI was then calculated.

RT3DE was performed 48 hours after PCI to assess global LV systolic function and LV dyssynchrony; immediately after RT3DE, myocardial contrast echocardiography was performed to assess infarct size. These echocardiographic examinations are part of the routine, comprehensive assessment of patients presenting with AMI in our clinics.

In addition, 30 subjects without evidence of structural heart disease and without known risk factors for coronary artery disease, matched for age, gender, and body surface area, who underwent RT3DE, were included as a control group. These subjects were derived from the echocardiographic database and were clinically referred for echocardiographic evaluation because of atypical chest pain, palpitations, or syncope without murmur.

To determine impairment of LV synchronicity after AMI, patient data were compared to data from controls. In addition, the relation between LV systolic function and other clinical and echocardiographic variables (including LV dyssynchrony, infarct size, and infarct location) was evaluated.

Patients underwent imaging in the left lateral decubitus position with a commercially available system (Vivid 7, GE Healthcare, Horten, Norway) equipped with a 3V phased array transducer (2.5 MHz). Apical full volume 3D datasets were acquired in harmonic mode, integrating, during a brief breath-hold, 8 R-wave–triggered subvolumes into a larger pyramidal volume (90° by 90°) with a complete capture of the left ventricle. The 3D datasets were digitally stored for off-line analysis.

Off-line analysis was performed by an observer who had no knowledge of patients' identity and myocardial contrast echocardiographic results. Dedicated software (4D LV-Analysis; TomTec, Munich, Germany) was used. The algorithm used by the software to calculate LV end-diastolic volume, LV end-systolic volume, and LVEF is described in detail elsewhere.[11] Briefly, a semiautomated method for the detection of the apical 4-chamber view and the 60° and 120° incremental views and for the tracing of the endocardial border in the entire 3D dataset (including LV trabeculations and papillary muscles within the LV volume) were used. Subsequently, a final reconstruction of the LV model was generated and LV volumes and LVEF were obtained. In addition, the same LV model was used for the assessment of LV dyssynchrony, as previously described.[12] Briefly, the LV model was automatically divided in 16 pyramidal subvolumes (6 basal segments, 6 mid segments, and 4 apical segments) based around a nonfixed central point. For each volumetric segment, the time–volume curve for the entire cardiac cycle was derived and the time taken to reach the minimum systolic volume was calculated. The SD of the time taken to reach the minimum systolic volume expressed as percent cardiac cycle (systolic dyssynchrony index [SDI]) was then calculated as a marker of global LV dyssynchrony.[12]

Immediately after RT3DE, myocardial contrast echocardiography was performed to evaluate myocardial perfusion, to assess infarct size after AMI. The same ultrasound system equipped with a 3.5-MHz transducer was used. The 3 standard apical views were acquired using a low-power technique (mechanical index 0.10 to 0.26). Background gains were set so that minimal tissue signal was seen, and the focus was set at the level of the mitral valve. Luminity (Bristol-Myers Squibb Pharma, Brussels, Belgium) was used as contrast agent. Each patient received an infusion of 1.3 ml of echocardiographic contrast diluted in 0.9% sodium chloride solution 50 ml through a 20-gauge intravenous catheter in a proximal forearm vein. Infusion rate was initially set at 4.0 ml/min and then titrated to achieve optimal myocardial enhancement without attenuation

artifacts.[13] Machine settings were optimized to obtain the best possible myocardial opacification with minimal attenuation. At least 15 cardiac cycles after high mechanical index (1.7) microbubble destruction [14] were stored in cine-loop format.

Analysis of myocardial contrast echocardiograms was performed off-line using EchoPAC 7.0.0 (GE Healthcare). To evaluate myocardial perfusion, the left ventricle was divided according to the 16-segment model of the American Society of Echocardiography.[15] A semiquantitative scoring system was used to assess contrast intensity after microbubble destruction: *(1)* normal/homogenous opacification; *(2)* decreased/patchy opacification; *(3)* minimal or absent contrast opacification.[14,16] A myocardial perfusion index, expressing infarct size, was derived by adding contrast scores of all segments and dividing by the total number of segments.[14, 16]

Continuous variables are expressed as mean±SD, when normally distributed, and as median and interquartile range, when not normally distributed. Categorical data are presented as absolute numbers and percentages.

Differences in continuous variables were assessed using Student's t test or Mann-Whitney U test, if appropriate. Chi-square test or Fisher's exact test, if appropriate, was computed to assess differences in categorical variables.

Univariate and multivariate regression analyses were performed to evaluate the relation between LVEF in patients with AMI and the characteristics of age, gender, coronary risk factors, infarct location, multivessel disease, Thrombolysis In Myocardial Infarction flow grade 3 after PCI, symptoms-to-balloon time, QRS duration, ST-segment resolution, peak troponin T, LV dyssynchrony (expressed as SDI), and infarct size (expressed as myocardial perfusion index). Only variables with a p value <0.1 at univariate analysis were entered as covariates in the multivariate model. To determine the potential incremental value of SDI

over the other variables, the R^2 of the multivariate model was compared to the R^2 of the same model without SDI.

A p value <0.05 was considered statistically significant. Statistical analysis was performed using SPSS 15.0 (SPSS, Inc., Chicago, Illinois).

RESULTS

Reliable real-time 3-dimensional echocardiographic and myocardial contrast echocardiographic data were obtained in 129 patients; consequently, 30 patients were excluded from further analysis. All control subjects had reliable real-time 3-dimensional echocardiographic data.

Clinical and echocardiographic characteristics of patients with AMI are listed in Table 1. Sixty patients (46%) had an anterior AMI; obstructive multivessel disease (i.e., >1 vessel with luminal narrowing ≥70%) was present in 46 patients (36%).

Compared to control subjects, patients with AMI had significantly lower LVEF (64±6% vs 46±9%, p <0.001) and significantly higher SDI (2.02±0.70% vs 5.24±2.23%, p <0.001). The observed impairment of LV synchronicity in patients with AMI is shown in Figure 1.

Patients with AMI were subdivided into 2 groups according to LV systolic function (LVEF ≥45%, n = 83; LVEF <45%, n = 46). Clinical and echocardiographic characteristics of these 2 groups are presented in Table 2. Patients with LVEF <45% had more frequently multivessel disease (p = 0.032), less frequently Thrombolysis In Myocardial Infarction flow grade 3 after primary PCI (p = 0.049) and higher peak troponin T (p = 0.006) compared to patients with LVEF ≥45% (Table 2).

Regarding LV synchronicity, patients with LVEF <45% had significantly higher SDI (p <0.001) compared to patients with LVEF ≥45% (Table 2).

Figure 2 shows the impairment of LV synchronicity in patients with AMI and LVEF <45% compared to those with LVEF ≥45%. Indeed, a significant relation (r = 0.69, p <0.001) was noted between LVEF and SDI.

Table 1. Clinical and echocardiographic characteristics of control subjects and patients with acute myocardial infarction

	Control subjects (n = 30)	AMI patients (n = 129)	p value
Age (years)	57±11	58±11	0.53
Men	23 (77%)	100 (78%)	0.92
Body surface area (m^2)	1.96±0.58	1.98±0.22	0.76
Diabetes mellitus	-	14 (11%)	-
Family history of coronary artery disease *	-	49 (38%)	-
Hypercholesterolemia †	-	19 (15%)	-
Hypertension ‡	-	47 (36%)	-
Current or previous smoker	-	76 (59%)	-
Anterior wall acute myocardial infarction	-	60 (46%)	-
Infarct-related coronary artery			
- left anterior descending	-	60 (46%)	-
- left circumflex	-	22 (18%)	-
- right	-	46 (36%)	-
Multi-vessel coronary disease	-	46 (36%)	-
Thrombolysis In Myocardial Infarction flow grade 3		109 (85%)	-
Symptoms-to-balloon time (minutes)	-	177 (134-219)	-
QRS duration (msec)		96±13	
ST-segment resolution (%)	-	62±31	-
Peak troponin T (μg/l)	-	3.10 (1.52-6.89)	-
Left ventricular end-diastolic volume (ml)	90±23	110±30	0.01
Left ventricular end-systolic volume (ml)	35±14	60±23	<0.001
Left ventricular ejection fraction (%)	64±6	46±9	<0.001
Systolic dyssynchrony index (%)	2.02±0.70	5.24±2.23	<0.001
Myocardial perfusion index	-	1.25 (1.09-1.50)	-

Data are expressed as mean±SD or median (interquartile range), and n (%). *. Defined when close relatives had premature coronary artery disease (men <55 years old and women <65 years old). †: defined as total cholesterol ≥240 mg/dl. ‡: defined as systolic blood pressure ≥140 mmHg and/or diastolic blood pressure ≥90 mmHg.

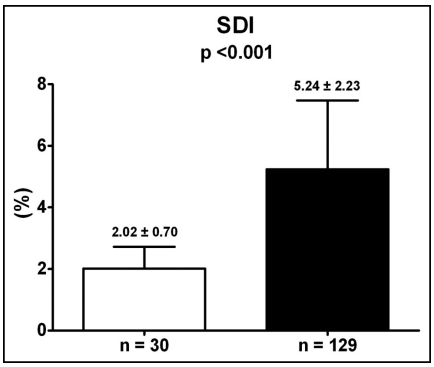

Figure 1. SDI in control subjects (white bar) and patients with AMI (black bar) (p <0.001).

Table 3 presents the results of univariate and multivariate regression analyses performed to determine factors related to LV systolic function. At univariate analysis, several variables were significantly related to LVEF. However, at multivariate analysis, only anterior location of AMI (beta −0.16, p = 0.037), SDI (beta −0.52, p <0.001), and myocardial perfusion index (beta −0.28, p = 0.034) were independent factors associated with LVEF. Adding SDI to the multivariate model significantly increased R2 from 0.45 to 0.52 (F change 16.9, p <0.001).

Figure 3 shows an example of a patient with severe impairment of LV systolic function and synchronicity after AMI.

DISCUSSION

The results of the present study show that LV synchronicity (assessed by RT3DE) is significantly impaired soon after AMI. The severity of this impairment is related to LV systolic function. In addition, the impact of SDI on LV systolic function was incremental to infarct size and anterior location of AMI.

The presence and clinical relevance of LV dyssynchrony in the setting of chronic heart failure has been extensively investigated in the previous decade; in this group of patients, loss of LV synchronous contraction is

related to impaired LV systolic function and poor hemodynamic status and is a predictor of worse outcome.[4-8] In addition, restoration of LV synchronicity, by cardiac resynchronization therapy, has been shown to reverse LV remodeling and to improve LV function and prognosis.[17-19]

Table 2. Clinical and echocardiographic characteristics of patients with acute myocardial infarction in relation to left ventricular systolic function

	LVEF ≥45% (n = 83)	LVEF <45% (n = 46)	p value
Age (years)	57±11	60±11	0.090
Men	60 (72%)	40 (87%)	0.056
Diabetes mellitus	9 (11%)	5 (11%)	1.00
Family history of coronary artery disease	31 (37%)	18 (39%)	0.84
Hypercholesterolemia	12 (15%)	7 (15%)	0.91
Hypertension	35 (42%)	12 (26%)	0.069
Current or previous smoker	47 (57%)	29 (63%)	0.48
Anterior wall acute myocardial infarction	34 (41%)	26 (57%)	0.090
Multi-vessel coronary disease	24 (29%)	22 (48%)	0.032
Thrombolysis In Myocardial Infarction flow grade 3	74 (89%)	35 (76%)	0.049
Symptoms-to-balloon time (minutes)	170 (127-215)	184 (150-231)	0.16
QRS duration (msec)	94±13	99±13	0.027
ST-segment resolution (%)	65±31	56±30	0.13
Peak troponin T (μg/l)	2.69 (1.23-5.39)	4.82 (1.85-11.02)	0.006
Left ventricular end-diastolic volume (ml)	105±25	118±38	0.042
Left ventricular end-systolic volume (ml)	51±14	75±28	<0.001
Left ventricular ejection fraction (%)	51±5	37±6	<0.001
Systolic dyssynchrony index (%)	4.29±1.44	6.95±2.40	<0.001
Myocardial perfusion index	1.19 (1.00-1.38)	1.56 (1.23-1.81)	<0.001

Data are expressed as mean±SD, median (interquartile range), or number of subjects (percentage).

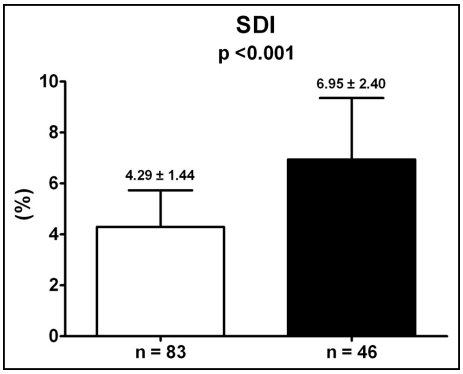

Figure 2. SDI in patients with AMI in relation to LV systolic function, namely LVEF ≥45% (white bar) and LVEF <45% (black bar) (p <0.001).

Table 3. Univariate and multivariate regression analyses to determine independent correlates of left ventricular systolic function in patients with acute myocardial infarction

	Univariate		Multivariate	
	β	p value	β	p value
Age	-0.17	0.058	0.025	0.72
Male gender	-0.14	0.10	-	-
Diabetes mellitus	0.017	0.85	-	-
Family history of coronary artery disease	0.092	0.30	-	-
Hypercholesterolemia	-0.031	0.73	-	-
Hypertension	0.051	0.57	-	-
Current or previous smoker	-0.005	0.96	-	-
Anterior wall acute myocardial infarction	-0.19	0.036	-0.16	0.037
Multi-vessel coronary disease	-0.19	0.032	-0.94	0.35
Thrombolysis In Myocardial Infarction flow grade 3	0.15	0.092	0.001	0.99
Symptoms-to-balloon time	-0.077	0.38	-	-
QRS duration	-0.17	0.061	-0.079	0.24
ST-segment resolution	0.21	0.015	0.028	0.69
Peak troponin T	-0.28	0.001	0.037	0.62
Systolic dyssynchrony index	-0.69	<0.001	-0.52	<0.001
Myocardial perfusion index	-0.65	<0.001	-0.28	0.034

The R^2 of the model selected at multivariate analysis was 0.52.

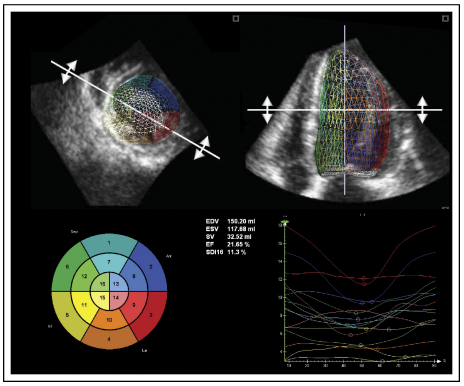

Figure 3. Example of a patient showing severe impairment of LV systolic function (LVEF 22%) and synchronicity (SDI 11.3%) after AMI.

More recently, LV dyssynchrony has been described to occur also in patients with AMI.[1-3, 20] However, the clinical meaning of this phenomenon has not been yet fully elucidated. In particular, it is unclear whether the presence of LV dyssynchrony after AMI independently influences LV function in these patients. Moreover, the detrimental effect of LV dyssynchrony in addition to other variables (e.g., infarct size and anterior location of AMI) on LV systolic function remains unknown.

In the present study, RT3DE was used to assess LV systolic function and LV synchronicity after AMI. This approach has been documented to provide highly accurate measurements of LVEF;[21] in addition, it is more robust than tissue Doppler echocardiography for the evaluation of LV dyssynchrony, being more reproducible and more consistent in differentiating healthy subjects from those affected by LV dyssynchrony.[22] Moreover, myocardial contrast echocardiography was used to obtain information about myocardial perfusion abnormalities after AMI and, hence, infarct size.[23]

In line with previous observations,[1] impairment of LV synchronicity (expressed as SDI) was observed in patients with AMI compared to control subjects. In addition, LV dyssynchrony was significantly associated to LV systolic function. Importantly, this relation remained

after adjustment for infarct size and anterior location of AMI, being incremental over these variables in determining LVEF.

LV dyssynchrony results in a nonhomogenous distribution of myocardial load and deformation and thus increases myocardial energy demand;[24] this may negatively influence the contractility of residual viable myocardium, thus further impairing LV function.

The results of the present study suggest that LV dyssynchrony soon after AMI has an additional detrimental impact on LV performance, beyond the infarct size itself; moreover, it may potentially contribute to the vicious circle of progression of LV dysfunction.[2] In this perspective, therapeutic approaches aiming to recover a more synchronous LV contraction (e.g., with cardiac resynchronization therapy) may be beneficial and improve LV systolic function, thus preventing LV remodeling. However, further studies are needed to support this hypothesis.

REFERENCES

1. Zhang Y, Chan AK, Yu CM, et al. Left ventricular systolic asynchrony after acute myocardial infarction in patients with narrow QRS complexes. Am Heart J. 2005; 149: 497–503

2. Mollema SA, Liem SS, Suffoletto MS, et al. Left ventricular dyssynchrony acutely after myocardial infarction predicts left ventricular remodeling. J Am Coll Cardiol. 2007; 50: 1532–1540

3. Delgado V, Sitges M, Vidal B, et al. Assessment of left ventricular dyssynchrony by real-time three-dimensional echocardiography. Rev Esp Cardiol. 2008; 61: 825–834

4. Baldasseroni S, Opasich C, Gorini M, et al. Left bundle-branch block is associated with increased 1-year sudden and total mortality rate in 5517 outpatients with congestive heart failure: a report from the Italian network on congestive heart failure. Am Heart J. 2002; 143: 398–405

5. Fauchier L, Marie O, Casset-Senon D, et al. Interventricular and intraventricular dyssynchrony in idiopathic dilated cardiomyopathy: a prognostic study with

Fourier phase analysis of radionuclide angioscintigraphy. J Am Coll Cardiol. 2002; 40: 2022–2030
6. Yu CM, Lin H, Zhang Q, et al. High prevalence of left ventricular systolic and diastolic asynchrony in patients with congestive heart failure and normal QRS duration. Heart. 2003; 89: 54–60
7. Bader H, Garrigue S, Lafitte S, et al. Intra-left ventricular electromechanical asynchrony (A new independent predictor of severe cardiac events in heart failure patients) . J Am Coll Cardiol. 2004; 43: 248–256
8. Penicka M, Bartunek J, Lang O, et al. Severe left ventricular dyssynchrony is associated with poor prognosis in patients with moderate systolic heart failure undergoing coronary artery bypass grafting. J Am Coll Cardiol. 2007; 50: 1315–1323
9. Thygesen K, Alpert JS, White HD, et al. Universal definition of myocardial infarction. Circulation. 2007; 116: 2634–2653
10. Nijveldt R, Beek AM, Hirsch A, et al. Functional recovery after acute myocardial infarction: comparison between angiography, electrocardiography, and cardiovascular magnetic resonance measures of microvascular injury. J Am Coll Cardiol. 2008; 52: 181–189
11. Soliman OI, Krenning BJ, Geleijnse ML, et al. A comparison between QLAB and TomTec full volume reconstruction for real time three-dimensional echocardiographic quantification of left ventricular volumes. Echocardiography. 2007; 24: 967–974
12. Kapetanakis S, Kearney MT, Siva A, et al. Real-time three-dimensional echocardiography: a novel technique to quantify global left ventricular mechanical dyssynchrony. Circulation. 2005; 112: 992–1000
13. Weissman NJ, Cohen MC, Hack TC, et al. Infusion versus bolus contrast echocardiography: a multicenter, open-label, crossover trial. Am Heart J. 2000; 139: 399–404
14. Dwivedi G, Janardhanan R, Hayat SA, et al. Prognostic value of myocardial viability detected by myocardial contrast echocardiography early after acute myocardial infarction. J Am Coll Cardiol. 2007; 50: 327–334
15. Lang RM, Bierig M, Devereux RB. F et al. Recommendations for chamber quantification: a report from the American Society of Echocardiography's Guidelines and Standards Committee and the Chamber Quantification Writing Group, developed in conjunction with the European Association of

Echocardiography, a branch of the European Society of Cardiology. J Am Soc Echocardiogr. 2005; 18: 1440–1463
16. Main ML, Magalski A, Kusnetzky LL, et al. Usefulness of myocardial contrast echocardiography in predicting global left ventricular functional recovery after anterior wall acute myocardial infarction. Am J Cardiol. 2004; 94: 340–342
17. Yu CM, Chau E, Sanderson JE, et al. Tissue Doppler echocardiographic evidence of reverse remodeling and improved synchronicity by simultaneously delaying regional contraction after biventricular pacing therapy in heart failure. Circulation. 2002; 105: 438–445
18. Bleeker GB, Mollema SA, Holman ER, et al. Left ventricular resynchronization is mandatory for response to cardiac resynchronization therapy: analysis in patients with echocardiographic evidence of left ventricular dyssynchrony at baseline. Circulation. 2007; 116: 1440–1448
19. Ypenburg C, van Bommel RJ, Borleffs CJ, et al. Long-term prognosis after cardiac resynchronization therapy is related to the extent of left ventricular reverse remodeling at midterm follow-up. J Am Coll Cardiol. 2009; 53: 483–490
20. Chang SA, Chang HJ, Choi S.I, et al. Usefulness of left ventricular dyssynchrony after acute myocardial infarction, assessed by a tagging magnetic resonance image derived metric, as a determinant of ventricular remodeling. Am J Cardiol. 2009; 104: 19–23
21. Badano LP, Dall'Armellina E, Monaghan MJ, et al. Real-time three-dimensional echocardiography: technological gadget or clinical tool?. J Cardiovasc Med. 2007; 8: 144–162
22. Conca C, Faletra FF, Miyazaki C, et al. Echocardiographic parameters of mechanical synchrony in healthy individuals. Am J Cardiol. 2009; 103: 136–142
23. Hayat SA, Senior R. Myocardial contrast echocardiography in ST elevation myocardial infarction: ready for prime time?. Eur Heart J. 2008; 29: 299–314
24. Prinzen FW, Hunter WC, Wyman BT, et al. Mapping of regional myocardial strain and work during ventricular pacing: experimental study using magnetic resonance imaging tagging. J Am Coll Cardiol. 1999; 33: 1735–1742

Chapter 13

Temporal Evolution of Left Ventricular Dyssynchrony After Myocardial Infarction: Relation With Changes in Left Ventricular Systolic Function

Gaetano Nucifora, Matteo Bertini, Nina Ajmone Marsan, Arthur J. Scholte, Hans-Marc J. Siebelink, Eduard R. Holman, Martin J. Schalij, Ernst E. van der Wall, Jeroen J. Bax, Victoria Delgado

Eur Heart J Cardiovasc Imaging 2012:13;1041–1046

ABSTRACT

Aims. The relationship between temporal changes in left ventricular (LV) dyssynchrony and LV functional recovery after acute myocardial infarction (MI) remains unclear. Accordingly, the aim of the present study was to evaluate the temporal evolution of LV synchronicity after acute MI, and to explore the relationship between changes in LV systolic function and LV synchronicity.

Methods and results. In 193 patients with a first acute MI, LV dyssynchrony (SDI) and global systolic function were evaluated with real-time three-dimensional echocardiography 48 h after percutaneous coronary intervention and at 6 months follow-up. Changes in LV systolic function and synchronicity were evaluated at the follow-up and the relationship between these changes was explored. A total of 59 (40%) patients had an anterior acute MI. Median peak value of troponin T was 2.97 μg/L (1.41–6.06 μg/L). Mean LVEF was 47±8% and mean SDI was 5.01±2.10%, respectively. At 6 months follow-up, a significant improvement in LVEF (50±9 vs. 47±8%; $p < 0.001$) and SDI (4.52±1.97 vs. 5.01±2.10%; $p = 0.003$) was noted. A strong correlation was found between LVEF change and SDI change ($\beta = -0.63$; $p < 0.001$). At multivariate analysis, SDI change was an independent factor associated with changes in LVEF. Importantly, an addition of SDI change to the multivariate model significantly increased the R2 from 0.41 to 0.57 (F change 49.0, $p < 0.001$).

Conclusion. A temporal evolution of LV synchronicity was observed after a first, mechanically reperfused, acute MI. The reduction in LV dyssynchrony independently influenced LV functional recovery in these patients.

INTRODUCTION

Recently, impairment of the synchronicity of left ventricular (LV) contraction has been described in the acute phase of myocardial infarction (MI);[1–4] in this setting, the presence of LV dyssynchrony has been shown to have a detrimental effect on haemodynamic function, mid-term LV remodelling, and long-term prognosis.[1–4] However, scarce data are available regarding the temporal evolution of LV dyssynchrony during the follow-up. In addition, the relationship between temporal changes in LV dyssynchrony and LV functional recovery remains unclear. Accordingly, the aim of the present study was two-fold: *first*, to assess the temporal evolution of LV synchronicity after acute MI, and *second*, to explore the relationship between changes in LV systolic function and LV synchronicity.

METHODS

Patient population

One-hundred ninety-three consecutive patients admitted with a first ST-segment elevation acute MI were selected from an ongoing registry.[2] Patients with a QRS complex duration >120 ms were excluded from the study.

The diagnosis of acute MI was made on the basis of typical electrocardiographic changes and/or ischaemic chest pain associated with increased plasma levels of cardiac biomarkers.[5] Immediate coronary angiography and primary percutaneous coronary intervention (PCI) of infarct-related artery were performed in all the patients. The infarct-related artery was identified by the site of coronary occlusion during coronary angiography and electrocardiographic criteria. Troponin T levels were determined at admission and at 6, 12, and 18 h of admission. Real-time three-dimensional echocardiography (RT3DE) was performed 48 h after PCI to assess global LV systolic function and LV dyssynchrony; in

addition, the presence and grade of mitral regurgitation and diastolic dysfunction were evaluated with two-dimensional colour, pulsed, and continuous wave Doppler echocardiography. At 6 months follow-up, RT3DE was repeated and global LV systolic function and LV dyssynchrony were re-assessed. Accordingly, changes in LV systolic function and synchronicity were evaluated at follow-up and the relationship between these changes was explored. These echocardiographic examinations were performed as part of the routine, comprehensive assessment of patients presenting with acute MI in our clinic, and not purely for study purposes. Clinical, angiographic, and echocardiographic data were prospectively collected in the departmental cardiology information system (EPD-Vision®) and retrospectively analysed.

Real-time three-dimensional echocardiography

Patients were imaged in the left lateral decubitus position with a commercially available system (Vivid 7, GE Healthcare, Horten, Norway) equipped with a 3V-phased array transducer (2.5 MHz). Apical full-volume three-dimensional data sets were acquired in harmonic mode, integrating, during a brief breath-hold, eight R-wave-triggered sub-volumes into a larger pyramidal volume (90° by 90°) with a complete capture of the LV. The 3D data sets were digitally stored and a dedicated software (4D LV-Analysis©; TomTec, Munich, Germany) was used for the offline analysis. The algorithm used by the software to calculate LV end-diastolic volume (EDV), LV end-systolic volume (ESV), and LVEF is described in detail elsewhere.[6,7] Briefly, a semi-automated method for the detection of the apical four-chamber view and the 60° and 120° incremental views and for the tracing of the endocardial border in the entire 3D data set (including LV trabeculations and papillary muscles within the LV volume) is used. Subsequently, a final reconstruction of the LV model is generated and LV volumes and LVEF are obtained. Qualitative assessment of regional wall motion was performed according to the 16-segment model of the American Society of Echocardiography and the global wall motion

score index (WMSI) was calculated for each patient.[8] In addition, the same LV model was used for the assessment of LV dyssynchrony, as previously described.[9] Briefly, the LV model was automatically divided in 16 pyramidal sub-volumes (six basal segments, six mid segments, and four apical segments) based around a non-fixed central point. For each volumetric segment, the time–volume curve for the entire cardiac cycle is derived and the time to minimum systolic volume (Tmsv) is calculated. The standard deviation (SD) of the 16 segments Tmsv expressed in percentage of cardiac cycle (the systolic dyssynchrony index, SDI) was then calculated as a marker of global LV dyssynchrony.[9]

As previously reported,[2] a normal control group value of SDI was 2.02±0.70%; significant mechanical dyssynchrony was defined as an SDI > 3 SD above the mean for normal subjects (4.12%).

Two-dimensional echocardiography

Two-dimensional echocardiography was performed with the same commercially available system (Vivid 7 Dimension, GE Healthcare) equipped with a 3.5 MHz transducer. Standard Doppler and colour-Doppler data were acquired from parasternal and apical views (four-, two-, and three-chamber) and digitally stored in cine-loop format; analyses were subsequently performed offline using EchoPAC version 7.0.0 (GE Healthcare, Horten, Norway).

The severity of MR was quantitatively determined by integrating different echocardiographic parameters such as vena contracta width and regurgitant volume measured with the proximal isovelocity surface area method, as recommended.[10] As previously described,[11] transmitral and pulmonary vein pulsed-wave Doppler tracings were used to classify diastolic function as *(i)* normal; *(ii)* diastolic dysfunction grade 1 (mild); *(iii)* diastolic dysfunction grade 2 (moderate); *(iv)* diastolic dysfunction grade 3 (severe).

Statistical analysis

Continuous variables are expressed as mean and standard deviation, when normally distributed, and as median and interquartile range, when not normally distributed. Categorical data are presented as absolute numbers and percentages. Differences in continuous variables between baseline and 6 months follow-up were assessed using the paired t test or the Wilcoxon singed rank test, if appropriate. Differences in continuous variables between two different groups were assessed using the Student t-test or the Mann–Whitney U-test, if appropriate.

The relationship between the changes in LVEF (ΔLVEF) and in LVESV (ΔLVESV) and the change in LV dyssynchrony (ΔSDI) after 6 months follow-up was evaluated with the linear regression analysis.

To evaluate the independent determinants of ΔLVEF at follow-up, univariate and multivariate linear regression analyses were performed. The following clinical and echocardiographic characteristics were included in the univariate model: age, gender, coronary risk factors, infarct location, multi-vessel disease, peak troponin T, symptoms onset to balloon time, baseline LVESV, baseline LVEF, baseline WMSI, presence of mitral regurgitation at baseline, presence of diastolic dysfunction at baseline, baseline SDI, and ΔSDI. Only significant variables at univariate analysis were entered as covariates in the multivariate model. Finally, in order to determine the potential incremental value of ΔSDI over the other variables, the R^2 of the multivariate model was compared with the R^2 of the same model without ΔSDI.

A two-tailed p value < 0.05 was considered statistically significant. Statistical analysis was performed using the SPSS software package (SPSS 15.0, Chicago, IL, USA).

RESULTS

A total of 36 patients were excluded from the analysis because of suboptimal RT3DE image quality data; in addition, 10 patients were lost at

follow-up. Consequently, a total of 147 patients were included in the final analysis.

Characteristics of the patient population

Baseline characteristics of the study population are summarized in Table 1. A total of 59 (40%) patients had an anterior acute MI; obstructive multi-vessel disease (i.e. more than 1 vessel with a luminal narrowing ≥70%) was present in 52 (35%) patients. The median peak value of troponin T was 2.97 μg/L (1.41–6.06 μg/L). Mean LVEF was 47±8% and mean SDI was 5.01±2.10%, respectively. A total of 87 (59%) AMI patients had an SDI higher than 4.12%, therefore having significant mechanical dyssynchrony.

Of note, anterior AMI patients had significantly worse SDI when compared with non-anterior AMI patients (6.06±2.58 vs. 4.31±1.32%; p <0.001). Conversely, no difference in SDI was observed between single-vessel and multi-vessel disease patients (4.83±1.87 vs. 5.35±2.46%; p = 0.19).

Evolution of LV volumes, systolic function, and LV dyssynchrony

At follow-up, a slight increase in LVEDV was observed (105±27 vs. 109±32 ml; p = 0.094), whereas LVESV remained unchanged (56±18 vs. 55±24 ml; p = 0.48); however, a total of 34 (23%) patients showed adverse LV remodelling (defined as an increase ≥15% of LVESV) [12,13] at 6 months follow-up.

A significant improvement in LVEF (47±8 vs. 50±9%; p <0.001) and SDI (5.01±2.10 vs. 4.52±1.97%; p = 0.003) was also noted (Figure 1). A total of 72 (49%) AMI patients remained with an SDI higher than 4.12%, therefore still having significant mechanical dyssynchrony at 6 months follow-up.

Table 1. Baseline characteristics of acute MI patients

Variable	n = 147
Age (years)	58±11
Male gender	116 (79%)
Diabetes	15 (10%)
Family history of CAD	59 (40%)
Hypercholesterolemia	23 (16%)
Hypertension	50 (34%)
Current or previous smoking	87 (59%)
Anterior myocardial infarction	59 (40%)
Infarct-related artery	
- left anterior descending coronary artery	59 (40%)
- left circumflex coronary artery	25 (17%)
- right coronary artery	63 (43%)
Multi-vessel disease	52 (35%)
Peak troponin T (μg/l)	2.97 (1.41-6.06)
Symptom onset to balloon time (minutes)	192±100
Medical therapy at discharge	
- Antiplatelets	147 (100%)
- ACE inhibitors and/or ARBs	147 (100%)
- Beta-blockers	143 (97%)
- Statins	146 (99%)
LVEDV (ml)	105±27
LVESV (ml)	56±18
LVEF (%)	47±8
WMSI	1.65±0.34
Mitral Regurgitation	
- absent/mild/moderate/severe	100 (68%)/43 (29%)/3 (2%)/1 (1%)
Diastolic dysfunction	
- absent/grade 1/grade 2/grade 3	59 (40%)/79 (54%)/7 (5%)/2 (1%)
SDI (%)	5.01±2.10

ACE: angiotensin-converting enzyme; ARBs:, angiotensin receptor blockers; CAD: coronary artery disease; EF: ejection fraction; EDV: end-diastolic volume; ESV: end-systolic volume; LV: left ventricular; MI: myocardial infarction; SDI: systolic dyssynchrony index; WMSI: wall motion score index.

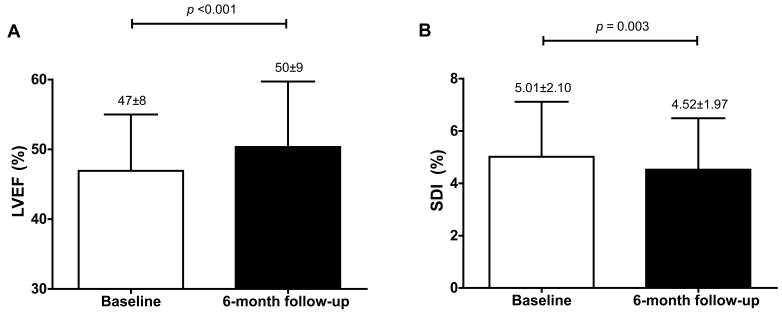

Figure 1. Changes in left ventricular ejection fraction (LVEF) and systolic dyssynchrony index (SDI) at 6-month follow-up. (**Panel A**) A significant increase in LVEF at 6 months follow-up. (**Panel B**) A significant decrease in SDI at 6 months follow-up.

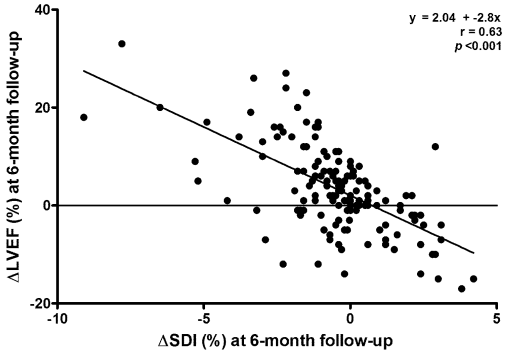

Figure 2. Relation between the change in left ventricular ejection fraction (ΔLVEF) and the change in systolic dyssynchrony index (ΔSDI) after 6 months follow-up in the study population. In patients with a decrease in SDI (restoration of LV synchronicity), LVEF improved. In contrast, in patients with an increase in SDI (impairment in LV dyssynchrony), LVEF decreased.

Of note, patients with anterior AMI improved in SDI to a larger extent when compared with non-anterior AMI patients (ΔSDI: −1.30±2.32 vs. 0.53±1.55%; p <0.001). Conversely, no difference in ΔSDI was observed between patients with single-vessel and multi-vessel disease (−0.55±1.85 vs. −0.39±2.27%; p = 0.66).

A strong correlation was found between ΔLVEF and ΔSDI ($\beta = -0.63$; p <0.001); importantly, patients having an improvement in LV synchronicity showed also an improvement in LVEF, while worsening in SDI was associated to a further decline in LVEF (Figure 2). A significant but weak correlation was observed also between ΔLVESV and ΔSDI ($\beta = 0.33$; p <0.001).

Table 2. Univariate and multivariate regression analyses to determine the independent correlates of change in LVEF at 6 months follow-up

	Univariate		Multivariate	
	β	**p value**	**β**	**p value**
Age	0.070	0.40	-	-
Female gender	0.081	0.33	-	-
Diabetes	-0.053	0.52	-	-
Family history of CAD	0.059	0.48	-	-
Hypercholesterolemia	-0.26	0.002	-0.12	0.038
Hypertension	-0.24	0.003	-0.11	0.057
Current or previous smoker	0.14	0.089	-	-
Anterior acute MI	0.16	0.047	0.017	0.78
Multi-vessel coronary disease	-0.048	0.56	-	-
Peak troponin T	-0.29	0.001	-0.35	<0.001
Symptom onset to balloon time	-0.017	0.84	-	-
Baseline LVESV	-0.031	0.71	-	-
Baseline LVEF	-0.39	<0.001	-0.30	<0.001
Baseline WMSI	-0.039	0.64	-	-
Presence of mitral regurgitation at baseline	-0.16	0.062	-	-
Presence of diastolic dysfunction at baseline	0.088	0.29	-	-
Baseline SDI	0.11	0.18	-	-
ΔSDI	-0.63	<0.001	-0.46	<0.001

The R^2 of the model selected at multivariate analysis was 0.57. Abbreviations as in Table 1.

Correlates of change in LV systolic function (LVEF) at 6 months follow-up

Table 2 shows the results of the univariate and multivariate regression analysis performed to determine the factors related to ΔLVEF between baseline and 6 months follow-up. At univariate analysis, several variables

were significantly related to ΔLVEF: hypercholesterolaemia, hypertension, anterior location of acute MI, peak troponin T, baseline LVEF, and ΔSDI. At multivariate analysis, hypercholesterolaemia, peak troponin T, baseline LVEF, and ΔSDI were independent factors associated with ΔLVEF. More importantly, the addition of ΔSDI to the multivariate model significantly increased the R2 from 0.41 to 0.57 (F change 49.0, p <0.001). This underscores the strong and independent relationship between these two parameters of LV mechanical performance (LVEF and SDI).

DISCUSSION

The present study demonstrates that after a first-reperfused acute MI, an improvement in LV global performance occurs with an improvement of LV systolic function (LVEF) and of LV synchronicty. Changes in LV synchronicity at 6 months follow-up are significantly and independently related to changes in LV systolic function.

Temporal evolution of LV systolic function and LV dyssynchrony after acute myocardial infarction

In the present study, an improvement in LVEF was shown at 6 months follow-up in patients with a first acute MI successfully reperfused. Of note, LV functional recovery (expressed as positive ΔLVEF) was significantly and inversely related to peak value of troponin T (reflecting myocardial damage) and baseline LVEF. In addition, the inverse relationship between baseline LVEF and improvement in LV systolic function during follow-up is likely related to functional recovery of stunned myocardium.[14–16]

Furthermore, LV dyssynchrony early after acute MI has been related to LVEF and LV remodelling at follow-up.[1,2] Besides infarct size as quantified with levels of Troponin or extent of wall motion abnormalities, LV dyssynchrony has shown to be an independent determinant of LV remodelling after acute MI.[1] However, the relationship between changes in

LV dyssynchrony and LV systolic function over time after reperfused acute MI remained unknown. The present study shows that restoration of LV synchronicity was associated with improved LV systolic function after 6 months; conversely, in the subset of patients experiencing worsening of LV dyssynchrony, a further decline in LVEF was observed. Of note, the impact of change in LV synchronicity on the change in LV systolic function was independent and incremental to other baseline variables (including baseline peak troponin T and baseline LVEF). Previous experimental and clinical reports partially explained these observations;[17–20] the detrimental effects of LV dyssynchrony on LV performance may be incremental to the effects of LV structural changes. After acute MI, LV remodelling is characterized by hypertrophy and fibrosis of the non-infarcted regions and expansion and thinning of the infarct core.[21] These changes determine a redistribution of myocardial fibre strain with increasing myocardial work and energy demand.[17–19] The addition of LV dyssynchrony may impact negatively on myocardial fibre strain further impairing LV global performance and favouring LV remodelling.

Clinical perspective

The present study demonstrates that the impairment in LV synchronicity observed early after acute MI is not a permanent phenomenon. In the overall study population, restoration of LV synchronicity was observed, which was related to LV functional recovery. Conversely, progressive worsening of LV dyssynchrony during the follow-up appeared to be an ominous mechanism, which independently contributed to progression of LV dysfunction. Accordingly, beside the essential role of timely and effective revascularization of the culprit vessel, therapeutic strategies to restore a more synchronous LV contraction could potentially be useful in this group of patients.

Limitations

Some limitations should be acknowledged. First, only patients with ST-segment elevation AMI who underwent PCI were included; consequently, the results cannot be extrapolated to patients with non-ST-elevation AMI or patients who did not undergo reperfusion therapy. In addition, RT3DE image quality is highly dependent on the acoustic window; consequently, analysable 3D LV model may be technically difficult to acquire in some patients.[7] Peak troponin T levels measured within the first 18 h of admission may not accurately reflect the infarct size.[22] However, these peak levels are clinically relevant as they predict major cardiac events at follow-up. Finally, the present study did not focus on regional changes in LV mechanics.

CONCLUSION

A temporal evolution of LV synchronicity was observed after a first, mechanically reperfused, acute MI. The reduction in LV dyssynchrony independently influenced LV functional recovery in these patients.

REFERENCES

1. Mollema SA, Liem SS, Suffoletto MS, et al. Left ventricular dyssynchrony acutely after myocardial infarction predicts left ventricular remodeling. J Am Coll Cardiol 2007;50:1532-40.
2. Nucifora G, Bertini M, Marsan NA, et al. Impact of left ventricular dyssynchrony early on left ventricular function after first acute myocardial infarction. Am J Cardiol 2010;105:306-11.
3. Shin SH, Hung CL, Uno H, et al. Mechanical dyssynchrony after myocardial infarction in patients with left ventricular dysfunction, heart failure, or both. Circulation 2010;121:1096-103.
4. Zhang Y, Chan AK, Yu CM, et al. Left ventricular systolic asynchrony after acute myocardial infarction in patients with narrow QRS complexes. Am Heart J 2005;149:497-503.

5. Thygesen K, Alpert JS, White HD, et al. Universal definition of myocardial infarction. Circulation 2007;116:2634-53.
6. Soliman OI, Krenning BJ, Geleijnse ML, et al. A comparison between QLAB and TomTec full volume reconstruction for real time three-dimensional echocardiographic quantification of left ventricular volumes. Echocardiography 2007;24:967-74.
7. Nucifora G, Marsan NA, Holman ER, et al. Real-time 3-dimensional echocardiography early after acute myocardial infarction: incremental value of echo-contrast for assessment of left ventricular function. Am Heart J 2009;157:882e1-8.
8. Lang RM, Bierig M, Devereux RB, et al. Recommendations for chamber quantification: a report from the American Society of Echocardiography's Guidelines and Standards Committee and the Chamber Quantification Writing Group, developed in conjunction with the European Association of Echocardiography, a branch of the European Society of Cardiology. J Am Soc Echocardiogr 2005;18:1440-63.
9. Kapetanakis S, Kearney MT, Siva A, et al. Real-time three-dimensional echocardiography: a novel technique to quantify global left ventricular mechanical dyssynchrony. Circulation 2005;112:992-1000.
10. Lancellotti P, Moura L, Pierard LA, et al. European Association of Echocardiography recommendations for the assessment of valvular regurgitation. Part 2: mitral and tricuspid regurgitation (native valve disease). Eur J Echocardiogr 2010;11:307-32.
11. Lester SJ, Tajik AJ, Nishimura RA, et al. Unlocking the mysteries of diastolic function: deciphering the Rosetta Stone 10 years later. J Am Coll Cardiol 2008;51:679-89.
12. White HD, Norris RM, Brown MA, et al. Left ventricular end-systolic volume as the major determinant of survival after recovery from myocardial infarction. Circulation 1987;76:44-51.
13. Himelman RB, Cassidy MM, Landzberg JS, et al. Reproducibility of quantitative two-dimensional echocardiography. Am Heart J 1988;115:425-31.
14. Ripa RS, Nilsson JC, Wang Y, et al. Short- and long-term changes in myocardial function, morphology, edema, and infarct mass after ST-segment elevation myocardial infarction evaluated by serial magnetic resonance imaging. Am Heart J 2007;154:929-36.

15. Ndrepepa G, Mehilli J, Martinoff S, et al. Evolution of left ventricular ejection fraction and its relationship to infarct size after acute myocardial infarction. J Am Coll Cardiol 2007;50:149-56.
16. Christian TF, Gitter MJ, Miller TD, et al. Prospective identification of myocardial stunning using technetium-99m sestamibi-based measurements of infarct size. J Am Coll Cardiol 1997;30:1633-40.
17. Takeuchi M, Fujitani K, Kurogane K, et al. Effects of left ventricular asynchrony on time constant and extrapolated pressure of left ventricular pressure decay in coronary artery disease. J Am Coll Cardiol 1985;6:597-602.
18. Prinzen FW, Hunter WC, Wyman BT, et al. Mapping of regional myocardial strain and work during ventricular pacing: experimental study using magnetic resonance imaging tagging. J Am Coll Cardiol 1999;33:1735-42.
19. Sweeney MO, Prinzen FW. Ventricular pump function and pacing: physiological and clinical integration. Circ Arrhythm Electrophysiol 2008;1:127-39.
20. Lionetti V, Aquaro GD, Simioniuc A, et al. Severe mechanical dyssynchrony causes regional hibernation-like changes in pigs with nonischemic heart failure. J Card Fail 2009;15:920-8.
21. Gaudron P, Kugler I, Hu K, et al. Time course of cardiac structural, functional and electrical changes in asymptomatic patients after myocardial infarction: their inter-relation and prognostic impact. J Am Coll Cardiol 2001;38:33-40.
22. Arruda-Olson AM, Roger VL, Jaffe AS, et al. Troponin T levels and infarct size by SPECT myocardial perfusion imaging. JACC Cardiovasc Imaging 2011;4:523-33.

Summary and Conclusions

SUMMARY AND CONCLUSIONS

The general introduction of the thesis outlines the value of non-invasive imaging modalities (including coronary artery calcium scoring and multi-slice computed tomography [MSCT] coronary angiography, conventional echocardiography, myocardial deformation imaging, real-time three-dimensional echocardiography [RT3DE] and contrast-echocardiography) in the diagnostic process. The main applications are described in patients with suspected coronary artery disease and in patients with acute myocardial infarction (AMI).

Part I

The first part of the thesis discusses the clinical utility of non-invasive imaging modalities for diagnosis and risk stratification of patients with suspected coronary artery disease. In **Chapter 2**, an overview of the literature regarding the prognostic value of CACS assessment is provided; in addition, potential other applications of CACS assessment as well as the limitations of the technique are discussed. In **Chapter 3**, the prevalence of coronary artery disease across the Framingham Risk Score categories using CACS and MSCT coronary angiography was evaluated; a strong positive relationship was observed between Framingham Risk Score and the prevalence and extent of atherosclerosis. Especially in intermediate Framingham Risk Score patients, CACS and MSCT coronary angiography provided useful information on the presence of subclinical atherosclerosis. In these patients, who represent a substantial part of the population, clinical management is frequently uncertain and refinement of risk using atherosclerosis imaging may allow more appropriate targeting of preventive measures.

CACS and MSCT coronary angiography, despite providing meaningful information about the presence and extent of coronary atherosclerosis, do not provide information about the functional relevance of the observed coronary lesions. In **Chapter 4**, a better understanding of the

complementary information provided by these non-invasive methods (imaging of coronary atherosclerosis versus evidence of inducible ischemia), especially in relation to traditional risk assessment, is provided and a flow chart describing the proposed integration of non-invasive imaging of coronary arteries and stress testing into the traditional risk assessment of coronary artery disease events is presented.

In **Chapters 5 and 6** the prevalence of coronary artery disease, by means of MSCT, and of abnormal stress testing were evaluated among patients with paroxysmal or persistent atrial fibrillation and compared with patients without a history of AF. Interestingly, a higher prevalence of obstructive coronary artery disease was observed among patients with AF, while the prevalence of functionally-relevant coronary lesions was similar to non-AF patients. The higher burden of subclinical coronary atherosclerosis observed in patients with AF may explain the previously observed higher long-term risk of coronary artery disease event in this group; accordingly, more aggressive medical therapy and risk factor modification may be justified in AF patients.

The presence of cardiac and aortic calcium shares many risk factors and a similar cause with both systemic and coronary atherosclerosis; as shown in **Chapter 7**, a simple echocardiography-derived calcium score, obtained through the comprehensive assessment of the burden of cardiac and ascending aorta calcium, is able to predict CACS and the presence of obstructive coronary artery disease, assessed using MSCT coronary angiography. Accordingly, recognition of cardiac and ascending aorta calcium using transthoracic echocardiography, a simple, low-cost, radiation-free and widely available technique, may be used to optimize the identification of patients with obstructive coronary artery disease in clinical practice.

As previously observed by the Multiethnic Study of Atherosclerosis (MESA) study, a progressive impairment of myocardial contraction (despite normal left ventricular ejection fraction) is associated with an increasing severity of coronary atherosclerosis (detected by MSCT or

EBCT) in patients without known coronary artery disease. In **Chapter 8**, the relation between obstructive coronary artery disease (assessed by MSCT coronary angiography), left ventricular diastolic dysfunction, and subclinical left ventricular systolic dysfunction (assessed by speckle-tracking echocardiography) and the potential incremental value of left ventricular diastolic dysfunction and subclinical left ventricular systolic dysfunction over the initial estimate of pretest likelihood of obstructive coronary artery disease were investigated. Of note, both left ventricular diastolic dysfunction and subclinical left ventricular systolic dysfunction were independently related to obstructive coronary artery disease and the presence of subclinical left ventricular systolic dysfunction provided significant incremental value over the Duke Clinical Score for the identification of patients having obstructive coronary artery disease. Especially among the patients with low or intermediate Duke Clinical Score, the presence of subclinical left ventricular systolic dysfunction significantly increased the likelihood of having obstructive coronary artery disease. Accordingly, routine screening for subclinical left ventricular systolic dysfunction among patients without known coronary artery disease may possibly refine the traditional clinical assessment and may be useful for selection of further diagnostic tests.

Part II

In this part of the thesis the clinical value of novel echocardiographic techniques is evaluated in patients with AMI. At present, transthoracic echocardiography is a frequently used imaging modality in the management of patients with AMI. Echocardiography is a low-cost and safe modality, which can be easily applied at the bedside and is valuable for patient follow-up. The accuracy of RT3DE acquisitions with and without contrast early after AMI was investigated in **Chapter 9**; of note, the administration of contrast agents in these patients was of incremental value, improving endocardial border visualization and reproducibility of left ventricular function assessment. As shown in **Chapter 10**, the use of

echocardiographic contrast agents permits also the assessment of left ventricular fluid dynamics, which are related to the remodelling and deformation properties of the left ventricle. The assessment of vortex formation with contrast echocardiography represents indeed a novel measurement of left ventricular diastology; vortex formation time and morphology were indeed good correlated with infarct size and with left ventricular untwisting rate.

This technique also allows for the evaluation of myocardial perfusion and therefore of myocardial infarction extension, which is an important parameter to take into account in the evaluation of cardiac mechanics at short- and long-term follow-up after AMI. In fact, left ventricular function immediately after AMI was demonstrated to be independently associated with infarct size and left ventricular twist (**Chapter 11**). Of note, the impairment of left ventricular twist early after AMI was significantly and independently related to the occurrence of left ventricular remodelling at 6 months follow-up, representing a sensitive global parameter of left ventricular systolic performance after infarction.

Advances in echocardiographic techniques (i.e., tissue Doppler echocardiography, speckle-tracking echocardiography, and RT3DE) have demonstrated an impaired left ventricular synchronicity in patients with AMI; in **Chapters 12 and 13**, the relation between this decrease in left ventricular synchronicity and left ventricular systolic function at baseline and at 6 months follow-up was investigated. Early after AMI, the severity of impairment of left ventricular synchronicity had an additional detrimental impact on left ventricular performance, beyond the infarct size itself. The impairment in left ventricular synchronicity observed early after AMI is not however a permanent phenomenon in all patients; in patients having restoration of left ventricular synchronicity at 6 months follow-up, left ventricular functional recovery was also observed. Conversely, progressive worsening of left ventricular dyssynchrony during the follow-up appeared to be an ominous mechanism, which independently contributed to progression of left ventricular dysfunction.

Accordingly, beside the essential role of timely and effective revascularization of the culprit vessel, therapeutic strategies to restore a more synchronous left ventricular contraction could potentially be useful in this group of patients.

CONCLUSIONS

Non-invasive cardiac imaging modalities play a crucial role in the diagnostic process and clinical management of patients without known coronary artery disease and patients with AMI.

Non-invasive coronary angiography with MSCT has witnessed an enormous development in the last decade allowing accurate detection of significant coronary stenosis; its implementation in clinical practice helps to refine traditional patients' risk stratification.

Conventional two-dimensional echocardiography, the use of echo-contrast agents, myocardial deformation imaging, and RT3DE have been demonstrated to be useful techniques for the identification of patients with obstructive coronary artery disease and for the risk stratification of patients with recent AMI.

Samenvatting en Conclusies

SAMENVATTING EN CONCLUSIES

De inleiding van dit proefschrift beschrijft de waarde van niet-invasieve beeldvormende technieken (coronair calcium score scan, multi-slice CT (MSCT) coronair angiografie, myocard deformatie imaging, real-time 3D echocardiografie (RT3DE) en contrast-echocardiografie) voor het diagnostisch proces. De belangrijkste toepassingen hiervan worden beschreven in patiënten met verdenking op coronairlijden en in patiënten met een acuut hartinfarct.

Deel I

In het eerste deel van dit proefschrift wordt de waarde van niet-invasieve beeldvorming voor de diagnostiek en risico-stratificatie van patiënten met verdenking op coronairlijden besproken. **Hoofdstuk 2** verstrekt een overzicht van de literatuur over de prognostische waarde van een coronair calcium score scan; er wordt tevens ingegaan op eventueel andere toepassingen van deze calcium scan en er wordt beschreven wat de beperkingen aan deze techniek zijn. In **Hoofdstuk 3** werd in de verschillende Framinghame Risk Score categorieën de prevalentie van coronairlijden bestudeerd met behulp van de calcium score scan en MSCT coronair angiografie. Er bleek een sterk positieve relatie te zijn tussen de Framingham Risk Score en de prevalentie en ernst van de atherosclerose. Met name in patiënten met een intermediaire Framingham Risk score werd er met de coronair calcium score scan en de MSCT coronair angiografie nuttige informatie verschaft over de aanwezigheid van subklinische atherosclerose.

Het klinisch beleid is in deze patiënten, die een substantieel deel van de populatie vertegenwoordigen, nog vaak onzeker en met verfijning van het risico met behulp van beeldvorming van de atherosclerose zouden er meer geschiktere preventieve maatregelen genomen kunnen worden. Hoewel de coronair calcium scan en MSCT coronair angiografie zeer waardevolle informatie verschaffen over de aanwezigheid en uitgebreidheid van de

atherosclerose in de kransslagaders, wordt er geen informatie verkregen over de functionele relevantie van de geobserveerde coronair laesies. Een beter begrip van de aanvullende informatie die deze niet-invasieve beeldvorming verschaft ten opzichte van traditionele risico evaluatie en hoe afgebeelde coronair atherosclerose zich verhoudt tot induceerbare ischemie, wordt verstrekt in **Hoofdstuk 4**. Tevens wordt er aan de hand van een flow chart een voorstel gepresenteerd voor de integratie van niet-invasieve beeldvorming van de kransslagaders met stress-testing in de traditionele risico evaluatie voor ischemisch hartlijden. In **Hoofdstuk 5 en 6** werd de prevalentie van coronairlijden (op MSCT) en een abnormale stress-test bestudeerd in patiënten met paroxysmaal of persisterend atriumfibrilleren (AF) en vergeleken met patiënten zonder AF. Er bleek een hogere prevalentie te zijn van obstructief coronairlijden in de patiënten met AF ten opzichte van diegene zonder AF terwijl de prevalentie van functioneel relevante coronair laesies tussen beide groepen hetzelfde was. De grotere burden van subklinische coronair atherosclerose in de patiënten met AF verklaart wellicht het hogere risico dat deze patiënten hebben op hart- en vaatziekten gerelateerde events. Op basis hiervan zou agressievere medische behandeling en het strenger beperken van de risicofactoren in AF patiënten rechtvaardig zijn.

In **Hoofdstuk 7** wordt getoond dat veel van de risicofactoren voor cardiaal calcium hetzelfde zijn als die voor calcium in de aorta hetgeen zich uit in zowel systemische als coronair atherosclerose. Een op echocardiografie gebaseerde calcium score, verkregen bij grondige analyse van de cardiale en aorta calcium burden, bleek in staat te zijn de coronair calcium score en de aanwezigheid van obstructief coronairlijden op MSCT te kunnen voorspellen. Op deze manier kan het bij transthoracale echocardiografie herkennen van cardiaal calcium en calcium in de ascenderende aorta een eenvoudige, weinig-kostende en stralingsvrije techniek zijn die in de dagelijkse praktijk gebruikt kan worden voor het optimaliseren van de identificatie van patiënten met obstructief coronairlijden. Zoals eerder al werd geobserveerd in de Multiethnic Study

of Atherosclerosis (MESA) studie, is een progressieve verslechtering van de myocardiale contractie (ondanks een normale linker kamer ejectie fractie) geassocieerd met een toenemende ernst van coronair atherosclerose op multi-slice of electron-beam CT. In **Hoofdstuk 8** werd de relatie tussen obstructief coronairlijden (op MSCT coronair angiografie) en diastolische linker kamer dysfunctie en subklinische, systolische linker kamer dysfunctie (beoordeeld met speckle-tracking echocardiografie) onderzocht en werd er bekeken of het evalueren van hiervan een incrementele waarde had boven een initiële, pretest likelihood schatting op coronairlijden. Zowel diastolische linker kamer dysfunctie als subklinische, systolische linker kamer dysfunctie bleken onafhankelijk gerelateerd te zijn aan obstructief coronairlijden. Daarnaast verschafte de aanwezigheid van subklinische, systolische linker kamer dysfunctie een incrementele waarde voor het identificeren van patiënten met obstructief coronairlijden boven de Duke Clinical Score.
Met name bij patiënten met een lage of intermediaire Duke Clinical Score, verhoogde de aanwezigheid van subklinische, systolische linker kamer dysfunctie de kans op obstructief coronairlijden. Routine screening voor subklinische, systolische linker kamer dysfunctie in patiënten zonder bekend coronairlijden zou mogelijk de traditionele klinische benadering kunnen verfijnen en zou wellicht bruikbaar kunnen zijn voor het selecteren van andere diagnostische testen.

Deel II

In dit deel van het proefschrift werd de klinische waarde van nieuwe echocardiografische technieken in patiënten met een acuut hartinfarct bestudeerd. Op dit moment is transthoracale echocardiografie de meest gebruikte beeldvormingstechniek in het management van patiënten met een acuut hartinfarct. Echocardiografie is een weinig kostende en veilige techniek die gemakkelijk ook aan bed gebruikt kan worden en waardevol is voor de follow-up. De accuraatheid van RT3DE acquisities met en zonder contrast vroeg na het acute infarct werd onderzocht in **Hoofdstuk 9**.

Het toedienen van contrastmiddelen in deze patiënten bleek van toegevoegde waarde daar het de visualiteit van de endocardiale border verbeterde en de linker kamer functie reproduceerbaarder kon worden bepaald. Zoals laten zien in **Hoofdstuk 10**, maakt het gebruik van echocardiografische contrastmiddelen het mogelijk de linker kamer vloeistof dynamiek te kunnen bepalen; deze zijn gerelateerd aan remodelling en aan de deformerings eigenschappen van de linker kamer.

Het evalueren van de vortex formatie met contrast-echocardiografie is een nieuwe maat voor linker kamer diastologie. De vortex formatie tijd en morfologie bleken goed gerelateerd te zijn aan de infarct grootte en aan de linker kamer untwisting rate. Deze techniek maakt het verder ook mogelijk om de myocardiale perfusie te evalueren en daarmee dus ook de myocardiale infarct extensie. Dit is een belangrijke parameter in de evaluatie van de cardiale mechaniek op zowel korte als lange termijn follow up na het acute hartinfarct.

De linker kamer functie onmiddellijk na het acute hartinfarct bleek onafhankelijk te zijn gerelateerd aan infarct grootte en linker kamer twist (**Hoofdstuk 11**).

De vermindering van linker kamer twist vroeg na het acute hartinfarct was significant en onafhankelijk gerelateerd aan het ontstaan van linker kamer remodelling na 6 maanden follow-up en is dus een gevoelige, globale parameter van de systolische linker kamer performance na het infarct.

Ontwikkelingen in echocardiografische technieken (waaronder tissue Doppler echocardiografie, speckle-tracking echocardiografie en RT3DE) hebben een verminderde linker kamer synchroniciteit aangetoond in patiënten met een acuut hartinfarct. In **Hoofdstuk 12 en 13** werd de relatie tussen de vermindering in linker kamer synchronie en systolische linker kamer functie op baseline en na 6 maanden follow-up bestudeerd. Vroeg na het infarct heeft de ernst van vermindering in linker kamer synchroniciteit een extra schadelijke impact op de linker kamer performance, verder dan de infarct grootte an sich.

De vermindering in linker kamer synchroniciteit welke vroeg na het infarct gezien werd bleek echter niet een permanent fenomeen te zijn in alle patiënten. In patiënten waarbij na 6 maanden follow-up herstel van de linker kamer synchroniciteit gezien werd, was er ook herstel van de linker kamer functie. Omgekeerd bleek een toename van de linker kamer dissynchronie een omineus mechanisme te zijn, welke onafhankelijk bijdroeg aan de progressie van linker kamer dysfunctie. Naast een snelle en effectieve revascularisatie van de culprit laesie, zouden therapeutische strategieën die een meer synchrone linker kamer contractie nastreven, potentieel van waarde kunnen zijn in deze groep patiënten.

CONCLUSIES

Niet-invasieve cardiale beeldvormingstechnieken spelen een cruciale rol in het diagnostisch proces en klinisch management van patiënten zonder bekend coronairlijden en in patiënten met een acuut hartinfarct.
Niet-invasieve coronair angiografie door middel van MSCT heeft het laatste decennium een enorme ontwikkeling doorgemaakt waardoor er nu een accurate detectie van significante coronair stenosen mogelijk is. De implementatie hiervan in de dagelijkse klinische praktijk helpt de traditionele risico-stratificatie te verfijnen. Van conventionele 2D echocardiografie, het gebruik van echografische contrastmiddelen, myocardiale deformatie beeldvorming en van RT3DE is aangetoond dat dit waardevolle technieken zijn voor de identificatie van patiënten met obstructief coronairlijden en voor de risico-stratificatie van patiënten na recent acuut hartinfarct.

LIST OF PUBLICATIONS

1. **Nucifora G**, Cassin M, Brun F, Nicolosi GL. Infarto miocardico anteriore in etilista cronico in trattamento con disulfiram:descrizione di un caso. Ital Heart J Suppl 2004;5:900-904.
2. **Nucifora G**, Albanese MC, De Biaggio P, Caliandro D, Gregori D, Goss P, Miani D, Fresco C, Rossi P, Bulfoni A, Fioretti PM. Lack of improvement of clinical outcomes by a low-cost, hospital-based heart failure management programme. J Cardiovasc Med (Hagerstown) 2006;7:614-622.
3. **Nucifora G**, Gianfagna P, Badano LP, Piccoli G, Hysko F, Allocca G, Cinello M, Fioretti PM. Anomalous origin of the right coronary artery mimicking aortic dissection at transesophageal echocardiography. Int J Cardiovasc Imaging 2007;23:333-336.
4. Allocca G, Slavich G, **Nucifora G**, Slavich M, Frassani R, Crapis M, Badano L. Successful treatment of polymicrobial multivalve infective endocarditis. Multivalve infective endocarditis. Int J Cardiovasc Imaging 2007;23:501-505.
5. **Nucifora G**, Badano L, Hysko F, Allocca G, Gianfagna P, Fioretti P. Pulmonary embolism and fever: when should right-sided infective endocarditis be considered? Circulation 2007;115:e173-e176.
6. Proclemer A, Allocca G, Badano LP, Pavoni D, Baldassi M, **Nucifora G**, Facchin D, Fioretti PM. Fibrillazione atriale permanente e scompenso cardiaco: ablazione a radiofrequenza della giunzione atrioventricolare e terapia di resincronizzazione cardiaca. Revisione della letteratura e delle nuove tecniche di valutazione ecocardiografica. G Ital Cardiol (Rome) 2007;8:215-224.
7. **Nucifora G**, Badano LP, Allocca G, Gianfagna P, Proclemer A, Cinello M, Fioretti PM. Severe tricuspid regurgitation due to entrapment of the anterior leaflet of the valve by a permanent pacemaker lead: role of real time three-dimensional echocardiography. Echocardiography 2007;24:649-652.

8. **Nucifora G**, Hysko F, Vasciaveo A. Blunt traumatic abdominal aortic rupture: CT imaging. Emerg Radiol 2008;15:211-213.
9. **Nucifora G**, Badano LP, Viale P, Gianfagna P, Allocca G, Montanaro D, Livi U, Fioretti PM. Infective endocarditis in chronic haemodialysis patients: an increasing clinical challenge. Eur Heart J 2007;28:2307-2312.
10. Pinamonti B, Di Lenarda A, **Nucifora G**, Gregori D, Perkan A, Sinagra G. Incremental prognostic value of restrictive filling pattern in hypertrophic cardiomyopathy: a Doppler echocardiographic study. Eur J Echocardiogr 2008;9:466-471.
11. **Nucifora G**, Badano LP, Sarraf-Zadegan N, Karavidas A, Trocino G, Scaffidi G, Pettinati G, Astarita C, Vysniauskas V, Gregori D, Ilerigelen B, Marinigh R, Fioretti PM. Comparison of early dobutamine stress echocardiography and exercise electrocardiographic testing for management of patients presenting to the emergency department with chest pain. Am J Cardiol 2007;100:1068-1073.
12. Zakja E, Badano LP, Ventruto P, **Nucifora G**, Gianfagna P, Fioretti PM. Pulmonary embolism and fever: an indication for urgent echocardiography not reported in clinical guidelines? J Cardiovasc Med (Hagerstown) 2007;8:846-849.
13. **Nucifora G**, Hysko F, Vit A, Vasciaveo A. Pulmonary fat embolism: common and unusual computed tomography findings. J Comput Assist Tomogr 2007;31:806-807.
14. Cinello M, **Nucifora G**, Bertolissi M, Badano LP, Fresco C, Gonano N, Fioretti PM. American College of Cardiology/American Heart Association perioperative assessment guidelines for noncardiac surgery reduces cardiologic resource utilization preserving a favourable clinical outcome. J Cardiovasc Med (Hagerstown) 2007;8:882-888.
15. **Nucifora G**, Badano LP, Iacono MA, Fazio G, Cinello M, Marinigh R, Fioretti PM. Congenital quadricuspid aortic valve associated with obstructive hypertrophic cardiomyopathy. J Cardiovasc Med (Hagerstown) 2008;9:317-318.

16. **Nucifora G**, Benettoni A, Allocca G, Bussani R, Silvestri F. Arrhythmogenic right ventricular dysplasia/cardiomyopathy as a cause of sudden infant death. J Cardiovasc Med (Hagerstown) 2008;9:430-431.
17. Badano LP, Pezzutto N, Marinigh R, Cinello M, **Nucifora G**, Pavoni D, Gianfagna P, Fioretti PM. How many patients would be misclassified using M-mode and two-dimensional estimates of left atrial size instead of left atrial volume? A three-dimensional echocardiographic study. J Cardiovasc Med (Hagerstown) 2008;9:476-484.
18. **Nucifora G**, Pellegrini P, Hysko F, Rashidi R, Igidbashian DM. Thrombolysis in acute nonmassive pulmonary embolism: potential role of multidetector-row spiral computed tomography in decision making. Cardiovasc Revasc Med 2008;9:184-187.
19. Allocca G, Proclemer A, **Nucifora G**, Dall'Armellina E, Rebellato L. Monomorphic ventricular tachycardia in 'Brugada syndrome': clinical case and literature review. J Cardiovasc Med (Hagerstown) 2008;9:842-846.
20. **Nucifora G**, Ajmone Marsan N, Siebelink HM, van Werkhoven JM, Schuijf JD, Schalij MJ, Poldermans D, Holman ER, Bax JJ. Safety of contrast-enhanced echocardiography within 24 h after acute myocardial infarction. Eur J Echocardiogr 2008;9:816-8.
21. Spedicato L, Zanuttini D, **Nucifora G**, Sciacca C, Badano LP, Minen G, Morocutti G, Bernardi G, Fioretti PM. Transient left ventricular apical ballooning syndrome: a 4-year experience. J Cardiovasc Med (Hagerstown) 2008;9:916-921.
22. **Nucifora G**, Badano LP, Dall' Armellina E, Gianfagna P, Allocca G, Fioretti PM. Fast Data Acquisition and Analysis with Real Time Triplane Echocardiography for the Assessment of Left Ventricular Size and Function: A Validation Study. Echocardiography 2009;26:66-75.
23. Djaberi R, Schuijf JD, van Werkhoven JM, **Nucifora G**, Jukema JW, Bax JJ. Relation of Epicardial Adipose Tissue to Coronary Atherosclerosis. Am J Cardiol. 2008;102:1602-1607.

24. Allocca G, Vallone C, **Nucifora G**, Miani D, Facchin D, Proclemer A. A dramatic storm of idiopathic ventricular fibrillation. Clin Res Cardiol. 2009;98:62-5.
25. **Nucifora G**, Schuijf JD, van Werkhoven JM, Jukema JW, Djaberi R, Scholte AJ, de Roos A, Schalij MJ, van der Wall EE, Bax JJ. Prevalence of coronary artery disease across the Framingham risk categories: coronary artery calcium scoring and MSCT coronary angiography. J Nucl Cardiol. 2009;16:368-75.
26. **Nucifora G**, Badano LP, Sarraf-Zadegan N, Karavidas A, Trocino G, Scaffidi G, Pettinati G, Astarita C, Vysniauskas V, Gregori D, Ilerigelen B, Fioretti PM. Effect on quality of life of different accelerated diagnostic protocols for management of patients presenting to the emergency department with acute chest pain. Am J Cardiol. 2009;103:592-7.
27. Badano LP, **Nucifora G**, Stacul S, Gianfagna P, Pericoli M, Del Mestre L, Buiese S, Compassi R, Tonutti G, Di Benedetto L, Fioretti PM. Improved workflow, sonographer productivity, and cost-effectiveness of echocardiographic service for inpatients by using miniaturized systems. Eur J Echocardiogr. 2009;10:537-42
28. Mollema SA, **Nucifora G**, Bax JJ. Prognostic value of echocardiography after acute myocardial infarction. Heart 2009; 95:1732-1745
29. **Nucifora G**, Schuijf JD, van Werkhoven JM, Jukema JW, Ajmone Marsan N, Holman ER, van der Wall EE, Bax JJ. Usefulness of Echocardiographic Assessment of Cardiac and Ascending Aorta Calcific Deposits to Predict Coronary Artery Calcium and Presence and Severity of Obstructive Coronary Artery Disease. Am J Cardiol. 2009;103:1045-50.
30. **Nucifora G**, Marsan NA, Holman ER, Siebelink HM, van Werkhoven JM, Scholte AJ, van der Wall EE, Schalij MJ, Bax JJ. Real-time 3-dimensional echocardiography early after acute myocardial infarction: incremental value of echo-contrast for assessment of left ventricular function. Am Heart J. 2009;157:882.e1-8.

31. Pundziute G, Schuijf JD, van Werkhoven JM, **Nucifora G**, van der Wall EE, Wouter Jukema J, Bax JJ. Head-to-head comparison between bicycle exercise testing and coronary calcium score and coronary stenoses on multislice computed tomography. Coron Artery Dis. 2009;20:281-7.
32. Pundziute G, Schuijf JD, Jukema JW, van Werkhoven JM, **Nucifora G**, Decramer I, Sarno G, Vanhoenacker PK, Reiber JH, Wijns W, Bax JJ. Type 2 diabetes is associated with more advanced coronary atherosclerosis on multislice computed tomography and virtual histology intravascular ultrasound. J Nucl Cardiol. 2009;16:376-83.
33. Bertini M, **Nucifora G**, Marsan NA, Delgado V, van Bommel RJ, Boriani G, Biffi M, Holman ER, Van der Wall EE, Schalij MJ, Bax JJ. Left ventricular rotational mechanics in acute myocardial infarction and in chronic (ischemic and nonischemic) heart failure patients. Am J Cardiol. 2009;103:1506-12.
34. **Nucifora G**, Schuijf JD, van Werkhoven JM, Djaberi R, van der Wall EE, de Roos A, Scholte AJHA, Schalij MJ, Jukema JW, Bax JJ. Relation between Framingham risk categories and the presence of functionally-relevant coronary lesions as determined on multi-slice computed tomography and stress testing. Am J Cardiol. 2009;104:758-763
35. Ng CTA, Delgado V, Bertini M, **Nucifora G**, Shanks M, Ajmone Marsan N, Holman ER, van de Veire NRL, Y Leung D, Bax JJ. Advanced Applications of 3-Dimensional Echocardiography. Minerva Cardioangiolica 2009; 2009;57:415-41.
36. van Werkhoven JM, Bax JJ, **Nucifora G**, Jukema JW, Kroft LJ, de Roos A, Schuijf JD. The value of multi-slice-computed tomography coronary angiography for risk stratification. J Nucl Cardiol. 2009;16:970-80.
37. Bertini M, Ajmone Marsan N, Delgado V, J. van Bommel R, **Nucifora G**, Borleffs CJW, Boriani G, Biffi M, Holman E, Van Der Wall E, Schalij M, Bax J. Effects of cardiac resynchronization therapy on left ventricular twist. J Am Coll Cardiol. 2009;54:1317-25.

38. **Nucifora G**, Schuijf JD, Tops LF, van Werkhoven JM, Kajander S, Jukema JW, Schreur JHM, Heijenbrok MW, Trines SA, Gaemperli O, Turta O, Kaufmann PA, Knuuti J, Schalij MJ, Bax JJ. Prevalence of Coronary Artery Disease Assessed by Multislice Computed Tomography Coronary Angiography in Patients With Paroxysmal or Persistent Atrial Fibrillation. Circ Cardiovasc Imaging. 2009;2:100-106.
39. van Velzen JE, Schuijf JD, de Graaf FR, **Nucifora G**, Pundziute G, Jukema JW, Schalij MJ, Kroft LJ, de Roos A, Reiber JH, van der Wall EE, Bax JJ. Plaque type and composition as evaluated non-invasively by MSCT angiography and invasively by VH IVUS in relation to the degree of stenosis. Heart 2009;95:1990-6.
40. Ng ACT, Sitges M, Pham PN, Tran DT, Delgado V, Bertini M, **Nucifora G**, Vidaic J, Allman C, Holman ER, Bax JJ, Leung DY. Incremental Value Of Two-Dimensional Speckle Tracking Strain Imaging To Wall Motion Analysis For Detection Of Coronary Artery Disease In Patients Undergoing Dobutamine Stress Echocardiography. Am Heart J 2009;158:836-44.
41. Siebelink HM, Scholte AJ, Van de Veire NR, Holman ER, **Nucifora G**, van der Wall EE, Bax JJ. Value of contrast echocardiography for left ventricular thrombus detection postinfarction and impact on antithrombotic therapy. Coron Artery Dis. 2009;20:462-6.
42. Ng AC, Delgado V, Bertini M, van der Meer RW, Rijzewijk LJ, Shanks M, **Nucifora G**, Smit JW, Diamant M, Romijn JA, de Roos A, Leung DY, Lamb HJ, Bax JJ. Findings from left ventricular strain and strain rate imaging in asymptomatic patients with type 2 diabetes mellitus. Am J Cardiol. 2009;104:1398-401.
43. Ajmone Marsan N, JM Westeberg J, Ypenburg C, Delgado V, van Bommel RJ, Roes S, **Nucifora G**, van der Geest RJ, de Roos A, Reiber JC, Schalij M. Quantification of mitral regurgitation by real-time three-dimensional echocardiography: head-to-head comparison with 3D velocity-encoded magnetic resonance imaging. JACC Cardiovasc Imaging. 2009;2:1245-52.

44. Ng AC, Delgado V, van der Kley F, Shanks M, van de Veire NR, Bertini M, **Nucifora G**, van Bommel RJ, Tops LF, de Weger A, Tavilla G, de Roos A, Kroft LJ, Leung DY, Schuijf J, Schalij MJ, Bax JJ. Comparison of Aortic Root Dimensions and Geometries Pre- and Post-Transcatheter Aortic Valve Implantation by 2- and 3-Dimensional Transesophageal Echocardiography and Multi-slice Computed Tomography. Circ Cardiovasc Imaging. 2010;3:94-102
45. Bertini M, Delgado V, den Uijl DW, **Nucifora G**, Ng AC, van Bommel RJ, Borleffs CJ, Boriani G, Schalij MJ, Bax JJ. Prediction of Cardiac Resynchronization Therapy Response: Value of Calibrated Integrated Backscatter Imaging. Circ Cardiovasc Imaging. 2010;3:86-93.
46. de Graaf FR, Schuijf JD, van Velzen JE, **Nucifora G**, Kroft LJ, de Roos A, Schalij MJ, Jukema JW, van der Wall EE, Bax JJ. Assessment of global left ventricular function and volumes with 320-row multidetector computed tomography: A comparison with 2D-echocardiography. J Nucl Cardiol. 2010;17:225-31.
47. Bertini M, Sengupta PP, **Nucifora G**, Delgado V, Ng AC, Marsan NA, Shanks M, van Bommel RR, Schalij MJ, Narula J, Bax JJ. Role of left ventricular twist mechanics in the assessment of cardiac dyssynchrony in heart failure. JACC Cardiovasc Imaging. 2009;2:1425-35.
48. **Nucifora G**, Schuijf JD, Delgado V, Bertini M, Scholte AJ, Ng AC, van Werkhoven JM, Jukema JW, Holman ER, van der Wall EE, Bax JJ. Incremental value of subclinical left ventricular systolic dysfunction for the identification of patients with obstructive coronary artery disease. Am Heart J. 2010;159:148-57.
49. **Nucifora G**, Bertini M, Marsan NA, Delgado V, Scholte AJ, Ng AC, van Werkhoven JM, Siebelink HM, Holman ER, Schalij MJ, van der Wall EE, Bax JJ. Impact of left ventricular dyssynchrony early on left ventricular function after first acute myocardial infarction. Am J Cardiol. 2010;105:306-11.
50. Pundziute G, Schuijf JD, van Velzen JE, Jukema JW, van Werkhoven JM, **Nucifora G**, van der Kley F, Kroft LJ, de Roos A, Boersma E, Reiber

JH, Schalij MJ, van der Wall EE, Bax JJ. Assessment With Multi-Slice Computed Tomography and Gray-Scale and Virtual Histology Intravascular Ultrasound of Gender-Specific Differences in Extent and Composition of Coronary Atherosclerotic Plaques in Relation to Age. Am J Cardiol. 2010;105:480-486.

51. Shanks M, Ng AC, van de Veire NR, Antoni ML, Bertini M, Delgado V, **Nucifora G**, Holman ER, Choy JB, Leung DY, Schalij MJ, Bax JJ. Incremental prognostic value of novel left ventricular diastolic indexes for prediction of clinical outcome in patients with ST-elevation myocardial infarction. Am J Cardiol. 2010;105:592-7.
52. **Nucifora G**, Ajmone Marsan N, Bertini M, Delgado V, Siebelink HM, van Werkhoven JM, Scholte AJ, Schalij MJ, van der Wall EE, Holman ER, Bax JJ. Reduced left ventricular torsion early after myocardial infarction is related to left ventricular remodeling. Circ Cardiovasc Imaging. 2010;3:433-42.
53. **Nucifora G**, Bax JJ, van Werkhoven JM, Boogers MJ, Schuijf JD. Coronary Artery Calcium Scoring in Cardiovascular Risk Assessment. Cardiovasc Ther. 2010; Cardiovasc Ther. 2011;29:e43-53
54. Barison A, Aquaro GD, Todiere G, **Nucifora G**, Corciu AI, Pasanisi E, Neglia D, Coceani M. Intramural myocardial hemorrhagic rupture in a patient with metastatic cancer and myocardial infarction. J Cardiovasc Med (Hagerstown). 2011;12:277-9
55. Bertini M, Delgado V, **Nucifora G**, Marsan NA, Ng AC, Shanks M, Van Bommel RJ, Borleffs CJ, Ewe SH, Boriani G, Biffi M, Schalij MJ, Bax JJ. Effect of cardiac resynchronization therapy on subendo- and subepicardial left ventricular twist mechanics and relation to favorable outcome. Am J Cardiol 2010;106:682-7.
56. **Nucifora G**, Todiere G, De Marchi D, Barison A, Aquaro GD, Lombardi M, Pingitore A. Severe involvement of pulmonary arteries in Takayasu arteritis: magnetic resonance imaging. Clin Res Cardiol 2011;100:89-92
57. Bertini M, Ng AC, Borleffs CJ, Delgado V, Wijnmaalen AP, **Nucifora G**, Ewe SH, Shanks M, Thijssen J, Zeppenfeld K, Biffi M, Leung DY, Schalij MJ,

Bax JJ. Longitudinal mechanics of the periinfarct zone and ventricular tachycardia inducibility in patients with chronic ischemic cardiomyopathy. Am Heart J. 2010;160:729-36.

58. **Nucifora G**, Schuijf JD, van Werkhoven JM, Trines SA, Kajander S, Tops LF, Turta O, Jukema JW, Schreur JH, Heijenbrok MW, Gaemperli O, Kaufmann PA, Knuuti J, van der Wall EE, Schalij MJ, Bax JJ. Relationship between obstructive coronary artery disease and abnormal stress testing in patients with paroxysmal or persistent atrial fibrillation. Int J Cardiovasc Imaging. 2011;27:777-85
59. Bertini M, Delgado V, **Nucifora G**, Ajmone Marsan N, Ng AC, Shanks M, Antoni ML, van de Veire NR, van Bommel RJ, Rapezzi C, Schalij MJ, Bax JJ. Left ventricular rotational mechanics in patients with coronary artery disease: differences in subendocardial and subepicardial layers. Heart. 2010;96:1737-43.
60. **Nucifora G**, Aquaro GD, Masci PG, Barison A, Todiere G, Pingitore A, Lombardi M. Lipomatous metaplasia in ischemic cardiomyopathy: Current knowledge and clinical perspective. Int J Cardiol. 2011;146:120-2.
61. Shanks M, Bertini M, Delgado V, Ng AC, **Nucifora G**, van Bommel RJ, Borleffs CJ, Holman ER, van de Veire NR, Schalij MJ, Bax JJ. Effect of biventricular pacing on diastolic dyssynchrony. J Am Coll Cardiol. 2010;56:1567-75.
62. **Nucifora G**, Delgado V, Bertini M, Marsan NA, Van de Veire NR, Ng AC, Siebelink HM, Schalij MJ, Holman ER, Sengupta PP, Bax JJ. Left ventricular muscle and fluid mechanics in acute myocardial infarction. Am J Cardiol. 2010;106:1404-9.
63. Ng AC, Bertini M, Borleffs CJ, Delgado V, Boersma E, Piers SR, Thijssen J, **Nucifora G**, Shanks M, Ewe SH, Biffi M, van de Veire NR, Leung DY, Schalij MJ, Bax JJ. Predictors of death and occurrence of appropriate implantable defibrillator therapies in patients with ischemic cardiomyopathy. Am J Cardiol. 2010;106:1566-73.

64. Shanks M, Delgado V, Ng AC, van der Kley F, Schuijf JD, Boersma E, van de Veire NR, **Nucifora G**, Bertini M, de Roos A, Kroft L, Schalij MJ, Bax JJ. Mitral valve morphology assessment: three-dimensional transesophageal echocardiography versus computed tomography. Ann Thorac Surg. 2010;90:1922-9.

65. Scholte AJ, **Nucifora G**, Delgado V, Djaberi R, Boogers MJ, Schuijf JD, Kharagjitsingh AV, Jukema JW, van der Wall EE, Kroft LJ, de Roos A, Bax JJ. Subclinical left ventricular dysfunction and coronary atherosclerosis in asymptomatic patients with type 2 diabetes. Eur J Echocardiogr. 2011;12:148-155.

66. Delgado V, van Bommel RJ, Bertini M, Borleffs CJ, Marsan NA, Arnold CT, **Nucifora G**, van de Veire NR, Ypenburg C, Boersma E, Holman ER, Schalij MJ, Bax JJ. Relative merits of left ventricular dyssynchrony, left ventricular lead position, and myocardial scar to predict long-term survival of ischemic heart failure patients undergoing cardiac resynchronization therapy. Circulation. 2011;123:70-8.

67. **Nucifora G**, Aquaro GD, Pingitore A, Masci PG, Lombardi M. Myocardial fibrosis in isolated left ventricular non-compaction and its relation to disease severity. Eur J Heart Fail. 2011;13:170-6

68. Regoli F, Faletra FF, Scaglione M, **Nucifora G**, Moccetti T, Auricchio A. Pulmonary Vein Isolation Guided by Real-Time Three-Dimensional Transesophageal Echocardiography. Pacing Clin Electrophysiol. 2012; 35:e76-9

69. Faletra FF, Regoli F, **Nucifora G**, Auricchio A. Real-Time, Fluoroless, Anatomic-Guided Catheter Navigation by 3D TEE During Ablation Procedures. JACC Cardiovasc Imaging. 2011;4:203-6.

70. Faletra FF, **Nucifora G**, Ho SY. Imaging the atrial septum using real-time three-dimensional transesophageal echocardiography: technical tips, normal anatomy, and its role in transseptal puncture. J Am Soc Echocardiogr. 2011;24:593-9

71. Boogers MJ, van Werkhoven JM, Schuijf JD, Delgado V, El-Naggar HM, Boersma E, **Nucifora G**, van der Geest RJ, Paelinck BP, Kroft LJ, Reiber

JH, de Roos A, Bax JJ, Lamb HJ. Feasibility of diastolic function assessment with cardiac CT: feasibility study in comparison with tissue Doppler imaging. JACC Cardiovasc Imaging. 2011;4:246-56

72. Ng AC, Delgado V, Bertini M, Antoni ML, van Bommel RJ, van Rijnsoever EP, van der Kley F, Ewe SH, Witkowski T, Auger D, **Nucifora G**, Schuijf JD, Poldermans D, Leung DY, Schalij MJ, Bax JJ. Alterations in multidirectional myocardial functions in patients with aortic stenosis and preserved ejection fraction: a two-dimensional speckle tracking analysis. Eur Heart J. 2011;32:1542-50
73. **Nucifora G**, Pasotti E, Pedrazzini G, Moccetti T, Faletra FF, Gallino A. Cardiac fibroma mimicking hypertrophic cardiomyopathy: role of magnetic resonance imaging in the differential diagnosis. Int J Cardiol. 2012;154:e11-3
74. Aquaro GD, **Nucifora G**, Pederzoli L, Strata E, De Marchi D, Todiere G, Andrea B, Pingitore A, Lombardi M. Fat in left ventricular myocardium assessed by steady-state free precession pulse sequences. Int J Cardiovasc Imaging. 2012;28:813-21
75. Faletra FF, **Nucifora G**, Ho SY. Real-time 3-dimensional transesophageal echocardiography of the atrioventricular septal defect. Circ Cardiovasc Imaging. 2011;4:e7-9
76. **Nucifora G**, Faletra FF, Regoli F, Pasotti E, Pedrazzini G, Moccetti T, Auricchio A. Evaluation of the left atrial appendage with real-time 3-dimensional transesophageal echocardiography: implications for catheter-based left atrial appendage closure. Circ Cardiovasc Imaging. 2011;4:514-23
77. Regoli F, Faletra FF, **Nucifora G**, Pasotti E, Moccetti T, Klersy C, Auricchio A. Feasibility and acute efficacy of radiofrequency ablation of cavotricuspid isthmus-dependent atrial flutter guided by real-time 3D TEE. JACC Cardiovasc Imaging. 2011;4:716-26.
78. **Nucifora G**, Faletra FF. Current applications of contrast echocardiography. Minerva Cardioangiol. 2011;59:519-32.

79. **Nucifora G**, Miani D, Piccoli G, Proclemer A. Cardiac magnetic resonance imaging in Danon disease. Cardiology. 2012;121:27-30.
80. Bertini M, Ng AC, Antoni ML, **Nucifora G**, Ewe SH, Auger D, Marsan NA, Schalij MJ, Bax JJ, Delgado V. Global longitudinal strain predicts long-term survival in patients with chronic ischemic cardiomyopathy. Circ Cardiovasc Imaging. 2012;5:383-91.
81. Faletra FF, **Nucifora G**, Regoli F, Ho SY, Moccetti T, Auricchio A. Anatomy of pulmonary veins by real-time 3D TEE: implications for catheter-based pulmonary vein ablation. JACC Cardiovasc Imaging. 2012;5:456-62.
82. **Nucifora G**, Stolfo D, Daleffe E, Piccoli G, Copetti R, Proclemer A. Early repolarization in arrhythmogenic left ventricular cardiomyopathy: insights from cardiac magnetic resonance imaging. Int J Cardiol. 2012;159:66-8.
83. **Nucifora G**, Bertini M, Ajmone Marsan N, Scholte AJ, Siebelink HM, Holman ER, Schalij MJ, van der Wall EE, Bax JJ, Delgado V. Temporal evolution of left ventricular dyssynchrony after myocardial infarction: relation with changes in left ventricular systolic function. Eur Heart J Cardiovasc Imaging. 2012;13:1041-6
84. Miani D, **Nucifora G**, Piccoli G, Proclemer A, Badano LP. Incremental value of three-dimensional strain imaging in Danon disease. Eur Heart J Cardiovasc Imaging. 2012;13:804
85. Abate E, Hoogslag GE, Antoni ML, **Nucifora G**, Delgado V, Holman ER, Schalij MJ, Bax JJ, Marsan NA. Value of three-dimensional speckle-tracking longitudinal strain for predicting improvement of left ventricular function after acute myocardial infarction. Am J Cardiol. 2012;110:961-7
86. Grillone S, **Nucifora G**, Piccoli G, Gianfagna P, Hysko F, Pavoni D, Slavich G, Proclemer A, Gasparini D. Biventricular non-compaction demonstrated on multi-slice computed tomography with echocardiographic correlation. J Cardiovasc Med (Hagerstown). 2013;14:677-80.

87. Zanuttini D, Armellini I, **Nucifora G**, Carchietti E, Trillò G, Spedicato L, Bernardi G, Proclemer A. Impact of emergency coronary angiography on in-hospital outcome of unconscious survivors after out-of-hospital cardiac arrest. Am J Cardiol. 2012;110:1723-8

88. Bertini M, Höke U, van Bommel RJ, Ng AC, Shanks M, **Nucifora G**, Auger D, Borleffs CJ, van Rijnsoever EP, van Erven L, Schalij MJ, Marsan NA, Bax JJ, Delgado V. Impact of clinical and echocardiographic response to cardiac resynchronization therapy on long-term survival. Eur Heart J Cardiovasc Imaging. 2013;14:774-81.

89. **Nucifora G**, Miani D, Di Chiara A, Piccoli G, Artico J, Puppato M, Slavich G, De Biasio M, Gasparini D, Proclemer A. Infarct-like acute myocarditis: relation between electrocardiographic findings and myocardial damage as assessed by cardiac magnetic resonance imaging. Clin Cardiol. 2013;36:146-52.

90. Zanuttini D, Armellini I, **Nucifora G**, Grillo MT, Morocutti G, Carchietti E, Trillò G, Spedicato L, Bernardi G, Proclemer A. Predictive value of electrocardiogram in diagnosing acute coronary artery lesions among patients with out-of-hospital-cardiac-arrest. Resuscitation. 2013;84:1250-4.

91. **Nucifora G**, Aquaro GD, Masci PG, Pingitore A, Lombardi M. Magnetic resonance assessment of prevalence and correlates of right ventricular abnormalities in isolated left ventricular noncompaction. Am J Cardiol. 2014;113:142-6

92. Abate E, Hoogslag GE, Leong DP, Bertini M, Antoni ML, **Nucifora G**, Joyce E, Holman ER, Siebelink HM, Schalij MJ, Bax JJ, Delgado V, Ajmone Marsan N. Association between multilayer left ventricular rotational mechanics and the development of left ventricular remodeling after acute myocardial infarction. J Am Soc Echocardiogr. 2014;27:239-48

93. Muser D, **Nucifora G**, Gianfagna E, Pavoni D, Rebellato L, Facchin D, Daleffe E, Proclemer A. Clinical spectrum of isolated left ventricular noncompaction: thromboembolic events, malignant left ventricular

arrhythmias, and refractory heart failure. J Am Coll Cardiol. 2014;63:e39

94. Armellini I, Zanuttini D, **Nucifora G**, Proclemer A. Role of emergent coronary angiography in post-cardiac arrest care: from literature review to clinical practice. G Ital Cardiol (Rome). 2014;15:79-89
95. Fabris E, Morocutti G, Sinagra G, Proclemer A, **Nucifora G**. Uncommon cause of ST-segment elevation in V1-V3: incremental value of cardiac magnetic resonance imaging. Clin Res Cardiol. 2014;103:825-8.
96. **Nucifora G**, Muser D, Masci PG, Barison A, Rebellato L, Piccoli G, Daleffe E, Toniolo M, Zanuttini D, Facchin D, Lombardi M, Proclemer A. Prevalence and prognostic value of concealed structural abnormalities in patients with apparently idiopathic ventricular arrhythmias of left versus right ventricular origin: a magnetic resonance imaging study. Circ Arrhythm Electrophysiol. 2014;7:456-62
97. **Nucifora G**, Muser D, Morocutti G, Piccoli G, Zanuttini D, Gianfagna P, Proclemer A. Disease-specific differences of left ventricular rotational mechanics between cardiac amyloidosis and hypertrophic cardiomyopathy. Am J Physiol Heart Circ Physiol. 2014;307:H680-8.
98. Sechi A, **Nucifora G**, Piccoli G, Dardis A, Bembi B. Myocardial fibrosis as the first sign of cardiac involvement in a male patient with Fabry disease: report of a clinical case and discussion on the utility of the magnetic resonance in Fabry pathology. BMC Cardiovasc Disord. 2014;14:86.
99. Muser D, Piccoli G, Puppato M, Proclemer A, **Nucifora G**. Incremental value of cardiac magnetic resonance imaging in the diagnostic work-up of patients with apparently idiopathic ventricular arrhythmias of left ventricular origin. Int J Cardiol. 2015;180:142-44

CURRICULUM VITAE

Dr. Gaetano Nucifora was born on October 27th, 1976 in Udine, Italy. He obtained his high school diploma in 1995 from Liceo Classico "Jacopo Stellini" in Udine, Italy. In 2002, he graduated cum laude from the Medical School at the University of Udine, Italy and in 2006 he completed his Cardiology training at the University of Trieste, Italy. After a three-month period as consultant cardiologist at the Hospital of Gorizia, Italy, he underwent a two-year cardiac imaging research fellowship at Leiden University Medical Center, Leiden, the Netherlands under the mentorship of Prof. Dr. Jeroen J. Bax. He then underwent a one-year fellowship consisting of clinical cardiac magnetic resonance imaging training at the Fondazione CNR/Regione Toscana Gabriele Monasterio, Pisa, Italy. In 2010 dr. Nucifora was appointed as senior researcher in cardiovascular imaging at the Fondazione Cardiocentro Ticino, Lugano, Switzerland and in 2011 as consultant cardiologist at the University Hospital "Santa Maria della Misericordia", Udine, Italy. His primary clinical and research areas of interest include novel echocardiographic techniques for the assessment of myocardial mechanics and the evaluation of cardiac anatomy and valvular function and the application of non-invasive cardiac imaging techniques (real-time 3D transesophageal echocardiography, cardiac magnetic resonance and cardiac computed tomography) to clinical cardiac electrophysiology.

ACKNOWLEDGMENTS

I would like first to thank prof. Paolo M. Fioretti (past director of the Cardiology Department of the University Hospital of Udine, Italy), dr. Luigi P. Badano (past director of the echo-lab of the University Hospital of Udine, Italy) and prof. Ugolini Livi (director of the Cardiac Surgery Department of the University Hospital of Udine, Italy) who proposed me to come to Leiden to work under the supervision of Prof. Jeroen J. Bax and helped and supported me during this two-year fellowship.

This thesis was also possible thanks to all the friends, colleagues and staff I had the opportunity to meet and work with at the Department of Cardiology of the Leiden University Medical Center. In particular, I cannot forget Victoria, Nina, Matteo, Arnold, Rutger, Miriam and Agnieszka; thank you for the nice discussions we had, for your advices and support, and for your friendship. Also, thanks to to Philippe van Rosendael for the precious help.

Finally, I would like to thank my wife Fjoralba and my mama, for their love, support and encouragement during my foreign experience and my papa, my first teacher and protector through my life.